UNIVERSITY OF LONDON THESIS

Degree MD Year 2005 Name of Author CROSSMAN John Edward

Morphogenesis of the cervical vertebrae

A computer investigation into
developmental mechanisms

John Edward Crossman

A thesis submitted for the degree of MD
at the faculty of Medicine,
University of London, 2005

Supervisor: Professor Alan Crockard
National Hospital for Neurology and Neurosurgery
Queen Square
London WC1N 3BG

ProQuest LLC
789 East Eisenhower Parkway
P.O. Box 1346
Ann Arbor, MI 48106-1346

Abstract

In mammals the presence of a vertebral column defines the phylum and provides protection and support for essential organ systems such as those of respiration, locomotion and neurological function. Congenital abnormalities of the vertebral column in the human are uncommon but they can lead to spinal instability and accelerated degenerative change. They are also often associated with other system abnormalities.

Because our understanding of the developmental process is incomplete, and there is little clinical and / or scientific evidence on which treatment decisions can be based, it is difficult for doctors to decide on the best treatment for affected individuals. With this in mind, the aim of this work has been to construct a theoretical model of vertebral body morphogenesis in order to investigate and clarify mechanisms of normal development and how they might be altered in the formation of congenitally abnormal vertebrae.

As a first step a classification system of vertebral malformations was developed from a study of the clinical and scientific literature. Using cellular automata techniques on a personal computer a model of vertebral body morphogenesis was then constructed and this was used to generate and test hypotheses regarding the aetiology of the observed malformations.

The results of this work suggest that during normal development:

(i) sclerotomal cells migrate medially without significant cranial or caudal deviation

(ii) cellular replication is necessary for normal formation of the cellular condensation which will ultimately develop into the vertebral body.

Abnormal vertebrae were found to be a consequence of

(i) abnormal spatial arrangement of the sclerotomal cells resulting from malsegmentation of the paraxial mesoderm or

(ii) decreased or absent sclerotomal cell replication

The causes of the malsegmentation and abnormal cellular replication in the human embryo is not certain. However animal models have suggested exposure to common environmental teratogens such as sodium valproate and alcohol can cause malsegmentation before the embryo's mother even realises she is pregnant.

Acknowledgements

I am grateful to Professor Alan Crockard, who introduced me to the complexities of congenital abnormalities of the spine, and allowed me to study the patients under his care. He allowed me the time to think about this problem, and has provided inspiration and encouragement throughout the long gestation of this work.

I am also grateful to the late Professor Peter Thorogood who was instrumental in the early stages of this work, and to Professor Jonathan Bard who maintained a biological realism following Peter Thorogoods untimely death.

I also wish to thank Fiona, my wife and my parents, Ian and Clare, for their unstinting support, advice and encouragement.

Chapter list

Detailed contents list

Figure list

Table list

1 Introduction: the enigma of the embryo

morphogenesis *n* the origin and development of a part, organ or organism
Chambers English Dictionary 1998

1.1 THE VERTEBRAL COLUMN

The assembly of the embryo from the female egg and male sperm represents the enigma of the embryo. This task of constructing the embryo through the mechanisms of morphogenesis – cellular growth, replication and organisation – is guided by the genetic information from the mother and father which through interaction with the local environmental factors constructs the phenotype – the embryo.

The aim of this thesis is to investigate how morphogenesis of the vertebral column occurs in the normal mammalian embryo and ways in which these mechanisms might be disturbed leading to formation of the congenital abnormalities of the vertebral column such as those described later in this chapter.

The vertebral column is literally the back bone of the human, and consists of seven cervical vertebrae, 12 thoracic vertebrae, 5 lumbar vertebrae, 5 sacral vertebrae, fused to form the sacrum and a varying number of coccygeal vertebrae. The function of the cervical region of the spine is to allow the head a wide range of movement whilst the body remains unmoved. To this end the vertebrae are relatively small and mobile. The facet joints, through which the vertebrae articulate are more horizontally

placed than in other regions which allows flexion, extension, rotation and lateral flexion movements of this region to occur. The first and second cervical vertebrae are known as the atlas and axis respectively and have a different form from the remaining cervical vertebrae. These vertebrae, with the occipital bone in the base of the skull form the occipito-atlanto-axial osseous-ligamentous complex which is highly specialised and allows skull on neck axial rotation and flexion-extension movement[1].

The thoracic vertebrae articulate with the ribs and support the thoracic cavity. The bodies are larger than in the cervical region, and progressively enlarge towards the lumbar spine. The spinous processes, which initially overlap the caudal vertebra, become progressively shorter. The facet joints are more vertically orientated, and permit a degree of flexion and extension movement, as well as rotation. The rib cage, however, restricts the functional range of movement, but also provides stability to this region[2].

The lumbar vertebrae are the largest in the body. They support the abdominal cavity, and transmit the weight of the body from the upper region of the spine to the pelvis through the sacrum. The arrangement of the facet joints permits flexion / extension movement and lateral flexion.

The whole spine bony-ligamentous complex encases and protects the spinal cord from external injury and excessive movement. The spinal musculature, configuration of the pelvis and shoulder girdle permit an erect posture.

1.2 DISEASES OF THE VERTEBRAL COLUMN

The vertebral column is susceptible to diseases ranging from metabolic disorders of bone metabolism such as osteogenesis imperfecta and rickets, through inflammatory diseases such as rheumatoid arthritis and the HLA-B27 associated arthritidies, infections of the vertebrae and disk

spaces to primary tumours of the bone and cartilage and metastatic tumours. Trauma is also a major contributor to spinal pathology. Mechanical arthritis of the lumbar spine is reaching epidemic proportions in the western world. Reports suggest that the life time prevalence of back pain in the population is now between 60-80%[3].

1.3 EVOLUTIONARY DEVELOPMENT OF THE SPINE

The vertebral column has evolved from the notochord. In the adults of the low order organisms such as the jawless fishes, the adult notochord is different to that seen in the embryo. The adult notochord contains an outer elastic sheath and an inner fibrous sheath. This allows the organism to flex the body wall, as in swimming. This notochord has additional cartilaginous modifications - an dorsal arch to encase the spinal cord with a neural spine and an incomplete anterior hemal arch[4].

Cartilaginous and bony fishes subsequently developed centra - the precursors of the vertebral bodies - of which adjacent pairs articulated with each other on primitive disks derived from the notochord. There is little regional difference through the vertebral column. The first vertebra is modified for articulation with the skull. In the caudal region some bony fishes and many cartilaginous fishes have two vertebrae per muscle segment and pair of spinal nerves. This pattern is known as diplospondyly and the significance is debated. It may simply be a consequence of inbreeding and genetic malformation.

As organisms transferred from a water borne to a land borne existence, new stresses were placed on the spine, which it had to resist in some places and allow extra flexibility in others. These organisms developed firm centra with intervertebral joints which permitted modification to allow and restrict movement.

Amniotes developed a multitude of variations to support their different habitats. Mammals are unique in having bony caps to the vertebrae as

part of the growth process. They, with few exceptions have seven cervical vertebrae, irrespective of whether the neck is short or long. There are about twenty trunk vertebrae which are more prominently regionalised than other groups into anterior thoracic and posterior lumbar vertebrae.

1.4 THE OBJECTIVE OF THIS WORK

Many children with congenital abnormalities of the vertebral column, such as those seen as part of the Klippel-Feil syndrome are referred to the Cranioverterbal Disorders Clinic at Great Ormond Street Hospital. It was the objective of this work to develop a computer simulation which could be used to explore how these congenital vertebral abnormalities, such as a block vertebra or hemivertebra might arise. This knowledge might then be used to further the clinical management of these childrens condition.

1.4.1 What was investigated ?

In order to achieve this objective, mechanisms of cellular morphogenesis described in the literature were studied, and a computer program to manipulate "virtual" cells – the morphogenetic toolkit – was developed. The available literature on normal and abnormal vertebral column development was reviewed and a theoretical model of the migration of the sclerotomal cells to surround the notochord – the stage considered most likely to be responsible congenital vertebral abnormalities – was constructed.

This model was then implemented in a computer program, using the morphogenetic toolkit to control the behaviour of the sclerotomal cells. It should be emphasised that whilst the response of these “virtual cells” to other cells in the vicinity and to a diffusible morphogen pre-ordained within the computer program, the pattern formed by the cells was not. The computer program was then tested, initially using normal development and subsequently abnormal development using it to investigate how the organisation – or dis-organisation such as occurs in malsegmentation of the somites – of the sclerotomal cells alters the morphology of the cellular condensation.

Having identified a possible mechanism for the creation of abnormal vertebra, this could then be used to consider the nature of the insult giving rise to the congenitally abnormal vertebra.

1.4.2 What was the outcome measure ?

Direct comparison of the morphology of the cellular condensation with the abnormal vertebra seen in the clinic is not a valid comparison, as the cellular condensation undergoes chrondrification / ossification during which the fine details of the structure are created. Outcome was therefore restricted to (i) the necessary morphogenetic mechanisms necessary to simulate the formation of the cellular condensation, and (ii) observations such as whether the disk space between the adjacent vertebrae was preserved, the degree to which cellular mixing from adjacent somites occurred, and whether the sclerotomal cells crossed over the midline.

1.5 OVERVIEW OF HUMAN EMBRYOLOGICAL DEVELOPMENT

In order to understand how the vertebral column is built and how congenital abnormalities might arise, it is necessary to understand how the normal human body is "built". This section is an overview of basic human embryology. A more detailed overview of the molecular construction of the human vertebral column is given in Chapter 5.

A new human embryo is formed following fertilisation of the maternal egg by the paternal sperm. Following fusion of the egg and sperm, the fertilised oocyte is transported along the fallopian tube to the uterus. This process takes about one week, during which cellular division of the oocyte is occurring to form a blastomere and subsequently a blastocyst containing an inner cell mass surrounded by outer trophoblast cells. The blastocyst implants in the uterine wall at the beginning of the second week of development. The trophoblastic cells subsequently form the placenta and fetal membranes, whilst the inner cell mass or embryoblast forms a bilaminar embryonic disk consisting of ectoderm and endoderm[5].

At the beginning of the third week, formation of the mesodermal cell layer transforms the bilaminar embryo to a trilaminar structure. The mesodermal layer is formed by ectodermal cells migrating into the space between the ectoderm and endoderm, through the primitive groove in the primitive streak. The primitive streak first arises as a caudal ectodermal thickening which grows cranially. At the junction of the middle and anterior third of the embryo, the primitive streak forms the primitive node through which cells invaginate and form the notochordal process, a rod like structure extending cranially. Anterior to the notochord, in the midline the endoderm and ectoderm are closely applied and this region is known as the prechordal plate, which will give rise to the head region. Posterior to the primitive streak the endoderm and ectoderm are also closely applied and this forms the future cloacal membrane.

After 21 days somites start to form in the mesodermal layer, in a cranial to caudal direction. At the same time in the midline the ectodermal layer is forming the neural tube which will ultimately give rise to the spinal cord. The sclerotome cells are formed by differentiation of the somite and it is these cells which migrate to surround the notochord and subsequently form a cellular condensation around the notochord and anterior part of the neural tube. This cellular condensation then undergoes chondrification and subsequently ossification to form the vertebral body and lateral vertebral elements.

1.6 CONGENITAL ABNORMALITIES

Abnormalities present at birth, or believed to have been present at birth, but discovered later are known as congenital abnormalities or birth defects. These abnormalities, for example heart defects, or in the case of the spine, fusion between two adjacent vertebrae have occurred during the embryonic development of the organism, whilst *in utero*. Similar abnormalities may develop after birth and are termed acquired abnormalities. For instance, inflammatory diseases, such as rheumatoid arthritis can result in adjacent vertebrae fusing in the cervical spine. Such a fusion is termed acquired[6].

1.6.1 Klippel-Feil syndrome

This is the best known congenital abnormality of the neck. The syndromic triad of a short neck, low hairline and restricted neck movements caused by multiple cervical vertebral fusions was first described by Klippel and Feil[7]. The original case is illustrated in Figure 1-1. Klippel-Feil syndrome will be further discussed in Chapter 2.

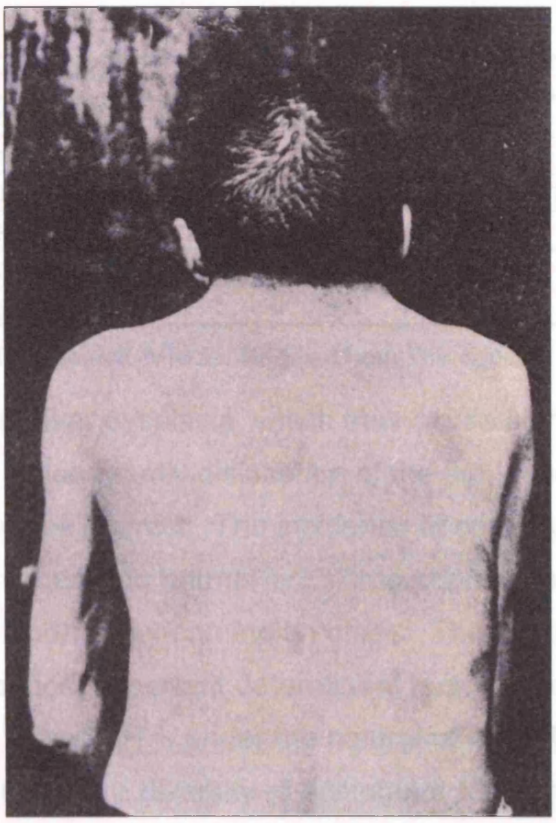

Figure 1-1: the case discussed in the original paper by Klippel and Feil

1.6.2 Relationship of genotype to phenotype

The origin of a congenital abnormality may lie in the genotype of the individual, or may result from an interaction between the genotype and the environment[8]. The phenotype is the form that an individual takes, and includes appearance, behaviour and biochemical make up. It is therefore possible for an individual to possess an entirely normal genotype, yet an abnormal phenotype.

1.6.3 The role of the environment

In many cases, a combination of a genetic abnormality combines with an environmental influence to produce a congenital abnormality which has a multifactorial origin. The genetic abnormality maybe mono or polygenetic, or related to a chromosome abnormality. Thorogood has outlined the possible aetiological categories of congenital defect, and this is given in Table 1-1[8].

Causes of congenital defects
chromosomal abnormalities eg trisomies, translocations
polygenic disorders
single gene mutations eg achondroplasia, aperts syndrome
environmental / teratogenic factors
multifactorial aetiology
unknown aetiology

Table 1-1: Causes of congenital defects. Modified from Thorogood

In congenital acetabular dysplasia, which may cause a shallow acetabulum, and consequently dislocation of the hip, genetic and behavioural influences interact. The incidence of congenital dislocation of the hip (CDH) is higher than normal in Eskimo populations, but lower than normal in certain North American Indian tribes. The depth of the acetabulum is the most important determinant factor as to whether an individual suffers from CDH is under the control of multiple genes. Within both populations there is a diversity of acetabular sizes, relating to the polygenetic control. Following birth, Lapps and North American Indian infants are often swaddled, with both legs splinted together, hips and knees fully extended. The southern Chinese and African Negro infants are often carried on their mother backs with their legs held in abduction. The legs in abduction promote development and deepening of the acetabulum, and hence lower the risk of CDH[9].

Physical factors during the embryonic development *in utero* are also considered important. The development of the os odontoideum, long debated and previously considered a consequence of mal-segmentation is now thought more likely to occur when the transverse ligament of the atlas

acts as a "cheese wire", and divides the odontoid process from the body of the axis[10].

1.6.4 Teratology

The word teratogen is derived from the Greek expression meaning "monster formers"[11]. Teratogens are usually chemical agents, often drugs, that interfere with the normal developmental process and result in the formation of congenital defects. Common examples are alcohol and the anti-convulsant drugs phenytoin and sodium valproate. Other agents also possess teratogenic properties. Common agents with known teratogenic properties are listed in Table 1-2 (from Brown[11]).

Chemical	Use	Effects	Molecular site of action
ACE inhibitors	antihypertensive	patent ductus arteriosus, oligohydramnios, renal abnormalities, skull hypoplasia	ACE (kinase II)
Diethylstilboestrol	anti-miscarriage	multiple defects of (male and female) reproductive tract, vaginal adenocarcinoma	oestrogen receptor
Phenytoin	anti-convulsant	nail and digit hypoplasia, fetal hydantoin syndrome	?
Ethanol	recreational drug	growth and mental retardation, craniofacial and cns defect	?
Retinoids	anti-acne	craniofacial, cardiac, CNS malformation, thymic aplasia	retinoid receptors
Streptomycin	anti-tuberculous	deafness	?

Thalidomide	sedative	phocomelia, ear defects, oesophageal atresia, tetralogy of Fallot, renal agenesis	?
Valproic acid	anti-convulsant	spina-bifida, cardiac defects, fetal valporate syndrome	?
Warfarin	anti-coagulant	nasal hypoplasia, bone stippling	?

Table 1-2: List of teratogenic agents, effect and site of action (where known). From Brown

The mechanism of action of the teratogenic agents varies widely. Often one agent acts at several different sites to produce an effect. The ability of the agent to disrupt the developmental process will alter depending on the developmental processes occurring at the time of exposure. The embryo is most sensitive to exposure during the period of embryogenesis (up to about 9 weeks post ovulation) when the basic form of the heart, kidneys and lungs is developing. Following this period, teratogenic insult causes failure of differentiation eg renal, sexual genitalia and central nervous system[12].

The timing and duration of exposure can be of critical importance. If the organism is exposed, for example during the formation of the seventh pair of somites, and as a consequence, malsegmentation occurs at this level, then abnormal vertebrae may result. However, the embryo maybe able to "repair" the abnormal developmental process, and allow somitogenesis to continue in the normal manner. The site of action of the teratogen may also be important, and a teratogen disrupting the lateral and paraxial mesoderm, may result in abnormalities affecting the kidney and vertebral column. This scenario is seen in the MURCS (Mullerian duct aplasia, renal aplasia, cervicothoracic somite dysplasia) syndrome discussed later[13].

Teratogenic agents are used in developmental biology in order to investigate mechanisms of development[11]. The rationale for the use of

these agents is normally to determine how normal development is affected if a particular "component of the equation" is removed. It is also possible to work backwards and attempt to find a teratogen with a similar outcome to a known congenital abnormality. In this situation, it is possible to conclude that the agent may result in the congenital abnormality, or that the stage in the developmental process that was altered is a critical factor in the normal development of the organism.

1.6.5 Fetal alcohol syndrome

This syndrome is an example of how teratogenic factors in the maternal environment can result in multiple abnormalities in development, none of which are serious enough to result in a spontaneous abortion. Infants suffering from fetal alcohol syndrome typically have a small head size, indistinct philtrum, narrow upper lip and low nasal bridge. The brain is smaller than normal, and neural and glial migration is disordered. Prominent cell death occurs in the frontonasal processes and cranial nerve nuclei. Functionally, these children have a low IQ and restricted mental function[12].

A mouse model has shown developmental abnormalities occurring in the formation of the midline of the brain and facial skeleton structures within 12 hours of ingestion of alcohol[14]. In the human time scale of embryonic development, a mother may ingest a teratogen before she even realises she has become pregnant.

It is likely that alcohol exerts its teratogenic effect through several mechanisms. Anatomical evidence indicates that migration of neural crest cells is impaired. Superoxide production is increased following alcohol ingestion and this can result in increased cell death. Alcohol also has a direct action on a cell adhesion molecule L1, and reduces its ability to "stick" cells together, so preventing cellular condensation, a necessary pre-requisite for morphogenesis[14].

1.6.6 Retinoic acid

Retinoic acid (RA) is a naturally occurring teratogenic compound. Within the developing embryo, RA functions as a transmitter within the HOX gene control cascade. The developmentally active forms of retinoic acid - *trans* retinoic acid and 9-*cis* retinoic acid - bind to retinoic acid receptors, which in turn are then able to bind to retinoic acid response elements containing two or more copies of the sequence GGTCA. Several HOX genes contain retinoic acid response elements in their promoters[14].

Exposure of the developing organism to teratogenic concentrations of retinoic acid results in brachial arch and aortic arch abnormalities, thymus deficiencies and central nervous system abnormalities. Of more interest to the work discussed in this thesis is the observation of homeotic transformations in the spine of mice exposed to retinoic acid during embryogenesis[15].

1.7 EPIDEMIOLOGY OF CONGENITAL ABNORMALITIES

Estimates for the incidence of congenital abnormalities vary depending on the source of data and the time of examination of the affected individuals[16]. Abnormalities maybe single or multiple. Between 3 to 14 percent of newborn individuals have a single malformation, and 0.7 percent of newborn individuals have multiple major malformations[17]. The frequency of malformations at conception is higher than that at birth, but a large number of these fetuses are spontaneously aborted. The birth incidence of major congenital malformations is given in Table 1-3.

Organ system	Incidence / 1000 births
Brain	10
Heart	8
Kidney	4
Limbs	2
Other	6
Total	30 / 10000

Table 1-3: Birth incidence of major congenital malformations. From Connor and Ferguson-Smith

Multiple malformations are present in 0.7 percent of newborns. The different combinations of malformations maybe either random or

syndromic. Examination of infants at the end of their first year of life further increases the incidence of congenital abnormalities.

The current incidence of congenital malformations of the cervical vertebra is not known. Many of these malformations do not result in clinically significant symptoms, and so do not come to light. Brown etal examined the cervical region of 1400 vertebral columns, and found 75 fusions, of which 10 were considered to be congenital. They also reviewed all of the cervical spine x-rays performed at the Mallinckrodt Institute of Radiology during 1963 and found seven congenital fusions in 1158 studies[18]. Sporadic simple malformations are much less likely to be discovered than more complex malformations involving other systems, perhaps leading to spinal cord malformation and dysfunction in which the structural vertebral abnormality is interesting but of no specific clinical significance. Inherited malformations have been described and are detected by pedigree screening[19,20].

1.8 SUMMARY

This chapter has discussed the aims and reasons for undertaking the work described in this thesis. It has also provided a general introduction to the vertebral column, congenital abnormalities and mammalian embryology. The subsequent chapters will discuss more fully the range of cervical spine congenital abnormalities, the molecular basis of vertebral column development and the development of, and experiments performed using the computer simulator.

2 Congenital abnormalities of the cervical spine

This chapter discusses the range of abnormalities observed, and a developmental classification system. The more common syndromic causes of congenital vertebral abnormalities are then reviewed.

2.1 THE SPECTRUM OF CERVICAL SPINE CONGENITAL ABNORMALITIES

Many different vertebral abnormalities have been demonstrated, from simple fusions of two adjacent vertebral bodies to more complex and severe malformations involving whole regions of the spine, including the absence of vertebral elements, for example hemi vertebra or the posterior elements leading to a spina bifida and/or fusion of other elements across the disk space. Such a case is shown in Figure 2-1. These congenital vertebral abnormalities may be associated with other central nervous system abnormalities, including spinal cord dysraphism and Chiari hindbrain malformations[21,22]. Neurological deficit may occur, and may either be a direct consequence of the malformation, or develop as a result of the malformation, for example, a child with a myleomeningocoele may not have lower limb function as a direct consequence of the malformation. In this situation the vertebral abnormality of absent posterior elements is likely to be caused by the underlying malformation of the neural tube. On the other hand, vertebral congenital abnormalities, for example malformation of the atlas may cause damage to the cervical spinal cord causing an acquired high cervical myleopathy[23-25].

Figure 2-1: an example of a patient with a complex vertebral malformation. This patient has axial and subaxial abnormalities including vertebral body fusions, absent and malformed posterior elements

2.2 THE SEQUALE OF CONGENITAL VERTEBRAL ABNORMALITIES

In most cases a congenital abnormality of a subaxial cervical vertebra is only discovered when the affected individual undergoes investigation for another non-related reason, for instance cervical spine trauma. Single level isolated abnormalities do not usually cause neurological impairment or excessive neck pain, and are not usually of particular import. An "unbalanced" malformation, such as a hemi vertebra is a cause of scoliosis[26,27] although this is not common in the cervical region.

Abnormalities of the cervical vertebrae extending over several levels can be associated with excessive motion and instability at disk spaces. Such a case is illustrated in Figure 2-2. This is frequently associated with neck pain, and may lead to compression of the spinal cord. The clinical management of such a case is not certain with opinion divided amongst (i) early surgical fusion, which will protect the abnormal level, but accelerate degenerative changes at the adjacent level, and if fusion is performed in the immature spine might interfere with the normal growth, and (ii) observation, which avoids the potential adverse effects of early surgery

discussed above, but if the degenerative changes progress to cause spinal cord damage, this is unlikely to be reversible, even after surgery. A radiological kinematic study has found increased movement in the upper cervical spine in patients with Klippel-Feil, compared to the normal population, and the authors have suggested that this places individuals with Klippel-Feil at increased risk of neurological sequelae[28].

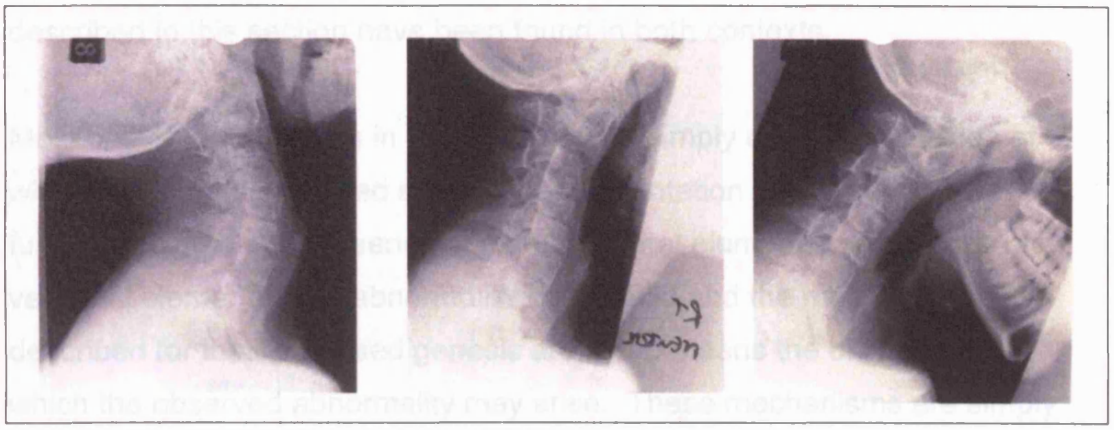

Figure 2-2: patient with Klippel-Feil and excessive movement at C2-3. Dynamic plain films, from left to right, in extension, neutral and flexion.

2.3 CONGENITAL VERTEBRAL ABNORMALITIES IN OTHER ANIMALS

Congenital abnormalities of the cervical vertebra are well recognised in other mammals[29,30]. An entire pedigree of an extended family of Arabian horses with familial occipito-atlanto-axial malformation has been published[31]. In this condition, the affected horses suffer from congenital fusions of the occipital bone to the atlas and axis, and because in the horse, the head is dependant, instability, as a consequence of the malformation at this level may result in high cervical compression with myleopathy.

Abnormalities in mice have been extensively catalogued[32] have provided useful laboratory models for investigation into the cause of the phenotype.

2.4 CLASSIFICATION OF CONGENITAL VERTEBRAL ABNORMALITIES

Many abnormalities in the cervical spine and skull base have been observed and multiple different mechanisms have been proposed for their genesis. This section attempts to classify the abnormalities observed on an embryological basis, irrespective of whether the abnormality occurs as part of a syndrome, or is an isolated event. Most of the abnormalities described in this section have been found in both contexts.

Most of the abnormalities in the spine can be simply divided into fusion of what should be segmented structures, segmentation of what should be fused structures and presence of extra vertebral elements, or absence of vertebral elements. The abnormalities observed and the mechanisms described for their proposed genesis are by no means the only way in which the observed abnormality may arise. These mechanisms are simply a suggested hypothetical possibility, based on the embryological development, and provide potential ideas to be tested on the computer simulator, as described later in the thesis.

2.4.1 Failure of fusion

This is a theoretical abnormality, that may occur during the development of the clivus. During the development of the skull base, the five occipital sclerotomes fuse to form the basi-occipital bone[33,34]. This is accompanied by a reduction in the expression of Pax-1, which is probably the reason an intervertebral disk does not form between the sclerotomes, and hence allowing the fusion to occur. The presence of a completely segmented clivus has not been described in the clinical literature, possibly, because it is associated with other fatal abnormalities, however, the presence of occipital vertebra has been described in animal models[35].

2.4.2 Failure of segmentation

This is the most common abnormality observed in the cervical spine. The degree of fusion between the components of the vertebrae varies. Most commonly, fusion occurs between the bodies of the affected vertebrae,

although rudimentary disk formation is often apparent. Fusion between the facet joints and of the posterior elements may also occur, although this is less frequent. Often the vertebrae involved are misshapen, with a decreased anterior-posterior dimension and increased lateral measurement[36]. This is described as "waisting".

2.4.3 Accessory vertebral components

The presence of hemi vertebra are in-frequently observed, usually as part of a more complex segmentation abnormality. The hemi vertebra may cause the formation of a scoliosis, particularly when found within the thoracic spine.

Enlargement of the posterior elements has been described[37,38]. In both cases, an abnormally enlarged spinous process was observed, associated with compression of the spinal cord and neurological symptoms apparent of neck extension.

2.4.4 Absence of vertebral elements

Absence of the posterior elements of a vertebra, resulting in the formation of a bifida is not uncommon. In this situation, failure of the complete formation of the neural arch has failed, and as a consequence, the spinous process fails to form. This form of abnormality maybe associated with failure of the neural tube to close.

2.5 PATTERNS OF CONGENITAL ABNORMALITIES

The congenital abnormalities observed in the skull base and bony cervical spine can be largely divided into those affecting the skull base and axial spine, and those affecting the subaxial spine. Abnormalities of the spinal cord in this region tend to involve the upper cervical spine. It is important to acknowledge that congenital spine abnormalities can also occur as an isolated occurrence without other features. These abnormalities are usually the simplest, and consist of a block vertebrae in the mid subaxial cervical spine.

2.5.1 Klippel-Feil (KF) syndrome

This is the most well known of the clinical syndromes involving congenital cervical spine fusions and skull base abnormalities, found in approximately 1:42000 of the general population[39]. The clinical syndrome is a triad composed of a low posterior hairline, a short neck and limitation of neck movement. The clinical phenotype from the paper is shown in Figure 2-1 This gentleman possessed an extensive fusion of the entire cervical spine, as illustrated by photograph and drawing reproduced in Figure 2-3 and Figure 2-4 from the original paper.

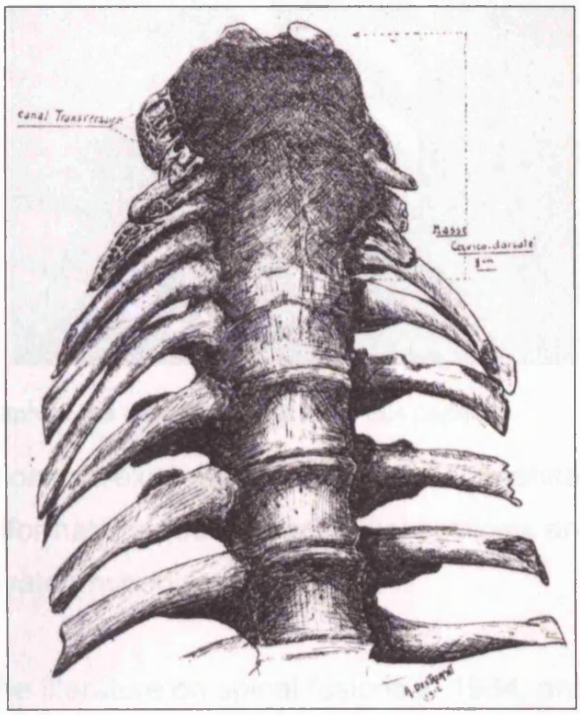

Figure 2-3: drawing of the spinal fusion found in the case described by Klippel and Feil

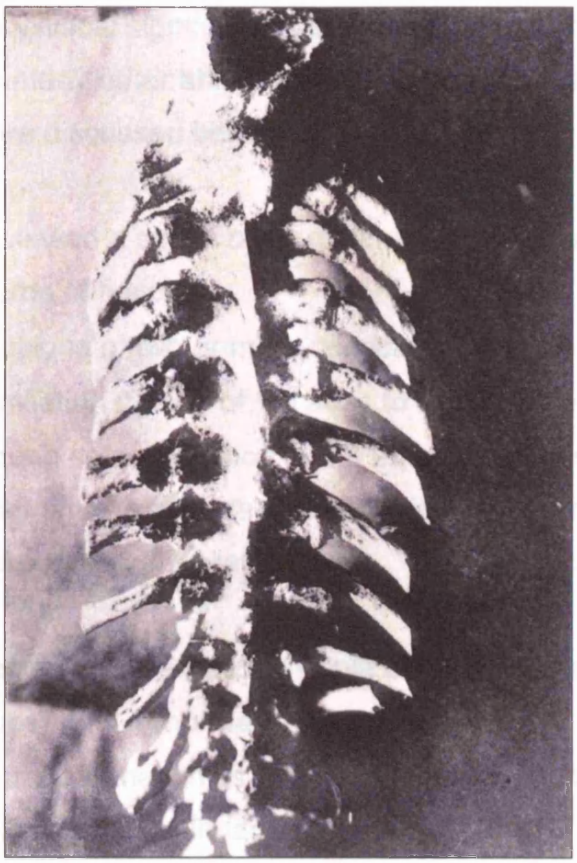

Figure 2-4: photograph of the case in Klippel and Feils paper

Other malformations co-exist with Klippel-Feil – congenital heart disease (30%), renal malformations (30%), congenital scoliosis and Sprengels shoulder (an elevated hypoplastic scapula).

Gray reviewed the literature on spinal fusions in 1964, and found a total of 462 cervical fusions[40]. The earliest congenital fusions were recognised in 500BC, and rediscovered in the 16th and 18th centuries. Gray reports that 75% of all fusions involve at least one of the atlas, axis or C3. Half of the cases reported had fusions of less than three levels, whilst a quarter of the cases were at the occipito-cervical level (O-C1). Fusion between the axis and C3 was most common. The degree of completeness of the fusion between the adjacent vertebrae varies. Most commonly, the anterior, lateral and posterior elements are fused (50%). In 18% of cases, fusion involved only the anterior elements, the lateral elements only in 3% and the posterior elements in 9%. Gray commented that congenital cervical fusions acted as a marker for other systemic malformations,

usually of greater clinical significance, and in addition to the defining triad of abnormalities, many other abnormalities are also associated with the syndrome, and are discussed below.

David etal[41,42] reviewed a series of 30 patients with cervical fusions and noted three patterns of fusion:

- subaxial fusions of two or more cervical vertebrae
- atlas assimilation (fusion of the atlas to the occipital bone)
- the "one bone spine" – fusion of the entire cervical spine

Approximately half of the cases described were asymmetrical between the left and right sides of the vertebral column.

David and colleagues outlined two possible developmental mechanisms to account for the observed abnormalities:

- homeotic transformation as a consequence of alteration of the anterior expression boundaries of the Hox genes
- impaired notochord function and / or Pax gene expression.

At the cranio-vertebral junction, a Chiari malformation sometimes associated with syringohydromyelia is observed. The combination of the hindbrain abnormalities with the KF abnormality is probably a reflection of disordered embryogenesis in the local anatomical region. Synkinesis is also observed, as a result of incomplete pyramidal tract decussation, especially with the split cord malformation[43].

Not all reported abnormalities associated with Klippel-Feil are found in any one individual, and the wide variety of abnormalities found suggest that KF is a consequence of at least several different perturbed developmental mechanisms.

Bony abnormalities of the cervical spine in KF syndrome occur in two distinct patterns, although the patterns may overlap, and co-exist. At the cranio-vertebral junction, occipitalisation of the atlas and block fusion of

C2-3, with a rudimentary dens or os odontoideum occurs. The second pattern of bony abnormality in the cervical spine with KF is that of subaxial fusions. The fusions may involve a single level, or be more extensive as illustrated by Klippel and Feil.

The first pattern is most likely to represent a homeotic transformation caused by exposure to a teratogen during pregnancy. Experimental exposure of mice to retinoic acid during development has resulted in similar abnormalities. The actual abnormality produced is dependant on the timing of the exposure. Kessel etal exposed mice to retinoic acid between seven and eight days following conception, that is whilst the mesodermal cell layer formation is occurring during gastrulation, and before segmentation of the paraxial mesoderm, which will eventually form the cervical spine has started to occur[44,45]. A range of time dependant abnormalities were noted to form affecting the morphology of the cervico-vertebral junction and remainder of the spine. The results of this experiment are in concordance with an experiment in which the cervical and thoracic somites / paraxial mesoderm were transplanted, but were found to continue to produce spinal elements appropriate to their original position[46]. It is interesting to note that Kessel etal did not observe the formation of block, hemi or fused vertebrae in this experiment.

Several mechanisms have been suggested to account for the development of vertebral fusions. The origin of the abnormality is probably multifactorial, in so far as several of the mechanisms act in concert which results in the fusion. Bavrinck and Weaver have proposed that disruption of the embryonic subclavian artery results in failure of the intersegmental arteries at the time of resegmentation, and henceforth a fusion[47]. Depending on the timing of the subclavian artery disruption, different abnormalities resembling the KF, Poland and Mofius abnormalities arose.

Familial KF has been reported in the literature[19,39,48,49]. Clarke published the first report of a genetic abnormality segregating with the clinical abnormality. In the family reported, an inversion on chromosome 8 - inv (8) (q22.2q23.3) - was found to be associated with vertebral fusions and malformation of the laryngeal cartilages[50]. Ohashi has also reported the presence of a reciprocal transformation in a 6 year old girl with sporadic KF syndrome[20].

2.5.2 Multiple segmentation vertebral defects

In this condition multiple segmentation defects of the ribs and vertebral bodies are found. Jarcho and Levin first described the condition as "short trunk dwarfism" in 1938. The vertebral body defects vary, and consist of fusion or absence of vertebrae, hemi vertebrae and butterfly vertebrae. The ribs vary in number and shape and maybe fused. The spine maybe kyphotic and / or scoliotic, and a pectus deformity can occur.

All regions of the spine can be affected. The associated malformations usually correspond with the site of the vertebral abnormalities. The condition has variable expression and can be transmitted as an autosomal dominant, autosomal recessive or occur as a new mutation[51].

2.5.3 Fetal alcohol syndrome

Fetal alcohol fusion is most common over a single level, related to teratogenic insult occurring between the 24th to 28th day of development. It is associated with cardiovascular system abnormalities, in distinction to KF, which is usually associated with genitourinary system abnormalities[52].

2.5.4 MURCS and Brachio-oto-renal syndrome

The MURCS syndrome - mullerian duct aplasia, renal agenesis / aplasia and cervical-thoracic spine dysplasia syndrome has been proposed to explain the association between cervical spine and genito-urinary system abnormalities[53]. The aetiology of MURCS is thought to be similar to that of branchio-oto-renal syndrome, in that both propose the association of abnormalities is a consequence of the cells that form the eventually

disparate organ systems originating in close proximity, and being exposed to a locally acting teratogenic insult.

2.5.5 Craniosynostoses

Cervical fusions are also associated with craniosynostoses. In Crouzons, Aperts, Pfeiffer and Saethre-Chotzen syndromes, congenital spinal fusions are found[54,55]. These are considered most likely to be progressive fusions, that is, the number of levels involved in the fusion increases with age. In the case of Aperts, Crouzons and Pfeiffers syndromes, the fusions maybe a consequence of a mutation in the FGF receptor gene, which has been found to occur in these syndromes[56,57].

2.5.6 Environmental agents

The role of teratogens in the aetiology of the malformations has been discussed above. However, as stated earlier, these malformations are often multifactorial in genesis, and mechanical factors may alter the phenotype. Klippel and Feils case displayed a complete fusion from the atlas to C7. More recently a series of cases reported by David etal[42] dicusses three cases with extensive cervical fusions. Case 1 is fused from the clivus to the upper thoracic spine, apart from a single motion segment at C4-5. It may well be that this level was also initially fused, but mechanical forces during the prenatal and post natal period resulted in a fracture of the mesenchymal analage or chrondrified unit to create a motion segment in much the same way as Crockard and Stevens have postulated for the formation of an os odontoideum, occurring in Down syndrome, Morquios disease, spondyloepiphyseal dysplasia, multiple epiphyseal dysplasia and pseudo-achondroplasia[10].

2.6 SUMMARY

This chapter has discussed the range of, and consequences of cervical spine vertebral abnormalities documented in the literature, and provided a theoretical classification of these abnormalities. The most common syndromic associations of cervical vertebral malformations have also been discussed.

3 Developmental mechanisms of morphogenesis

This chapter discusses the (i) cellular mechanisms and interactions responsible for morphogenesis and (ii) key developmental genes in the formation of the vertebral column. It is a general introduction into the principles and mechanisms that underlie the process of morphogenesis.

3.1 CELLULAR MECHANISMS OF MORPHOGENESIS

Bard[58] has listed the cellular properties which he considers necessary for cells to build structures in the organism. These properties are shown in Table 3-1.

Property		description
Movement	contact guidance	cellular migration guided by extracellular matrix molecules
	haptotaxis	movement of cells up a concentration gradient of an ECM molecule
	chemotaxis	movement of cells up a diffusible morphogen concentration gradient
	contact inhibition of movement	response to collision between two cells
Matrix production		secretion of ECM by cells
Condensation formation		aggregation of cells due to 1) increased cell adhesion molecule production, 2) increased cellular replication / growth, 3) loss of ECM, 4) cell traction
Growth		cell division, or cell enlargement, or increased ECM production
Death		usually apoptosis

Table 3-1: Cellular properties responsible for morphogenesis(Bard, morphogenesis, page 275).

The mechanisms underlying morphogenesis have been subject to biological and computational experiments to investigate the factors that control the movement or migration of cells within the in vitro and in vivo during the morphogenetic process. Cellular movement in the embryo can

occur either as part of a sheet of cells, such as occurs in the formation of the heart, or individually, for example migration of the sclerotome to create the vertebral body condensation or neural crest migration.

Migration of cells is not the only mechanism through which cellular condensation may occur. Other mechanisms such as (i) locally increased cellular proliferation, (ii) reduction in the extracellular matrix keeping the cells apart, (iii) increase in cellular adhesiveness and (iv) movement towards a focus. It is likely that a combination of factors contribute to condensation formation, rather than any one particular mechanism.

The majority of experimental evidence about the behaviour of mesenchymal cells during morphogenesis has been derived from experiments performed using fibroblasts, which are considered to have similar properties to those of mesenchymal cells.

Fibroblast morphology varies depending on their environment, or culture medium. The *in vivo* morphology is similar to that found in three dimensional collagen gels, however, when the cell is transferred to two dimensional world, such as that of the plastic culture dish, the cellular morphology becomes the shape of a fan, with a broad ruffling membrane over the leading curve of the fan, and a narrow trailing edge. *In vivo* and in three dimensional collagen gels, individual fibroblasts have a long bipolar shape, with small active pseudopodia at the leading edge. In condensations, the cells become more plump, and have fewer pseudopodia present[59-62].

Most cells can be induced to move when in a plastic culture dish. However, in the embryo, most cells move only very small distances. The neural crest cells move large distances, and the conditions required in order to allow the cells to move have been suggested as (i) removal of physical barriers such as the basal lamina, (ii) alterations in cellular adhesion, (iii) creation of space for the cell to move into, and (iv) activation of the locomotor apparatus[63].

Epithelial-mesenchymal transformation is a mechanism which allows the removal of the physical barrier to cellular migration. The epithelial somite breaks up to form a loose mesenchymal collection of cells, the ventro-medial quadrant of which forms the sclerotome, which subsequently migrate to the notochord and form the vertebral body anlage.

Random cellular movement has been demonstrated to occur in fibroblasts[64,65] Ambrose noted "that movements of cells when isolated and spreading on a glass are largely at random"[66].
The movement of mouse fibroblasts in tissue culture was further analysed by Gail and Boone[64]. Using time lapse photography at 2.5 hourly intervals the movement of mouse fibroblast cells in glass flasks containing Dulbecco-Vogt medium was recorded. Their results demonstrate that fibroblast cells have a tendency to persist in their direction of motion over successive 2.5 hour intervals but this is not detectable at 5 hourly intervals. They used a modified random walk model to measure "D*" – described as an augmented diffusion constant.

Observations at more frequent time intervals have demonstrated that cellular movements are more randomly based and are better described by a Brownian motion model rather than the random walk model used by Gail and Boone[67].

In the random walk, while the direction of travel is random, the vector of travel is constant, whilst in Brownian motion, both the direction and vector are random[68]. In this work, the Brownian motion model was preferred, as it was considered that this better represented the biological reality of observed fibroblast movement, albeit *in-vitro*.

However, it is directed cellular movement, ie cellular migration that is important in morphogenesis. Chemotaxis, haptotaxis and contact guidance are all mechanisms through which cellular movement can be directed.

3.1.1 Chemotaxis

The movement up a chemical concentration gradient – has been demonstrated to occur in the aggregation of solitary haploid amoebae cells of *Dictyostelium Discoideum*, to form a multicellular pseudoplasmodium or slug. Time lapse micro cinematography has demonstrated the cells form radial streams, which successively merge to form larger streams as the different streams converge on a central point[69]. The chemotactic substance was identified as cAMP by Konijn etal[70] and Bonner[71], and this process has subsequently been the topic of much research, including modelling of the process using computer techniques[72,73]. This topic is further discussed below. The ability of *Xenopus* blastula cells to express different genes dependant on the concentration of activin has also recently been demonstrated[74,74]. This demonstrates that the blastula cells are able to sense their position in a concentration gradient, and that this is able to influence individual cell behaviour.

3.1.2 Haptotaxis

This is the movement of cells up an adhesion gradient and has been demonstrated to guide a neuronal growth cone[75], and has also been suggested to guide primary mesenchymal cells during sea-urchin morphogenesis. The primary mesenchymal cells deploy processes, in an attempt to reach the region of maximal adhesiveness[76]. The extension of the processes or filopodia was studied *in vivo* in three dimensions and time by Malinda etal[77]. In this study, the filopodia were (i) transient in nature, (ii) initial direction of filopodia extension was random, (iii) closer to the target site, more filopodia were distributed towards the target.

It has also been shown that gastrulating cells will express receptors for adhesion molecules of the integrin family – a molecule found in the extracellular matrix in developing embryos. The control of the expression of the integrins is unknown, but it is postulated that the expression of these molecules will alter and guide the movement of the gastrulating cells[[78].

3.1.3 Contact guidance

Contact guidance is the guidance of migrating cells by molecules laid down in the substratum[79]. The movement of migrating mesenchymal cells in the developing telocast fin was observed by Wood and Thorogood[80]. They observed the mesenchymal cells followed collagen fibrils. Cell migration on fibronectin has also been observed in gastrulating embryos, and a gradient of fibronectin has been demonstrated in the path of migration between the endoderm and mesoderm for cells migrating to form the heart[81,82]. This process is likely to represent a combination of contact guidance and haptotaxis.

3.1.4 Contact mediated inhibition of movement

The movement of cells results in collisions between cells. If one moving cell meets another, the first cell becomes quiescent and movement of the cells will cease. Abercrombie suggested this mechanism could be responsible for the movement of cells from a region of high density to low density[83]. This behaviour was demonstrated to occur by Bard and Hay in 3D collagen gels and in the corneal stroma[61] and also subsequently demonstrated by Wood and Thorogood[80].

3.2 MECHANISMS OF CELLULAR INTERACTION

Co-ordination of cellular behaviour is of crucial importance in morphogenesis. Cellular movement, condensation, proliferation and death are to a large degree under the control of the cellular external environment. A variety of different stimuli have been implicated in the selection of the cellular response to the environment, including long range diffusible stimuli, the presence or absence of adhesion molecules on the surrounding cells, growth factors produced by the cell or local companions, and the extra-cellular matrix[33,84].

3.2.1 Induction

Waddington defined the ability of one tissue to influence another tissue as *induction*[85]. *Competence* is the ability of the second tissue respond to the signal. Induction maybe either instructive or permissive. Instructive induction occurs when the signal influences the type of cells that develop from another tissue. Permissive induction is defined as allowing a group of cells to continue to develop, without influencing the pathway along which the cells differentiate. During development, reciprocal interactions often occur between two tissues, with the role of inducer and competent tissue being exchanged several times.

The first example of an inducer was reported by Spemann, who discovered the organiser region in amphibians[86]. Spemann grafted the dorsal lip of an early frog blastopore to the ventral edge of another frog embryo, of the same age. The embryo subsequently developed a well defined partial second embryo, consisting of a second head and neck region, but joined at the tail. This is interpreted as addition of a second anterior axis. The transplant of an organiser from a late gastrula results in duplication of posterior structures.

For any interaction between tissues, the following questions arise when attempting to understand the embryological mechanism involved:[33]

- the location of the tissue source for the inductive signal
- properties of the inductive signal
- mode of intercellular transmission
- how do the responding cells process the signal
- how do signals affect differentiation / morphogenesis of competent tissue

In attempting to answer these questions, experimental work is vital. Often, an answer to one question is required before another question can be attempted, however, the effect of the signal on tissue differentiation and morphogenesis is usually obvious.

3.2.2 Location of the tissue source for the inductive signal

This is often resolved along the lines of Waddingtons classical experiment, when the anterior lip of the blastopore was removed, and re-implanted in another area of competent tissue.

3.2.3 Properties of the inductive signal

In order for the properties of the inductive signal to be determined, the source of the signal, and the actual signal must be identified. An example of this process was the identification of *sonic hedgehog*, the signal secreted by the notochord, which promotes the differentiation of the somite to sclerotome and to express the gene Pax-1. Sonic hedgehog was initially identified by using a gene probe derived from the Drosophilia *hedgehog* gene, which functions as a segment polarity signalling protein[87].

3.2.4 Mode of intercellular transmission

Fans experiments, in which he elucidated the mechanism of action of sonic hedgehog through a combination of isolating the cells secreting hedgehog from the target cells, and use of a hedgehog analogue in vitro, reveal the way in which the mechanism of action of the hedgehog molecule was shown to be a long range diffusible signal, rather than an intermediate signal involved in a genetic cascade[88].

3.2.5 How do responding cells process the signal

Two basic mechanisms exist by which cells respond to extra-cellular signals or extracellular signals are transduced: (i) through membrane bound receptor complexes, and (ii) via steroid receptors[89].

Ligands to membrane bound receptors do not have to pass through the cell membrane, and are consequentially more diverse in nature. The

ligands can be protein hormones or signalling molecules, cytokines, growth factors, or other molecules such as those attached to the cell wall of other cells. In this way, one cell is able to exert its affect on its neighbour. In order to have an effect, the receptor must be able to influence the intra-cellular environment. To this end there are several basic mechanisms, such as ionic channels, receptors bound to tyrosine kinase and adenylate cyclase. The basic activation mechanisms are reused, and cellular activation - or inhibition - is achieved through the cell membrane mounted receptor. Activation of an ionic channel leads directly to an alteration in the permeability of the channel, usually to a specific ion. Activation of other receptors, bound to enzymes, results in changes in second messenger molecules, such as intracellular protein molecule phosphorylation / dephosphorylation, which in turn alters the internal cellular biochemistry, with consequent alterations in the activity of enzymes, ionic channels, actin / myosin locomotion systems and gene control proteins.

The most important cellular transduction mechanisms are

- receptor-tyrosine kinase pathway, activated by FGF, EGF, PDGF
- hedgehog pathway, activated by the different hedgehogs
- Smad pathway, activated by the TGF-β ligands
- Wnt / Frizzled pathway

Steroid receptors are either soluble cytosolic or nuclear proteins, and therefore require the ligands to be able to pass through the cell membrane, before binding to the receptor. Steroid receptors are thought to regulate the transcription of gene products such as proteins. The speed of action of the hormone is therefore dependant on the time taken to synthesis the protein, and thus is usually slow in onset.

3.2.6 How do signals affect differentiation / morphogenesis

Differentiation of a cell is dependant on the expression of different components of the DNA. Morphogenesis is equally complex, and involves the co-ordinated assembly to cells to build structures. Morphogenesis occurs through cellular movement, condensation, proliferation and death, and it is through alterations in these cellular activities that the signals affect morphogenesis. For example, the compaction stage during somite formation has been shown to co-incide with an up-regulation of the expression of surface adhesion molecules, and it maybe that, as discussed below, an extracellular signal is received, which in turn through the intra-cellular biochemical "machinery" results in an up regulation of the surface expression of the adhesion molecules. As a consequence of adhesion molecule expression, the cells bind together more closely, resulting in the observed cellular compaction[90].

3.3 SIGNALLING METHODS

Co-ordinate behaviour of many cells is essential if cells are to build the complex structures found in organisms. The co-ordination of the cells is dependant on intercellular signalling. Four principle methods of intercellular signalling have been experimentally identified:

- cell-cell direct contact
- cell-adhesion molecule
- extracellular matrix molecules
- growth factors

3.3.1 Cell-cell direct contact

Gap junctions between the cells allow dispersion of signalling molecules, usually peptides between cells. This method of communication is thought to be important during early blastomere formation but does not appear to have a major role in morphogenesis.

3.3.2 Cell-adhesion molecules

Many different adhesion molecules have been isolated. Two major classes exist: those dependant on calcium - the cadherins, and the others - cell adhesion molecules (CAMS). Expression of the molecules are the cell membrane is usually a consequence of an inductive signal, and control of cellular activity is therefore indirect. Expression of cell adhesion molecules can result in cell compaction as occurs in somitogenesis when N-CAM expression is increased, or can be involved in binding to constituent molecules within the extracellular matrix[91].

3.3.3 Extracellular matrix molecules and receptors

Many molecules have been found to be present in the ground substance or extracellular matrix. Examples include lamin and fibronectin in the basal lamina of epithelial cells, and collagen, proteoglycans, and glycoproteins. These molecules may interact with growth factors and thereby encode spatial or temporal information and influence cellular movement and / or migration. Molecules such as hyaluronic acid and collagens may take on structural roles. Hyaluronic acid swells when in contact with water and creates and maintains space between cells in the developing embryo[92].

Cells are often induced to express a receptor which binds to extracellular matrix molecules. The integrins are a group of membrane bound receptors, expression of which has been demonstrated to increase during gastrulation and is a component of the mechanism of the inward migration of cells through the primitive streak to create the mesoderm layer of cells[93].

3.3.4 Growth factors and receptors

A huge diversity of growth factors - small molecules usually peptides or glycoproteins - exists. These signalling molecules affect cellular differentiation, migration and may promote or reduce cellular growth. The

molecules may influence the cell secreting the molecule - autocrine - or locally surrounding cells - paracrine. Within any one family of growth factors or their receptors considerable diversity exists. In certain situations considerable overlap between different growth factors within the same family exists in activating a receptor. In other situations, however, highly specific interactions between a single growth factor and receptor are required for receptor activation to occur.

3.4 APOPTOSIS

Apoptosis is a terminal state of cell differentiation, resulting in cell death, which occurs without local inflammation or release of the cellular lysosomal contents, in contradistinction to cell death occurring as a result of necrosis. Apoptosis may occur in cell populations or individual cells. The apoptotic process was originally described in 1972 by Kerr[94]. Apoptotic figures can be recognised in histological sections by nuclear chromatin condensation and cell shrinkage / rounding which occurs or by the use of immuno-assay.

Apoptosis has been increasingly recognised to occur during embryonic development, and is important in the development of the digits and forearm bones. Neuroblasts which project to incorrect targets fail to receive appropriate neurotropic factors and undergo apoptosis. Experimental evidence from has suggested that apoptosis is the default state for all cells, survival of the cell only occurring in the presence of one or more specific growth factors. Whilst the opposite of a developmental mechanism, morphogenesis clearly is involved in development of structure.

3.5 THE ROLE OF HOX GENES IN MAMMALIAN DEVELOPMENT

The HOX genes play a major role in specification of positional identity in the embryonic anterior-posterior axis and are expressed in the developing nervous system, somites and limbs[33]. The HOX genes belong to a larger

group of genes known as homeobox genes. Homeobox genes encode a sequence of 183 base pairs coding for 61 amino acids at the C terminal end of the protein. The protein function as a transcription factor, and thereby controls expression of downstream genes encoding growth factors, expression of cell adhesion molecules and extracellular matrix, all of which are involved in embryonic morphogenesis.

The homeotic genes were initially discovered in *Drosophilia*, and in mammals are found clustered on four chromosomes. Each of the *Drosophilia* genes is represented in the mammalian genome, some genes have several representations on the different chromosomes and these are referred to as paralogous groups. Genes in the same paralogous groups, whilst possessing similar anterior-posterior expression domains have different dorso-ventral domains in the developing central nervous system. The genes are numbered 1 to 13 from cranial to caudal according to their position on the chromosome. Each gene is also expressed in order - known as co linearity - along the chromosome from the 3' to 5' end.

The expression domain of the Hox genes in the somites overlaps, and the combination of genes expressed at any one point on the AP axis is known as the Hox code. The Drosophila, murine and human Hox genes are illustrated in Figure 3-1. Disruption of the expression domain of the Hox genes results in an alteration of the vertebra phenotype, known as a homeotic transformation[44].

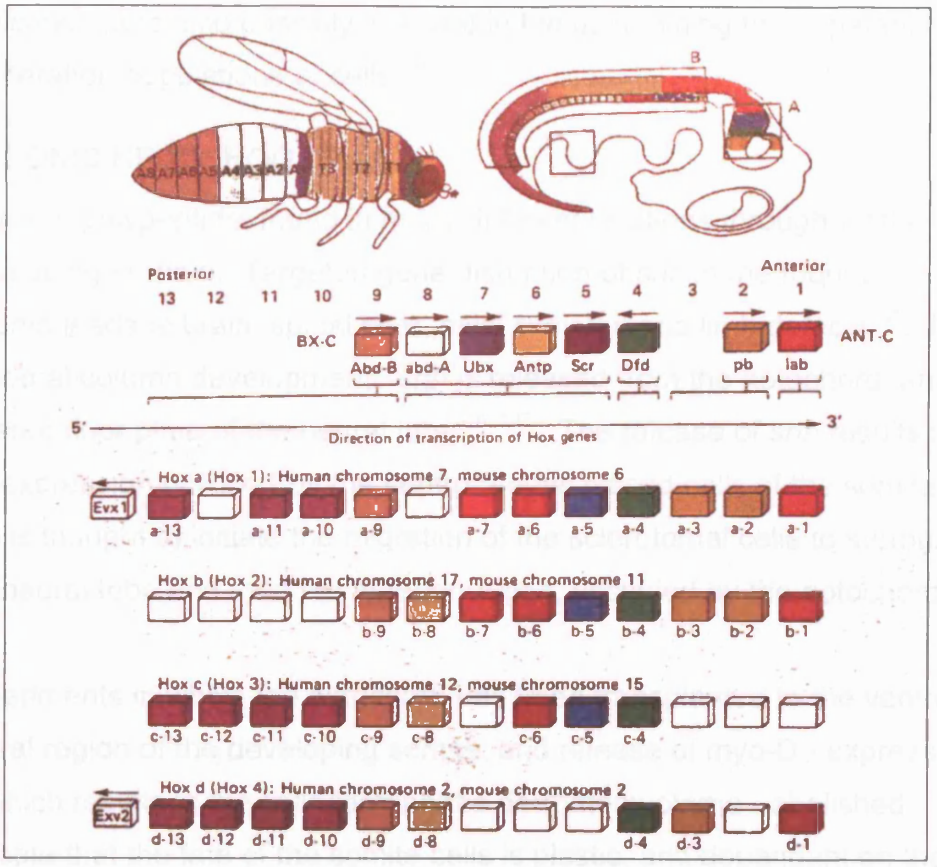

Figure 3-1: Drosophilla, murine and mammalian Hox genes

3.6 PAX GENES

Pax genes are also part of the family of genes that possessing a homeobox[33]. These genes also possess are region known as paired. In the formation of the vertebral column, the expression of Pax-1 is dependant on release of sonic hedgehog by the notochord[95,96]. Pax-1 is an initial marker for the sclerotomal cells, migrating from the ventro-medial aspect of the somite to surround the neural tube and notochord[97,98]. Expression of Pax-9 by the sclerotomal cells occurs later and is restricted to the more laterally placed cells around the neural tube[78,99]. Pax-1 expression in the vertebral body anlage is down regulated, however remains high in the location of the developing inter-vertebral disk. Pax-1 expression is also down regulated between the occipital somites, which fuse and ultimately form the occipital bone[34]. For these reasons, it has been hypothesised that in the development of the vertebral column, Pax-1 and Pax-9 are functioning as genes controlling cellular proliferation and

replication, and also possibly involved in the maintaining the separation of proliferation populations of cells[100].

3.7 SONIC HEDGEHOG (*SHH*)

Shh is a polypeptide, found in many different locations throughout the developing embryo. Targeted gene disruption of *shh* in the murine embryo leads to brain, spinal cord, axial skeleton and limb defects[101]. In vertebral column development, *shh* is released from the notochord, and anterior floor plate of the neural tube[102,103]. The release of *shh* results in the expression of Pax-1 by the ventro-medial placed cells of the somite, and is thought to initiate the migration of the sclerotomal cells to surround the neural tube and then the anterior region, occupied by the notochord.

Experiments in which the notochord has been transplanted to the ventro-lateral region of the developing somite, and release of myo-D - expression of which results in the cells forming the dermatomyotome - abolished indicate that the fate of the somite cells is plastic, and dependant on the diffusion of *shh*, the concentration of *shh* in the normal embryo being greater than myo-D[104].

3.8 SUMMARY

Morphogenesis is a co-ordinate process through which structures are built by individual cells acting in concert. Cells respond to multitude of environmental clues, including concentration gradients of morphogens and specific molecules in the extracellular matrix, which form a co-ordinate system. Cellular behaviour is governed by the cell position in the co-ordinate system, rather than by an intracellular "blueprint".

4 Models in developmental biology

A model is concept that simplifies and thereby enhances understanding of the process that it represents. The term model in developmental biological parlance covers a multitude of areas, ranging from simplified spatial representations of morphological processes, through animations constructed on graphics workstations, to test tube systems of developmental processes and mathematical systems that mimic cellular behaviour.

In this chapter, the models employed in developmental and molecular biology are discussed. Different models have been developed with different aims. Models formed from paper or wax aim to increase the understanding of spatial structure, and animations to increase understanding of how the spatial structure changes over time. Mathematical models exist to simulate the behaviour of the cells or biological system, and in some cases to attempt to predict the cause of an abnormality.

4.1 REPRESENTATIONS OF BIOLOGICAL DEVELOPMENT

This section discusses the development of models illustrating the spatial development of structures within the embryo. The aim of these models is to understand the spatial arrangement, and changes that occur in spatial arrangement during embryogenesis. Conventionally, embryos are sectioned in the axial, sagittal or coronal plane, and so the structures are visualised in a series of two dimensional slices, and a three dimensional appreciation of the embryonic structures is only obtained by mentally integrating the structures as visualised in the sliced embryo.

The mind model suffers from several disadvantages – it is difficult to handle, to rotate, scale and disassemble, and it can not be shared amongst co-workers. For these reasons, early developmental biologists created three dimensional models from wax and plaster. More modern materials have also been used to construct three dimensional representations, and include the use of plastic and cardboard.

With the advent of the high speed computer graphics work station, the construction of a virtual model of the embryo became possible. This technique allows the user to examine the model from any orientation, and additionally sophisticated techniques allow interactive slicing of the model in any plane, so the different layers of the embryo can be peeled back, in order to more fully understand the embryonic systems spatial arrangement.

More recently, several groups have been able to demonstrate the animated development of the embryo using a computer technique known as "morphing". This is a computer imaging technique whereby the is supplied with images of the developmental process at different stages. The user identifies equivalent points in each image, for instance components of the same vertebrae and the computer generates a series of images stepping from the earlier stage to the later stage. These images can then be animated and give the illusion of the actual developmental process. This technique has been used by the St Andrews group to reappraise cardiac development[17], and has also been employed by David etal to illustrate the development of the odontoid process, atlas and axis, and resolve a previous developmental controversy, by demonstrating the odontoid process chondrifies from the body of the axis, rather than comprising the body of the atlas[105].

Whilst these techniques are excellent aids to understanding the spatial structure of the embryo, and a sequence of models through time, or a computer animation through time is able to demonstrate how structures develop and integrate, models such as these do not explain the cellular

interactions and behaviour underlying the morphogenetic processes that occur in building the embryo, nor how abnormalities in these processes may lead to the creation of congenital abnormalities.

4.2 THEORETICAL BIOLOGY

4.2.1 The Turing Legacy

Alan Turing (1912-1954) was a Cambridge mathematician who played a major role in deciphering the German Enigma ciphers during the second world war. He subsequently investigated chemotaxis and published his work entitled *The Chemical Basis of Morphogenesis* in 1952[106]. Turing was fascinated by the apparent symmetries and patterns that exist in nature, and sought a mathematical explanation. Building on Waddingtons hypothesis of *evocators*, Turing described mathematically a system of two diffusible chemicals or morphogens - defined by Turing as a *form producer*, and somehow able to persuade tissue to develop along different lines than it would have otherwise done so. Turing defined the relationship between genes and morphogens such that *"genes catalyse production of morphogens, which in turn maybe catalytic. Eventually the chain leads to morphogens whose duties are not catalytic, but possess some other function, eg alteration in growth rate"*. In describing a system of two morphogens mathematically Turing assumed that the system was in steady state. Turing ignored the mechanical interactions such as masses, velocities of cell movement and forces between cells, and instead explored the way in which a steady state system could become unstable, and the resultant morphogen concentrations at different locations within the mass of tissue. Using a pair of standard diffusion equations for each morphogen X and Y, Turing was able to write

$$\left.\begin{aligned}\frac{dXr}{dt} &= f(X_r, Y_r) + \mu\left(X_{r+1} - 2X_r + X_{r-1}\right)\\ \frac{dYr}{dt} &= g(X_r, Y_r) + \nu\left(Y_{r+1} - 2Y_r + Y_{r-1}\right)\end{aligned}\right\} 1$$

where *X* and *Y* are the morphogens, *r* the distance from the source and *u* and *v* diffusion co-efficients.

Turing was then able to solve the equations for X_r and Y_r using the equations given below

$$X_r = h + \sum_{s=1}^{N} \left(A_s e^{P_s t} + B_s e^{P' s t} \right) \exp\left[\frac{2\pi \, irs}{N} \right]$$

$$Y_r = k + \sum_{s=1}^{N} \left(C_s e^{P_s t} + D_s e^{P' s t} \right) \exp\left[\frac{2\pi \, irs}{N} \right]$$

Exploring these equations, Turing found that when minor asymmetries or in homogeneities arose in the system, there were four possible patterns of morphogen distribution that could arise in both lines and arrays of cells:

1. a drift in the concentration of a morphogen within a cell, resulting in a dappled pattern;
2. oscillatory drift from homogeneity state;
3. drift from homogeneity in opposite directions in contiguous cells;
4. stationary wave patterns, increasing in amplitude with time.

Turing considered that pattern four was best represented in the biological world, and likened the formation of the standing waves to the development of *hydra*. The lack of high speed digital computers in Turings time restricted his exploration of the biological system described.

Bard and Lauder were able to utilise a high speed computer in the mid 1970s to more fully explore the Turing reaction diffusion system. Bard and Lauder divided the patterns occurring in embryos into those that are size–invariant, known as regulative systems, and those in which removal of part of the embryonic tissue results in a deficient adult – mosaic systems[107].

Investigation of a one dimensional system, using a row of cells, with two morphogens, Bard and Lauder found:

1. the number of peaks of morphogen concentration is proportional to the number of cells in the row.

2. if a row of sixty cells were cut in half, the resultant pattern remained unchanged from that occurring with a contiguous line of sixty cells.
3. the wavelength of the generated pattern is inversely proportional to the speed of the reaction.
4. These findings are compatible with a system able to form mosaic patterns, but are not size-invariant.

Using a two dimensional system, Bard and Lauder found, that using a narrow rectangle or cylinder, an unpredictable pattern of blotches or strips arose. Bard and Lauder considered the Turing model able to develop biological patterns, using realistic biological assumptions for the parameters, however, the systems were not thought reliable enough given the minor fluctuations resulting in different patterns.

Gierer and Meinhart also investigated the use of reaction-diffusion systems as positional mechanisms in developmental biology[108]. They developed two models, the first of which involved two morphogenetically active substances, known as the activator and inhibitor. The activator stimulated its own production (autocatalysis), and production of the inhibitor, whilst the inhibitor repressed formation of the activator. The activator and inhibitor were removed or decayed at a rate proportional to their concentration, and both substances diffused, the inhibitor more rapidly than the activator. A symmetry breaking event, ie a local in homogeneity such as a local increase in the concentration of the activator will result in the creation of a concentration gradient, and the activator will increase with a sharp concentration peak, whilst the concentration of the inhibitor will also increase, albeit with a somewhat shallower, but broader peak. As Slack has demonstrated, alteration of the field size reveals the concentration gradient is preserved to a large degree[109].

The second model developed by Gierer and Meinhardt also possessed the ability to generate repeating patterns. The model consists of two substances, whose synthesis is locally mutually exclusive, however activate one another at a distance, with a common repressor, the

synthesis of which is dependant on the concentration of both substances and which inhibits the production of both substances. Each substance *S* decays into a substance *s*, both of which are highly diffusible, and each of which activates the generation of the other substance of the pair. This has the end result that synthesis of each substance is locally mutually exclusive, and each substance activates itself at short range and the other substance at long range.

The difference between the two models is most apparent in two dimensional space. The first model produces a pattern of spots as shown in Figure 4-1 , the other a pattern of strips as shown in Figure 4-2.

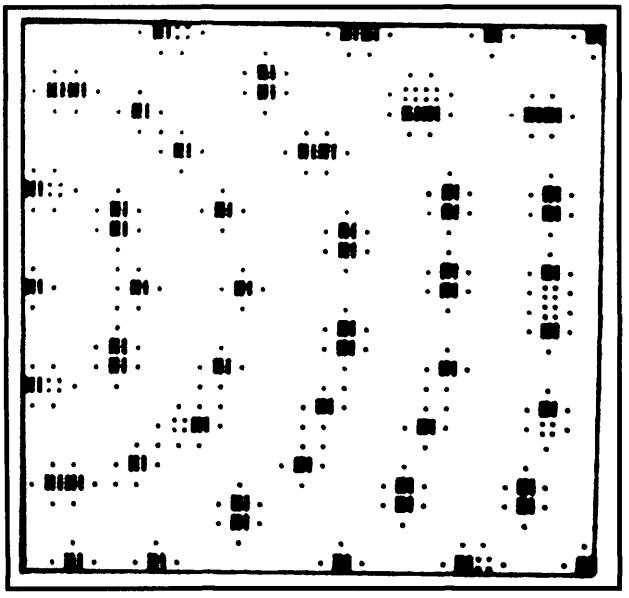

Figure 4-1:Pattern resulting from the first GM model

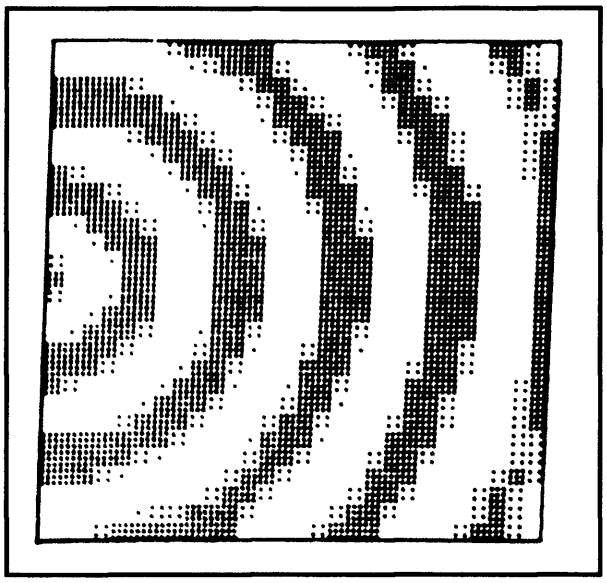

Figure 4-2:Pattern resulting from the second model

The patterns produced by the second model correlate well with the gene expression patterns seen in the generation of the segments and parasegments of *Drosophilia*[110], however, it is more difficult to relate these models to the form of primary segmentation that occurs in vertebrates.

4.3 CELLULAR AUTOMATA

"This is a technique which allows simulation of systems that numerically are too complex to represent mathematically by a series of simple rules that are easy to compute. Each cell or unit in the usually two dimensional simulation may have a series of states, and the rules within the system allow alteration of the state depending on the current state and state of the surrounding cells. A consequence of this is that the simulation is discrete in space, time and state. Biological simulations have been considered particularly suitable for cellular automata because there are few formal laws, such as exist in physics or mathematics, and the speed at which calculations can be performed enable a wide range of situations to be examined. Thus the simplified model can be useful in excluding certain mechanisms as unlikely to be those which occur in the real biology"[111].

In developmental biology, cellular automata systems have been used to model the creation of animal coat markings[112], and also the patterns found on shells[113]. Cellular automata systems have also been used to model the

relationship between ontologenetic changes and evolution[114]. More recently, a combination of cellular automata techniques – that is treating cells as discrete points, and the use of rules for cellular movement – in a continuous field of chemo attractant has been used to model the streaming of *Dictyostelium discoideum*. This approach has been successful in that the cells will form streams under biologically realistic conditions[73].

4.4 BIOLOGICAL MODELS OF ABNORMAL DEVELOPMENT

A number of strains of animals, usually mice and zebra fish exist, in which there are known or thought to be genetic mutations affecting the development of the axial and appendicular skeletons. These mutants were initially catalogued by Grüneberg[32], who classified them into several groups including (i) systemic disorders of the membranous skeleton, (ii) systemic disorders of the cartilaginous skeleton, (iii) disorders of the notochord, (iv) disorders of the unsegmented paraxial mesoderm, (v) disorders of segmentation and (vi) disorders of sclerotome differentiation.

The genetic mutations which affect vertebral column development have been catalogued by Dietrich and Kessel[115] and are listed in Table 4-1.

Process	Phenotype	Murine mutant	Gene
Gastrulation	Complex, includes vertebral agenesis	Brachyury, curtailed	T
Dorsoventral specification	Vertebral agenesis	truncate, Danforths short tail, Pintail, *shh -/-*	? ? ? *shh*
Somitogenesis	half and block vertebrae	pudgy	?
Sclerotome condensation	agenesis or malformation of corresponding elements	undulated	Pax-1
Neural tube closure	agenesis of dorsal neural arch	splotch	Pax-3
Axial specification	homeotic transformation	rachiterata Hox mutants	? Hox genes

Mesenchyme condensation, bone fracture repair	complex phenotype	short ear	BMP-5

Table 4-1: List of genetic mutations affecting murine vertebral column development

It is important to note that not all of the abnormalities have an associated gene – this maybe because a genomic abnormality does not exist, but the malformation is a result of, for instance, abnormalities of the extracellular matrix, intercellular binding, cell position, or the result of an environmental teratogen. Alternatively, the gene responsible for the phenotype might not yet have been discovered.

4.5 SUMMARY

Models are a useful tool for investigating the often complex processes and concepts in modern-day developmental biology. A variety of models have been developed, dependant on the particular quality under investigation. The use of modern computers has allowed more complex and sophisticated simulations of biological processes to be undertaken. The models can be used to undertake experiments that can not be performed in vivo, such as the work described in this thesis.

5 Molecular biology of subaxial cervical vertebra development

The purpose of this chapter is to review the current experimental literature relating to the formation of the vertebral body cellular condensation. An understanding of the process of somite formation, partitioning and sclerotome migration is important to place into context the experiments performed and reported in this thesis. In order to validate the virtual model described in Chapter 6, it is necessary to provide a detailed account of this stage of embryonic development.

The process of gastrulation creates the mesoderm which is initially unsegmented. The vertebrae develop from the paraxial region of the unsegmented mesoderm, which can be seen to condense into somites in a stepwise manner in a rostal to caudal direction. Each somite is then subdivided under the posterior influence of the surface ectoderm and dorsal neural tube into a dermatomyotome and anterior influence of the neural tube floor plate and notochord to form the sclerotome. The sclerotomal cells disaggregate, in contra-distinction to the dermatomyotome, and migrate medially to surround the notochord and neural tube to form a segmented prevertebral mesenchymal condensation. Each pre-vertebral condensation subsequent undergoes chondrification and later ossification forming the vertebral body and lateral elements. Paradoxically, the final phenotype of each vertebra has been demonstrated to be specified at the time of gastrulation[46]. Neural arch / spinous process formation is under the control of the Msx / BMP4 pathway[37,116,117].

Formation of a normal vertebra requires the paraxial mesoderm on each side of the neural tube and notochord to segment synchronously forming approximately symmetrical somites. Maturation of each somite is then controlled by inducers from the notochord / floor plate complex and surface ectoderm. This involves the co-ordinate interaction between the developmental processes regulating segmentation and midline inducer pathways. The process can be divided into the following stages, each of which will be discussed in greater detail below.

- formation of the paraxial mesoderm
- formation of the somite
- partitioning of the somite and sclerotome formation
- sclerotome migration and condensation
- chondrification / ossification

5.1 MOUSE DEVELOPMENTAL STAGES

Development of the embryo and the formation of new structures occurs continuously, however for the purpose of comparison between different organisms and species, development of organisms is usually said to take place in stages. Several systems of staged development exist for mouse development including those of Hamburger and Hamilton[118] and Theiler[119]. Human development is usually staged using the Carnegie system[120]. The tables in Appendix A list the main human and murine developmental stages.

5.2 FORMATION OF THE PARAXIAL MESODERM

Epiblast cells migrate through the primitive streak to form a new germ cell layer – the mesoderm. The mesoderm subsequently condenses either side of the notochord and neural tube to form paraxial mesoderm. Laterally, the mesoderm gives rise to the body wall, whilst a third category of mesoderm, placed between the lateral and medial – the intermediate mesoderm – gives rise to the urogenital system.

Fate mapping has allowed identification of the cell population destined to form the paraxial mesoderm, and it appears that the allocation of the

paraxial mesodermal cells to their particular anterior - posterior identity ie vertebral phenotype takes place at during the process of gastrulation[46].

5.3 FORMATION OF THE SOMITE

Two processes appear to take place concurrently during somite formation (i) specification of the developmental unit which results in the process of segmentation of the paraxial mesoderm, and (ii) epithelisation prior to formation of the somite

In classical chick embryological studies, the paraxial mesoderm is seen to condense in a rostal-caudal manner at approximately 90 minute intervals to form somites symmetrically either side of the neural tube, whilst new mesodermal cells enter the paraxial compartment posteriorly as a consequence of gastrulation[33]. Following cellular compaction, the somites subsequently epithelialise and form a central somitocoele[121]. The formed somites then partition into the dermatomytome and sclerotome, whilst new somites are forming caudally from the unsegmented paraxial mesoderm.

5.3.1 Segmentation and generation of anterior-posterior polarity

Segmentation refers to the generation of an individual developmental unit, of which the somite is the product, and the sclerotome and dermatomyotomes develop from. Anterior-posterior (A/P) polarity refers to the subdivision of the developmental unit into cranial and caudal regions.

There are well described differences between the caudal and cranial half of each somite which arise during somitogenesis[122]. Using light microscopy, the cranial half of the somite is noted to have a dense and compact cellularity compared to the loosely arranged cells in the caudal half[33]. Peanut lectin binding molecules, chondroitin sulphate proteoglycans T-cadherin and ephrins are all preferentially expressed in the caudal half of the somite[123].

The differential expression is responsible for the maintenance of boundaries between the adjacent somites, and prevents unlike halves of

somites mixing. If "like" somite halves are transplanted to be next to each other, extensive mixing of the cell populations occurs[124]. Additionally transplantation of unlike halves generates a boundary between the two. Many factors are also expressed prior to the condensation of the paraxial mesoderm at the anterior edge of the segmental plate[125].

Segmented patterns of expression of many genes within the somite and in presomitic units within the anterior segmental plate has been described, including Notch, Delta homologues, scleraxis, Meso-1, FGFR-1[125,126]. The segmental expression of these genes is incompletely understood, but appears to be co-ordinating distinct processes necessary for normal somitic development – segmentation and generation of A/P polarity.

Experimental evidence suggests that the segmentation process requires a molecular oscillator, as hypothesised by Cooke and Zeeman in 1976. From the initial demonstration of pulsed expression of mRNA of *c-hairy* in the presomitic mesoderm[127] more details of the molecular oscillator have become apparent, in particular the central role of the *notch-delta* pathway as reviewed by Pourquie[128]. Several transcription factors of the Hairy / Enhancer of Split (HES) family, *Lunatic fringe* and *Delta-C* have been demonstrated to exhibit cyclical expression. Current evidence suggests that *notch* activation causes the expression of transcriptional repressors of the HES family and other cyclic genes. An additional gene *Axin2*, part of the *Wnt* pathway has also been demonstrated to possess cyclical expression. Mutation of the *Wnt* pathway results in disruption of the expression of *Lunatic fringe* and *axin2* suggesting that *Wnt* acts upstream of the *notch* pathway, although the details are uncertain.

Notch is a transmembrane protein which binds to transmembrane Delta-Serrate-Lag-2 ligands on adjacent cells, hence only has influence on cells that are adjacent. Ligand binding releases the intracellular notch domain, which associates with RBP-Jκ protein, and turns on the expression of downstream genes including c-hairy1. Ligand-notch affinity can be

modulated by Fringe performing post-translational modification of the extra cellular notch domain[129].

Dll1 and *Dll3* – *delta* homologues – have been demonstrated in subsets of cells adjacent to the border in either half of the somite, suggesting a role in boundary formation and or maintenance. Kusumi etal[130] have demonstrated that the murine mutant *pudgy* is caused by loss of function of *Dll3*. In pudgy mutants the rostal and caudal sclerotome formation is disrupted[131], and this implies that boundary formation / maintenance and A/P polarity mechanisms are linked[132].

5.3.2 Epithelialisation

Concurrent with segmentation, under the control of the notch pathway, the mesenchymal cells in each developmental unit undergo transition to an epithelial ball structure. The subsequent partial epithelial to mesenchymal transition results in the regionalisation of the somite into the sclerotome and dermatomyotome[133]. *Paraxis*, a bHLH transcription factor, is initially expressed in the rostal unsegmented mesoderm, and subsequently in the epithelial ball. Mutation of the paraxis gene abolishes somite formation, whilst formation of other segmented structures such as the peripheral nervous system occurs normally. Restriction of the *ephrin-B2* and *Dll1* to the caudal sclerotome is lost in the mutant, as is that of *Notch1*[134].

Lack of *paraxis* transcription in mice results in somites that do not epithelialise[135]. However, normal segmentation was observed and the normal sclerotome (*Pax-1 / 9, scleraxis*) and myotome (*myf-5*, *myogenin*) markers were observed, although the pattern of expression observed was not normal[125]. Somites do not form in *Pax-1* null mutants, although the segmented pattern of the mesoderm is formed and the segmented form of the peripheral nervous system is established.

In mice with mutant *N-cadherin*, disrupted epithelial formation of the somites occurs and it is interesting to speculate on whether a *N-cadherin* is a downstream target of paraxis[136].

5.4 PARTITIONING OF THE SOMITE AND SCLEROTOME FORMATION

Following creation of the somite, it is patterned or partitioned into the sclerotome, which consists of the cells that will ultimately form the ossified vertebral column and the dermatomyotome which will form the body wall skin and musculature.

The current understanding of somite partitioning is based on inductive signals for different parts of the somite locale regulating the local expression of different molecular markers by the different parts of the somite. The pre-sclerotome region expresses *Pax-1*, whilst the pre-dermatomyotome region expresses *Myf5* and *MyoD*. Prior to partitioning, the whole somite initially expresses *Pax-3*, however ventral somitic expression decreases following the development of the sclerotome, whilst that in the dermatomyotome is retained[137,138].

A cascade of transcriptional regulators appear to control the expression of *Myf5* and *MyoD* in the myotome and *Pax-1* in the sclerotome. The major regulators are:

- *Sonic hedgehog*, released from the notochord and anterior neural tube
- *BMP4*, released from the lateral plate
- *Wnt 1/7a*, released from the dorsal neural tube and surface ectoderm

A complex regulatory pathway controls the expression and allocation of myogenital precursor cells to the epaxial and hypaxial compartments, and will not be discussed further.

5.4.1 Development of the sclerotome

That the axial structures of the notochord and neural tube are necessary for the development of the chondrogenic vertebral column or somite chondrogenesis has been known since Hoadleys experiments in 1925[139]. Prior to the advent of molecular biology, many experiments were

performed to assess the role of the notochord and neural tube on somite chondrogenesis, and subsequently in an attempt to elucidate the inducer. From the in vitro work the concept of a diffusible or secreted inducer arose[140].

Advances in molecular biology have shown that the gene *Pax-1* is expressed in a segmented pattern in the ventral region of the somite. This is the region of the somite which gives rise to the sclerotomal cells[98]. *Pax-1* was identified in mice by homology to the Drosophilia segmentation gene *gooseberry*. Experimental work has subsequently demonstrated *Pax-1* is initially expressed in the sclerotomal cells, but becomes progressively restricted in expression to the caudal cells of the somite and subsequently to the region ultimately destined to form the intervertebral disk[78,98,141,142]. There is a difference in expression between the avian and murine embryos as *Pax-1* mRNA is detected in the chondrocytes of immature vertebral bodies[140,142,142]. Important confirmatory evidence of the role of *Pax-1* in the development of the sclerotome was found when the murine mutant *undulated*, which has deficient sclerotome formation was found to have a point mutation in the *Pax-1* gene[141,143,144].

Pax-9 was isolated through homology with *Pax-1*[78,142]. Whilst expression of *Pax-9* mRNA is similar to that of *Pax-1*, *Pax-1* is initially expressed in the ventromedial aspect of the somite, compared with *Pax-9* which is initially highest in the dorsolateral region of the somite, before coming restricted to the caudal half of the sclerotome and ultimately the intervertebral disk.

The identification of *Pax-1* [98] allowed experimental workers to initially determine that expression of *Pax-1* required the presence of a long range diffusible factor secreted by the notochord / floor plate of the neural tube. Subsequently Fan and Tessier-Lavigne[87] determined this factor to be *sonic hedgehog (shh)*. Experimental work has demonstrated *shh* to be the major factor in the initiation of the expression of *Pax-1* by the sclerotome. However, Chiang[101] demonstrated using *shh* knockout mice that the

sclerotome initially forms normally, but that the expression of sclerotome is smaller in size and the level of *Pax-1* expression is correspondingly reduced. McMahon[145] demonstrated the mouse Noggin gene is expressed at the time of sclerotome formation, and homozygous Noggin mutants demonstrate delayed expression of *Pax-1*. It appears that normal expression of *Pax-1* requires synergy between *shh* and *Noggin*.

5.5 SCLEROTOME MIGRATION AND CONDENSATION

A condensation of sclerotomal cells around the notochord/neural tube is formed by the migration of sclerotomal cells medially following down regulation of *N-cadherin*. The cellular migration gives rise to the perinotochordal tube described by Williams[146] and Christ and Wilting[147]. The mechanism and factors controlling the migration are not well understood.

Newgreen investigated the migration of sclerotomal cells in the perinotochordal space. He took a section of notochord / neural tube with sclerotomal cells and placed it at right angles to a more caudal section of the notochord / neural tube on either a collagen gel or extra cellular matrix (ECM) of chick embryo cells[148]. The second more caudal notochord / neural tube complex did not have sclerotomal cells attached because it was obtained from a more caudal position in the embryo. Sclerotomal cells cultured on the collagen gel were seen to heap up against the second notochord / neural tube complex, whilst those cultured on the chick ECM maintained an even anterior migration boundary.

Newgreen also investigated the in vivo stages of migration of the sclerotome to surround the notochord[148]. He described

1) Following segmentation, outline of the ventral part of the somite adjacent to the notochord is increasingly broken by long filopodia.
2) Tongues of loosely arranged cells stretched ventrally from the body of the somite along the medial walls of the paired aorta and contacted the endoderm. Cells fused with the contra lateral

sclerotome around the notochord with preservation of the perinotochordal space.

3) A clear cell free space persisted around the notochord initially, which subsequently narrowed and became densely and evenly occupied by cells.

From the results of these experiments and other work reported earlier[149,150], it was concluded that

1) Sclerotomal cells are able to migrate and adhere to collagen and fibronectin gels.
2) The distribution of the ECM may influence sclerotome morphogenesis.

It has been speculated that the sclerotomal cells may migrate up a concentration gradient from the somite toward the notochord / neural tube[151], although one has not yet been demonstrated. However, it has been demonstrated that the notochordal sheath is metabolically active, and contains many collagens, proteoglycans and glycoproteins[152,153]. Smits and Lefebvre[154] have demonstrated absence of *Sox5* and *Sox6* activity results in down regulation of extra cellular matrix genes surrounding the notochord, including collagen 2, *aggrecan* and *perlecan*. However, sclerotome cell migration was not inhibited.

5.5.1 Interaction between Pax-1 and Pax-9

The expression of *Pax-1* precedes that of *Pax-9*. Pax-1 expression is initially found throughout the sclerotome, and later is maximal in the posterior ventromedial sclerotomal compartment[78]. *Pax-9* however, is maximal in the posterior ventrolateral region of the sclerotome.

5.6 CHONDRIFICATION AND OSSIFICATION

Recent experimental evidence has demonstrated *Bapx1* gene is essential for the formation of the axial skeleton and of spleen[155]. Initiation of chondrogenesis in the notochordal condensation is under the control of the *Bapx1* gene.

Analysis of the role of *Bapx1* in murine embryos has demonstrated that *Bapx1* is expressed in vertebral pre-cartilaginous condensations that will undergo endochondral ossification, and expression of the gene is necessary for the transition from prechondroblast to chondrocyte in mesenchymal cells adjacent to the notochord[156]. Subsequently Rodrigo etal[157] have demonstrated that *Bapx1* expression is directly regulated by *Pax-1* and *Pax-9*.

Bapx1 has homology to the *Drosophilia bagpipe* gene, a major determinant of mesodermal differentiation[158]. Expression studies have demonstrated that *Bapx1* is expressed in the splanchnic mesoderm and the sclerotomal component of the somite, and subsequently the migrating sclerotome which forms the notochordal cluster, and subsequently in all cartilaginous condensations fated to undergo endochondral ossification[159]. Targeted mutations of the *Bapx1* gene in mice demonstrated a phenotype without the vertebral centra and intervertebral disk. The appearance of the lateral vertebra was normal[155,156]. Expression of late markers of sclerotomal development such *Pax-1* and *Gli2* in the *Bapx1 -/-* mutant were normal, as was the expression of earlier patterning markers. Expression of the *alpha1 (II) collagen* gene was missing the ventromedial aspect of the vertebra. *Pax-1* and *Pax-9* were confirmed to act as direct transcriptional regulators of *Bapx1* by Rodrigo etal[157].

This work is in accordance with that performed by Zeng etal[160] which demonstrated that forced expression of *Nkx3.2* promotes axial chondrogenesis by promoting the expression of *Sox9* in the presence of BMP signals. Additionally, *Sox9* and *Nkx3.2* are mutual inducers in the presence of BMP signals. Zeng and colleagues have suggested that *shh* and BMP act to establish a positive regulatory *Nkx3.2 / Sox9* loop in which *Sox9* subsequently initiates chondrocyte differentiation[160].

5.7 SUMMARY

Formation of the somite and its subsequent division into the sclerotome and dermatomyotome requires the co-ordinate action of several complex

genetic processes. The normal consequence of these processes is progressive localisation of *Pax-1* expression into the caudal ventromedial region of each somite[97].

6 Theoretical model

The work presented in this chapter is based on a theoretical formulation of the developmental processes taking place during the morphogenesis of the vertebral column which have been modelled using a computer. In this work, the model simulates the stage of development from formation of the sclerotome to development of the pre-vertebral cellular condensation. As discussed earlier in Chapter 5, there is a certain body of experimental evidence which suggests that malsegmentation of the paraxial mesoderm leading to irregular somite formation and consequent irregular sclerotome formation is a cause of congenital vertebral abnormalities. The theoretical model has been constructed to model normal development and to investigate how altering the model (simulating mutations) can generate the types of abnormalities seen in congenital birth defects of the vertebral column, as previously discussed in Chapter 2.

This chapter describes the components of the theoretical model, and the computer software, hardware and display techniques used to visualise the model during simulation.

6.1 COMPUTER HARDWARE

Several different computer systems were used during the course of this work. Each system was based on the Intel Pentium processor and had an integral hard disk drive to store results and programs, and high resolution graphics display for visualisation of results. A typical machine configuration would be an Intel Pentium III processor 300 MHz clock speed, 40 Gbytes of hard disk storage, 128 Mbytes of RAM and a high

resolution graphics adaptor card, usually 1024 x 768 pixels at 32 bits per pixel.

6.2 COMPUTER SOFTWARE

6.2.1 Operating system and programming language

The C++ programming language, as described by Stroustrup[161] was used to develop the project software. Initial development employed the Redhat Linux operating system, running Motif on X-Windows and OpenGL graphics. However, development was switched to a Microsoft Windows NT platform using Microsoft Visual C++ version 5 with the OpenGL library in August 1997 because of the complexity of the Motif graphics user interface. Current development and simulations employ Windows 2000 and Visual C++ version 6.

6.2.2 Graphics extensions

Display of the results in three dimensions is a key component of this work. For this reason, the OpenGL graphics library was used to provide a "ready-made" three dimensional rendering library. This is a fast library which provides three dimensional low level graphics primitives, and allowed maximal resources to be concentrated on the thesis work.

6.3 METHODS OF DISPLAY

6.3.1 Three dimensional sphere view

This was the standard view used in development and when running simulations. A sphere is placed at the location of each cell within the simulation. The colour of the sphere is dependant on the type of the cell represented. The resultant model was three dimensional and was viewed on the computer monitor in a simulated three dimensions (actually in two dimensions) and could be rotated and translated in three dimensions. Essentially this view displays an implicit surface, and therefore surface detail and inter-relationships are well shown and easily assessed, however the internal structure of the objects displayed is not appreciated. A typical view is illustrated in Figure 6-1. In embryo orientation, this view is a

simulated ventral view, that is the neural tube lies furthest from the observer, with the notochord in front, and the sclerotomal cells migrate anteriorly, that is out of the screen or page to surround the anterior region of the neural tube and notochord.

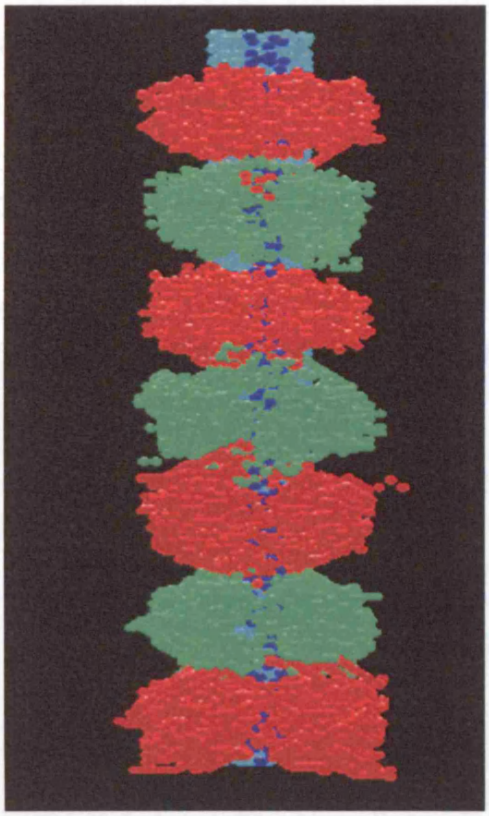

Figure 6-1: Three dimensional sphere view.

The notochord is in blue, the neural tube behind the notochord in cyan. Either side of the neural tube / notochord are sclerotomal cells in alternating red and green which reflects their origin from adjacent somites. The alternation of the colours allows determination of cellular mixing between adjacent somites.

The three dimensional sphere view was the "work horse" view and used during development, for creation of the animations and for general assessment of the morphology of the shape of the somite derivatives. The three dimensional surface viewed aided this task, particularly when display of the fixed central structures (neural tube / notochord complex) was turned off.

6.3.2 Three dimensional volume rendered view

This view was created by using the marching cubes algorithm[162] create an implicit surface[163]. Transparency could then be assigned to the somite derived structures, and using alpha (transparency) blending it then is possible "see through" the sclerotome groups of cells, and determine how these cells relate to the notochord / neural tube complex. This is demonstrated in Figure 6-2 and a limited animation is given on the animation CDROM. The sclerotome cells are in red and green, the neural tube in cyan and the notochord in blue.

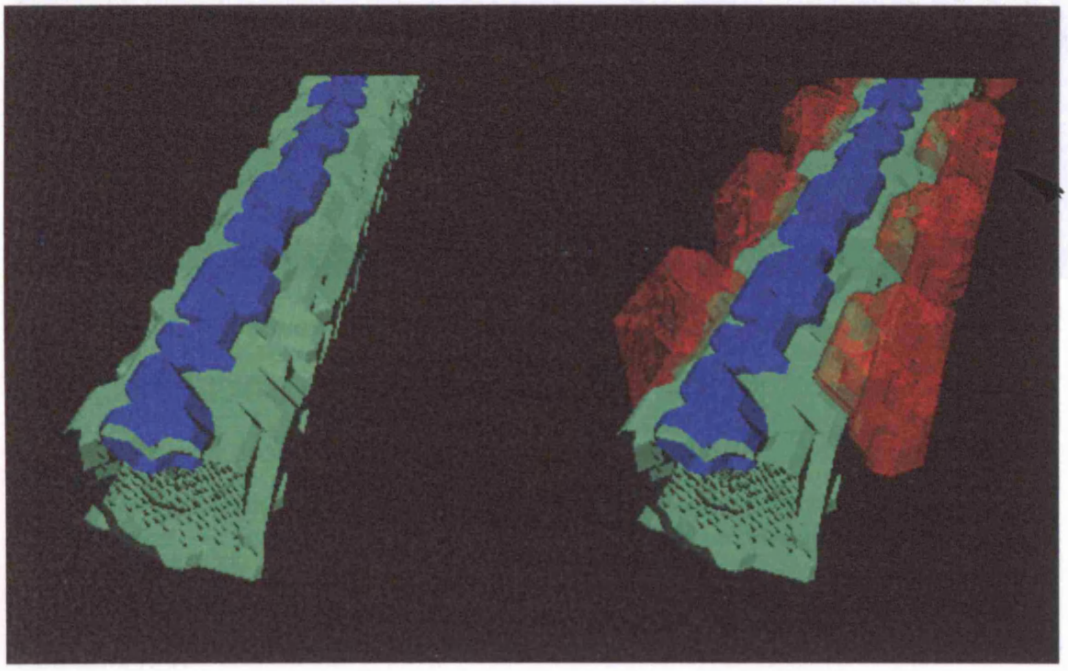

Figure 6-2: Three dimensional volume rendered view.

6.3.3 Two dimensional orthogonal views

These images were generated using the *ortho* viewer. This viewer allowed the user to select slices through the simulated model in three orthogonal planes. Using this system, the internal structure of each object was clearly apparent, and also the shape of the surface at that particular slice, however, appreciation of the overall morphology was extremely limited. A typical example of the output of the *ortho* viewer is given in Figure 6-3. The YZ plane is in the top left of the image, the XY in the top right and the XZ in the bottom right. The white dotted – dashed lines

either side of the model indicate the position of the orthogonal plane for each image. The orthogonal viewer was most useful for examining the internal structure of each object.

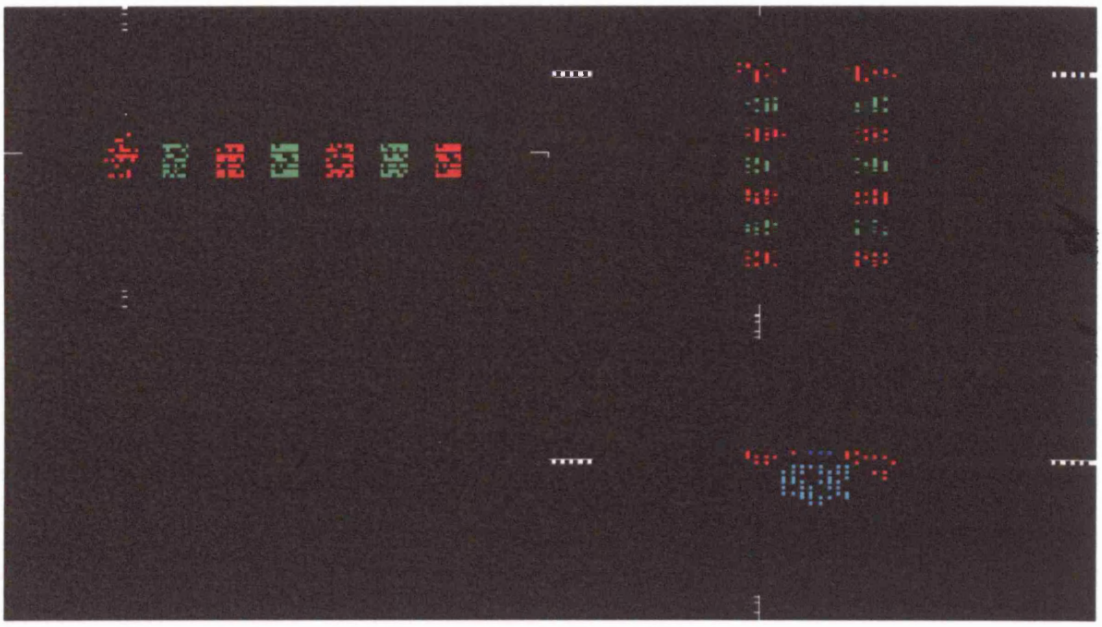

Figure 6-3: Two dimensional orthogonal views

6.4 COMPONENTS OF THE THEORETICAL MODEL

The theoretical model has the following components

- virtual world in which the simulation occurs and the cells reside
- virtual cells which perform the simulation
- secretion and diffusion of a morphogen to which the cells respond.

6.4.1 Virtual world

This is a computer array, or in mathematical terminology a matrix. The size of the array is specified by the user at the start of the simulation. Each location in the array has a size defined at 10 microns by 10 microns by 10 microns. This allows each location to accommodate one mesenchymal cell. Each location in the array is allowed to contain only one cell at any time, and a single cell can not be in more than one location at any time ie the cell can not overlap into two adjacent locations.

The computer array records whether each location is occupied, and if so the index number of the cell occupying the location. The index number of the cell is an array offset for the computer array holding the complete list of all cells active in the simulation. Each entry into this array contains the properties of the individual cell.

6.4.2 Morphogen secretion and diffusion algorithm

One of the cell properties allowed in the simulation is the ability to secrete a morphogen, which other cells are able to detect and migrate up a concentration gradient of the morphogen using the process of chemotaxis.

6.4.3 Morphogen secretion

The simulator iteratively determines which of the cells in the simulator are morphogen secretors. At every location where a morphogen secretor was present, the current morphogen concentration was increased by the value of the secretion constant, according to (1)

$$h_{x,y,z} = H_{x,y,z} + k_s \quad (1)$$

where $h_{x,y,z}$ is the new morphogen concentration, $H_{x,y,z}$ the current concentration at x,y,z and k_s the secretion constant.

6.4.4 Morphogen diffusion

Diffusion was first considered on a mathematical basis by Fick in 1855 who modified the heat transfer equations derived by Fourier in 1822[164]. The mathematical theory of diffusion in isotropic substance in one dimension is based on the assumption that the rate of transfer of diffusing substance through unit area of a section is proportional to the concentration gradient measured normal to the section, or

$$F = -D\frac{\partial C}{\partial x} \quad (2)$$

where F is the rate of transfer, C the concentration of the diffusing substance, x the linear dimension and D the diffusion constant. This is Ficks first law of diffusion.

Considering a cubic volume, (2) can be restated as a differential equation (3),

$$\frac{\partial C}{\partial t} = D\frac{\partial^2 C}{\partial x^2} \quad (3)$$

in one dimension, using the previous symbols.

Using a plane source, the solution to (3) is

$$C = \frac{A}{t^{\frac{1}{2}}}\exp(-x^2/4Dt) \quad (4)$$

in one dimension, using the previous symbols. However, it is computationally cheaper, instead of calculating (4) in three dimensions, for each morphogen source, for each cell in the simulation, to calculate diffusion of the morphogen throughout the virtual world, for each cycle of the simulation. Morphogen diffusion was therefore calculated as a two stage process. In the first stage, morphogen secretion was performed as detailed above. In the second stage, diffusion in three dimensions through the virtual world was considered by using the Fickian diffusion principle stated in three dimensions.

Using (1), and extrapolating to three dimensions, ie for 26 neighbours, the morphogen flux into or out of each location can be calculated for every location in the virtual world (personal communication, P V Thorogood, 1997)[108].

6.4.5 Virtual cells

The virtual cells reside in a three dimensional computer array (the virtual world), and have free movement within this array. The cells have the following conditions imposed

- the cells are not allowed to move off the array
- only one cell maybe in any one location of the array at one time

Each cell potentially has the basic properties listed in Table 6-1.

Property	Description

replication	ability to replicate and produce two identical cells
morphogen secretion	ability to secrete morphogen
movement: chemotaxis	migrates up a morphogen concentration gradient
movement: random	moves randomly
time that cell starts activity	cell unresponsive before start time
time that cell stops activity	cell unresponsive after end time

Table 6-1: Properties of each cell in simulation

Each cells properties are defined by the dataset loaded into the simulator program at the start of every simulation, as discussed in the Chapter 7. Each cell also had a type, which controlled the colour with which it was displayed in the simulation programs.

6.4.6 Vert programming language (VPL)

The simulator program vert was itself programmed prior to each simulation using a rudimentary programming language. This allowed greater versatility of the simulation scenarios that could be performed.

The commands available to program the simulator are listed in Table 6-2, with a description of each command.

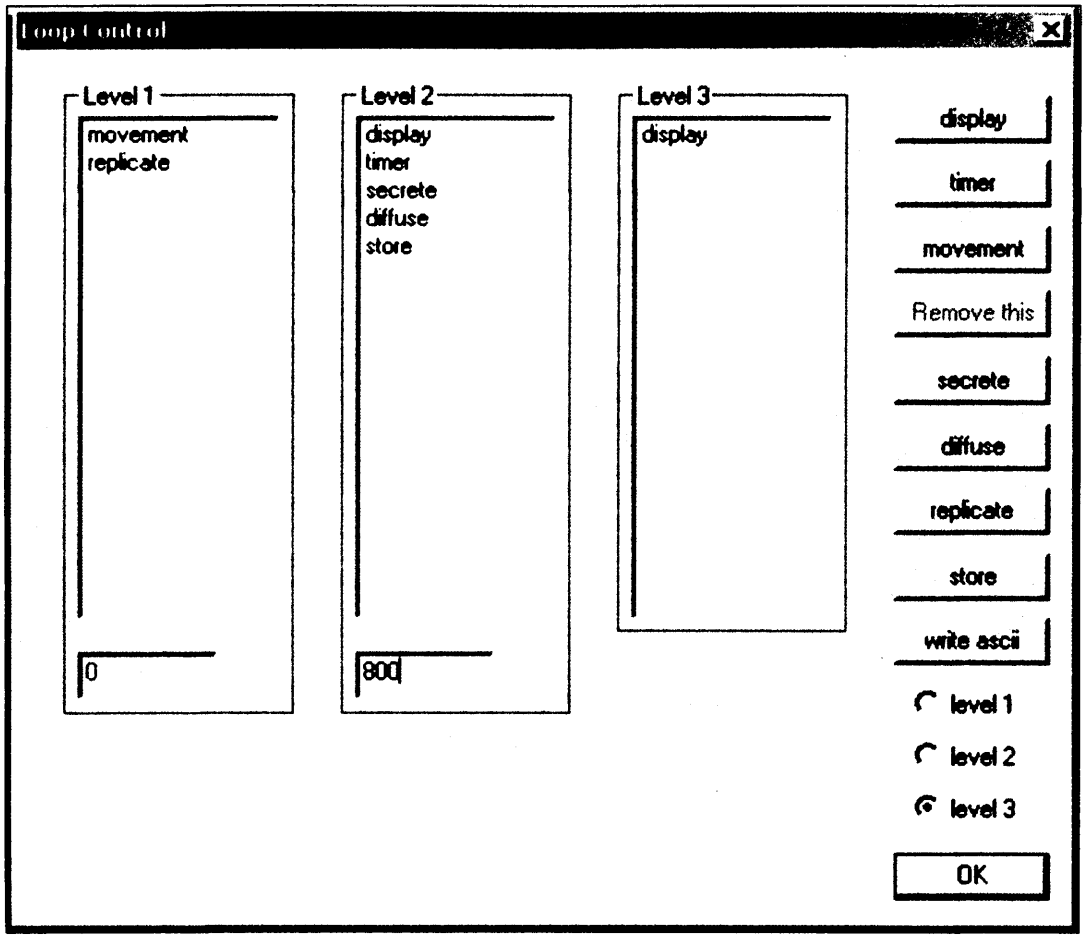

Figure 6-4: dialog box for VPL in simulator program

command	description
display	displays the position of each cell on the screen
timer	increments the simulation timer by one
movement	randomly selects a cell to move
secrete	causes all cells that are able to secrete morphogen to do so
diffuse	causes the morphogen to diffuse
replicate	randomly selects a cell to replicate
store	writes a copy of the screen image to disk for later analysis
write ascii	writes the current position of all cells for later analysis

Table 6-2: vert programming language commands

Figure 6-4 illustrates the dialog box used in vert to enter the program. There are three levels of nested program loops named Level 1, Level 2 and Level 3 at which program commands can be entered.

6.4.7 Control of the simulation

Control of the VPL simulation program is as shown in Figure 6-5. To start the VPL simulation, control is passed from the simulator program to the VPL control loop. Following completion of the VPL simulation program, control is passed back to the simulator program.

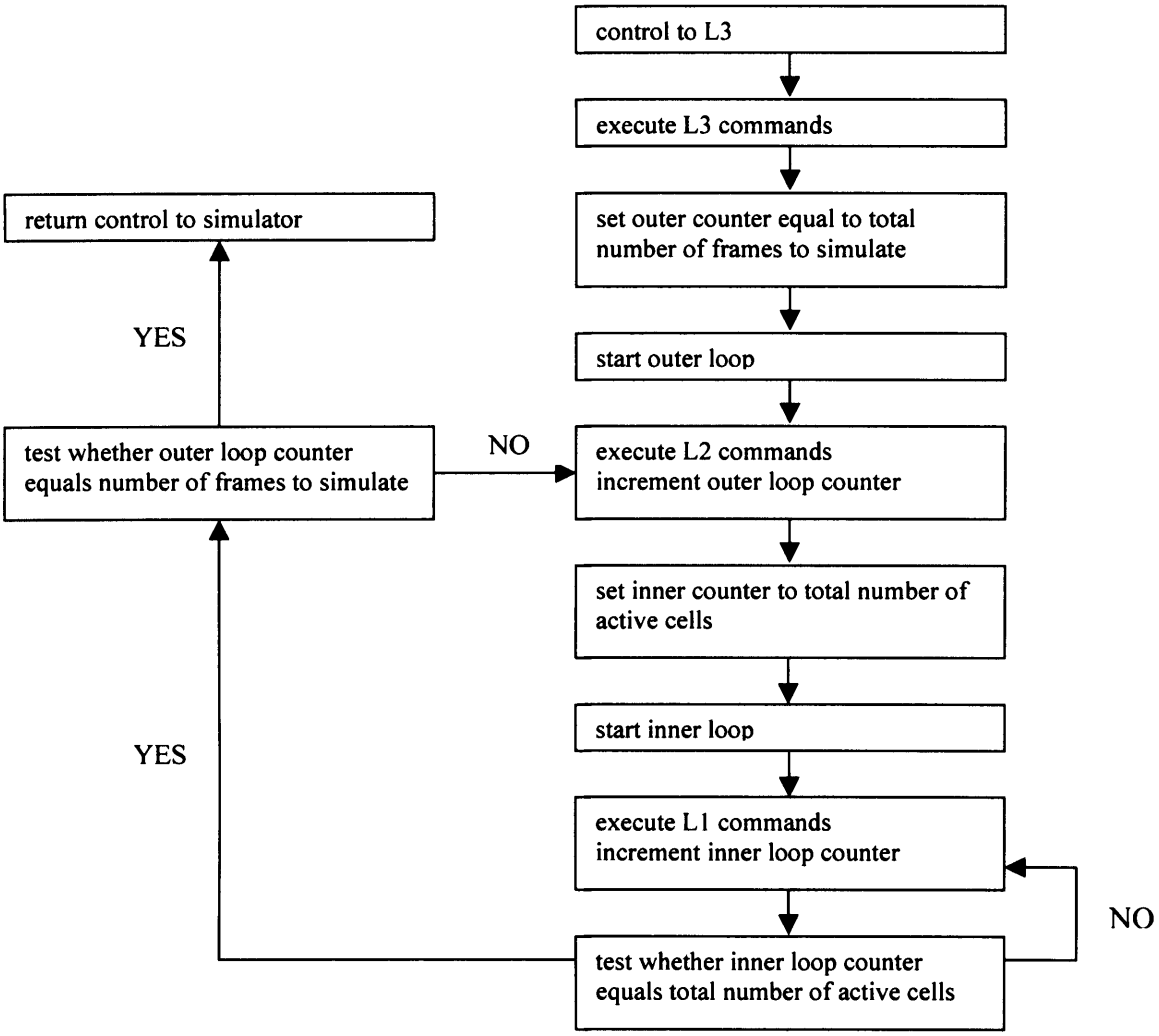

Figure 6-5: VPL control loop. (L3: Level 3, L2: Level 2, L1: Level 1)

6.5 SIMULATION DATA SETS

These are the computer files that contain the initial position of the cells in the simulation, and properties of each cell. Each file contains a notochord, neural tube and sclerotomal cells.

6.5.1 Notochord and neural tube

The dimensions of the notochord, neural tube and distance of the sclerotomal cells from the notochord / neural tube structure were taken from a photomicrograph of a mouse 9.5 days post conception (pc) in "The Atlas of mouse development"[165].

6.5.2 Sclerotome

The dimensions of the collection of sclerotomal cells was less easy to define because the cells destined to form the anterior cellular condensation that will ultimately form the vertebral body is not uniquely defined. There are several molecular markers of the sclerotome, *Pax-1* being the most commonly used. The initial experimental studies of *Pax-1* expression demonstrated a segmented pattern around the notochord at 9-10 days pc. Subsequently, at 14 days pc, *Pax-1* is found in the region of the forming intervertebral disk[98,141]. Experimental studies using several different forms of the *Pax-1* mutation *undulated* suggest that normal function of this gene is essential for normal vertebral column formation[144,166]. Complete absence of *Pax-1* results in a lack of formation of the vertebral bodies and intervertebal disks, although posterior element formation is normal[167]. Heterozygous mutants display vertebral body / disk malformation most prominently in the lumbar region. Further studies using *Pax-1* and *Pax-9* double mutants have demonstrated that a functional redundancy between *Pax-1* and *Pax-9* exists[96]. Homozygous double mutants demonstrate a low cellular proliferation rate in the sclerotomal region of the somite. Taken together, these experiments, with several others, suggest that the role of the *Pax 1/9* genes in vertebral column formation is to control cellular proliferation within the sclerotomal compartment. However, these experiments also demonstrate that whilst *Pax-1* identifies those cells fated to form the anterior cellular condensation, it does not distinguish these cells from those fated to form the intervertebral disk.

The best experimental description of *Pax-1* expression in the somite / sclerotome is that of Barnes etal[97] in the chicken. *Pax-1* expression is

shown initially in the ventromedial region of the somite, and subsequently localises to the caudal half of the somite, whilst remaining in ventromedial region at the time of cellular migration. This is illustrated Figure 6-6 from a paper by Barnes etal[97].

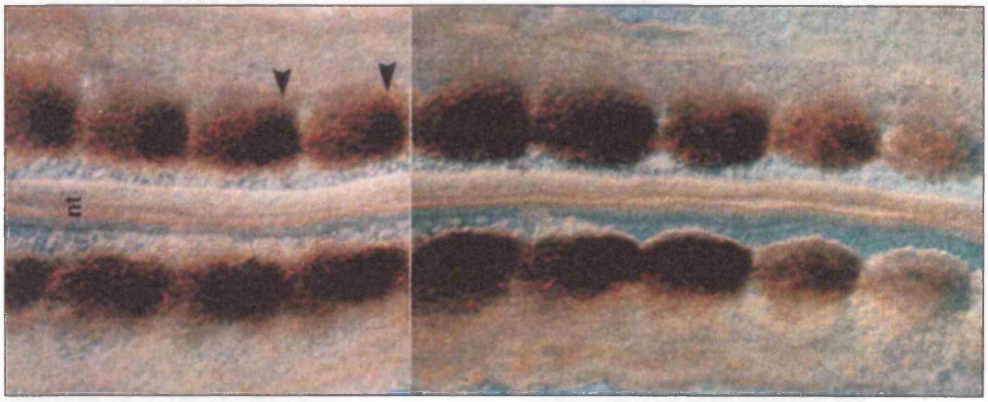

Figure 6-6: Chicken Pax-1 expression - in situ hybridization. From Barnes etal

It was therefore decided to represent the sclerotomal cells fated to form the anterior cellular condensation as shown with alternate blocks of cells, equally spaced by an absence of cells, shown in Figure 6-7.

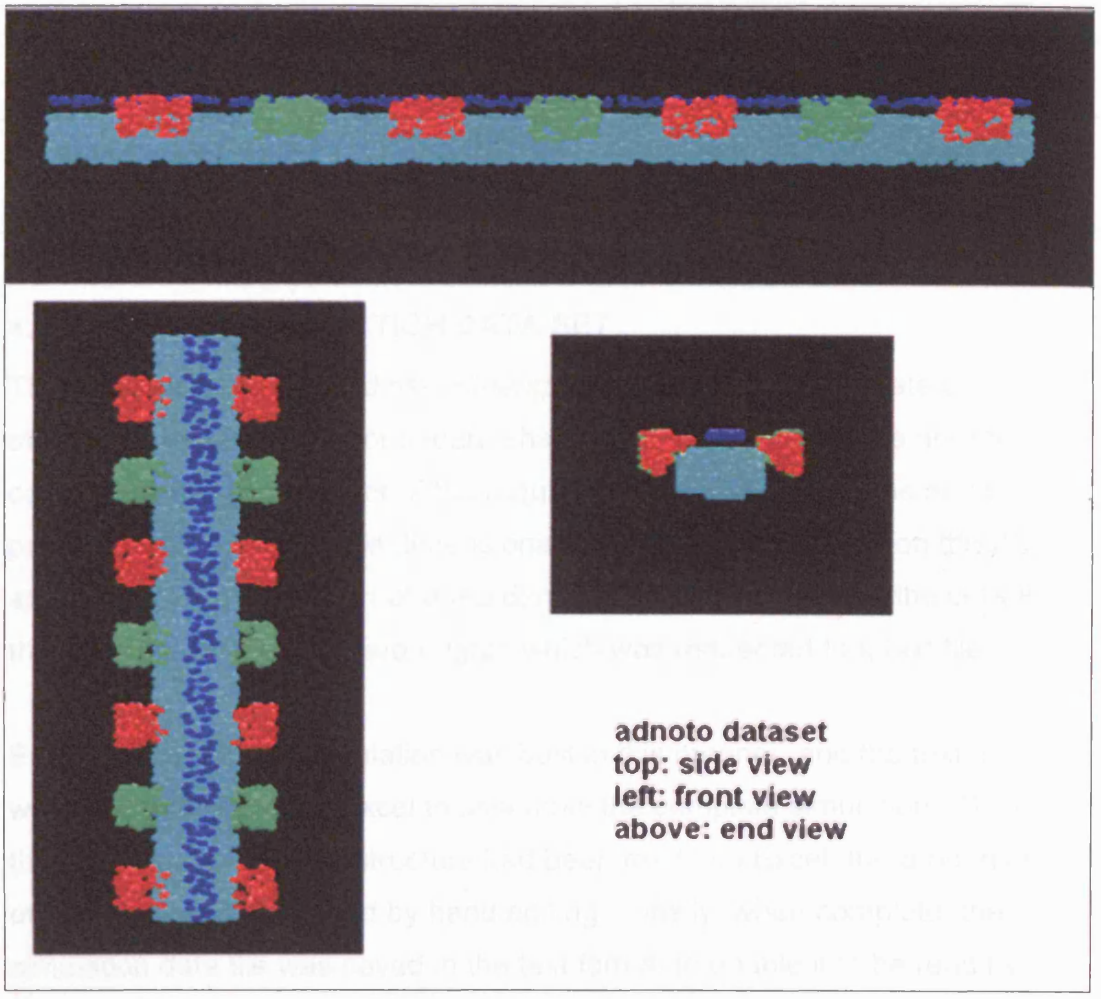

Figure 6-7: Arrangement of cells in theoretical model at start of simulation

6.6 CELLULAR PACKING DENSITY

The cell count per sclerotome has been approximated at half the number of cells per somite, using the data published by Tam (table 3)[168]. The total number of cells per structure, dimensions of each structure (in array voxels) and packing density of each structure in the dataset illustrated in Figure 6-7 are detailed in Table 6-3.

cell count	total number of cells	6019
	cells classified as neural tube	4625
	cells classified as notochord	221
	cells classified as sclerotome	1173
	average number of cells per individual sclerotome	1173 / 14 = 84

dimensions (volume in voxels)	neural tube	8 * 8 * 100 (6400)
	notochord	4 * 2 * 100 (800)
	individual sclerotome	4 * 7 * 7 (196)
packing density (cells per voxel)	neural tube	4625 / 6400 = 0.72
	notochord	221 / 800 = 0.28
	sclerotome	84 / 196 = 0.43

Table 6-3: Cell counts, dimensions and packing density per structure

6.7 BUILDING A SIMULATION DATA SET

The datasets were created using *triangle*, a program able to create solid structures, either triangle or square shape. The inputs to triangle are the co-ordinates of each corner of the required shape in the XY plane and the packing density. The three dimensional shape is then extruded on the Z axis. Triangle outputs a list of three dimensional co-ordinates of the cells in the structure on the standard output, which was redirected to a text file.

Each structure in the simulation was built in this manner, and the text file was read into Microsoft Excel to assemble the complete simulation. Once the co-ordinates of each structure had been read into Excel, the properties of each cell were assigned by hand editing. Finally, when complete, the simulation data file was saved in the text format to enable it to be read by the simulation program.

Adnoto - the basic dataset - was created to emulate the normal embryonic situation as described above, and is illustrated in Figure 6-7. Two additional datasets were created - *fused* and *deleted* - to test specific experimental hypotheses, as discussed in the experimental chapters. These datasets are illustrated in Figure 6-8.

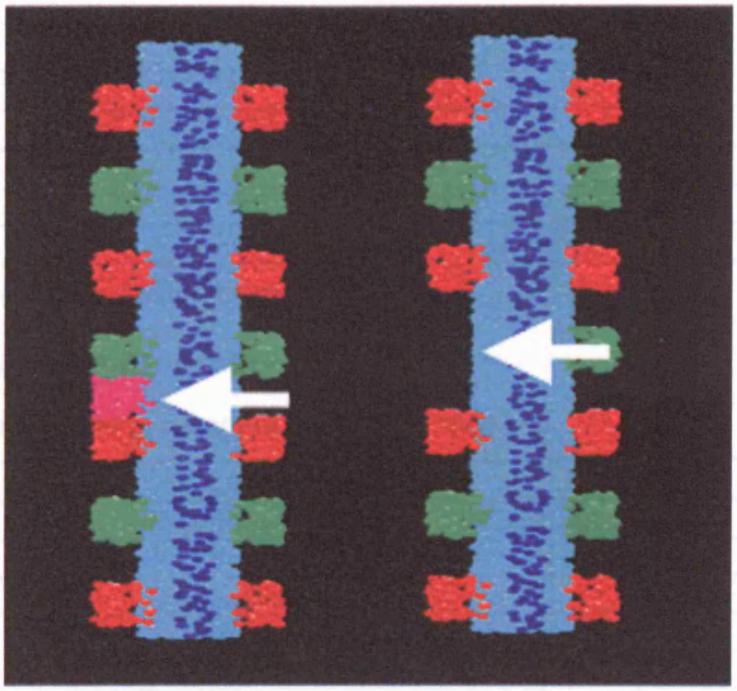

Figure 6-8: deleted (right) and fused (left) datasets. The arrows indicate were cells were added and removed to the adnoto dataset.

6.7.1 Data format

The simulation data file was read using the `fscanf(fp, "%s", &addr)` function. Numerical values are converted from an ascii representation to the appropriate numerical format using `_atol(char)` or `_atof(char)` functions.

6.8 SIMULATION PARAMETERS

The parameters consists of the constants and the program commands.

6.8.1 Simulation constants

The following simulation parameters were pre-defined, but could be altered by the user at the start of every simulation:

- replication constant
- diffusion constant
- secretion constant

In all of the simulation experiments described in this work, the standard values were accepted. These values are shown in Table 6-4. The values

chosen are "best estimates" of biological parameters (personal communication, P V Thorogood, 1997).

Simulation constant	value
replication	0.06
diffusion	0.0005
secretion	0.1

Table 6-4: Value of simulation constants

6.8.2 Simulation program

A typical simulation program is shown in Table 6-5.

Level 1	Level 2	Level 3
movement	time	display
replicate	display	
	secrete	
	diffuse	
	store	
	write image	

Table 6-5: A typical simulation program

By reference to Table 6-2 and Figure 6-5, it can be seen that this program will

- display the position of every cell in the simulation (Level 3)
- cause the morphogen to be secreted / diffuse and store the display / cell positions for later analysis (Level 2)
- randomly select cells for movement and replication (Level 1)

The outer counter (total number of frames to simulate) was usually set to 800.

6.9 SUMMARY

This chapter has described how the in vivo and in vitro experimental data has been translated into an experimental model, and how the experimental model has been implemented on a computer, and the assumptions made therein.

7 Materials and method

This chapter discusses the generic experimental method used in this thesis. Specific details for each experiment, including the hypothesis to be tested and results are given in the appropriate chapter.

7.1 PLAN OF EXPERIMENTAL WORK

In order to run a simulation, the initial position and types of all cells within the simulation had to be defined within the simulator program *vert*. This was performed by building a text file using Microsoft Excel spreadsheet containing the location, type and other cell properties of all cells as described previously. A standard template was defined and this was edited by hand to introduce additional cells or to remove cells from the simulation. The activation times of cells could also be altered.

The basic experimental structure was to as follows

- stage 1: define hypothesis to be tested
- stage 2: alter standard cell location template for hypothesis
- stage 3: use the simulator program *vert* to run the simulation. *vert* was programmed using VPL to output at each stage in the simulation cycle the position of each cell within the simulation for later analysis with the program *orthoview* and also save the screen display of the current location of the cells to disk for analysis.
- stage 4: create a movie of the simulation using the screen display images and either Adobe Premiere or Paint Shop Pro 3: Animation Shop.
- stage 5: analyse the internal structure of the models generated by the simulator and the movement of the cells on a frame by frame basis using *orthoview*.

As the work advanced, simulations with different aims were constructed. The different simulations can be divided into the following groups

- basic testing
- testing of normal biology
- robustness of the developmental mechanism
- testing abnormal biology
- testing virtual abnormal biology

7.1.1 Basic testing

How well do the individual morphogenetic toolkit algorithms emulate the observed biological behaviour of cells ? The algorithms and experiments performed are discussed in Chapter 8.

7.1.2 Normal biology

How well does the simulator emulate normal embryological development, and how close is the simulated outcome to that observed in the normal embryo ? The experimental methodology and results are presented in Chapter 9.

7.1.3 Experimental reliability

How different is the simulated outcome for experiments with identical starting conditions and data sets using the normal biological dataset ? Chapter 10 reports the methodology and results.

7.1.4 Mechanisms of development

Are cellular migration and replication both essential for formation of the normal phenotype ? Chapter 11 reports the experiments performed to dissect out the importance of these components of morphogenesis.

7.1.5 Abnormal biology - formation of a hemi vertebra

What happens to the simulation when the initial dataset is changed, for example a somite is removed ? This simulation will generate a phenotype which can then be compared with that of a human abnormality. The experimental design and results are reported in Chapter 12.

7.1.6 Virtual abnormal biology - formation of a fused vertebra

What is the phenotypic outcome of the simulation when the initial dataset if altered in a way that is not possible or may not have been performed in vivo ? The experimental design and results are reported in Chapter 13.

7.2 EXPERIMENTAL SIMULATION DATA FILES

These are the data files that contain the location of each virtual cell for the simulation program and are read into the simulator program prior to the start of each simulation. Each file contains the location, and other attributes – eg whether the cell is able to move, replicate, secrete a morphogen – about each of the approximately 6000 cells required for each simulation.

Three simulation files were created, one corresponding to each of the major virtual experiments. The files and the corresponding experiment are given in Table 7-1.

file name	experiment
adnoto.txt	experiment 1: testing normal biology
deleted.txt	experiment 2: formation of a hemi vertebra
fused.txt	experiment 3: formation of a fused vertebra

Table 7-1: List of data set filenames

Each file can be found on the animation CDROM.

7.3 MEASUREMENT OF OUTCOME

Accurate, reliable and reproducible measures of outcome that actually describe what has happened are a cornerstone of all branches of science. Poor measures abound and are notoriously deceptive and easily biased. In this work two different types of measure have been used: visual assessment and a visual mathematic technique for image comparison described later.

Shape and / or morphology is a difficult parameter to measure numerically. If a shape is regular, or predictable, linear measurements of predefined

axes can be calculated and quoted, and this will give a reproducible and quantifiable measure of the shape. Irregular or unpredictable shapes such as those encountered in these simulations are more difficult to measure in this manner, and the approach adopted for this work was to inspect the morphology of the cellular condensation using several different visualisation techniques and compare the morphology of the formed structures with those seen *in vivo*. In addition, the outcome of each experiment was also analysed using the generic outcome measures listed in Table 7-2 in a qualitative manner ie true or false.

Outcome measure	
1	Cell mixing from adjacent sclerotomes
2	Preservation of disk space between prevertebral cellular condensations
3	Presence of sclerotomal cell fusion across midline / around notochord
4	Formation of contralateral hemi prevertebral cellular condensation following removal of sclerotome
5	Formation of giant prevertebral cellular condensation when two adjacent sclerotomes were merged
6	Migration of cells across the midline ie from left side of notochord / neural tube to right side of notochord / neural tube

Table 7-2: Generic outcome measures

In Chapter 10 the reproducibility of the simulation is considered. In this chapter the condensation sizes are measured, as described within the chapter, and comparison repeated simulations with identical starting parameters was performed using a technique to plot the probability of any one location being occupied by a cell at a discrete point in the simulation.

7.3.1 Visualisation of results

The methods of display were discussed in 6. The VPL program displayed each new frame immediately following computation using the spherical three dimensional view. This view was also written to disk in order to generate an animation following the simulation. The *orthoview* program was used to analyse the developmental mechanism.

7.4 SUMMARY

The general plan of the experimental work has been described in this chapter, as has the method of assessing outcome. The three dimensional sphere view was the "work horse" view and used during development for

creation of the animations and for general assessment of the morphology of the shape of the somite derivatives. The three dimensional surface viewed aided this task, particularly when display of the fixed central structures (neural tube / notochord complex) was turned off. Using this view with alpha blending of the lateral structures demonstrated their relationship to the central structures. The orthogonal viewer was useful for examining the internal structure of each object.

8 Morphogenetic toolkit

This chapter describes the morphogenetic algorithms that were implemented, based on the mechanisms discussed in Chapter 3, and the computer experiments performed to assess the behaviour of each algorithm.

8.1 MIGRATION UP A CONCENTRATION GRADIENT

This is a fundamental property of many developmental cells as discussed earlier in Chapter 3. In this work, the implementation of this property is considered the same whether migration up a concentration gradient of diffusible morphogen (chemotaxis) or a more fixed ground substance (haptotaxis) is being considered.

The algorithm was designed to move the cell from a region of low concentration to that of a higher concentration, avoiding locations occupied by other cells. Each cell was considered to possess three pseudopodia with "concentration sensors". Each pseudopodia sampled the morphogen concentration at an adjacent location to that of the cell. At the start of each simulation, the location sampled by each pseudopodia from each cell was randomly allocated. The pseudopodia possess "memory" and regenerability, in that the pseudopodia sampling the lowest concentration around the cell was destroyed and a new pseudopodia created in a random position.

The concentration gradient was calculated by subtracting the concentration at the current location from that at the pseudopodia sampled location. A positive result implied an uphill gradient, negative, a downhill gradient. The cell chose to move in the direction of the highest

concentration gradient sampled by the pseudopodia. If two or more pseudopodia sampled identical morphogen concentrations, a random choice between the two locations was made.

Two variations of the algorithm were implemented and can be selected in the simulator program using the *zero rule* check box. If the zero rule flag is set, the cell will not move if the morphogen concentration gradient at the cell current location is zero. If the zero rule flag is set, and the morphogen concentration gradient at the current location is zero, the cell will move in the direction of a random pseudopodia. No movement occurred if the concentration gradient was negative or downhill. A flow chart to explain the algorithm is in Figure 8-1.

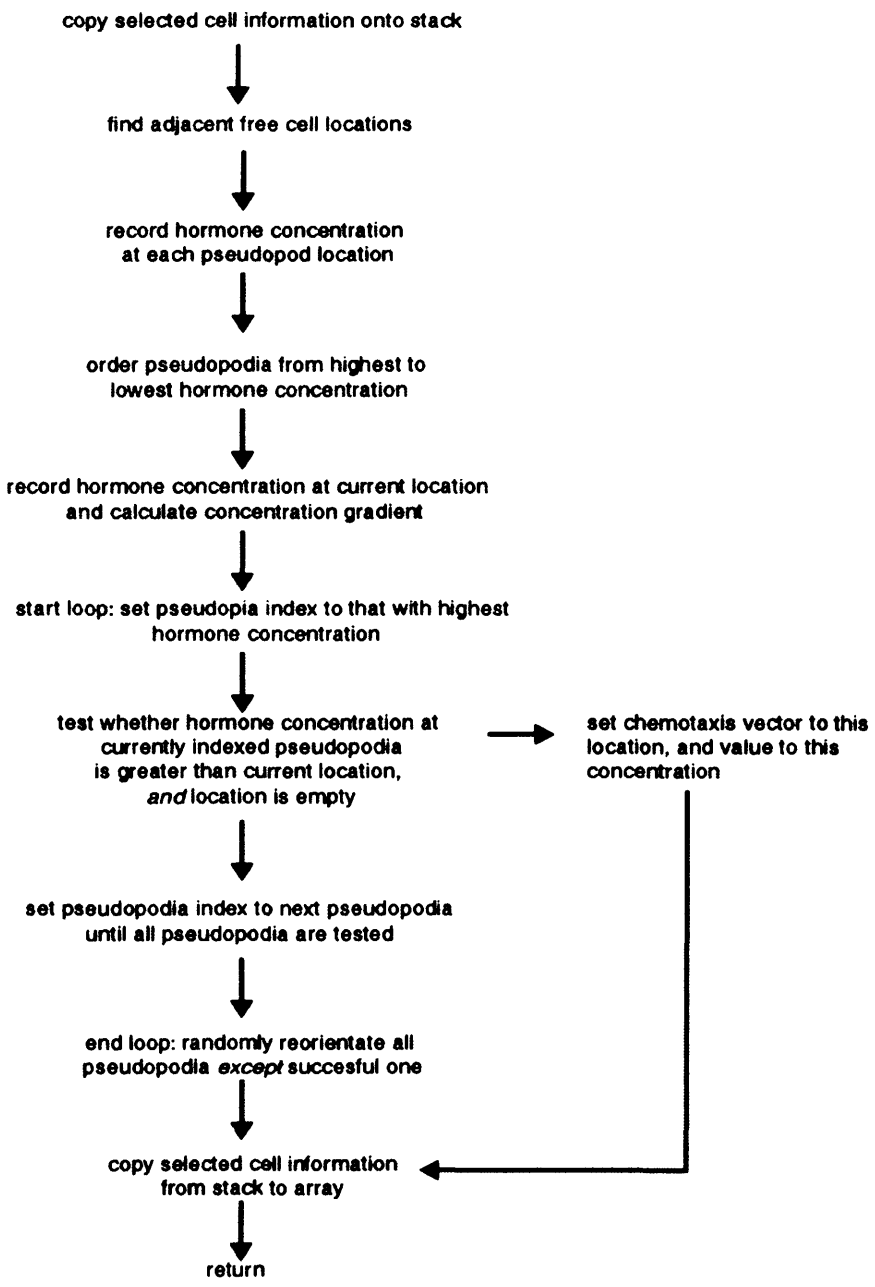

Figure 8-1: flowchart of chemotaxis algorithm

8.2 TESTING THE CHEMOTAXIS ALGORITHM

To characterise the behaviour of the algorithm, two test simulations were implemented using the simulator program *vert* – migration of randomly placed cells to a point source of diffusible morphogen and migration of a line of cells towards a line source of diffusible morphogen. A total of four simulations were performed, line source and point source, each with the zero rule reset and set.

8.2.1 Method

8.2.1.1 Point source

Ten cells were randomly scattered in a cube of dimensions 10 units by 10 units by 10 units and a point source emitter of diffusible morphogen placed at the centre of the volume.

Random movement was disabled, and simulations were with the zero rule flag set and reset. The cellular movement was therefore dependant only on the chemotaxis migration algorithm.

8.2.1.2 Linear source

Five hormone secreting cells were placed in a line, with seven cells able to migrate up a hormone concentration gradient. Random movement was disabled, and simulations were performed with the zero rule flag set and reset.

In each simulation, the simulator was programmed as shown in Table 8-1. Each simulation ran for 60 cycles. The default hormone constants of secretion and diffusion were not altered.

Level 1	Level 2	Level 3
movement	display	display
	timer	
	secrete	
	diffuse	
	store image	
	store binary	

Table 8-1: Simulator program

8.2.2 Results

The endpoint was clustering around the hormone source, and the migration path taken by the cells using animations generated from the simulations.

8.2.2.1 Point source

Clustering of the cells around the point source occurred in all cases. If the zero rule flag was set, all cells migrated towards the source, commencing migration as the hormone diffusion reached the different cellular locations. When the flag was reset, the majority of cells migrated towards the source, with occasional exceptions "escaping" the chemotactic influence due the random disposition of the pseudopodia.

8.2.2.2 Linear source

Clustering of the migratory cells around the linear arrangement of hormone cells was also observed in this simulation, with occasional escaping of migratory cells when the zero rule was reset.

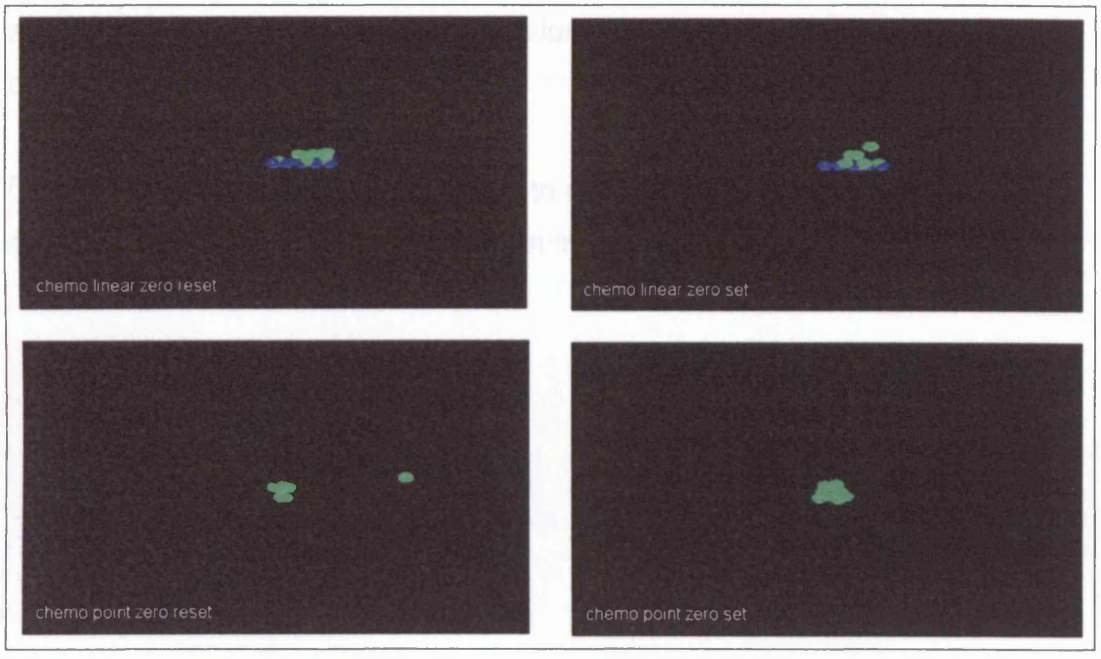

Figure 8-2: end frames for chemotaxis simulations

The complete animation of each of the simulations is presented on the accompanying animation CDROM.

8.3 CELLULAR REPLICATION

This is also a basic property of many developmental processes. In this work, replication of an individual cell occurred on a random basis and at a random orientation. A parent cell was replaced by two daughter cells with identical properties to the parent cell.

A cell was tested for replication by generating a random number less than 1.0, and testing this against the replication threshold. If the generated random number was less than the replication threshold, the cell could proceed to the replication cycle. A generated number greater than the random threshold terminated the individual cellular replication process at this stage.

In the replication cycle, the each potential cellular location surrounding the replicating cell was tested in a random order to determine whether it was occupied by another cell. If the location was empty, the parent cell was cloned, and the daughter cell placed in the tested location, and the algorithm terminated. If all of the locations around the replicating cell were occupied, replication did not occur.

Daughter cells achieved competence to replicate immediately. The replication algorithm flow chart is given in Figure 8-3.

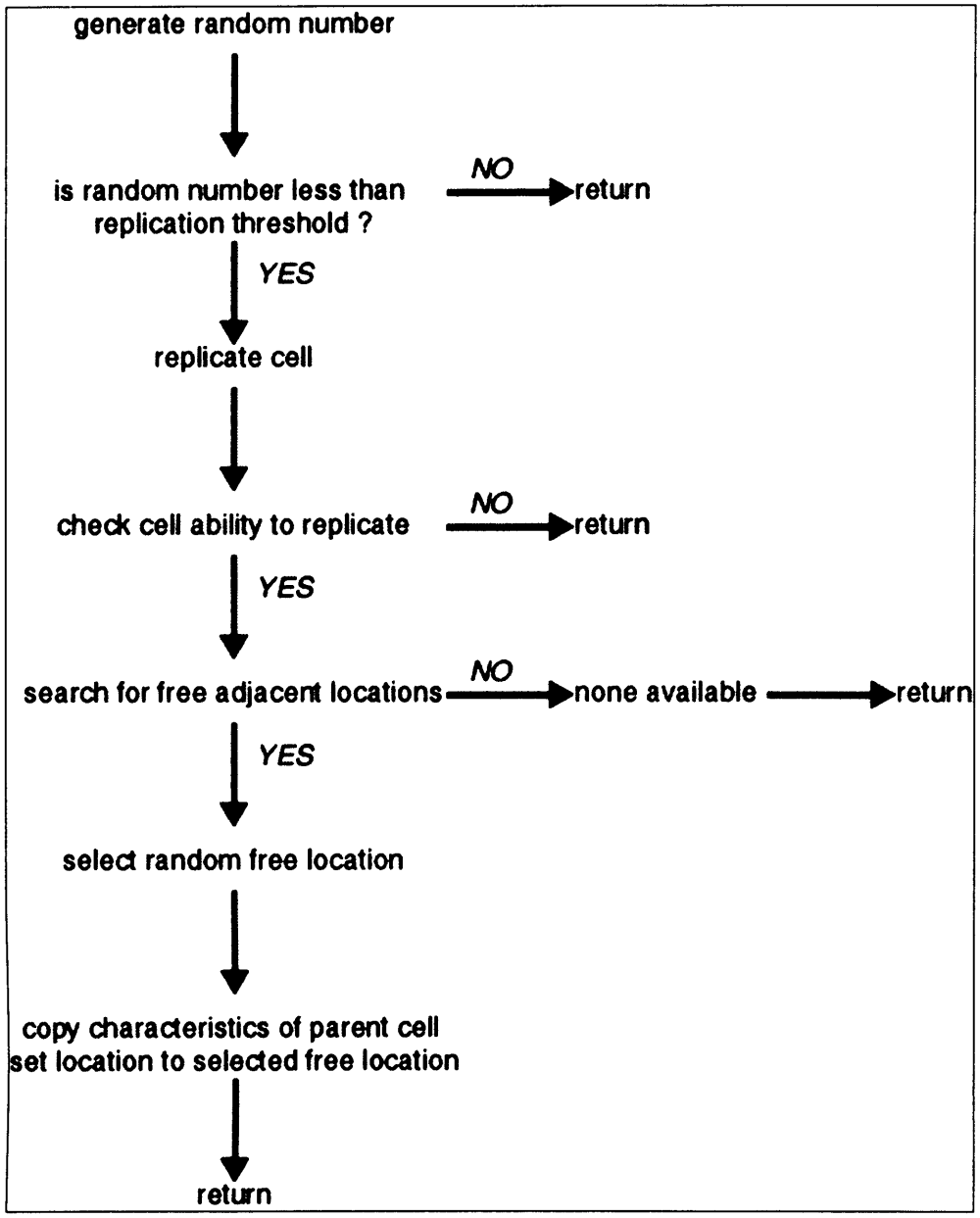

Figure 8-3: flowchart of replication algorithm

8.3.1 Method

Using the simulator program *vert* a volume of 10 units by 10 units by 10 units was filled with 9 randomly located cells. The simulator program included only the cellular replication algorithm. Outcome was assessed visually, using the *vert* display.

Increasing replication thresholds were tested against the same time period. The endpoint was the development of cellular clustering as judged visually.

The cell replication algorithm was tested using the standard *vert* simulator program given in Table 8-2.

Level 1	Level 2	Level 3
replicate	display	display
	timer	
	store image	
	store binary	

Table 8-2: Simulator program to test cellular replication algorithm

8.3.2 Results

Cellular replication occurred around existing cells. This occurred in a random fashion. The rate of growth of the cellular clusters increased as the replication threshold was increased. An animation demonstrating the cellular replication is presented on the CDROM.

8.4 RANDOM MOVEMENT

Cells on growth media appear to move in random directions in the absence of other directing forces. Directed cellular movement such as migration along a concentration gradient may also possess a random component.

The random movement algorithm was implemented by comparing a randomly generated number to a threshold value. If the threshold value was greater than the tested number, the cell was allowed to move randomly. The direction in which the cell moved was chosen by creating a list of vacant potential locations and randomly selecting a direction in which to move. Random movement was continued in that particular direction, unless a second random number between 0 and 1 was greater than the *kink* value, alterable through the software code. If the random number was greater than this value, the direction of the random movement was randomly reassigned. If random movement was enabled, but all of the potential surrounding locations were occupied, no movement occurred.

The random movement algorithm is shown in Figure 8-4.

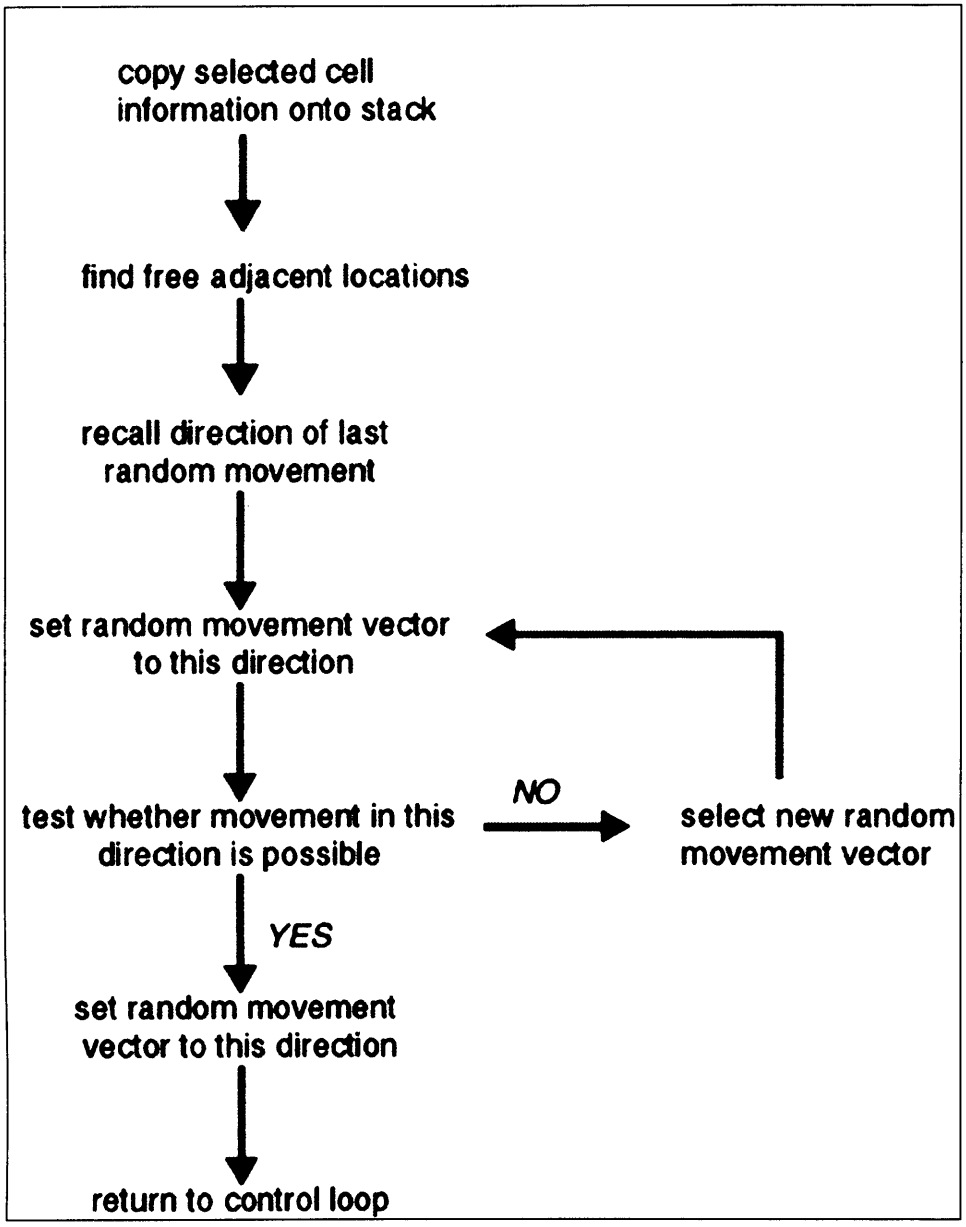

Figure 8-4: flowchart of random movement algorithm

8.4.1 Method

Two simulations using only the random movement code are presented. Both use the chemotaxis migration test data files (used to test the chemotaxis algorithm described earlier in this chapter) and the results are presented as a movie on the animation CDROM.

Using the program *vert* a volume of 10 units by 10 units by 10 units was filled with randomly located cells. The simulator program included only the random movement algorithm. Outcome was assessed visually, using the *vert* display.

The chemotaxis point source test file contained one immobile cell, and nine randomly placed movement cells. The chemotaxis linear source file contained five source cells and seven movement cells, both groups linearly arranged in parallel.

Level 1	Level 2	Level 3
random	display	display
movement	timer	
	store image	
	store binary	

Table 8-3: Simulator program used to test the random movement

8.4.2 Results

The cells were seen to migrate in a random fashion. Review of the animation of random movement demonstrates the cellular density was reduced from a relatively compact cluster of cells at the start of the simulation to a loose network.

8.5 INTERCELLULAR SORTING

Experiments where cells of two different types are mixed, and allowed to settle have demonstrated that cells will sort into groups of like cells surrounded by like cells. This can be explained on the basis that the intercellular bonds between like cells are greater than those formed between unlike cells. An algorithm was designed to reproduce this behaviour, however, despite intercellular movement occurred, sorting did not occur, and this algorithm was not further developed.

8.6 DISCUSSION

The individual morphogenetic algorithms and experimental behaviour of each algorithm as implemented in the simulator program *vert* is described above. Each algorithm and implementation appears to function in the manner that is intended, apart from the cellular sorting. Further development of the cellular sorting algorithm was not pursued further because this morphogenetic mechanism is not thought to play a major role in the development of the vertebral body condensation.

Each individual algorithm has been based on biological experimental work, as discussed in Chapters 3 and 6. Perhaps the greatest difficulty is that of observer bias influencing understanding of the actual biological process occurring. In the context of this work, this would lead to incorrect algorithmic design and implementation, which would alter the behaviour of the simulator program and obscure the true biological phenomena.

Additionally, there are a number of other points that should be considered in translating the true biological experimental cellular process to the simulated developmental process. Data on the behaviour and movement of individual sclerotomal cells in vivo and in vitro does not exist, and so the behaviour of sclerotomal cells has been inferred from that of other cells types used for in vitro and in vivo experiments and from theoretical analyses. Specifically, the behaviour of the following cells has been observed: primary mesenchymal cells during gastrulation, neutrophils after migration from a vessel, the behaviour of fibroblasts in a matrix gel, and a theoretical paper on pseudopodia formation[61,77,79,169-172]. Wood and Thorogoods paper on cell movement is an observed in vivo study of the cells in their natural habitat, however, even in this experiment, it is difficult to be absolutely certain of the influences on the cellular behaviour[80,173,174].

Vertebral condensation requires the co-ordinated movement of a large (or relatively large) number of cells. Each of the experiments reported above have examined the behaviour of only a small number of cells and whether a large number of cells migrating together will behave differently from a single cells is a further point. It is also conceivable that in this situation, cells may influence the behaviour of each other through intercellular bonding.

Many further experiments might have been performed to further investigate the behaviour of the individual algorithms, and how cell movement was altered by initial cellular placement, the position of the morphogen secreting cells and alteration of the cellular parameters such as cell migration velocity and frequency of cellular replication.

8.6.1 Morphogen directed cellular migration

Two scenarios were used to test this algorithm (i) migration towards a point source of morphogen and in anticipatation of later modelling of vertebral column development (ii) migration towards a linear source of morphogen. In each case, the cells migrated up the morphogen concentration gradient towards the source of morphogen. Migration was not always in a straight line towards the source because of the initial random placement of the pseudopodia on each cell, and whilst not so apparent in this simulation with only a few cells, the presence of a cell "in front" of another caused the behind cell to alter direction. A moderate degree of cellular compaction can be seen around the point source, although not every location is occupied. This is probably related to the limited time period for which the simulation was run, but also the random nature of the simulation. The more spread out nature of the linear morphogen source has resulted in a less compact "condensation" of cells, nevertheless, the cell have migrated to surround the source. Comparison of the animations of cellular migration towards the point and linear source reveals that, because of the more diffuse nature of the linear source, cellular movement is less inhibited by collisions occurring between two migrating cells.

The effect of the "zero rule" can be clearly seen when the simulations in which the "zero flag" has been set are compared with those in which the flag is reset. As described above, when the "zero flag" was reset, the majority of cells migrated towards the morphogen source, with the occasional cell escaping. An occasional cell escapes because of the random motion influence, it starts to migrate in a direction opposite to that of the morphogen source, and whilst the source diffuses, in the limited time allowed for the simulation, the diffusion edge of the morphogen source never "catches up" to influence cellular migration. This mechanism, if implemented in biological cells would allow individual cells to actively seek out morphogen sources. However, as these simulations

demonstrate, it can lead to cellular loss. The relative number of cells escaping is few, and will be seen to be fewer in the later simulations.

In conclusion, the slightly different algorithms have demonstrated is that the important factor is the generic algorithm implementing migration, rather than the refinements of the actual migration algorithm.

8.6.2 Cellular replication

In early mammalian embryonic development, the cleavage of the blastomeres occurs at particular orientations. The initial cleavage is a normal division of the on the cellular meridian, however in the second division, rotational cleavage occurs, that is one cell divides on its meridian, whilst the other divides on the cellular equator[175]. Cell division may also not occur in synchrony. The differences in the plane of cellular division are presumably related to the establishment of the different components of the early embryo.

In this work, replication can occur in any direction in which there is space for the parent cell to replicate into. A more sophisticated replication algorithm would be have to only allow the cell to replicate towards a morphogen source, but there is no experimental evidence to suggest this actually occurs in the development of the vertebral column. Sclerotomal cells may not be competent to replicate whilst migrating towards a morphogen source, in contradistinction to the cells in this simulation, which are allowed to replicate at any point during the simulation.

8.6.3 Random movement

It is difficult to be certain in biological experiments whether the random movement observed is truly random, as it is not possible to be certain that the cells are not responding to an unknown stimulus, however, the movement observed does appear to be without pattern or form. In the experiments performed and the results presented above true random motion occurs, without formation of any discernable structures. Whilst this experiment has not been performed with large numbers of cells, or over

extended periods of time, it implies that the formation of structures observed in the simulations performed with the program *vert* are directed and a response to the morphogen concentration gradient.

8.7 SUMMARY

The algorithms and code implementation described in this chapter form the basis for the simulator program *vert*. The experiments described demonstrate the behaviour of the algorithms to be similar to that observed in biological experiments, and therefore a reasonable basis for more complex simulations described in later chapters investigating the developmental mechanisms involved in vertebral column formation and malformation.

9 Experiment 1: testing normal biology

This experiment was designed to assess the ability of the simulation program to emulate the normal development of the sclerotomal cells in forming the putative anterior vertebral body cellular condensation.

The simulation commenced with the sclerotomal cells placed laterally as described in the theoretical model. A morphogen gradient was then established and the cells migrated in response to this gradient.

In the mammalian embryo, development of the cranio-caudal axis and formation of the sclerotomes occurs concurrently. In order to simulate this, whilst the notochord and neural tube cells were present throughout the computer experiment the notochord and sclerotomal cells were segmentally activated in a cranio-caudal direction. Successive groups of sclerotome cells were activated in a craniocaudal direction every 100 outer loop cycles.

9.1 HYPOTHESIS

The system will emulate the normal embryological development, using chemotaxis directed cellular migration, cellular replication and random movement. Formation of pre-vertebral cellular condensations around the anterior part of the notochord / neural tube complex, similar to those observed *in vivo* in the mammalian embryo will occur.

9.2 METHOD

The initial arrangement of the cells using the dataset *adnoto* in the simulator was as shown in Figure 9-1. Each sclerotome segment was activated for two hundred outer loop cycles (Table 9-1).

Sclerotome number^	start time#	finish time#
1	0	200
2	100	300
3	200	400
4	300	500
5	400	600
6	500	700
7	600	800

Table 9-1: Timing of notochordal cells activation. ^counting from cranial to caudal (top to bottom in the computer images # in simulator program cycles

The simulator was programmed to perform 800 outer loop cycles in total. The standard VPL simulation program (Table 6-5) and constants (Table 6-4) were used in the simulation. The output was analysed using an animation created by the 3 Dimensional spherical view, VRML models and orthoview.

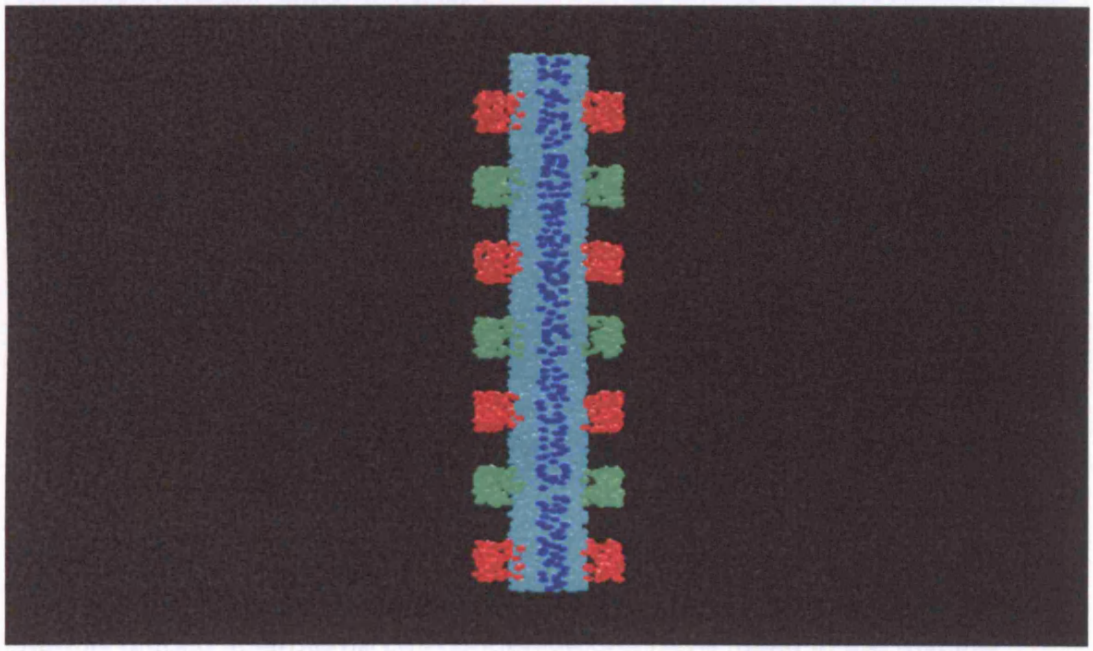

Figure 9-1: initial appearance of the cells in the simulator. This is a three dimensional sphere view. The sclerotome cells are red and green, the notochord is cyan and the neural tube is blue.

9.3 OUTCOME MEASURE

The outcome main measure of the experiment was how closely the structure developed at the end of the simulation period resembled that developed in the murine embryo at approximately 11.5-12 days post

conception (plate 26b figure e, page 136, Kaufman, The Atlas of mouse development[165]). The actual developmental mechanism of morphogenesis was analysed using the orthogonal visualisation program orthoview.

The generic outcome measures (Table 7-2) were also assessed.

9.4 RESULTS

The final frame of the simulation is shown in Figure 9-2.

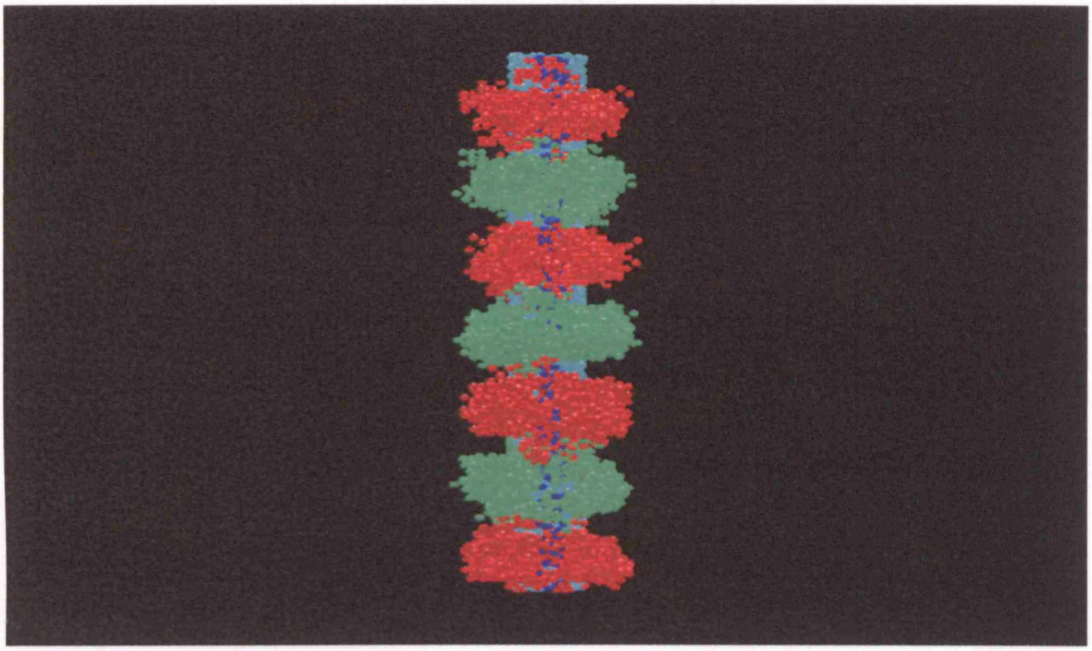

Figure 9-2: final frame of simulation. The sclerotome cells have migrated and formed cellular condensations surrounding the notochord / neural tube complex.

The sclerotomal cells have migrated from their initial lateral position to surround the midline notochord / neural tube structure, and the initially two laterally placed sclerotome cell condensations have fused in the midline and formed a single condensation – the prevertebral analgan – which will in due course will undergo chondrification and subsequently ossification to form the vertebral body. No mixing of the cells from the different sclerotome condensations is observed, and the position of the presumptive intervertebral disk is preserved between the cellular condensations.

Comparison between Figure 9-3 and Figure 9-4 demonstrates the similarity in the morphology of the computer generated condensation to that see in the developing mouse. Whilst the computer simulator does not model the developing dorsal root ganglion and peripheral nerve, it can be seen that the computer generated prevertebral cellular condensation occupies a similar position to that seen in Figure 9-3, although the size of the condensation across the midline enveloping the notochord is rather waisted when compared to that seen in the mouse.

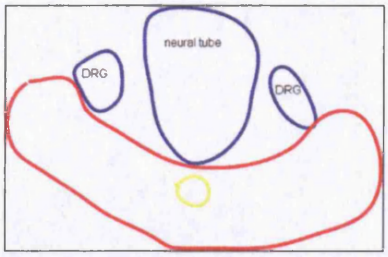

Figure 9-3: tracing of plate 26b figure 4 from Kaufman (DRG dorsal root ganglion, yellow notochord, red prevertebral cellular condensation)

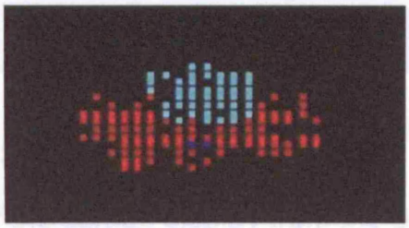

Figure 9-4: simulation output after 800 cycles

In terms of the generic outcome measures, cell mixing has not occurred between the adjacent sclerotomes, the disk spaces have been preserved, and fusion has occurred across the midline around the notochord. Measures 4 and 5 are not relevant to this experiment and it is not possible to determine 6 in this experiment.

9.4.1 Orthoview analysis

Using the orthogonal viewer in combination with the computer generated animation (on animation CDROM), it can be seen that the cells in the sclerotome initially separate, and then migrate in a fairly direct manner towards the midline. Cells surround only the ventral third of the notochord / neural tube complex, in keeping with the experimentally derived finding that the neural arch is formed under control of a different mechanism and

later in the developmental process, as discussed earlier. Packing density in the midline condensation increases largely as a consequence of cell replication rather than recruitment of further more laterally placed cells.

9.4.1.1 Initial position of cells

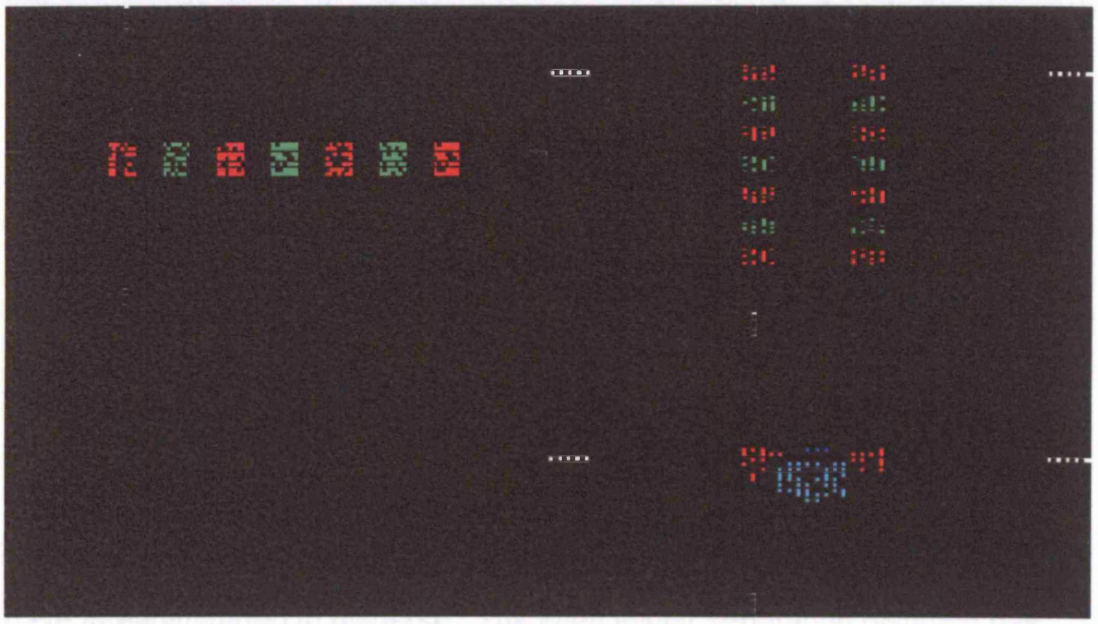

Figure 9-5: frame 0001 x 23 y 31 z 31

Figure 9-5 is a copy of the screen display from the program *ortho*, and illustrates the starting position of cells in the *adnoto* data set. A plane through the most rostal, animal right, more ventral than the notochord has been chosen for this figure. The image illustrates the starting arrangement of the sclerotome cells either side of the notochord / neural tube complex. As described previously, this is a complete data set, with normal arrangement of the sclerotomal cells – represented in red and green – notochordal cells in blue and neural tube in cyan.

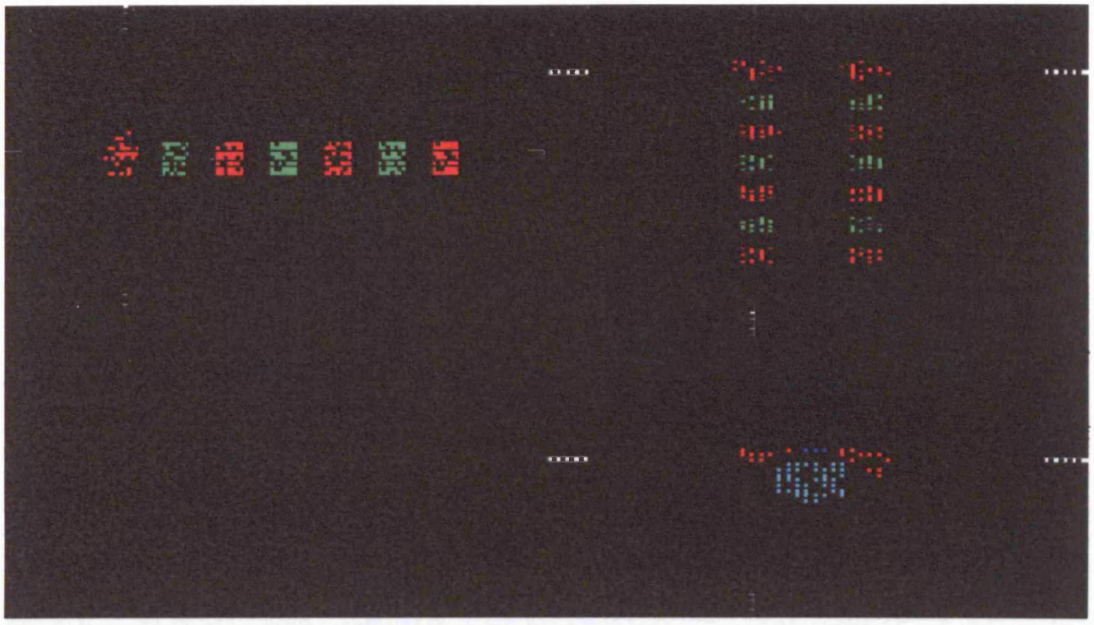

Figure 9-6: frame 0006 x 23 y 31 z 31

Figure 9-6 is the sixth frame of the simulation. Compared to the first frame, the sclerotomal cells of the most cranial collection can be seen to have already started to disperse. The intercellular separation distance has increased and consequentially the condensation size has enlarged. Cells are starting to migrate towards the notochord.

9.4.1.2 Sclerotomal cell migration

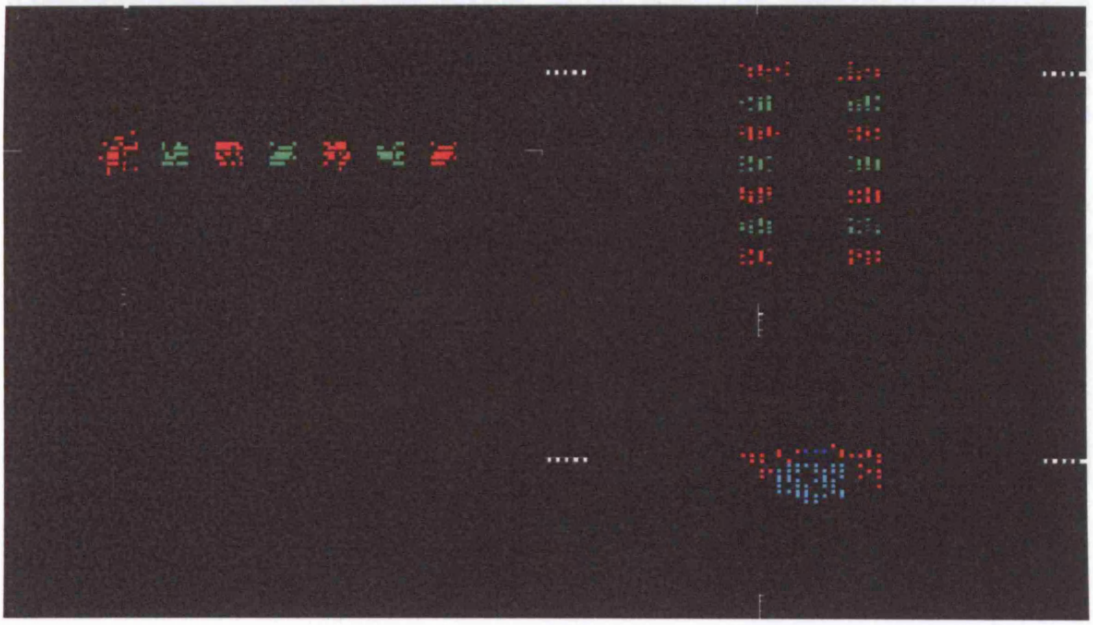

Figure 9-7: frame 0012 x 24 y 31 z 31

This view illustrates how the cells having reached the notochord, are starting to pass around the notochord, forming a perichordal sheath.

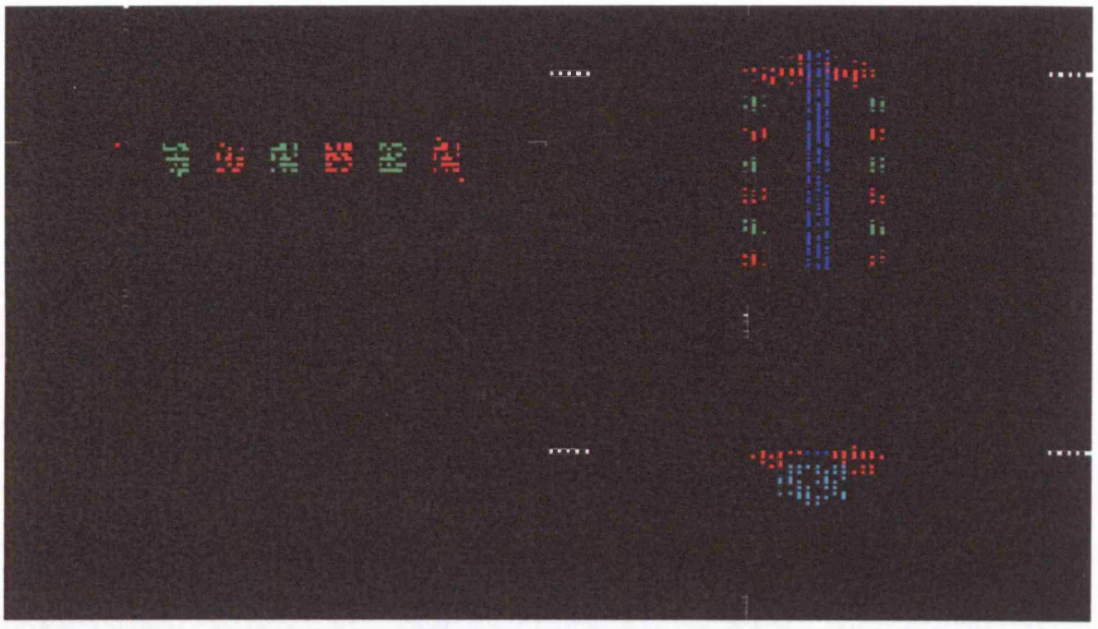

Figure 9-8: frame 0025 x 22 y 33 z 31

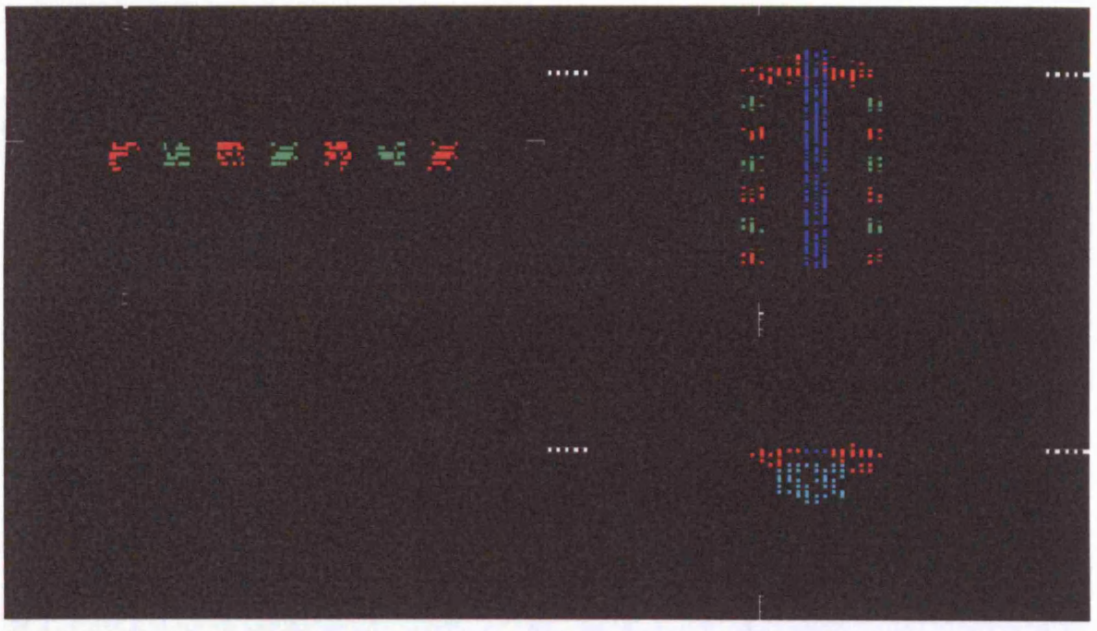

Figure 9-9: frame 0025 x 24 y 33 z 31

Figure 9-8 and Figure 9-9 illustrate how the red sclerotomal cells can be seen to have migrated ventromedially from their original lateral position, with respect to the neural tube. The cells are continuing to "heap up" around the notochord, with a few starting to pass ventral to the notochord.

9.4.1.3 Sclerotomal-notochord interface

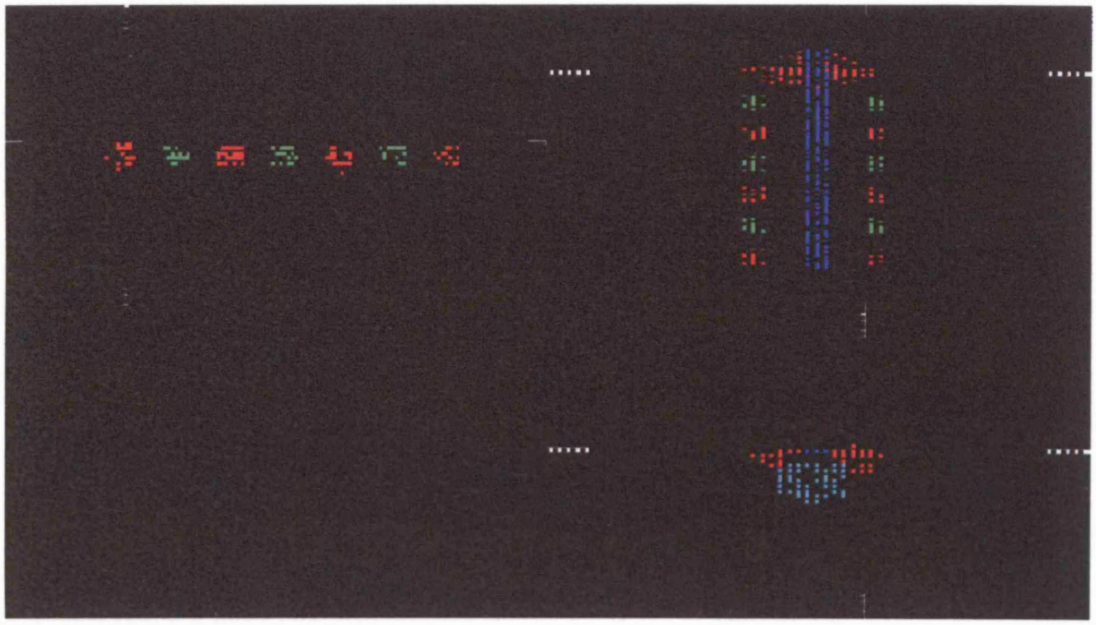

Figure 9-10: frame 0031 x 25 y 33 z 31

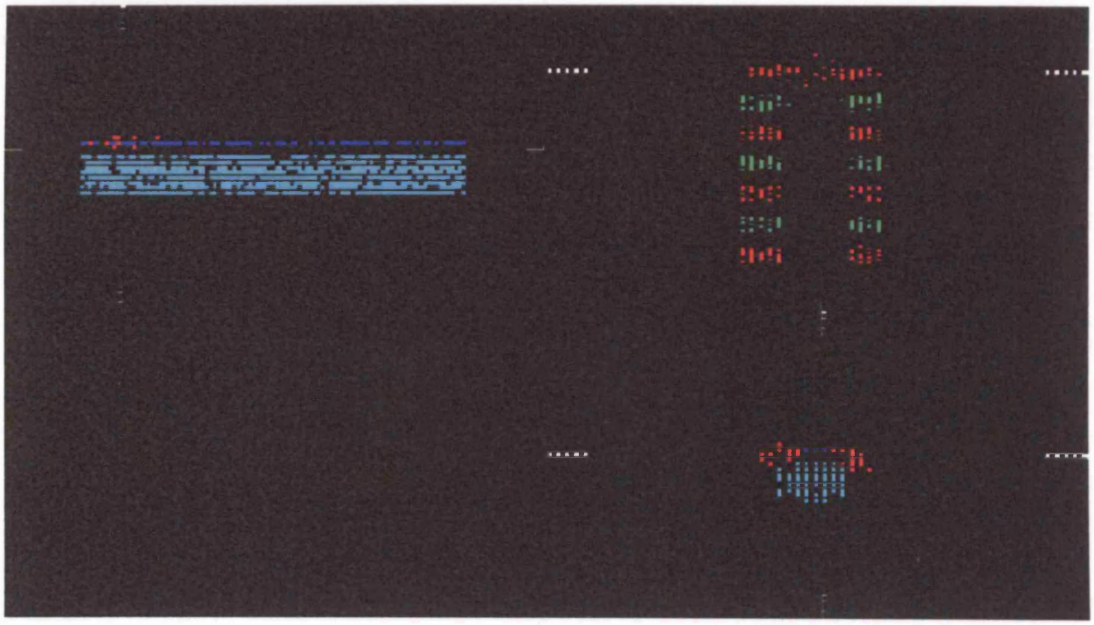

Figure 9-11: frame 0078 x 31 y 32 z 30

Figure 9-10 and Figure 9-11 although widely spaced in time illustrate how the interface between the notochord and the sclerotomal cells is starting to expand in the cranial and caudal directions, although there is little further migration around the notochord towards the midline.

9.4.1.4 Intersclerotomal cleft formation

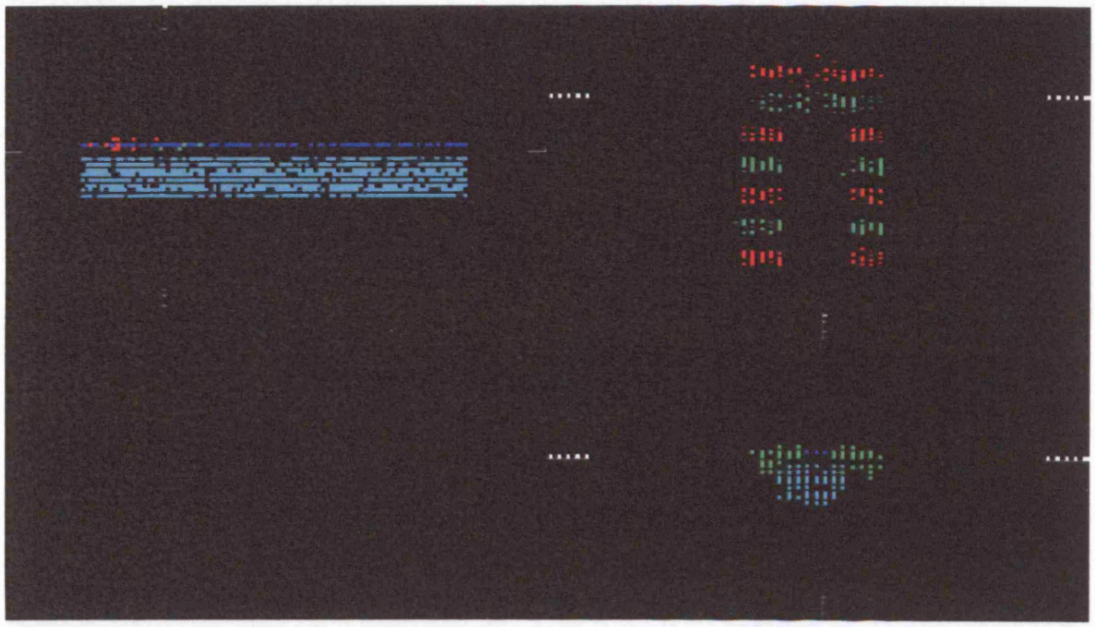

Figure 9-12: frame 0166 x 31 y 32 z 41

This frame (Figure 9-12) is midway through the activation of the second sclerotomal condensation. It illustrates preservation of an inter sclerotomal cleft – the putative disk space – between the first and second sclerotomes, although this is more obvious laterally.

9.4.1.5 Examination of the perinotochordal condensation

Figure 9-13 to Figure 9-16 are slices of the same frame, successively moving through the ventral plane.

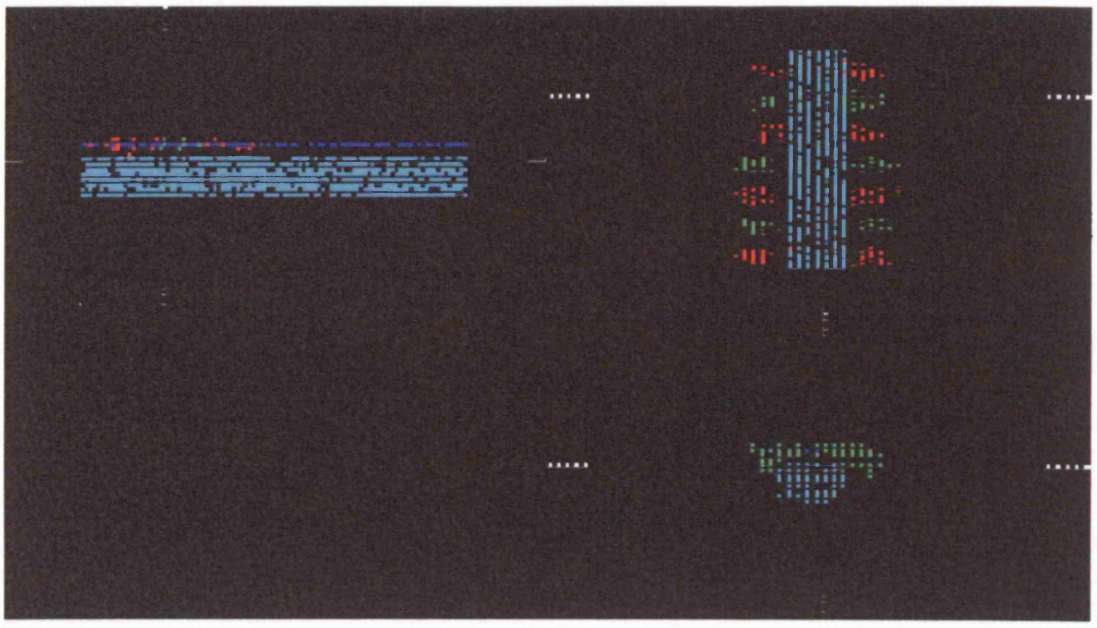

Figure 9-13: frame 0290 x 31 y 30 z 41

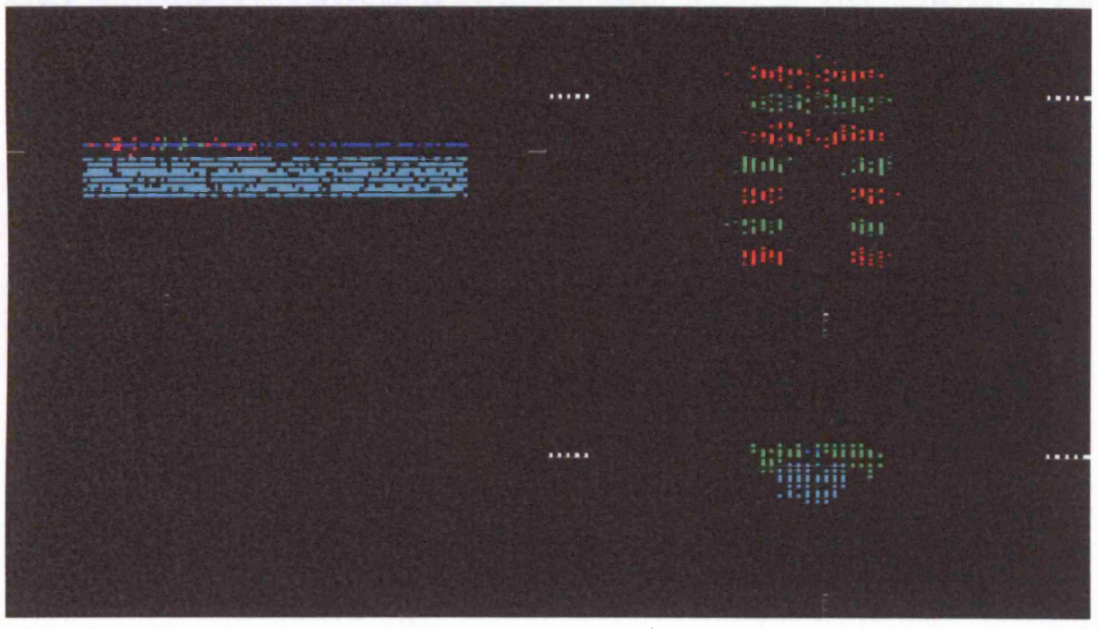

Figure 9-14: frame 0290 x 31 y 32 z 41

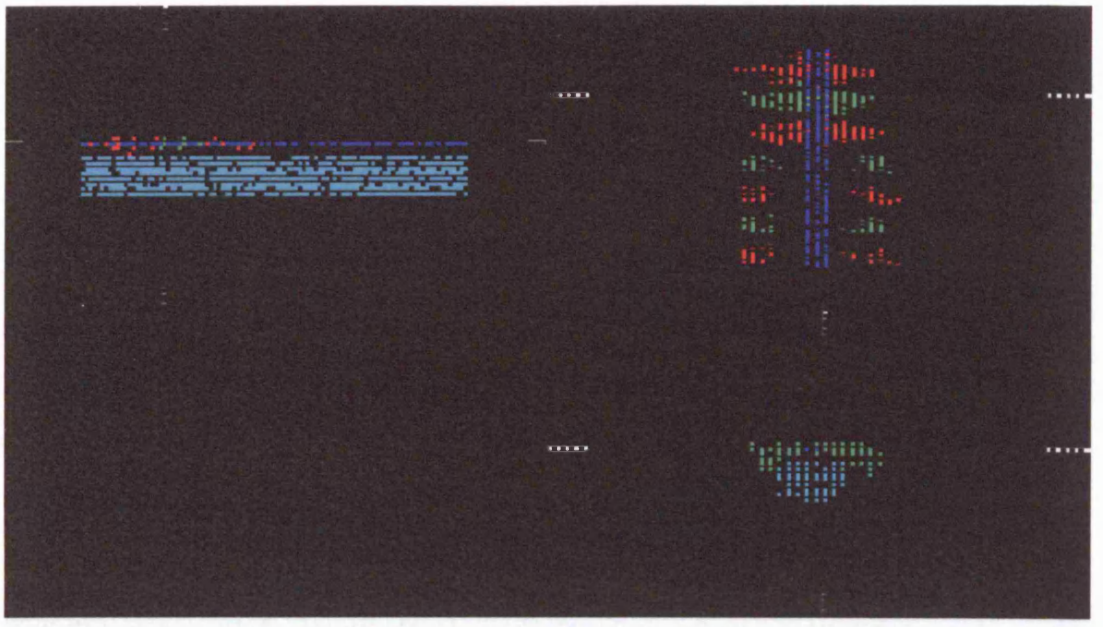

Figure 9-15: frame 0290 x 31 y 33 z 41

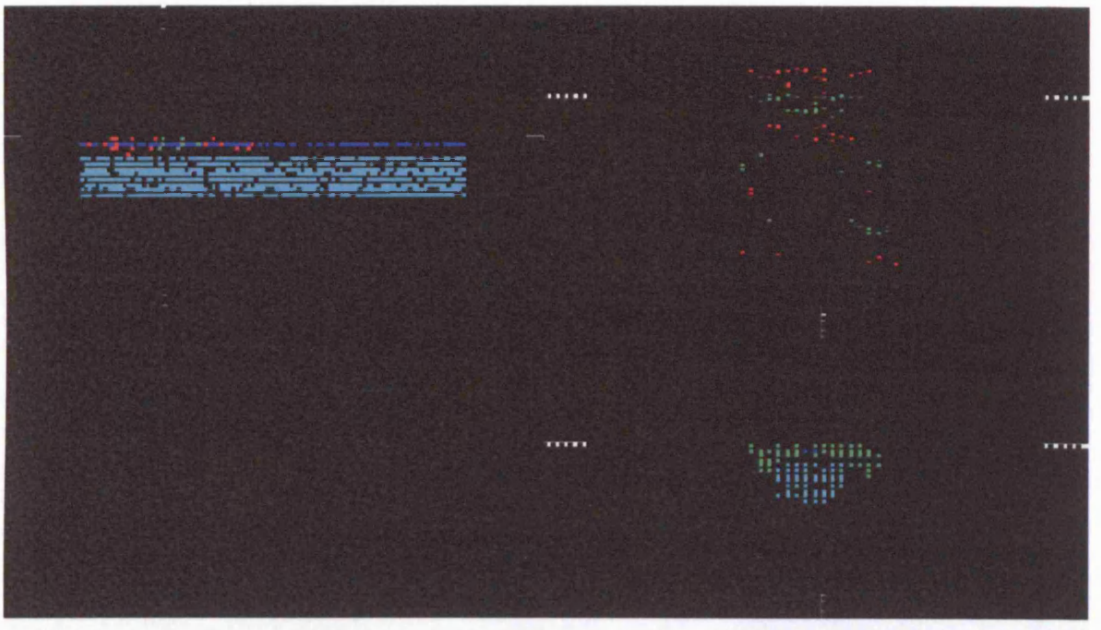

Figure 9-16: frame 0290 x 31 y 34 z 41

These figures illustrate how sclerotomal cells have migrated at this stage to surround the notochord dorsally and ventrally. The putative disk space remains preserved.

9.4.1.6 Comparison of young and old perinotochordal condensations

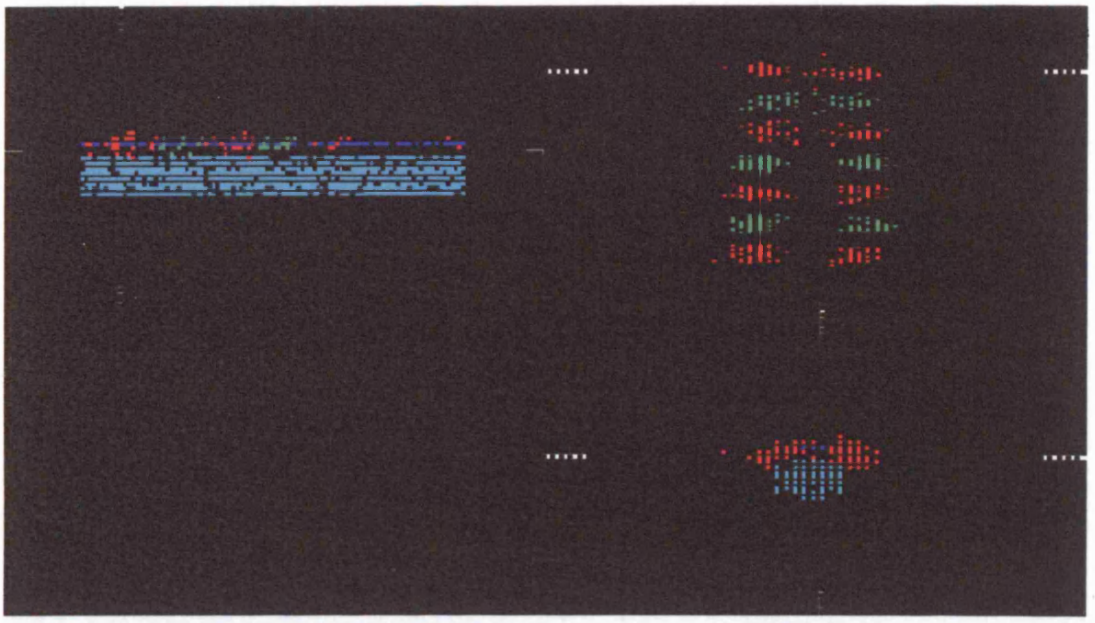

Figure 9-17: frame 0467 x 31 y 31 z 30

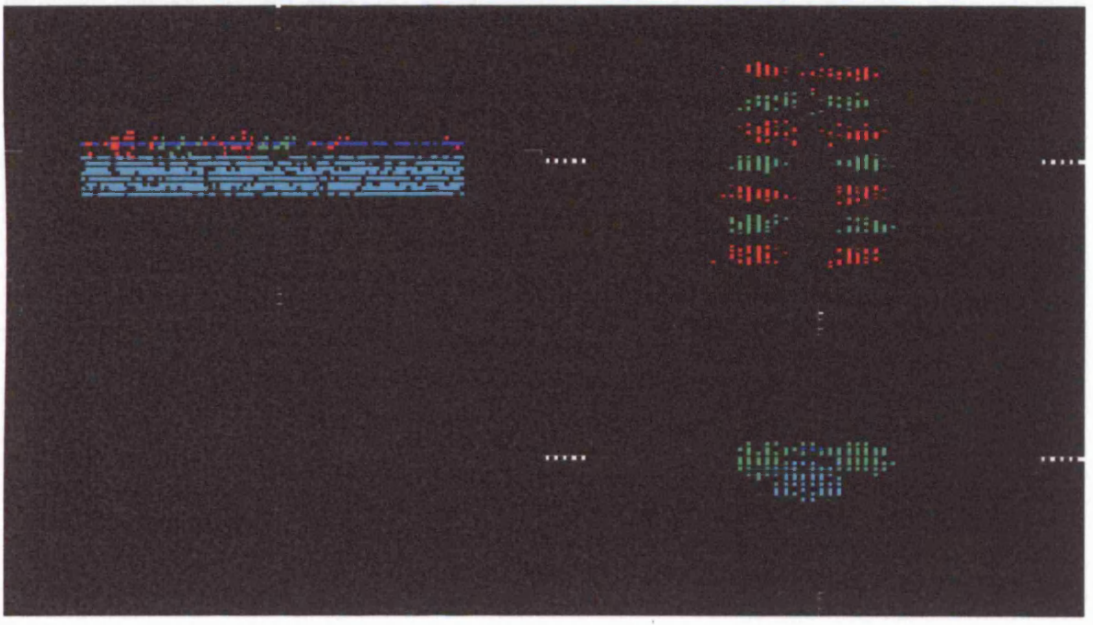

Figure 9-18: frame 0467 x 31 y 31 z 71

Figure 9-17 and Figure 9-18 compare the morphology of the condensation between an older stage (most cranial condensation) (Figure 9-17) and a younger stage (fourth condensation) (Figure 9-18). There is little difference between the two stages, although the views in the dorso-ventral and

cranio-caudal planes suggests that the condensation appears to "thin out" with time and conform more closely to the edge of the neural tube.

9.4.1.7 Examination of perinotochordal condensations in the sagittal plane

Figure 9-19 though to Figure 9-31 are successive cuts through the simulation from the lateral edge of the right sclerotome through to the lateral edge of the left sclerotome, and demonstrate the morphology of the cellular condensation in the sagittal plane.

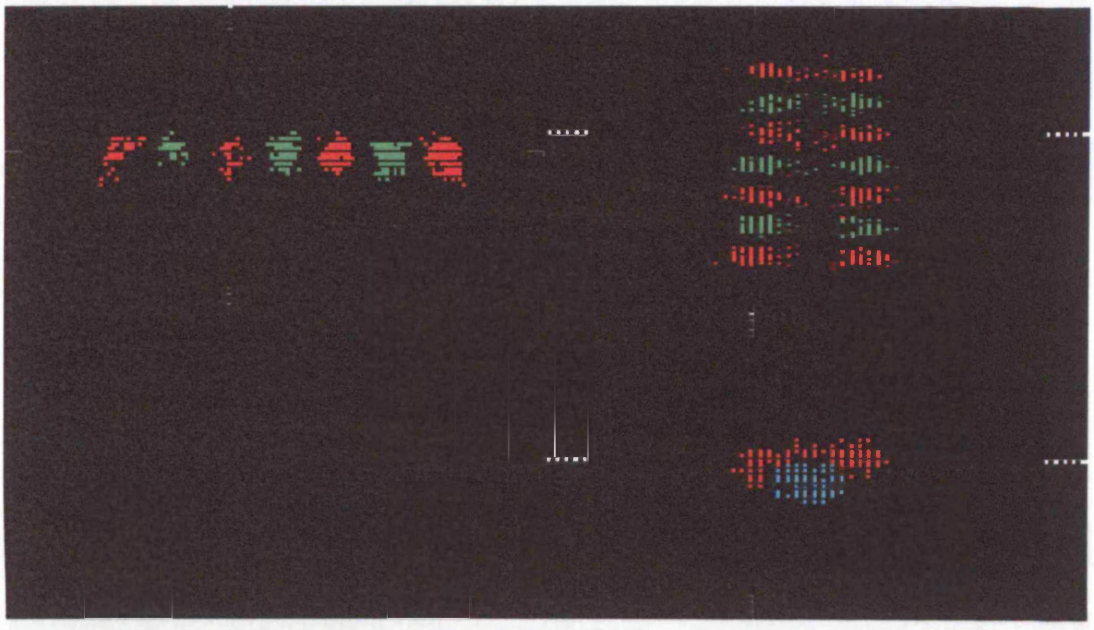

Figure 9-19: frame 0575 x 23 y 31 z 58

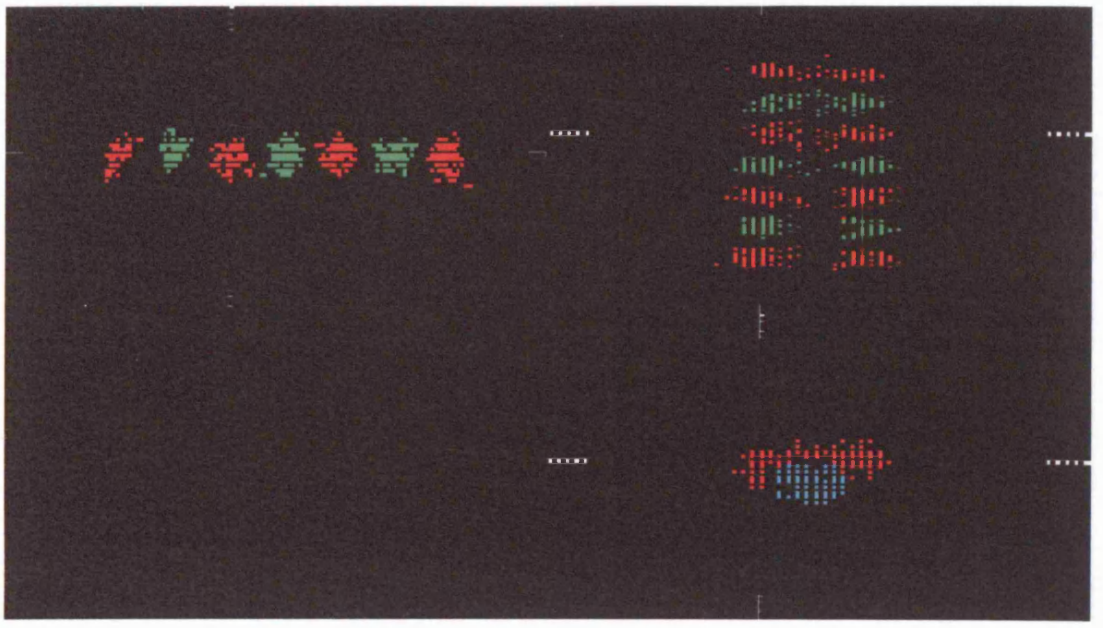

Figure 9-20: frame 0575 x 24 y 31 z 58

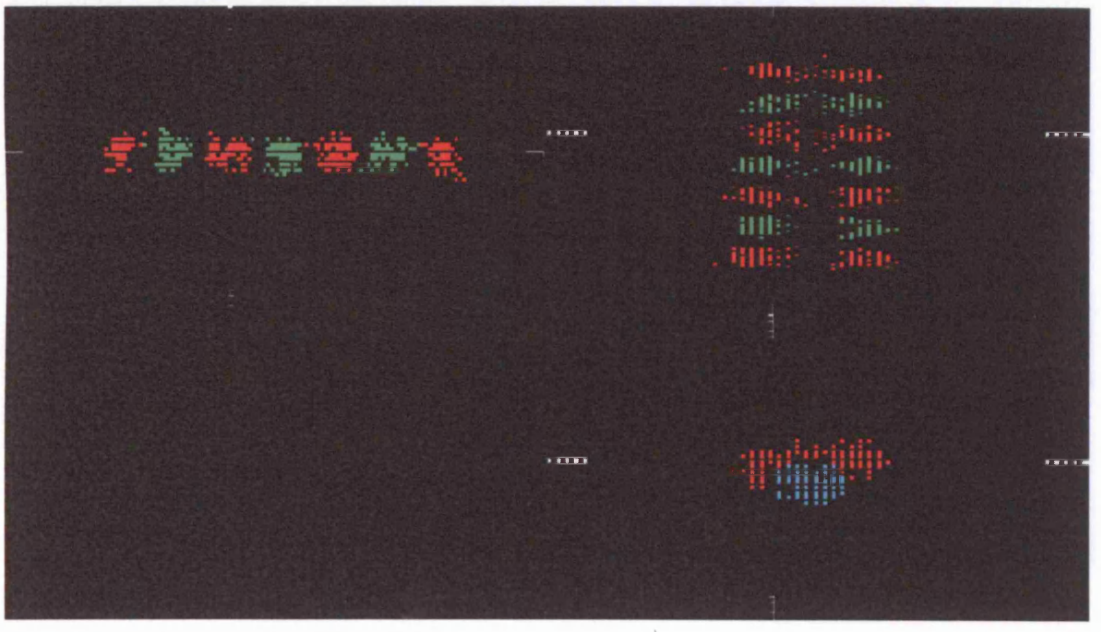

Figure 9-21: frame 0575 x 25 y 31 z 58

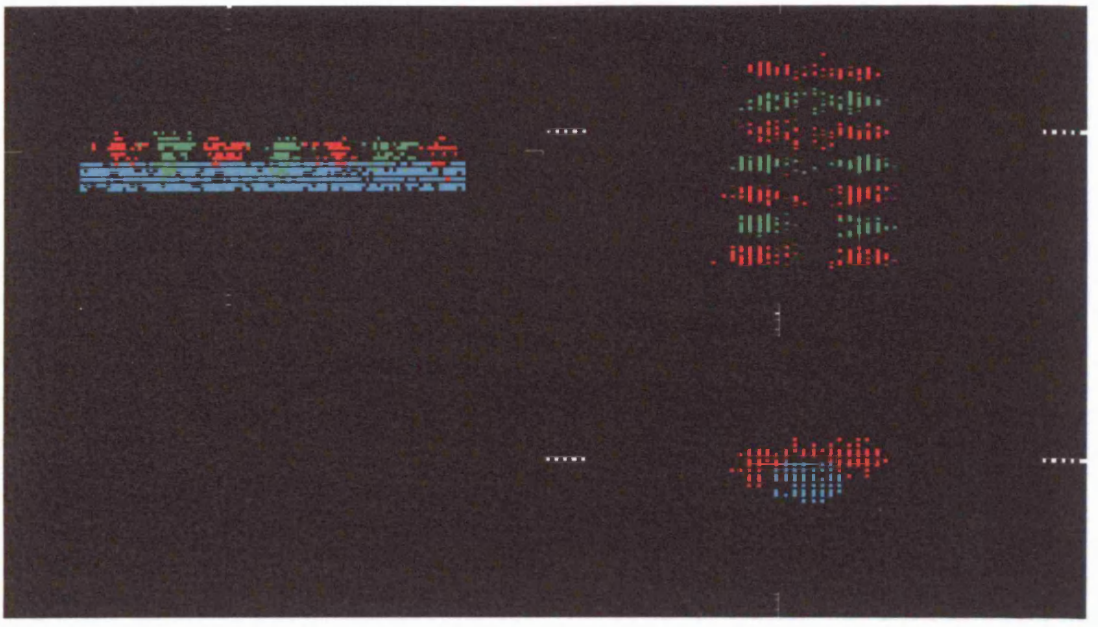

Figure 9-22: frame 0575 x 26 y 31 z 58

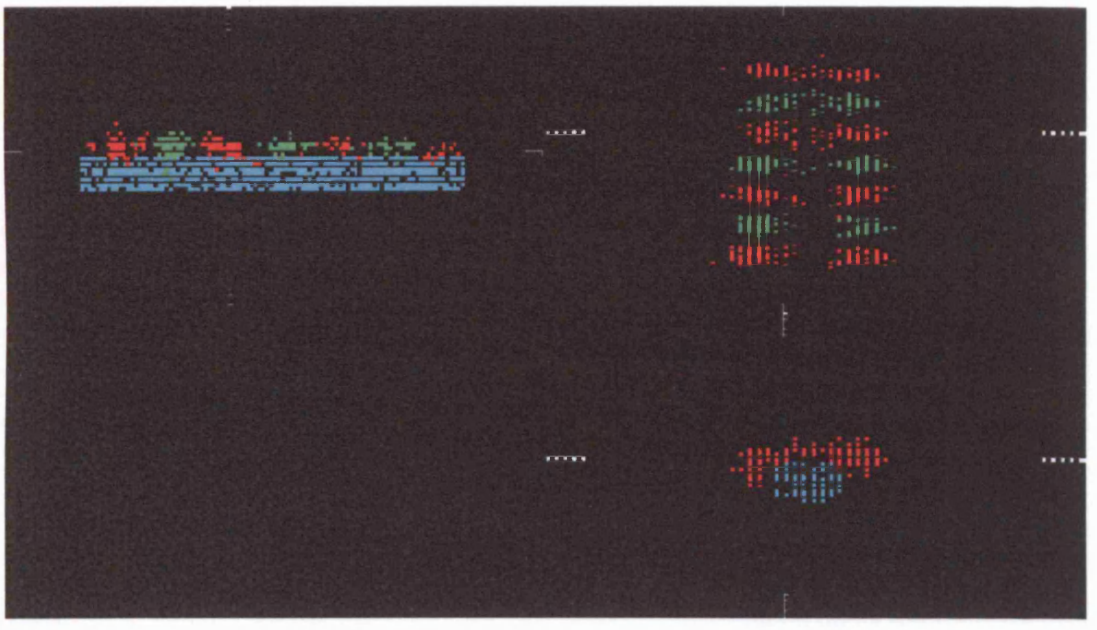

Figure 9-23: frame 0575 x 27 y 31 z 58

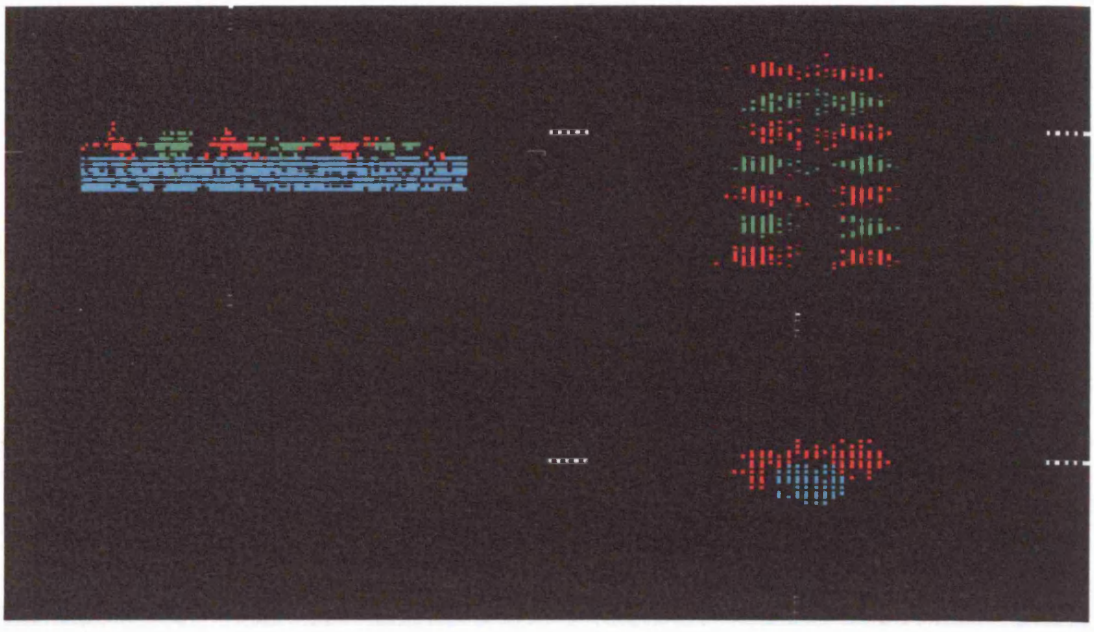

Figure 9-24: frame 0575 x 28 y 31 z 58

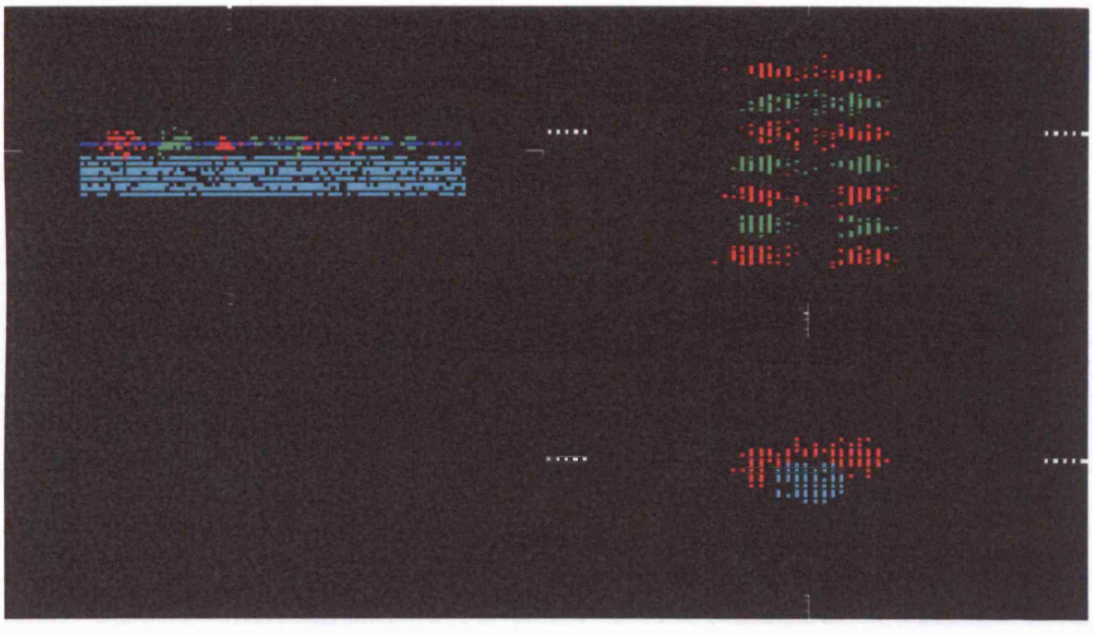

Figure 9-25: frame 0575 x 29 y 31 z 58

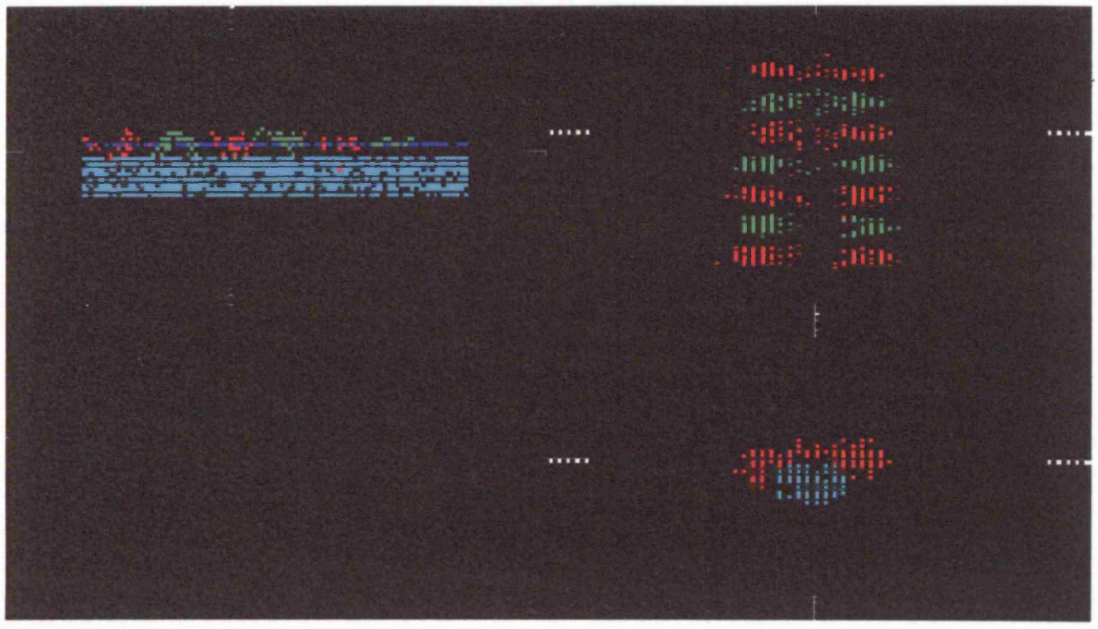

Figure 9-26: frame 0575 x 30 y 31 z 58

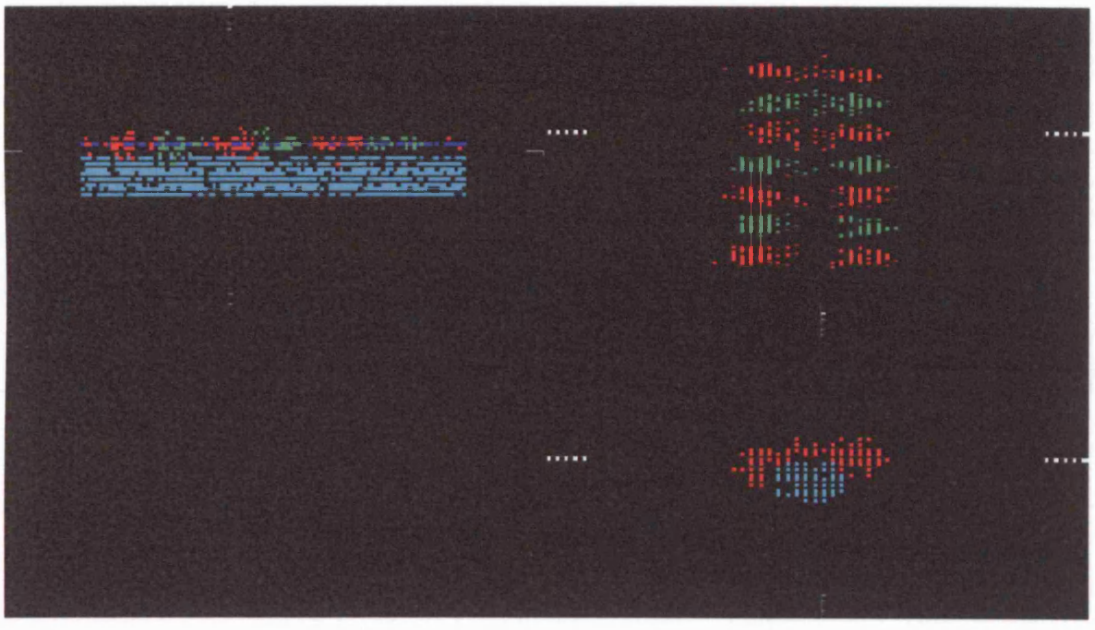

Figure 9-27: frame 0575 x 31 y 31 z 58

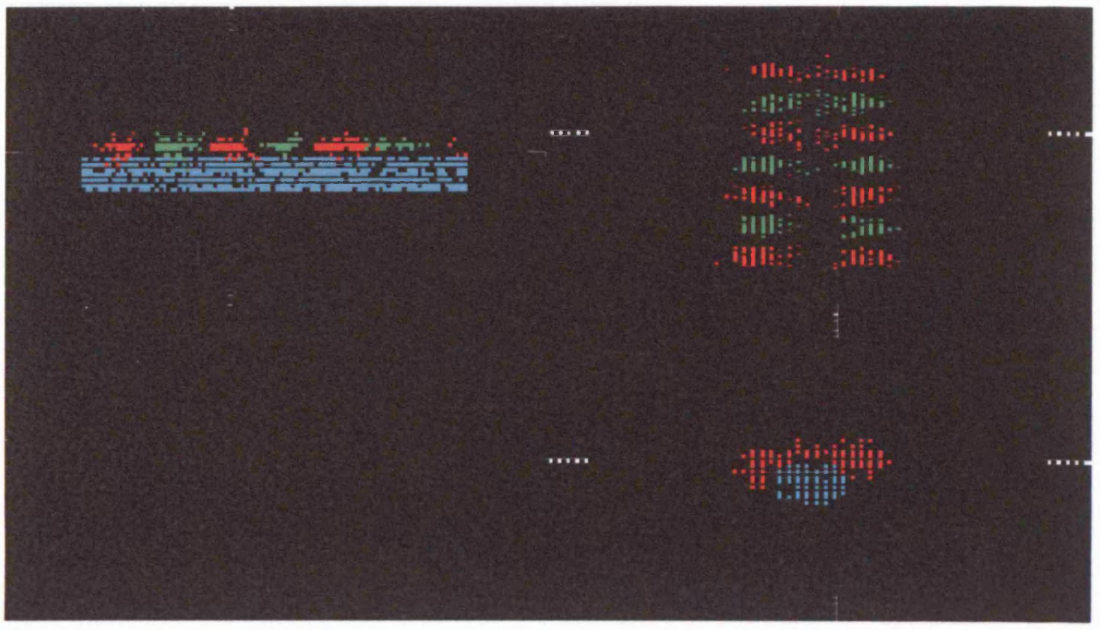

Figure 9-28: frame 0575 x 32 y 31 z 58

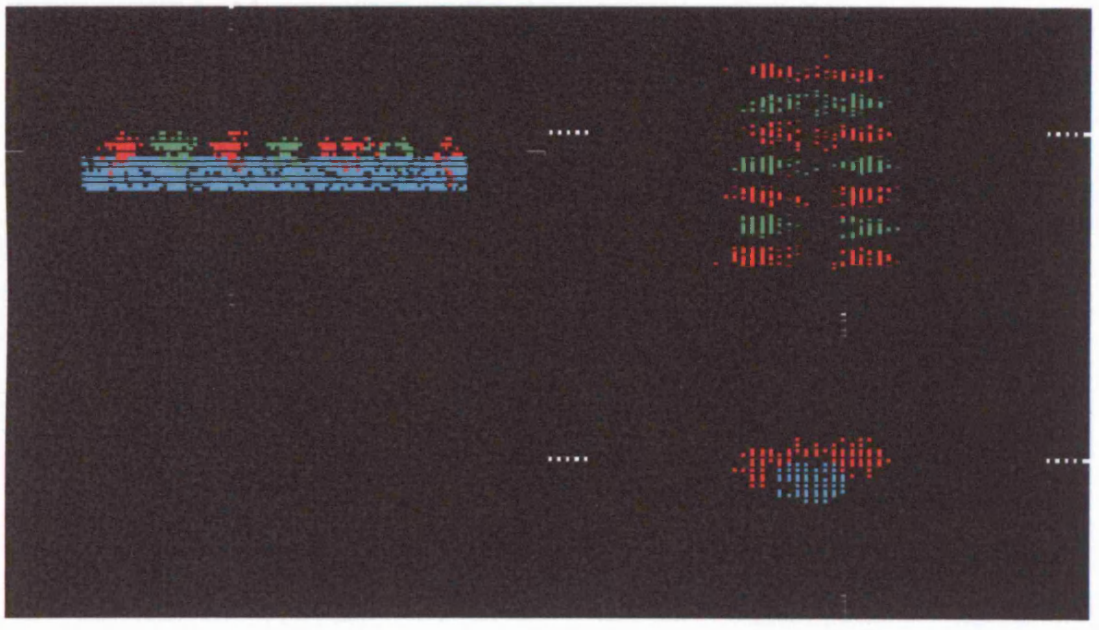

Figure 9-29: frame 0575 x 33 y 31 z 58

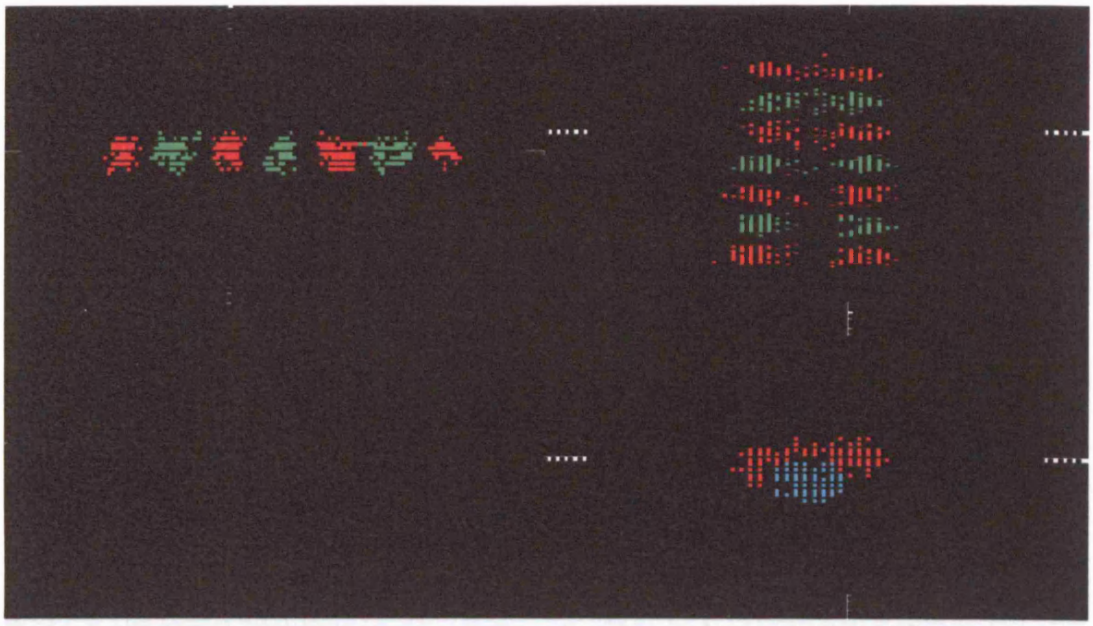

Figure 9-30: frame 0575 x 34 y 31 z 58

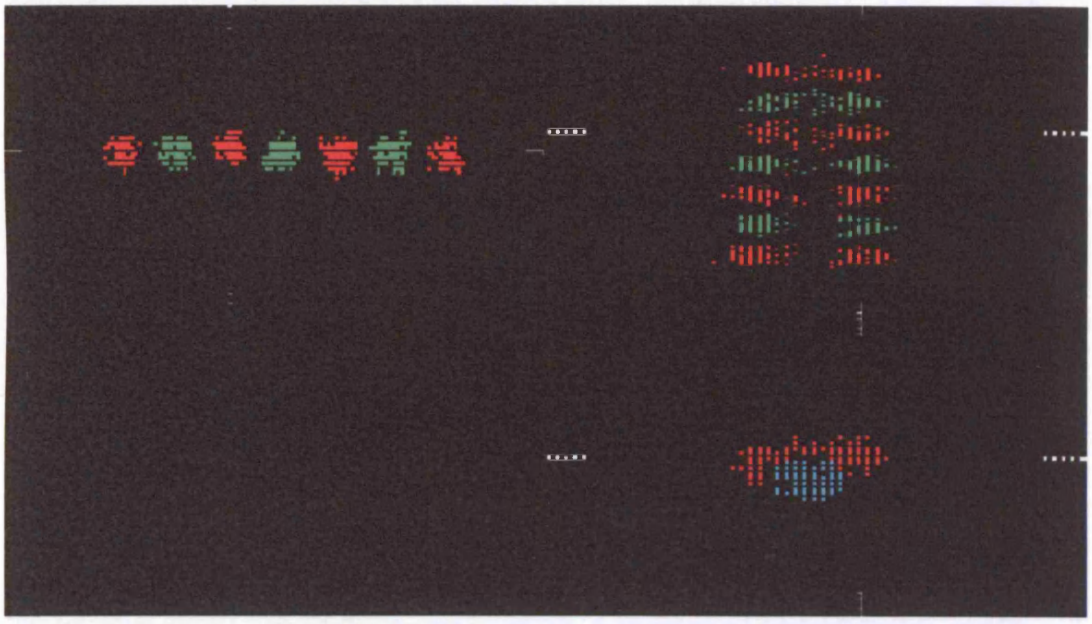

Figure 9-31: frame 0575 x 35 y 31 z 58

Figure 9-19 to Figure 9-31 demonstrate how the putative disk space – the space between adjacent sclerotomal cells – is preserved around the notochord – the medial compartment – and away from the notochord – the lateral compartment. Cells can also be seen to have migrated ventrally and dorsally around the notochord.

9.4.1.8 Role of cellular replication on cellular condensation formation

Figure 9-32 to Figure 9-34 demonstrate condensations with greater maturity than illustrated in Figure 9-19 to Figure 9-31.

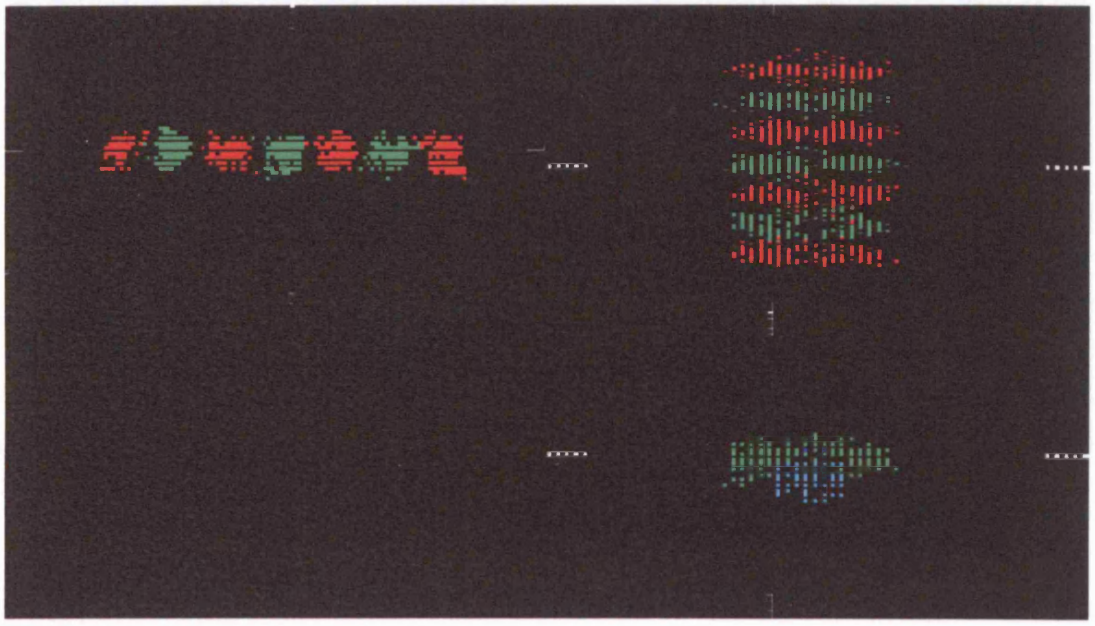

Figure 9-32: frame 0668 x 25 y 32 z 74

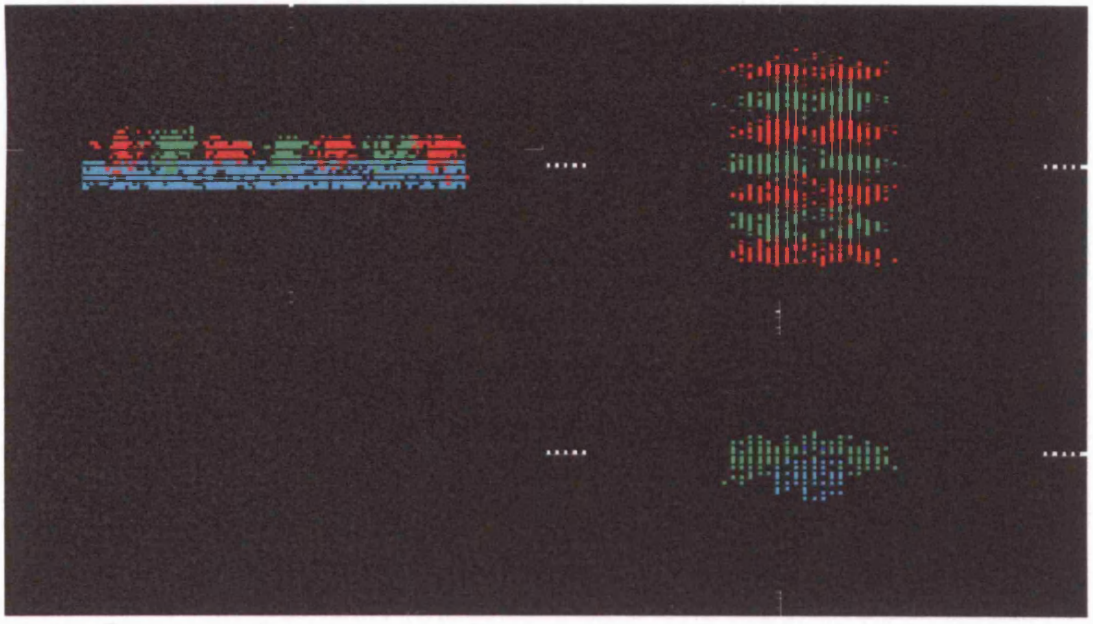

Figure 9-33: frame 0668 x 26 y 32 z 74

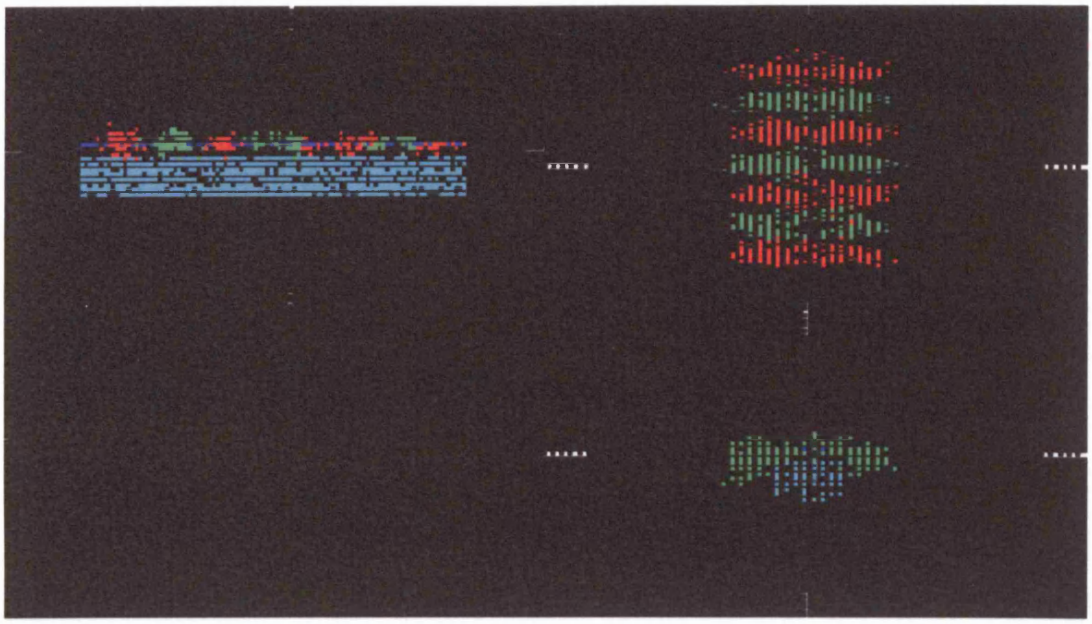

Figure 9-34: frame 0668 x 29 y 32 z 74

Whilst migration of the majority of cells depicted has been arrested, the condensations have continued to increase in size as a consequence of cellular replication. However, the inter sclerotomal clefts – putative disk spaces – remain preserved, and minimal intermingling of the adjacent sclerotomal populations has taken place.

9.5 DISCUSSION

This experiment has demonstrated that the simulator is able to emulate normal mammalian development. Whilst there is not exact concordance between the morphology of the computer and animal cellular condensations, the characteristics of the condensations in terms of cellular distribution are similar, that is restricted to the anterior region of the neural tube, around the neural elements, and surrounding the notochord.

This result implies that the morphogenetic mechanisms of chemotaxis and replication are sufficient to mimic the formation of the prevertebral cellular condensation. The theoretical model of notochord / anterior neural tube secreting morphogen, creating a concentration gradient of morphogen up which the sclerotomal cells migrate has been shown to be a potential mechanism through which this process might occur in the embryo.

Using the computer animation of this developmental process and the orthogonal viewer, it can be seen that most cells take a fairly direct route when migrating up the concentration gradient. The cells are seen to migrate in an orderly fashion on the animation towards the cellular condensation. Once this has been reached, migration ceases, and the condensation increases in size through cellular replication.

9.6 SUMMARY

This experiment has demonstrated that the theoretical model of vertebral column development outlined earlier using chemotaxis and cellular replication to build a prevertebral cellular condensation is one way in which this process might occur and a potential explanation how this process occurs in the embryo.

10 Experiment 2: experimental reliability

Within the simulation, there are random processes included in an attempt to emulate the demonstrably random nature of the cellular movements. This work describes two analyses to measure the reliability of the simulator program to produce consistent results in terms of the morphology of the prevertebral cellular condensation.

The random processes in the simulator program are:

1) selection of the cell to attempt movement at program level one.

2) random assignment of pseudopodia when movement in a particular direction is blocked by another cell occupying the selected location

3) random ability to replicate, and within this process the random location of the daughter cell

4) a random movement vector is added to the chemotaxis movement vector to produce the final movement vector.

5) when a cell is moving in the concentration gradient and has to "choose" between two or more alternative directions, this choice is made using random selection.

Most computer languages possess a pseudo-random number generator, which returns a relatively short sequence of numbers before the sequence repeats. In order to obtain truly random numbers, Knuths portable random number generator – rand3 – from Numerical recipes in C was used in *vert*[176] to generate a random number for the random processes described above.

To compare the reliability of *vert*, the simulator program was used to generate four simulations, labelled `29jan02a` to `29jan02d`, each with identical starting data and simulation parameters. Every 100th frame of the simulation was compared by visual inspection and using a program *imcf*.

10.1 VISUAL INSPECTION

Every 100th frame of the simulation datasets were compared in terms of condensation shape and size, whether adjacent condensations had fused in the craniocaudal and lateral medial axes. In order to increase the objectivity of the comparison Adobe Photoshop, version 5 (Adobe Systems, Incorporated, California, USA) was used to measure the maximum craniocaudal (height) and lateral to lateral (width) dimension of each formed pre-vertebral analgan.

10.2 IMAGE COMPARISON – *IMCF*

Imcf was written for this work. The program calculates the probability that a particular location (x,y,z) is occupied by a sclerotomal cell given a comparable series of frames from separate simulations. This is achieved by counting the number of times each location is occupied in the series of stimulations. The number of times each location is occupied is then stored at that location on an identically sized output array. The probability of location (*x,y,z*) being occupied by a sclerotomal cell is then found using the standard formula for probability:

$$P_{x,y,z} = \frac{n_{x,z,y}}{t}$$

where n is the number of times the location (*x,y,z*) was occupied and t is the total number of simulations analysed.

In order to identify those locations which formed the core of the structure formed by the sclerotomal cells, each location is then divided into a high probability, low probability and not occupied by a cell location.

The result is displayed graphically in three dimensions using Iris Explorer. A colour encoded sphere is displayed at each location of the output array. The colour of each sphere is shown in Table 10-1.

Probability	Colour
0.00 (location unoccupied)	black
0.01-0.25	green
0.26-0.49	blue
0.50-0.74	red
0.75-1.00	white

Table 10-1: Table of colour coded probability

An opacity value is assigned to each of the spheres as well as a colour. This has the effect of rendering the red and white spheres translucent and allows the internal structure of the object to be appreciated.

Imcf is executed from the command line and requires a single argument - the is the name of a text file containing up to ten binary vert output files that are to be compared. The colour map is illustrated graphically by the dialog box of the Generatecolormap module in Iris Explorer in Figure 10-1.

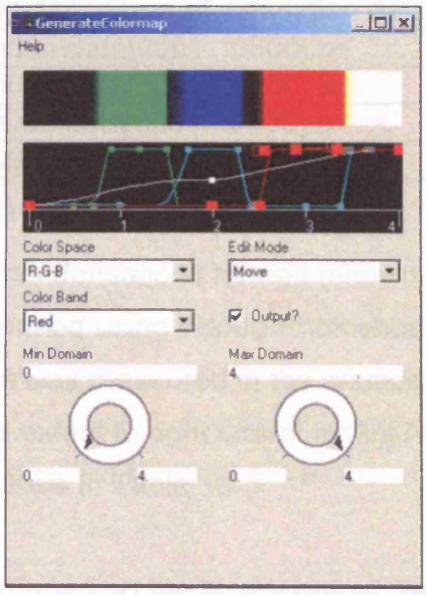

Figure 10-1: generatecolormap dialog box used to colour encode the probability of a location being occupied

10.3 HYPOTHESIS

That the morphology of the pre-vertebral condensations formed by successive simulations using identical parameters will be unchanged.

10.4 METHOD

10.4.1 Dataset creation

The basic test dataset adnoto and standard simulation program (Table 6-5) were used to generate four consecutive simulations using the standard simulation constants (Table 6-4). Screen images for visual analysis, and binary data files suitable for analysis by *imcf* of every 100th frame were written to the computer hard disk. The output files for each simulation were stored in the directories `e:\data\29jan02a` through to `e:\data\29jan02` on the simulation computer and are labelled as such in the illustrations in this chapter.

10.4.2 Dataset analysis

The filenames of the datasets generated is given in Table 10-2. The table also records the filename of the binary image files output by *vert* and subsequently analysed by *imcf*.

Directory name of simulation dataset
E:\data\29jan02\29jan02a\data[0001...0800].txt
E:\data\29jan02\29jan02b\data[0001...0800].txt
E:\data\29jan02\29jan02c\data[0001...0800].txt
E:\data\29jan02\29jan02d\data[0001...0800].txt

Table 10-2: Directory name of each simulation dataset

Visual analysis of the condensations formed (shown in Figure 10-3 to Figure 10-9) was performed using Adobe Photoshop. Each formed pre-vertebral condensation was measured in the craniocaudal dimension (height) and left lateral extent to right lateral extent (width) dimensions and the size recorded, in pixels in Table 10-3.

Imcf analysis was performed on the binary output files generated by *vert* and yielded Figure 10-12 and Figure 10-13.

10.5 RESULTS

10.5.1 Visual analysis

Images for comparison were displayed side by side using the 3D spherical view. The cellular condensations were visually inspected for size and location.

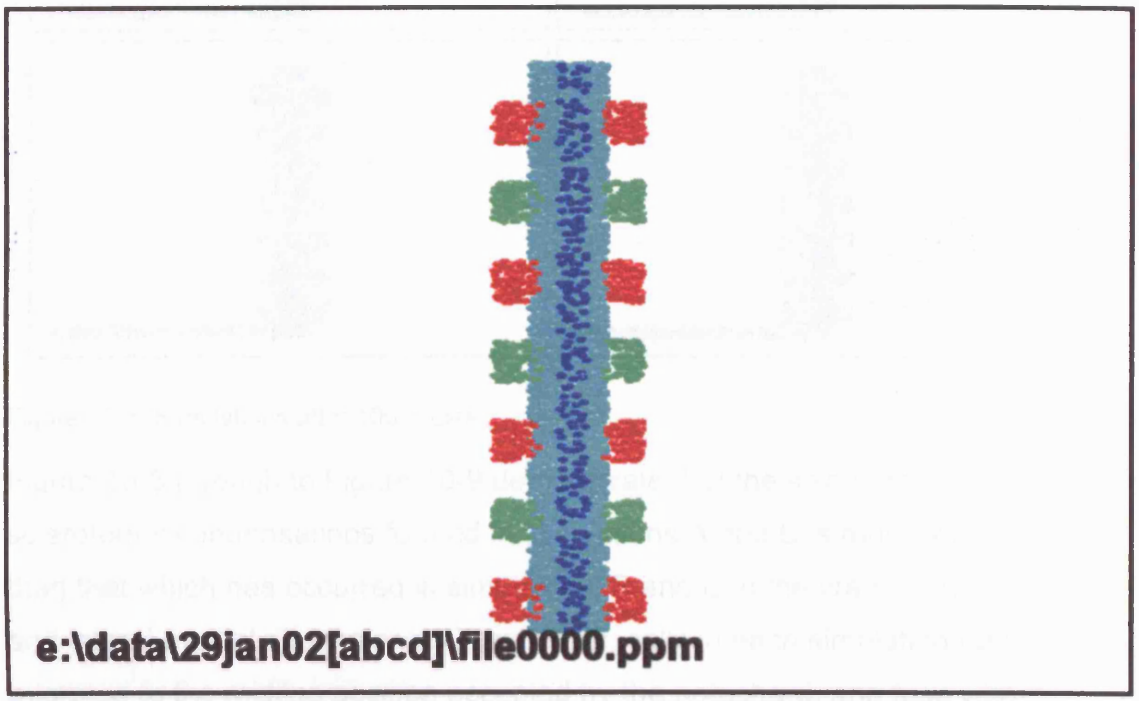

Figure 10-2: Starting position of cells in *adnoto* dataset. The legend e:\data\29jan02[abcd]\ indicates the simulation dataset the image is taken from (a to d). filename*nnnn*.ppm indicates the number of cycles completed by the simulations when the image was generated

As before in experiment 1, using the *adnoto* data set, the cranial sclerotome cells start migration immediately, ie after 0 program cycles. Subsequent sclerotome cells (in a cranio-caudal direction, as in the embryo) begin migration after every one hundred program cycles.

Figure 10-3 is taken at the end of the development of the first pre-vertebral condensation, and subsequent figures at the end of development of the subsequent vertebral condensations.

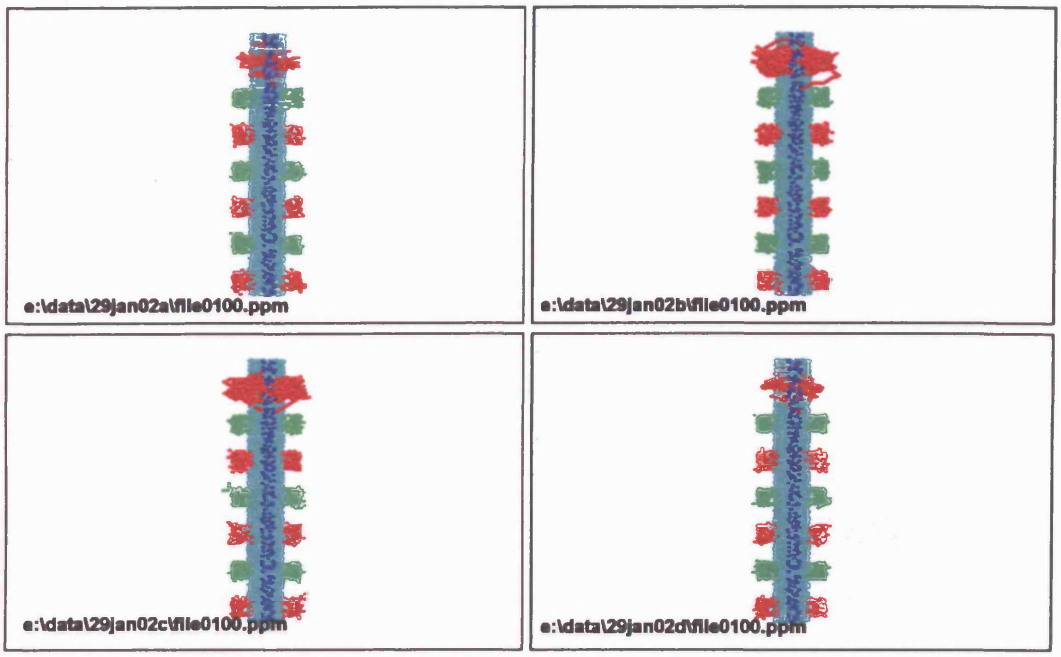

Figure 10-3: Simulations after 100 cycles

Figure 10-3 through to Figure 10-9 demonstrate that the size of the sclerotomal condensations formed in simulations A and D is much less than that which has occurred in simulations B and C in the cranio-caudal and lateral-medial dimensions. Despite this, cells in each simulation have migrated to the midline position occupied by the notochord, and fuse with the corresponding cell mass from the contralateral side to form the cellular condensation. A midline ventral cleft between the groups of cells from each side is apparent in simulations *a* and *d* for another further 400 program cycles, by which time replication of the cells in the condensation has occurred into the cleft, and thereby removing it.

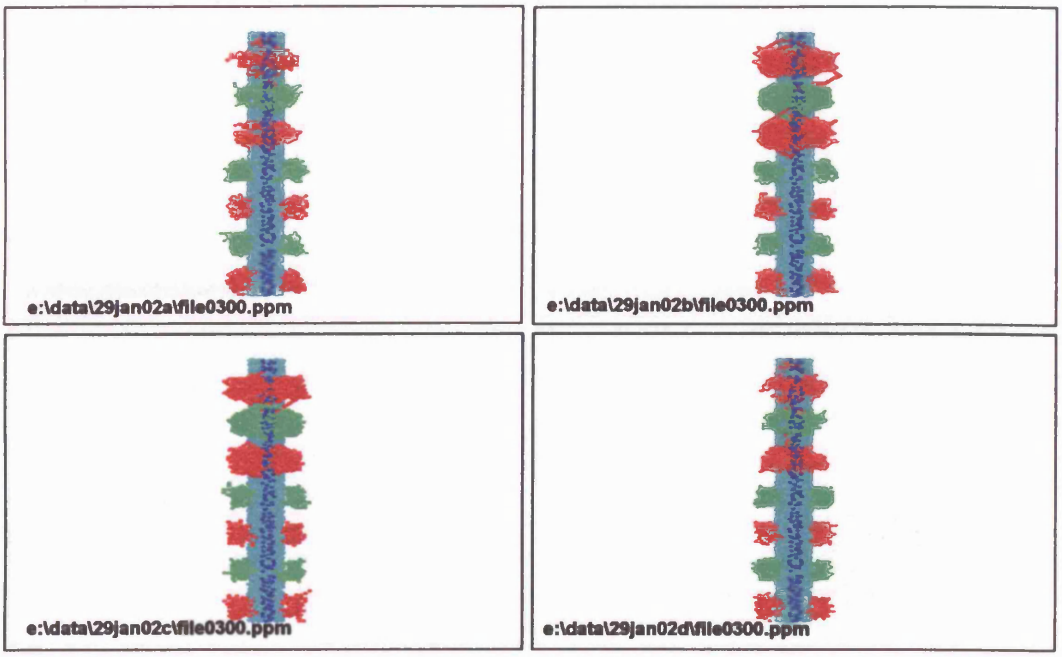

Figure 10-4: Simulation after 300 cycles

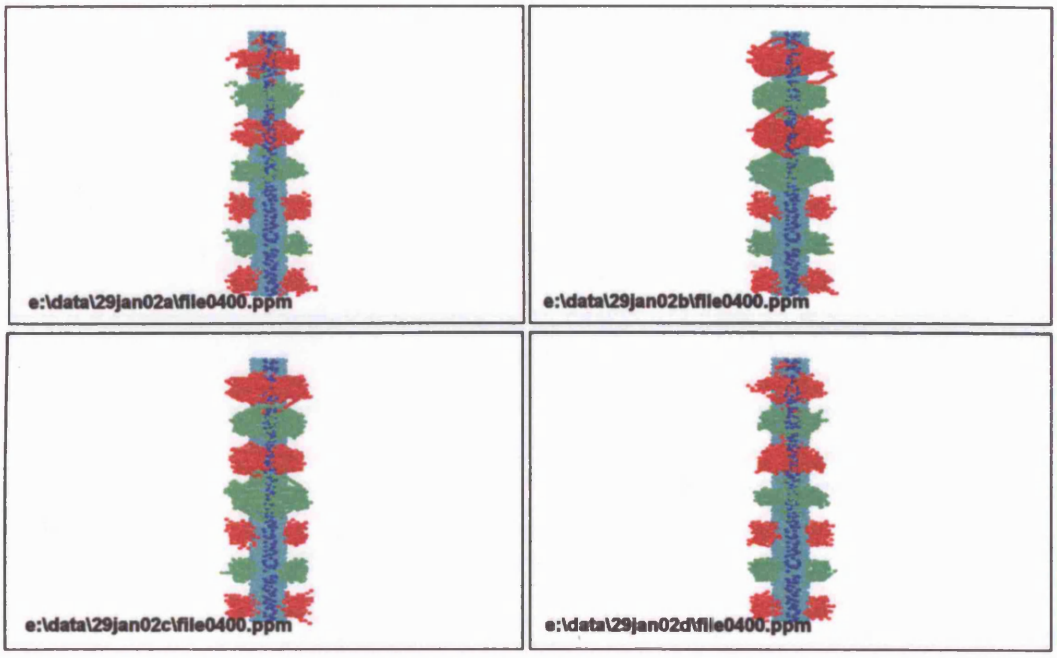

Figure 10-5: Simulation after 400 cycles

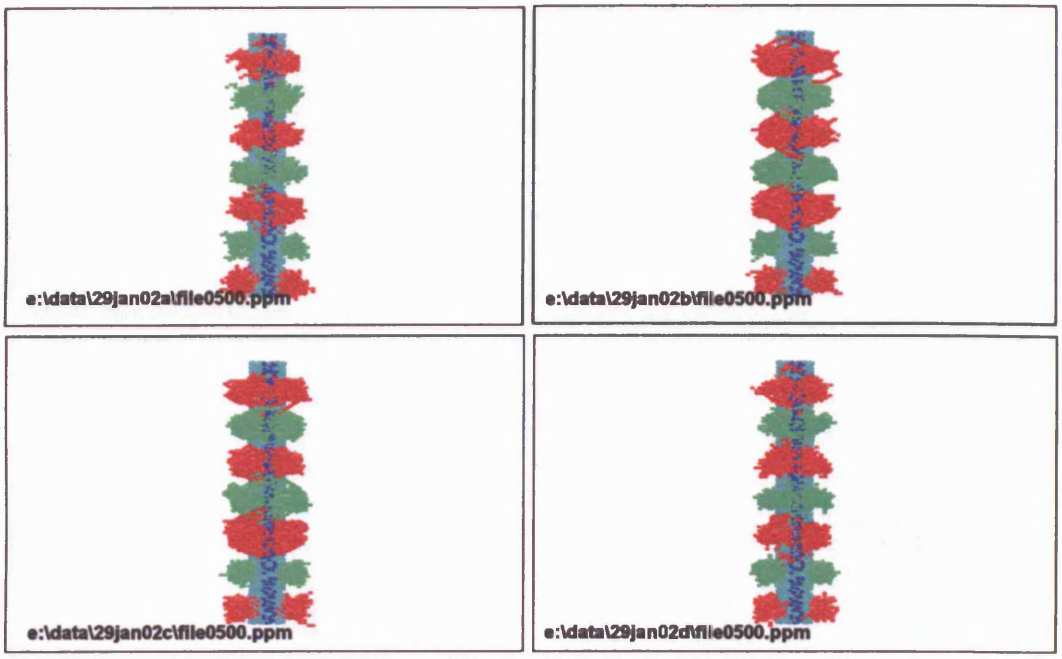

Figure 10-6: Simulation after 500 cycles

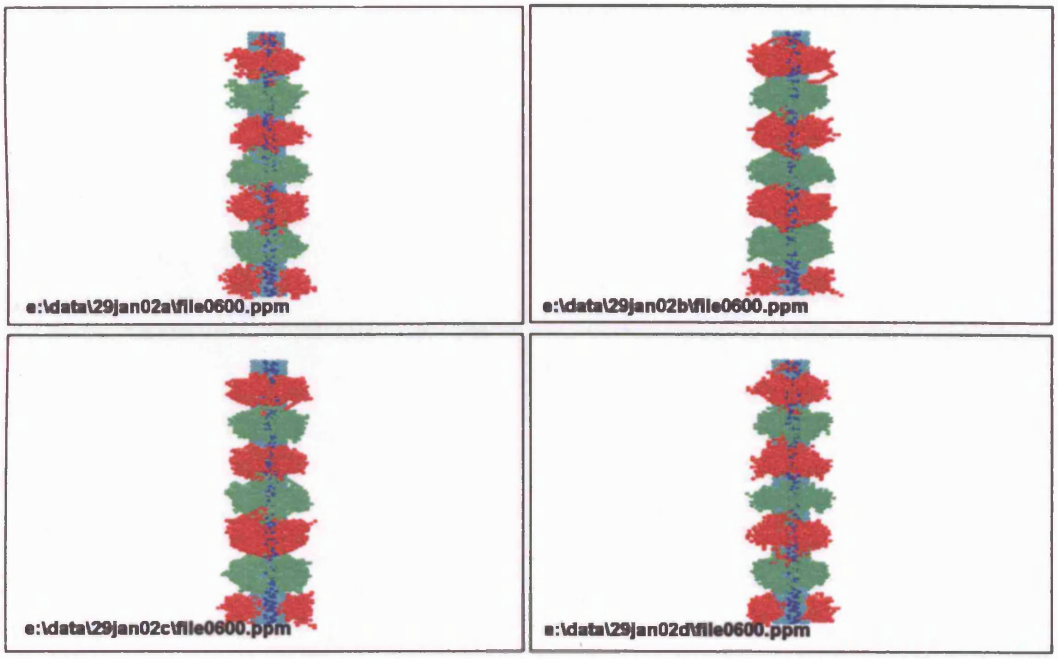

Figure 10-7: Simulation after 600 cycles

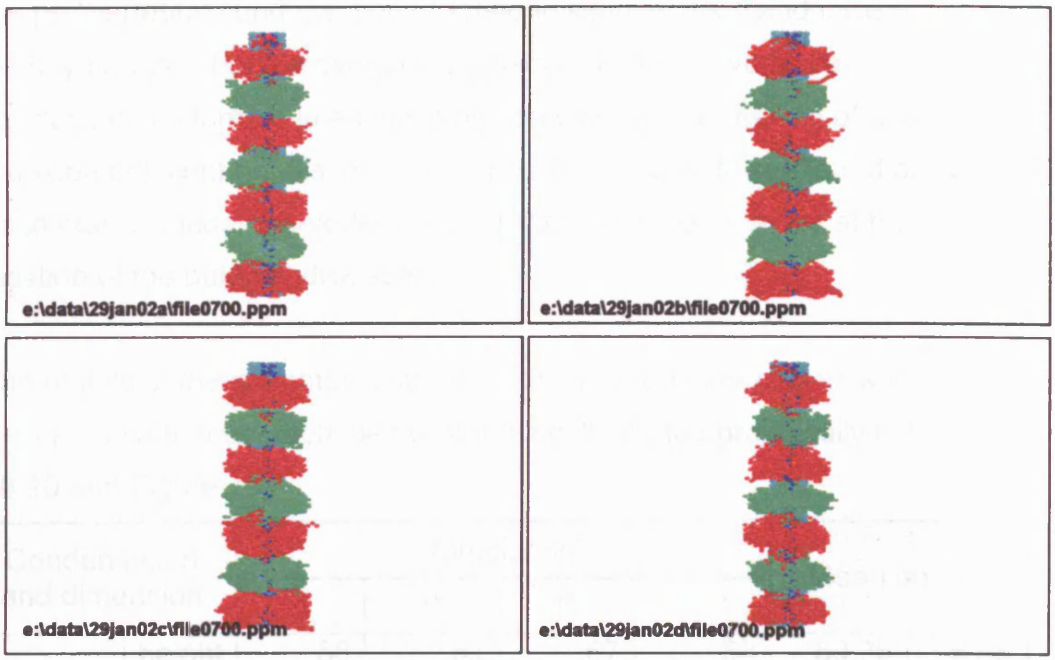

Figure 10-8: Simulation after 700 cycles

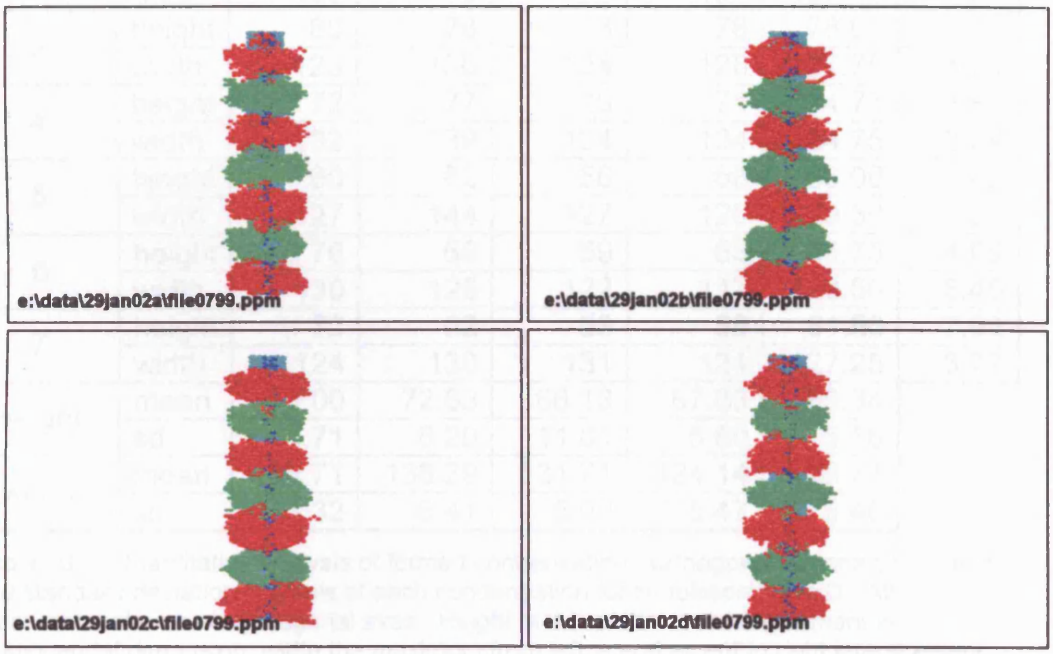

Figure 10-9: Simulation after 799 cycles

Overall it can be seen the fusion across the midline of the migrating sclerotome cells occurs at the same time in each simulation, and that in simulations *b* and *c* there appeared to be many more sclerotome cells in the condensations earlier in the simulation, probably due to a greater number of cell replications taking place. By the end of each simulation,

the pre-vertebral condensations formed in simulations *b* and *c* were slightly broader, but the overall morphology of the pre-vertebral condensations formed in each simulation was similar. Mixing of cells between adjacent populations did not occur and a cleft was found between each cranio-caudal pre-vertebral condensation in each series at the location of the putative disk space.

The results of the quantitative analysis of the three dimensional spherical view are given in the table below, and also illustrated graphically in Figure 10-10 and Figure 10-11.

Condensation and dimension		Simulation				Mean and sd	
		A	B	C	D		
1	height	58	61	67	53	59.75	5.85
	width	121	150	149	122	135.50	16.18
2	height	76	74	59	75	71.00	8.04
	width	130	130	135	124	129.75	4.50
3	height	80	78	78	76	78.00	1.63
	width	123	136	124	128	127.75	5.91
4	height	72	77	79	71	74.75	3.86
	width	132	139	134	134	134.75	2.99
5	height	60	82	56	66	66.00	11.43
	width	127	144	127	120	129.50	10.21
6	height	70	69	59	65	65.75	4.99
	width	130	125	122	117	123.50	5.45
7	height	72	62	53	59	61.50	7.94
	width	124	130	131	124	127.25	3.77
height	mean	71.00	72.63	66.13	67.63	69.34	
	sd	5.71	6.20	11.01	5.60	5.56	
width	mean	126.71	136.29	131.71	124.14	129.71	
	sd	3.32	6.41	5.00	5.47	3.40	

Table 10-3: Quantitative analysis of formed condensation - orthogonal dimensions, mean and standard deviation in pixels of each condensation for simulations A to D. All measurements are on orthogonal axes. Height is the maximum measurement in craniocaudal dimension, width the maximum from left lateral extent to right lateral extent.

This analysis demonstrates the average height and width of the cellular condensations created by each simulation was similar (Figure 10-10). However, Figure 10-11 demonstrates that variability does exist in condensation size - a trend towards the condensations in the centre of the craniocaudal dimension, ie the 3rd and 4th being larger than the more peripheral condensations.

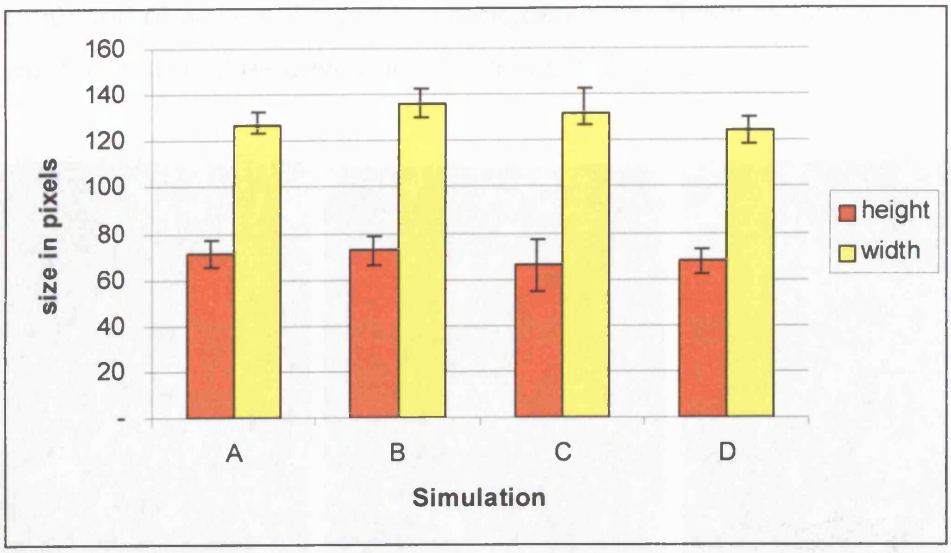

Figure 10-10: the graph demonstrates the average condensation size and standard deviation (error bars) created in each simulation.

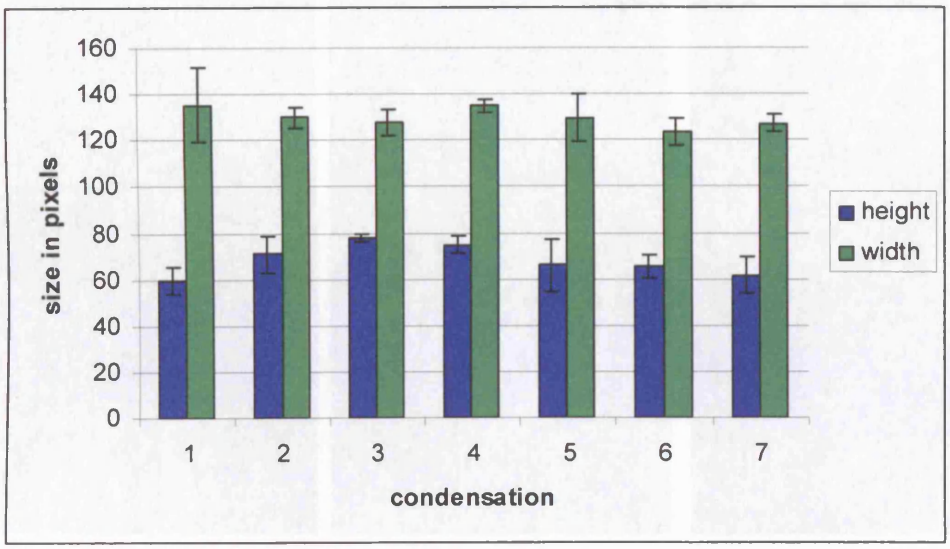

Figure 10-11: graph to demonstrate the average size of each condensation created in simulations A to D, where 1 is the most cranial and 7 the most caudal. Error bars indicate the standard deviation.

10.5.2 Imcf analysis

Figure 10-12 and Figure 10-13 demonstrate the probability of cellular occupancy as calculated by *imcf* at 100 cycle intervals throughout the simulation. Between every sclerotomal cellular condensation, an intersclerotomic cleft has been preserved. The majority of each structure

is composed of white cells and this indicates a significant similarity between the structures developed in each simulation.

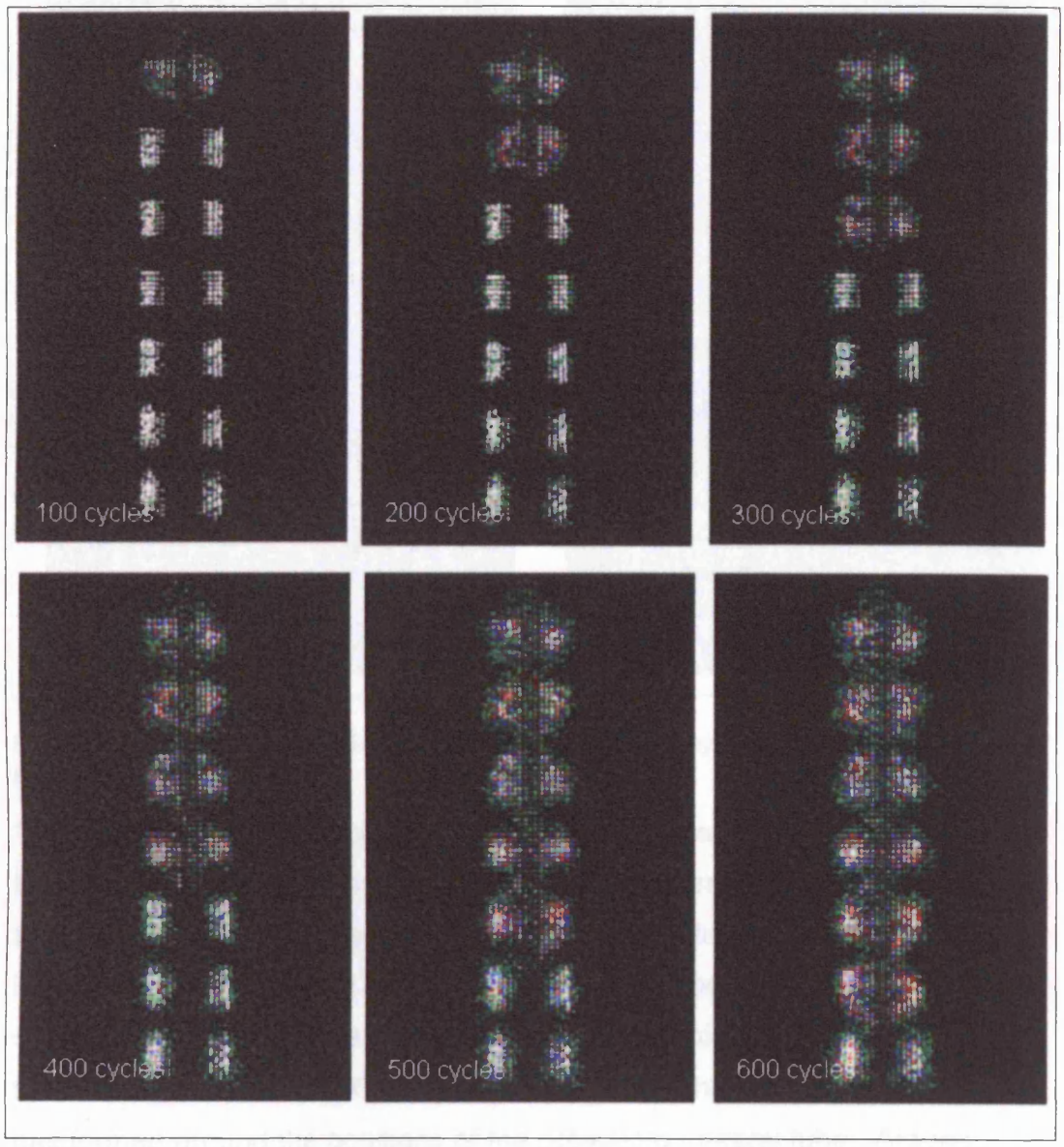

Figure 10-12: probability of cellular occupancy calculated by *imcf* at 100 cycle intervals. 100 cycles is shown at the top left, 600 cycles at the bottom right.

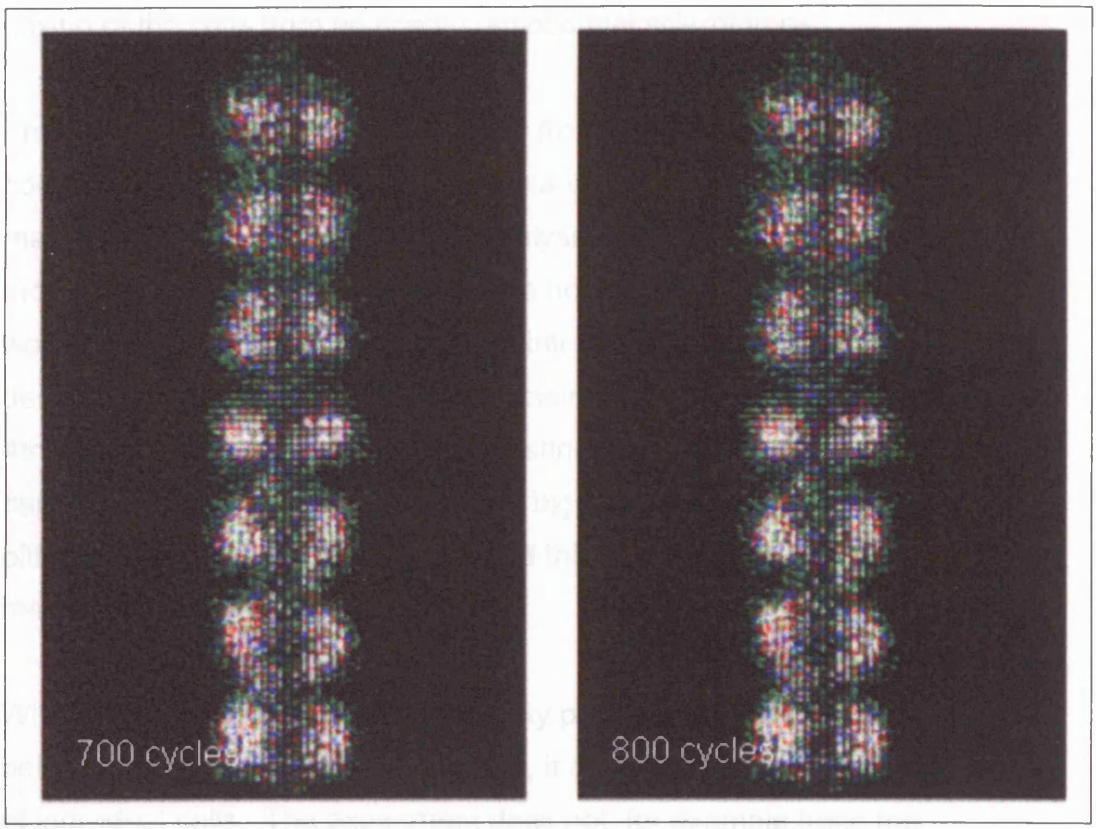

Figure 10-13: probability of cellular occupancy as calculated by *imcf* at 100 cycles intervals

This analysis does not provide information on cellular mixing, which must be obtained from the 3D spherical view. From the images, it can be seen that although fusion of the sclerotomal cellular condensation has occurred in every case, the highest density of white cells is found either side of the midline, with an hourglass constriction across the midline. Examination of the three dimensional VRML model demonstrates how the condensation has formed around the positions of the notochord / neural tube. Around the edge of each condensation a rim of red cells can be seen.

10.6 DISCUSSION

Review of the results presented in the visual analysis and *Imcf* analysis sections demonstrate that there is a significant similarity between the structures developed in each simulation despite the random processes built into the simulation. Additionally, there is consistently preservation of

an inter somitic cleft at the site of the putative disk space, and a lack of mixing of the cells from adjacent craniocaudal sclerotomes.

The data presented here is formalised from four simulations, however, concurs with a much larger body of data visually rather than mathematically analysed. Further analysis of this data, particularly the movement of the cells in relation to the hormone concentration gradients would also provide additional insights into, at least, the simulated developmental process, and might explain the consistently larger 3rd and 4th cellular condensations. It is interesting to speculate that the mid to caudal mammalian vertebrae are also bigger than the vertebrae found at either end of the vertebral column, and this might be a potential mechanism for this variation.

Whilst this experiment on reproducibility provides information about the behaviour of the generality of the cells, it does not examine the behaviour of individual cells. The experiment does not, for example trace the pathways of individual cellular migration, which maybe geometrically linear or rather more random. The experiments also do not describe the behaviour of the cells when an individual cells collides with an established condensation – whether the cells simply accumulate and move no further, forming effectively a linear spur, or whether the cells spill around the condensation in an attempt to continue to move up the condensation gradient.

A fundamental weakness of the visual analysis is the method of measuring the size of each condensation. Given that these are three dimensional structures, measurement in two dimensions is somewhat simplistic. However, as inspection of the VRML model demonstrates, in 3 dimensions a complex shape around the neural tube / notochord is produced, and in fact, the most consistent dimensions are those that have been measured. These are also the simplest measurements. Accurate measurements of the dimensions of the three dimensional shape would be complex, and because of this, unreliable.

In conclusion, these experiments demonstrate a high degree of consistency between each simulation, and therefore indicates that the structures formed are not the result of chance, but occur as a result of the morphogenic influences on the sclerotomal cellular migration and replication.

10.7 SUMMARY

The experiment reported in this chapter has demonstrated that there is consistency in the form of the generated cellular condensations across several simulations, and that the shapes formed are not merely a consequence of the random functions employed within the simulator program.

11 Experiment 3: mechanisms of development

The aim of the work reported in this chapter is to determine whether both of the morphogenetic mechanisms employed in the work in Chapters 9 and 10 are required to form the pre-vertebral cellular condensation.

Animal experimental evidence suggests that whilst replication is important in generating a normal sized structure, segmentation will proceed in the absence of replication. Tam investigated this by using mitomycin C, exposing pregnant mice to mitomycin C at either 6.5 days pc or 7 days pc, during development of the primitive streak. Examination of embryos at 7.5 days pc and 8.5 days pc demonstrated small but morphologically normal embryos. At birth, normal size had been achieved, presumably through compensatory growth[177]. This scenario is examined in this chapter in the first experiment, where the cellular replication rate constant is reduced to 2%.

That cellular migration is required for the pre-vertebral cellular condensation formation is tested in the second experiment in this chapter. Dalgleish contended that the only mechanism required for the formation of the thoracic vertebrae in the rat was cellular replication[178]. Chernoff and Lash used cytochalasin D to inhibit cellular movement and found cellular movement and therefore somite formation did not occur[179]. The VPL program used in the second experiment does not include a cellular movement command, and hence only cellular replication occurs.

11.1 HYPOTHESIS

The work reported in this chapter tests the hypothesis that replication and cellular migration are required for the development of the pre-vertebral cellular condensation.

11.2 METHOD

Two experiments were performed, each with an identical initial arrangement of the cells, using the dataset *adnoto* as shown in Figure 9-1 on page 9-111.

The first experiment tested whether cellular migration alone would be sufficient to generate a structure similar to that found in Figure 9-2 on page 9-112. The value of the replication constants is given in Table 11-1 and the VPL simulation program used is shown in Table 11-2. Replication was decreased to 2% in this experiment.

Simulation constant	value
replication	0.02
diffusion	0.0005
secretion	0.1

Table 11-1: simulation constants for cellular migration experiment

Level 1	Level 2	Level 3
movement	time	display
replicate	display	
	secrete	
	diffuse	
	store	
	write image	

Table 11-2: VPL simulation program for cellular migration experiment

The second experiment tested whether cellular replication alone would create a structure similar to that found in Figure 9-2 on page 9-112. The VPL simulation program used is shown in Table 11-4 and the replication constants in Table 11-3. Replication was unaltered from the default value of 6%, but cells were unable to migrate.

Simulation constant	value
replication	0.06
diffusion	0.0005
secretion	0.1

Table 11-3: simulation constants for cellular replication experiment

Level 1	Level 2	Level 3
replicate	time	display
	display	
	secrete	
	diffuse	

	store	
	write image	

Table 11-4: VPL simulation program for cellular replication experiment

Each sclerotome segment was activated for two hundred outer loop cycles. The simulator was programmed to perform 800 outer loop cycles in total. The output was analysed using an animation created by the 3 Dimensional spherical view and VRML models.

11.3 OUTCOME MEASURE

The structure generated in each experiment was compared to that shown in Figure 9-2 using the generic outcome measures listed in Table 7-2.

11.4 RESULTS

11.4.1 Cellular migration

The structure formed at the end of the cellular migration experiment is shown in Figure 11-1 and in VRML format on the CDROM. An animation of the complete developmental sequence is given on the CDROM.

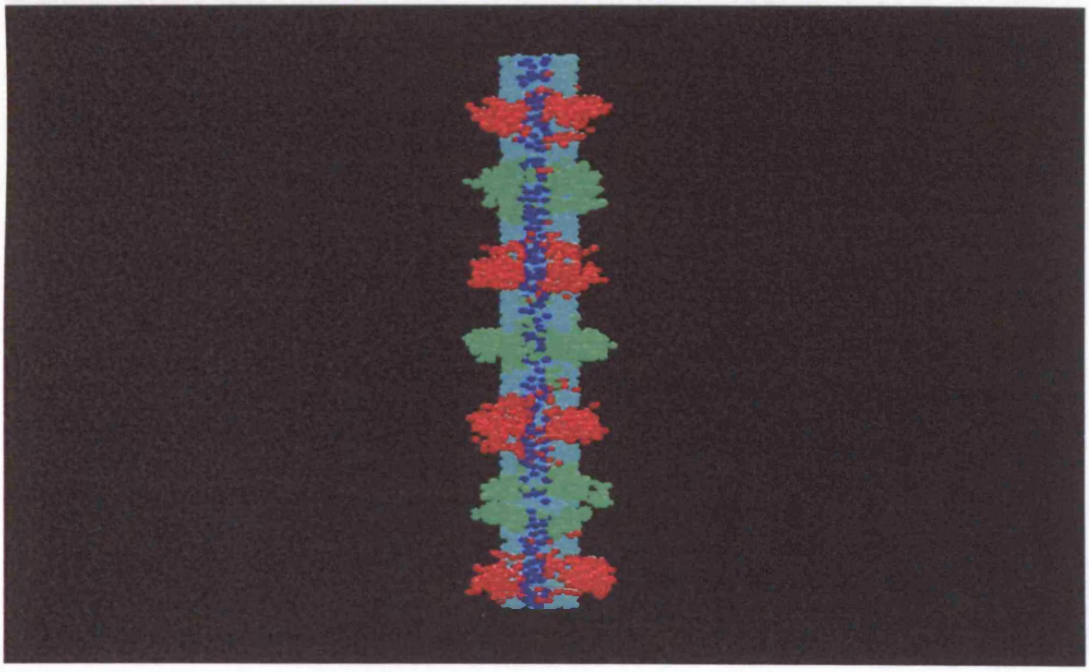

Figure 11-1: final frame of simulation. The cells have migrated to surround the anterior structures, but fusion has not taken place.

The figure demonstrates that whilst cells have migrated medially from their initial lateral position towards the midline structures, the largest density of

cells lies in a paramedian position, and the cells from either side do not meet across the midline to any significant degree – that is there is very little fusion of the cell masses from either side. The morphology of the cellular condensations has also altered from a more spherical shape to an elongated one. Analysis according to the generic outcome measures demonstrates that no cell mixing between adjacent cranio-caudal levels occurs (measure 1) and the disk space is preserved (measure 2). Fusion across and around the notochord might occur in that the cell masses from either side come close to the midline but do not generally meet (measure 3). Cells are not seen crossing the midline (measure 6). Measure 4 and 5 are not relevant to this experiment.

11.4.2 Cellular replication

The structure formed following completion of the cellular replication experiment is shown in Figure 11-2 and in VRML formation on the CDROM. An animation of the complete developmental sequence is given on the CDROM.

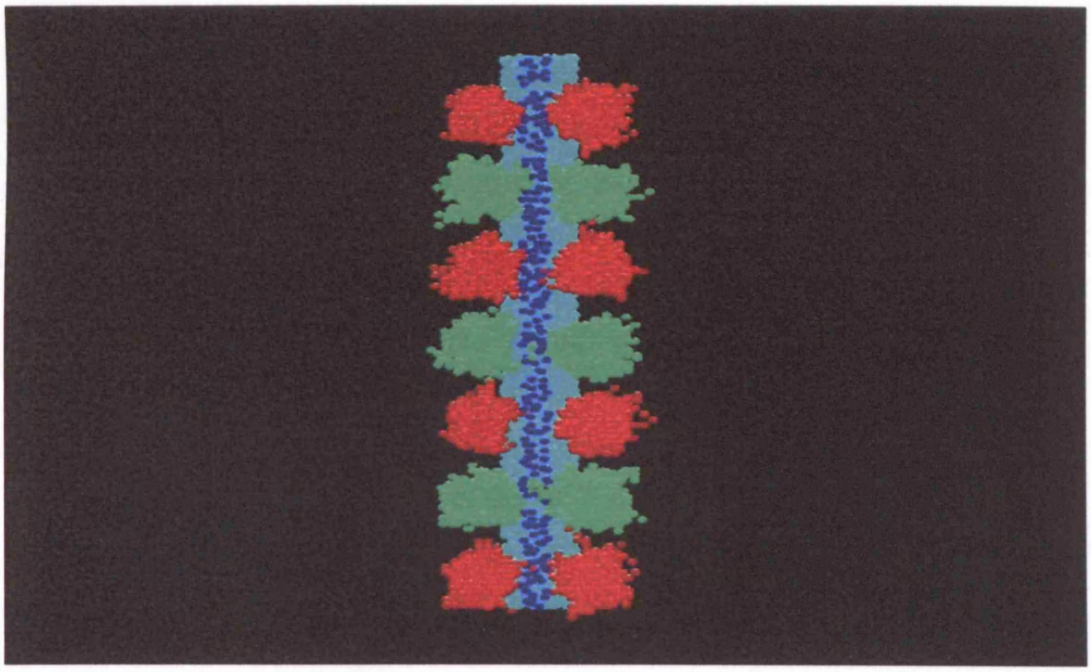

Figure 11-2: final frame of simulation. Cellular replication has increased the size of the sclerotomal cell cluster, but the replication has not resulted in an anterior cellular condensation.

The figure and animation clearly demonstrate that lack of cellular migration will result in two separate cellular condensations either side of the midline. The initial collection of sclerotomal cells simply progressively enlarges. The morphology of the cellular collection on either side of the midline does not significantly alter. In terms of the generic outcome measures, there is no cell mixing between adjacent levels (measure 1), and the disk space is preserved (measure 2). Fusion across and around the anterior midline structures does not occur (measure 3). Measures 4 and 5 are not relevant for this experiment. Cells do not migrate across the midline, or even reach it (measure 6).

11.5 DISCUSSION

The experiments reported in this chapter have demonstrate the requirement for the cellular migration and replication in forming the pre-vertebral cellular condensation. Lack or inhibition of either of these mechanisms might lead to the presence of two cellular condensations either side of the midline structures. Ultimately following chondrification and ossification, the expressed phenotype would be two hemi vertebrae at the same level. In the case of cellular migration without cellular replication, there are two other possible phenotypical outcomes. The cellular condensations might fuse across the midline, forming an anterior pre-vertebral cellular condensation. The morphology of this structure would be abnormal, but it might possibly regain a normal morphology during chondrification / ossification. An alternative outcome is that the two sclerotomal cellular condensations would become adjacent to each other, but the chondrification / ossification processes would not fuse the cells because of the reduced number of cells. This would lead to a form of a butterfly vertebra, as illustrated in Figure 11-3 from Sonel etal [180].

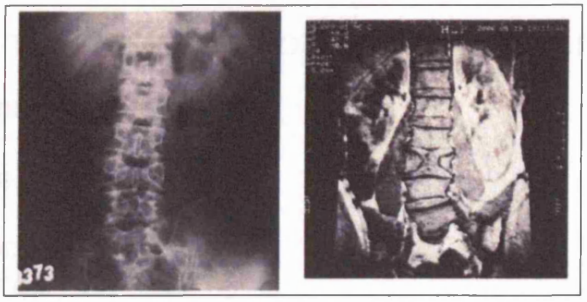

Figure 11-3: Plain film and corresponding MRI scan of a patient with a lumbar vertebra. From Sonel etal.

It could be argued that enough time is not given for the cells to migrate in the cellular migration experiment to move to the midline, and in the cellular replication experiment, if enough time is allowed for sufficient replications to occur, fusion will occur across the midline. However, one must also consider the other processes occurring in the embryo, and that these occur concurrently, and so it is unlikely that additional developmental time canbe be allocated for a specific process in order to allow it to "catch up" – instead, it is likely that the normal structure will fail to develop as postulated above.

11.6 SUMMARY

The experiments reported in this chapter have demonstrated the requirement for the cellular migration and cellular replication mechanisms in the formation of a normal pre-vertebral cellular condensation. Inhibition of either of these mechanisms might result in the formation of a hemi-vertebra, although in contradistinction to the hemi vertebrae discussed later, these would be paired across the midline.

12 Experiment 4: formation of a hemi vertebra

The experiments reported in Chapters 9 and 10 have demonstrated that when using the simulator with a normal dataset, a phenotype with normal appearance is generated and that the appearance of the phenotype is consistently unchanged over several simulations.

In order to attempt to elucidate the relationship between abnormal segmentation and the consequential phenotype, the experiments described in this chapter and the next were performed. If successful, these experiments would also demonstrate that not only did the simulator create a normal phenotype from a normal dataset, but also generated an abnormal phenotype consistent with that found experimentally from an abnormal dataset.

Bagnall etal[181,182] and Jungell-Wass etal[183] have described experiments in which a somite was surgically removed from a murine embryo, and the embryo then allowed to develop until sacrifice at a later time. Following surgical removal of an embryo, a contralateral hemi vertebra is always observed to form as demonstrated in Figure 12-1. The interpretation of this figure is that a hemi vertebra has formed on the non-operated side, which has fused with the caudal vertebra.

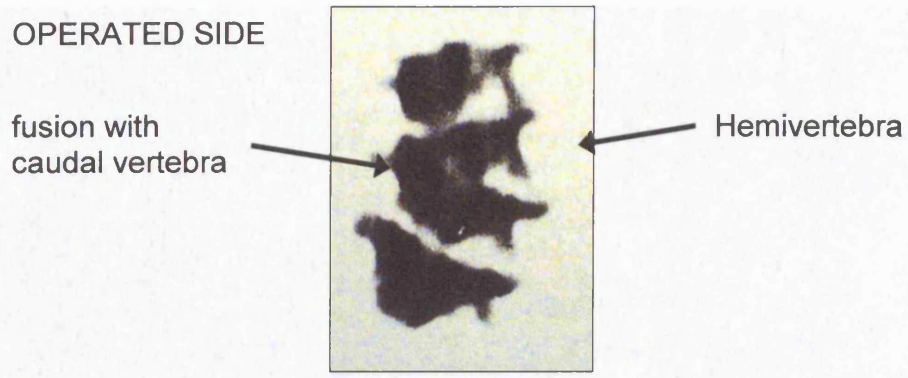

Figure 12-1: from Bagnalls paper on outcome following removal of a somite (figure 5) in Bagnall etal

In order to simulate this experiment, the dataset *deleted* was created from the *adnoto* dataset by removal of the fourth left sclerotomal condensation. The dataset was edited using Excel, and the cells that made up this condensation were deleted.

12.1 HYPOTHESIS

Using the simulator *vert*, the dataset *deleted*, and the standard simulator program (Table 6-5) and constants (Table 6-4), removal of a single sclerotomal condensation will result in the formation of a contralateral hemi vertebrae, similar to that observed *in vivo* by Bagnall and Jungel-Wass[181-183].

12.2 METHOD

The simulator program *vert* without modification was used in this experiment. An identical program to that used in the previous experiments was used, and data collected in the same manner ie every frame was stored on the hard disk as an image form and binary format for later analysis. Initial cell position was defined by the data file *deleted*. Identical activation cycle times and biological constants as those used in experiment 1 were used. The starting position of the cells can be seen below in Figure 12-2. The results were visualised and analysed using animations of the 3 Dimensional sphere view, VRML models and orthoview.

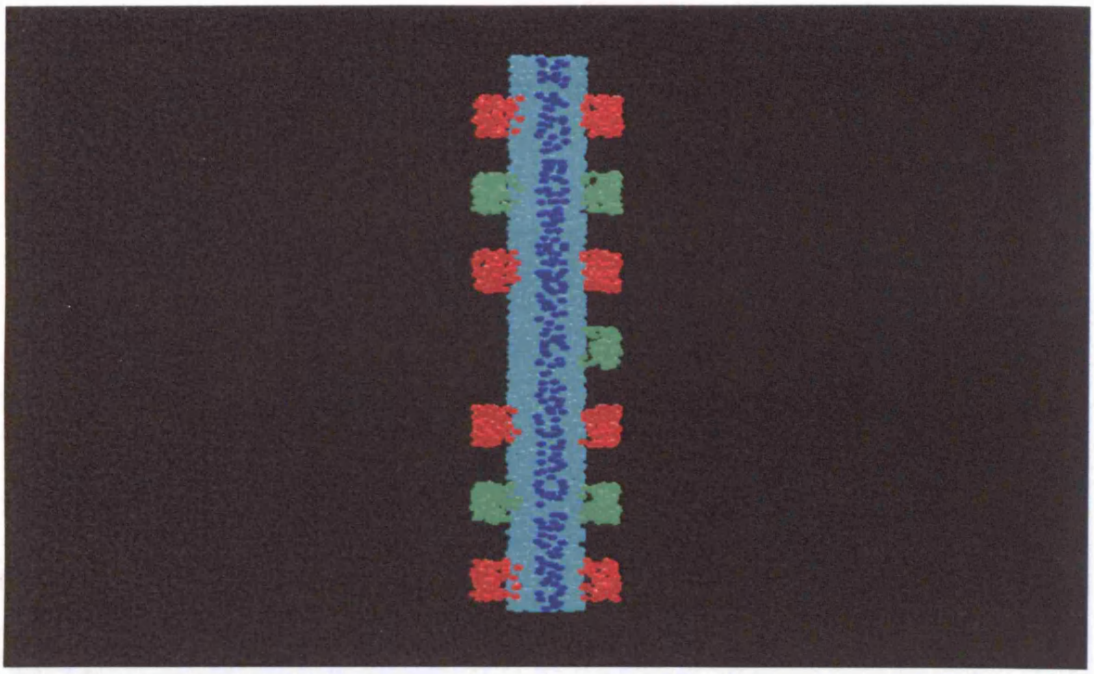

Figure 12-2: starting position of cells

12.3 OUTCOME MEASURE

The main outcome measure of this experiment was to determine the similarity of the structure built by the computer simulation with those found by Bagnall and Jungel-Wass in animal models. In results reported by Bagnall and Jungel-Wass, the animals were sacrificed after chrondification of the mesenchymal structures had occurred, hence were more advanced developmentally than the structure developed by the computer simulator. Additionally, the animal structures developed by the animal models were subject to muscular strain and hence deformity, as can be seen in Figure 12-1 from Bagnall[181], illustrating formation of a hemi vertebra.

There generic outcome measures were also assessed, in particular (1) mixing from adjacent sclerotomes, in this case into the space vacant as a consequence of removal of the sclerotome and (6) migration of cells from the left side of the midline across the midline to the right side.

12.4 RESULTS

A typical result is illustrated below in Figure 12-3, and in VRML format on the CDROM. An animation of the complete developmental sequence can also be found on the CDROM.

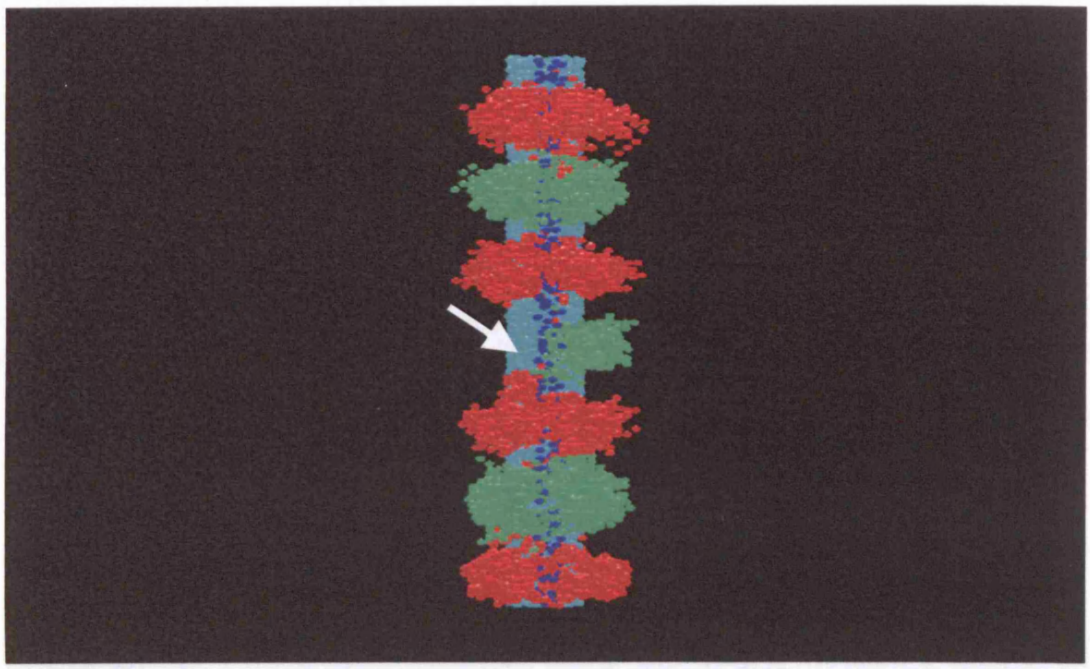

Figure 12-3: end frame of simulation (frame 799). The arrow points to a potential bridging between the adjacent cellular condensations.

This result is similar to that observed experimentally by Bagnell and Jungel-Wass[181-183] following removal of a single unilateral somite. The location of the missing cells remains unfilled by cells migrating from either the rostal or caudal sclerotomes. The cells from the contralateral sclerotome condensation have not crossed the midline. The disk spaces above and below the hemi vertebrae are preserved. Using the VRML viewer, the initial sclerotomal condensations can be seen to have migrated anteriorly from the initial lateral position to surround the notochord and neural tube structures. It is also interesting to note the small almost midline cranially orientated "spicule" on the left fourth condensation (arrow, Figure 12-3). The computer generated structures are mesenchymal, and it might be that when the chondrification process occurs, bridging would occur between the right fourth cellular condensation (hemi vertebra) and

the left fourth cellular condensation. Similar bridging is seen in the animal model results (Figure 12-1).

12.4.1 Orthoview analysis

12.4.1.1 Initial cell position

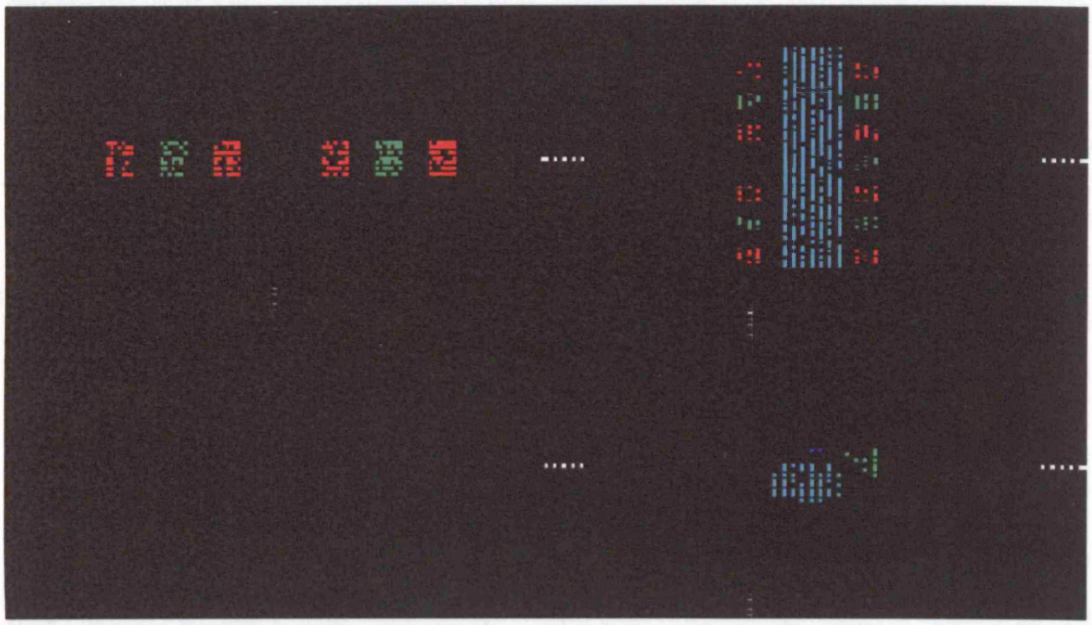

Figure 12-4: frame 0001 x 23 y 30 z 70

Figure 12-4 demonstrates the initial setup, with the absent fourth right sclerotome.

12.4.1.2 Initial development of cellular condensations

The normal pattern of development occurs until the region of the deleted sclerotome is reached and is illustrated in Figure 12-5 and Figure 12-6.

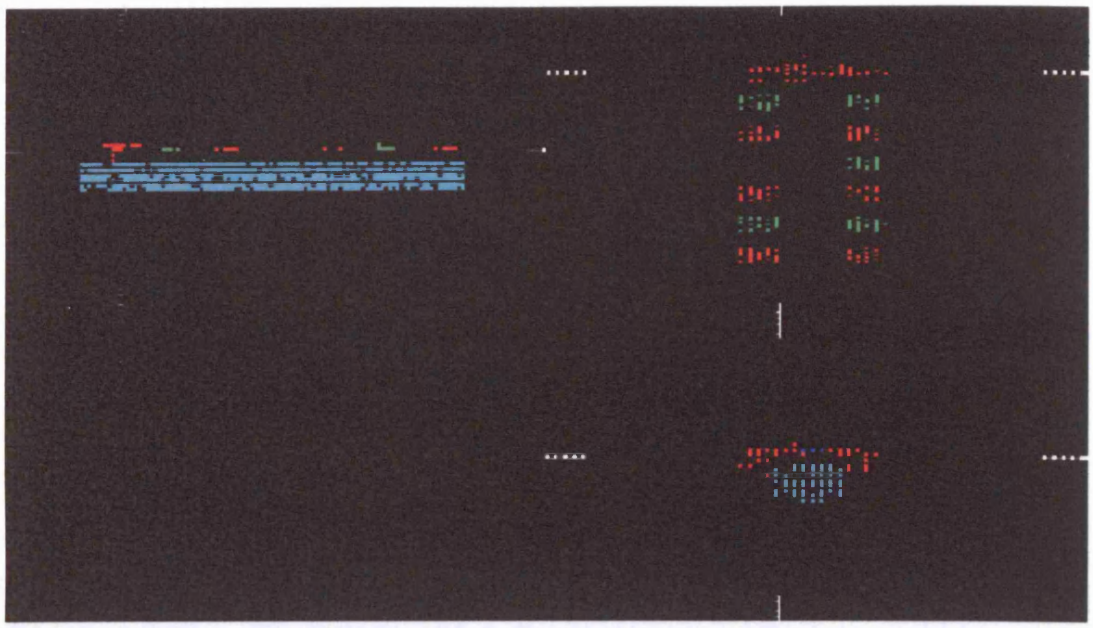

Figure 12-5: frame 0061 x 26 y 32 z 30

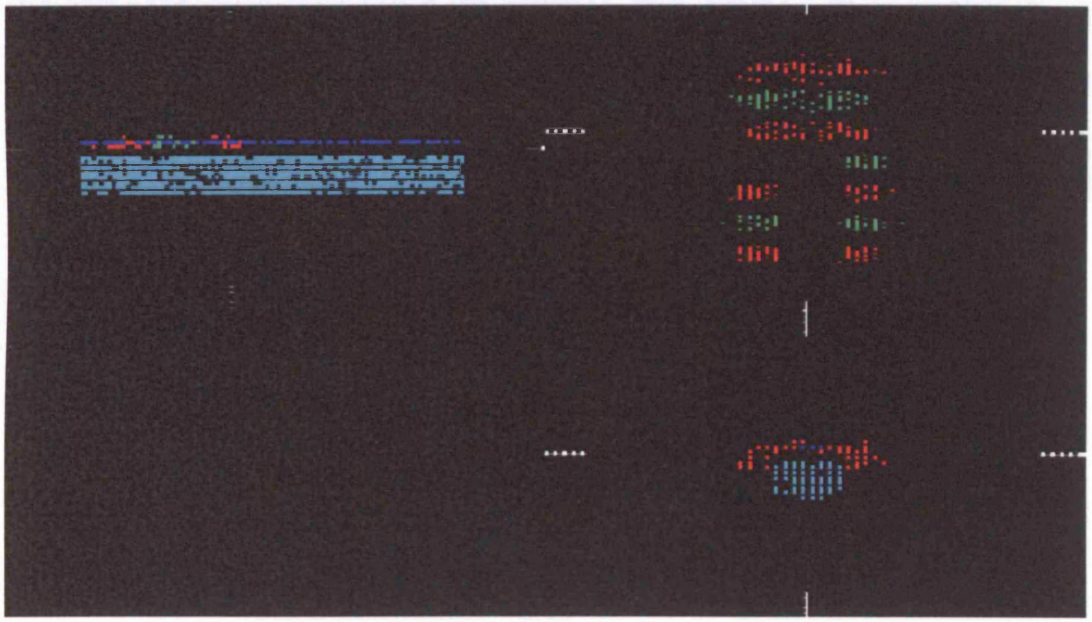

Figure 12-6: frame 0299 x 29 y 32 z 58

The sclerotomal cells can be seen to have migrated from the initial lateral position to surround the anterior notochord and neural tube. Pre-vertebral condensations similar to those seen in the previous experiments are formed.

12.4.1.3 Hemi vertebra development

At the level of the deleted sclerotome, spreading of the cells from the third sclerotome on the left side into the empty space resulting from the deleted sclerotome has not occurred. These cells have migrated in a fairly direct manner towards notochord / anterior neural tube.

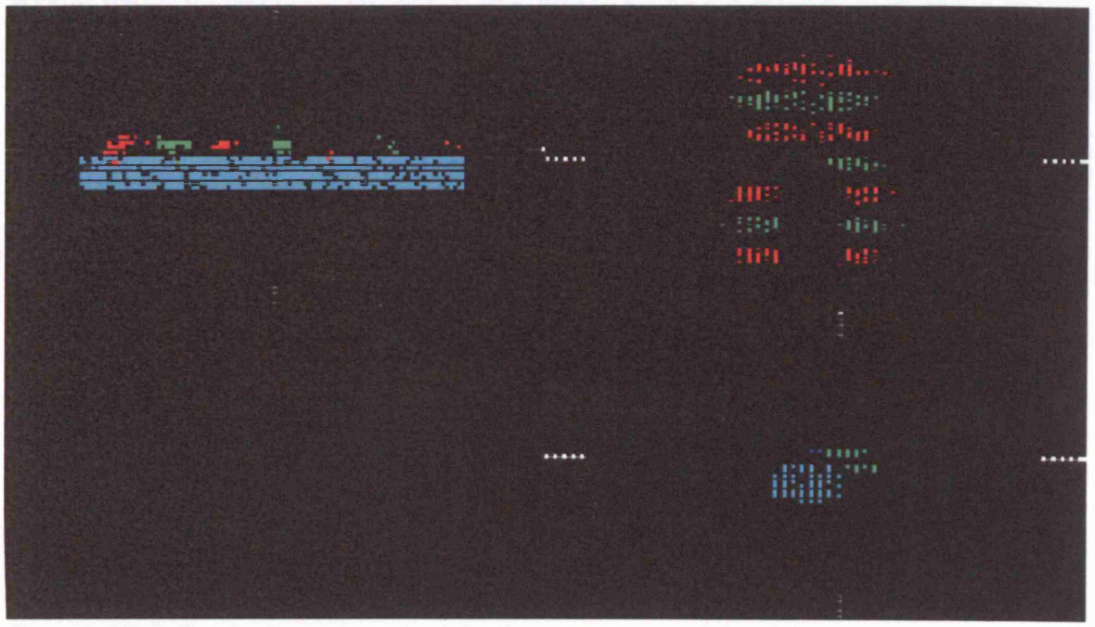

Figure 12-7: frame 0316 x 33 y 32 z 70

Early in the development of the right fourth condensation, the cells are migrating directly to the midline notochord, demonstrating normal morphology (Figure 12-7).

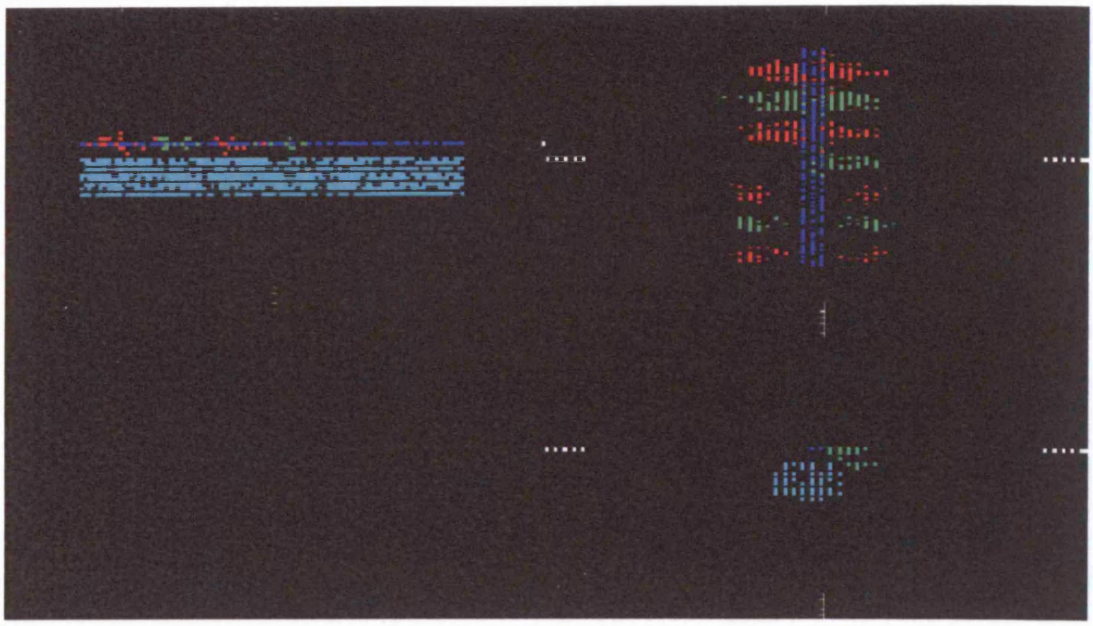

Figure 12-8: frame 0400 x 31 y 33 z 70

None of the contra-lateral sclerotomal cells are demonstrated to have crossed the midline notochord. This is demonstrated in Figure 12-8.

12.4.1.4 Development around the absent somite

Figure 12-9 illustrates normal early development of the fourth left sclerotome, without spreading of the sclerotomal cells in the cranial-caudal direction as they migrate towards the midline notochord.

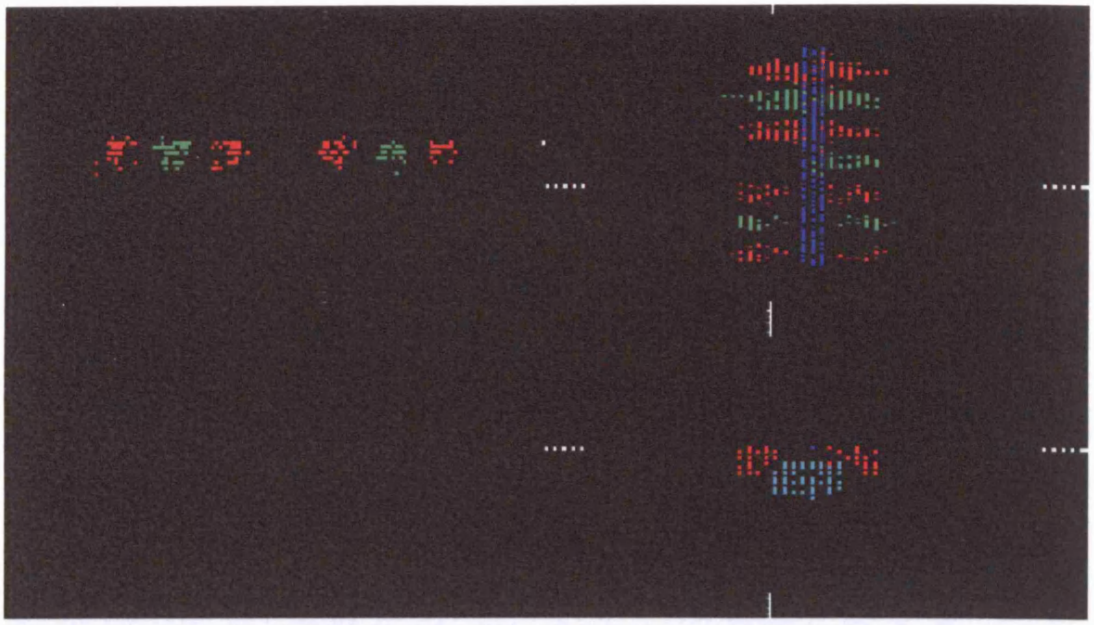

Figure 12-9: frame 0408 x 25 y 33 z 83

Later in the developmental process there is perhaps a small degree of excess spreading of the sclerotomal cells in the cranial direction as they migrate towards the midline as demonstrated in Figure 12-10 and Figure 12-11, when viewed from above, however, this is not confirmed on the longitudinal view (top left) in these figures.

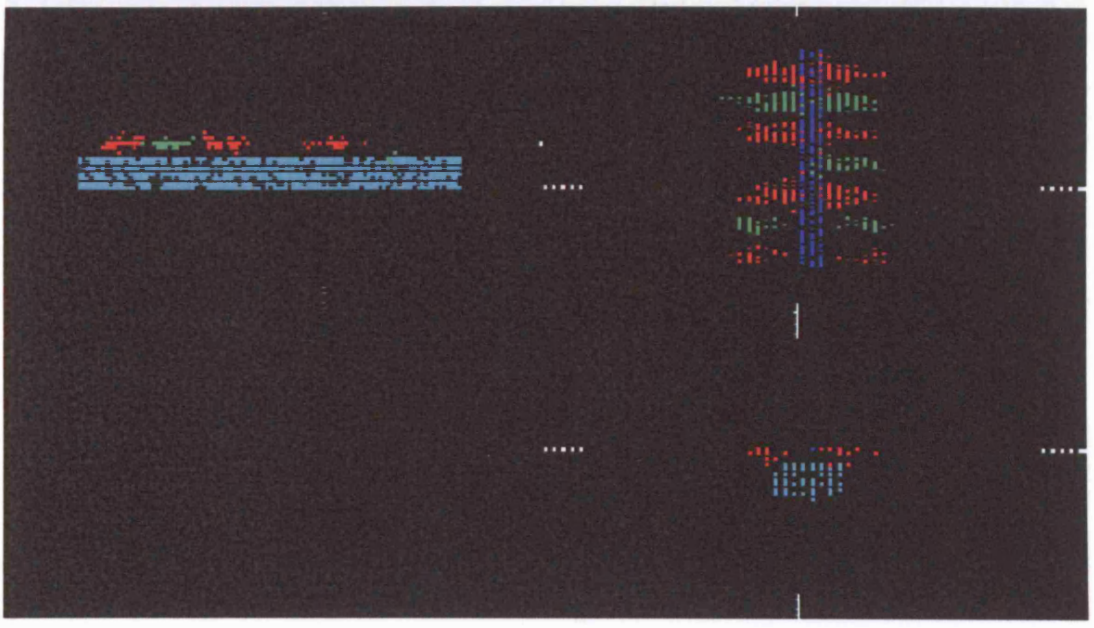

Figure 12-10: frame 0439 x 28 y 33 z 83

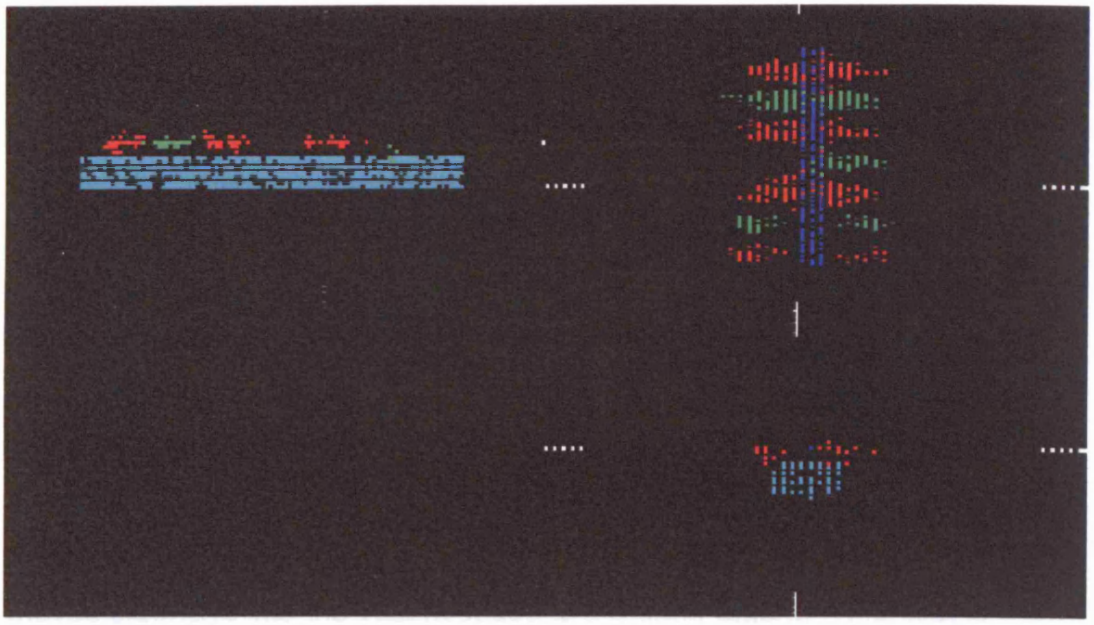

Figure 12-11: frame 0479 x 28 y 33 z 83

12.4.1.5 Subsequent development

The remainder of the developmental process is completed normally as seen in Figure 12-12.

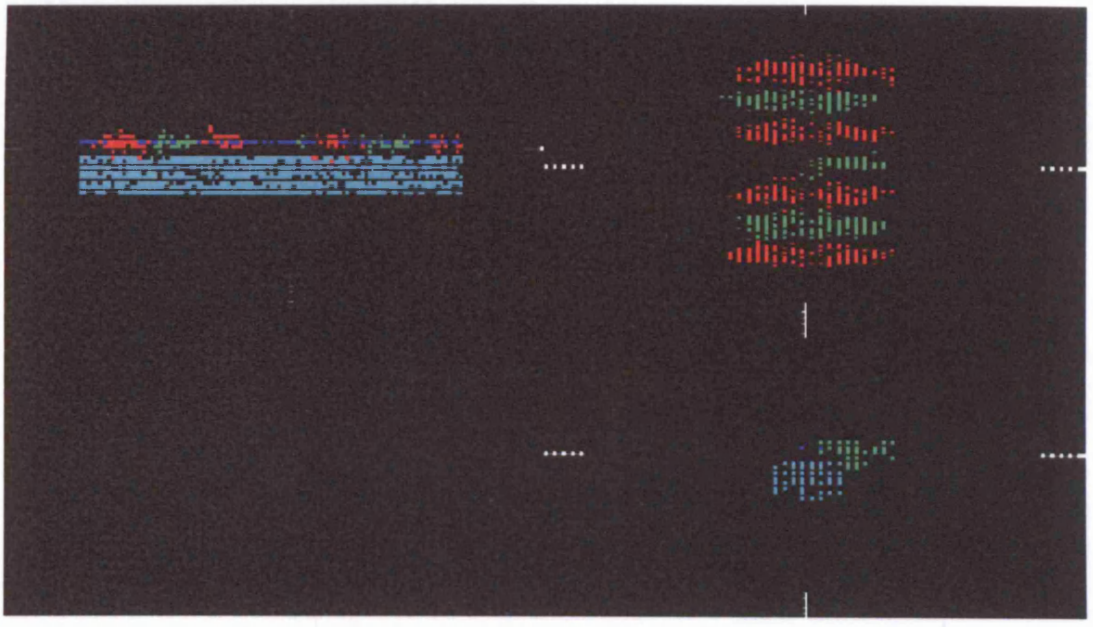

Figure 12-12: frame 0640 x 29 y 32 z 74

12.5 DISCUSSION

The experiment described in this chapter is similar in principle to those performed by Bagnall and Jungel-Wass. They found that removal of a somite – the source of the sclerotomal cells – caused a defect in the pre-vertebral cellular condensation on the same side as, and at the same level as the somite removal. They went on to conclude the eventual phenotype would be that of a contralateral hemi vertebra. Bagnall, in particular was concerned that surgical interference in the embryo might be a possible explanation for the observed results. The computer simulations reported in this chapter confirm his experimental findings.

It is interesting that the cells from the adjacent sclerotomes have not moved sideways into the vacant space to a greater extent. This, too, is similar to the observed findings in the biological experiments, and implies that the chemotactic migratory drive is significantly stronger than that of the random movement.

It is noteworthy that the sclerotomal cells from the contralateral side at the level of the missing sclerotome do not migrate across the midline into the vacant space. This is a further point of similarity to that of the biological experiments. The mechanism for this in the computer experiments is probably related to the fact that the midline contains the morphogen source, and if the cells were to pass over the midline, they would be passing down rather than up a concentration gradient. Correlation of the morphogen concentration gradient with cellular location would be required to confirm this, however. The contralateral disk spaces either side of the unilateral condensation are clearly preserved as would be expected.

Although the computer simulation ends with the formation of the pre-vertebral condensation, it can be inferred that the final phenotype following chondrification and ossification, would be that of a hemivertebra, similar to that seen in Figure 12-1, and that loss of the sclerotomal cells is a mechanism by which this abnormality might arise.

The formation of a potential bridge between the right sided hemivertebra and left fourth cellular condensation is fascinating in its similarity to the result reported by Bagnall and illustrated in Figure 12-1. Chondrification and subsequent ossification of this structure, when combined with the paraspinal musculature would act to generate a scoliosis convex to the right with the bridging across adjacent developmental levels.

12.6 SUMMARY

This experiment has demonstrated that a contralateral hemivertebra can be formed by loss of the ipsilateral sclerotome cell population at the same level. In concordance with *in vivo* experimental findings, cells from the adjacent sclerotomes do not migrate into the affected sclerotomal compartment and rescue cellular condensation formation. This represents a potential mechanism for formation of a hemivertebra.

13 Experiment 5: formation of a fused vertebrae

The outcome of the previous experiments has demonstrated that the simulation program *vert* is able to reproduce the normal developmental formation of the vertebral column in mammalian embryos by invoking the chemotactic and replication morphogenetic mechanisms

These experiments have demonstrated that the sclerotomal cells migrate in an almost linear manner from their initial lateral position to form the pre-vertebral cellular condensation surrounding the notochord / anterior neural tube complex. Hence, if a fused vertebrae were to be formed, it would be likely to result from a giant sclerotome.

Unfortunately, no direct experimental evidence exists on which to base the experiment described in this chapter. The paraxial mesoderm of the genetic murine mutant *Pudgy* does not segment normally, with formation of irregular somites, including giant somites, similar in morphology to those formed in embryos exposed to sodium valporate and anti-sense *Pax-1*[184,185]. As a consequence, the skeletal vertebral column is chaotic and malformed. However, direct observation of the morphogenetic process is not possible, and so it is not possible to draw conclusions regarding the initial arrangement of the sclerotomal cells and the resultant phenotype.

In order to test the assertion made above, that a fused vertebrae arises from a giant sclerotome, the normal dataset *adnoto* was modified using Excel to form the *fused* dataset. In the *fused* dataset, additional sclerotomal cells exist between the left fourth and fifth sclerotomal cell collections. These cells were made type 5, which is displayed in magenta on the simulator output, so their contribution to the developed structure

could be easily observed. They were allowed to start migration after 300 cycles, ie at the same time as the fourth sclerotomal cell collection, and finished migration after 600 cycles, ie when the fifth sclerotomal cell collection ended migration. Otherwise the properties with respect to replication and movement were identical to those of the other sclerotomal cells.

13.1 HYPOTHESIS

Using the simulator *vert*, the VPL program in Table 6-5 and the simulation constants in Table 6-4, and the dataset *fused*, addition of extra sclerotomal cells to form a giant sclerotomal cell collection, will result in the development of a giant hemivertebra.

13.2 METHOD

The simulator program *vert* without modification was used in this experiment. The simulator program was identical to that used in previous experiments, and the dataset *fused* was used to set up the initial starting positions of the sclerotomal cells. Identical cell cycle activation times and biological constants to those used in the previous experiments were used in this experiment. Every output frame of the simulation was stored on the simulator computer hard disk in visual and binary format for later analysis using the three dimensional spherical display and the *orthoview* program.

The starting position of the cells is shown in Figure 13-1. Note the additional cells in magenta between the fourth and fifth sclerotome cell collections on the left.

13.3 OUTCOME MEASURE

This chapter does not have an experimentally verified animal model. Assessment therefore has to be made along the lines of the generic outcome measures, specifically (1) cell mixing from adjacent sclerotomes, (2) preservation of disk space, (3) fusion across the midline structures, (5) formation of giant prevertebral cellular condensations and (6) migration of cells for one side of the midline to the other.

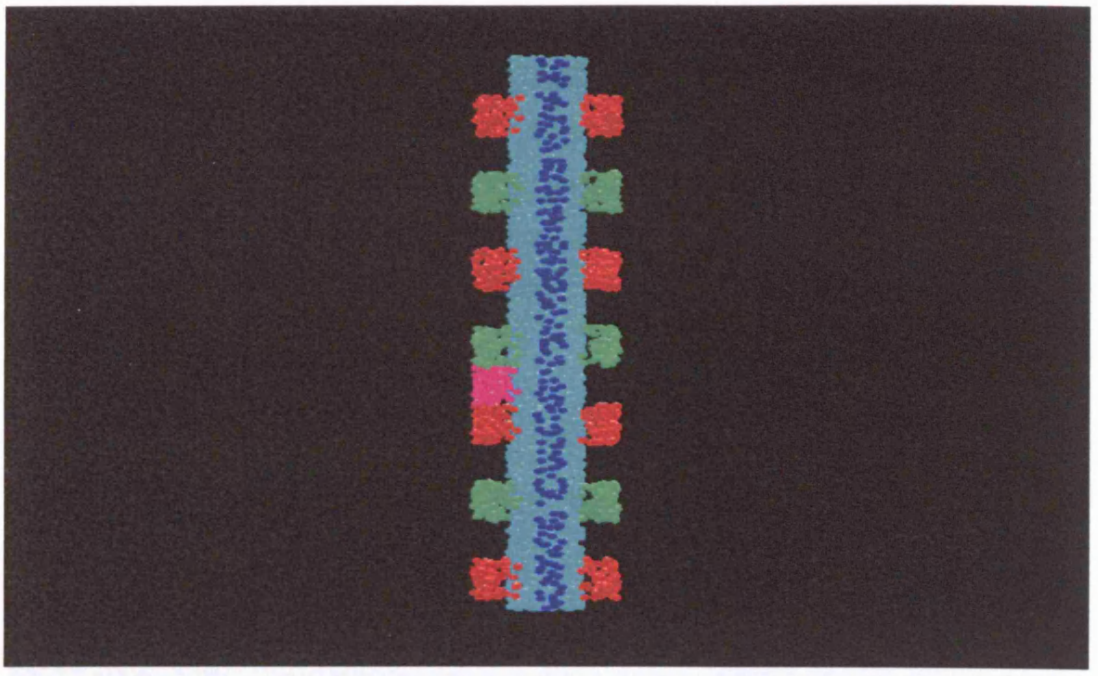

Figure 13-1: starting arrangement of cells

13.4 RESULTS

The final frame after 799 cycles of a typical simulation is shown in Figure 13-2. An animation of the developmental process is on the CDROM.

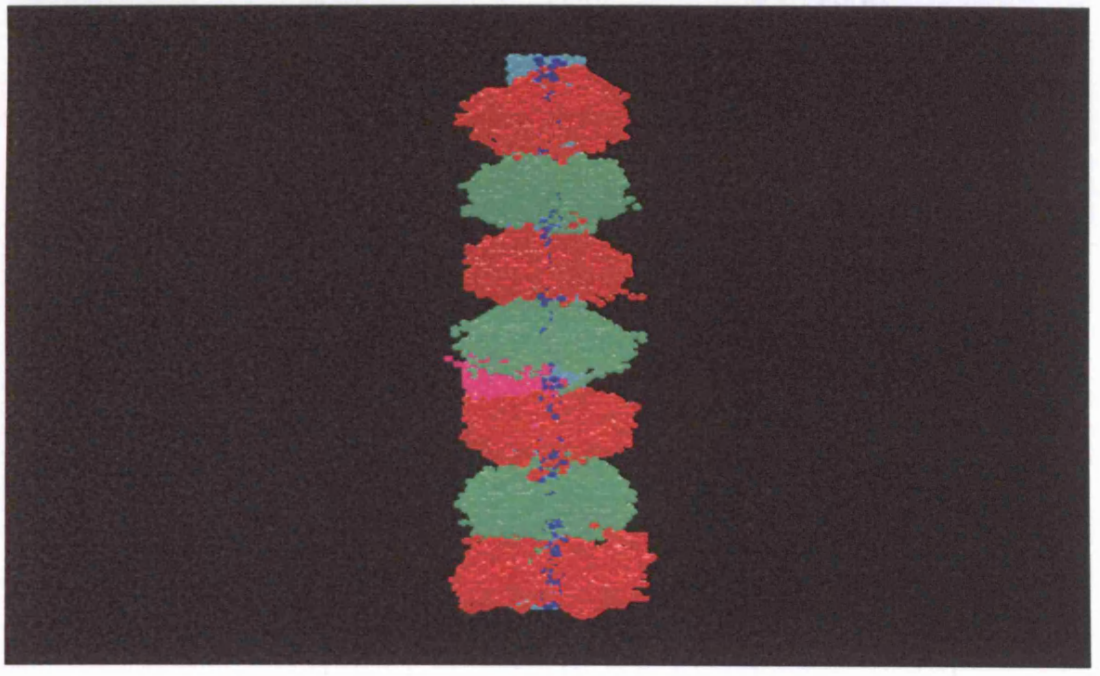

Figure 13-2: completed fused sclerotome simulation

Figure 13-2 demonstrates that the fused sclerotomal condensation has migrated to form a giant pre-vertebral cellular condensation, on the left. This is likely to result in a hemiblock vertebra phenotype. On the opposite side to the presumptive hemiblock vertebra the normal right fourth and fifth sclerotomal cell collections have migrated normally and fused across the midline with their opposite partners on the left. A putative disk space has also been preserved.

13.4.1 *orthoview* analysis

The following section examines the development of the condensations using *orthoview*.

13.4.1.1 Initial positions of cells

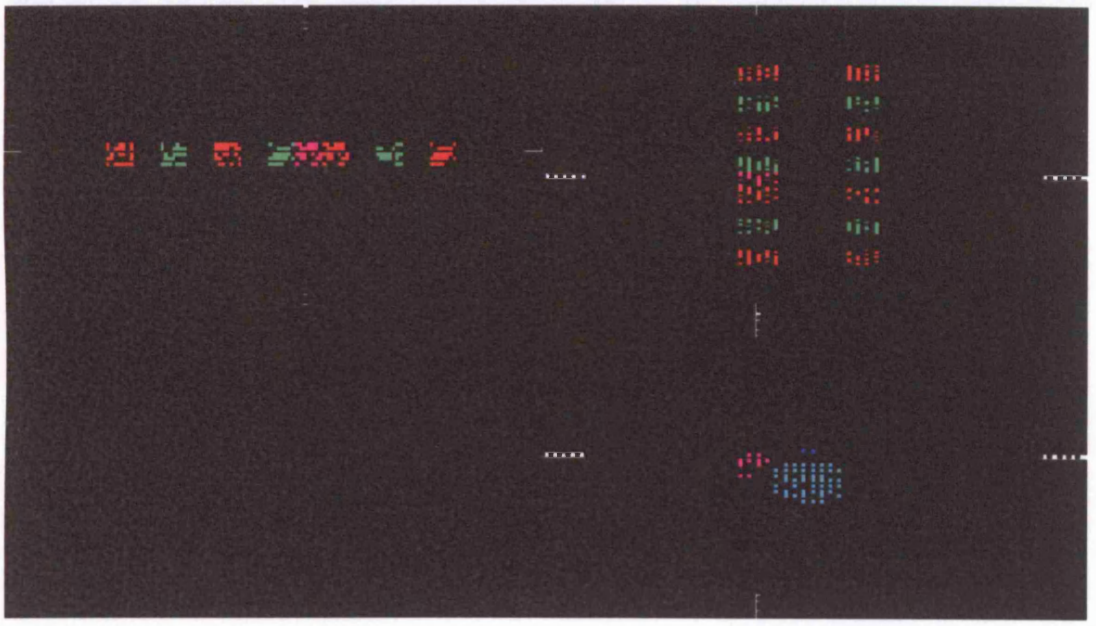

Figure 13-3: frame 0001 x 24 y 32 z 78

This is the initial frame of the simulation. The additional sclerotomal cells are represented in magenta.

13.4.1.2 Normal development prior to fused sclerotome

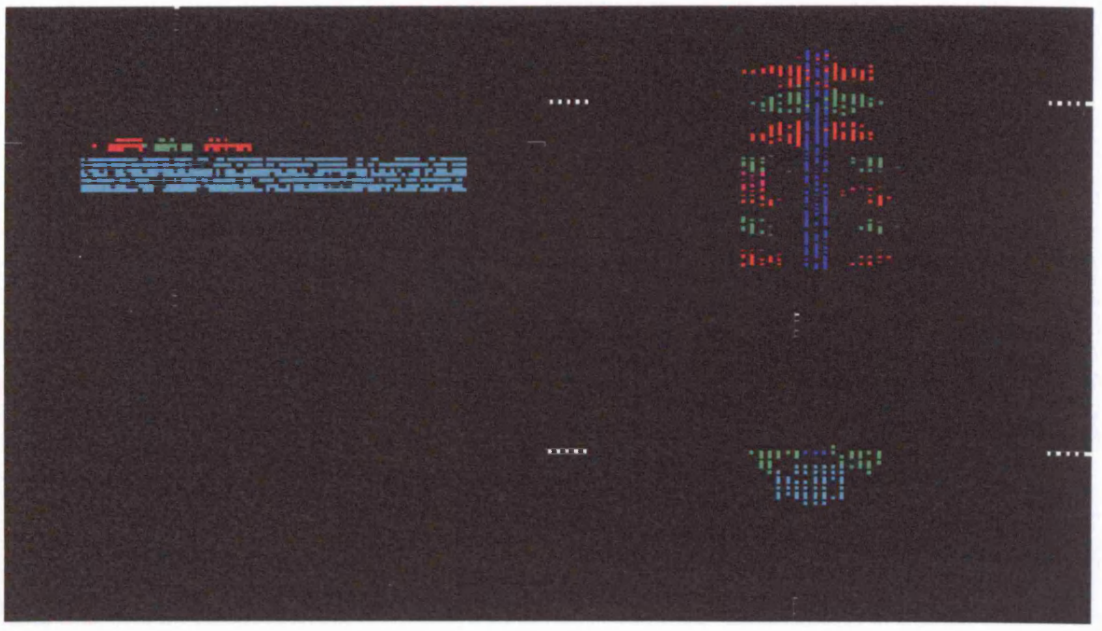

Figure 13-4: frame 0261 x 28 y 33 z 44

Three sclerotomes have now migrated towards the notochord. As seen in the simulation using the normal dataset, the cleft between the somites has been preserved, and the sclerotomal cells have migrated up to and surround the notochord.

13.4.1.3 Development of the fused sclerotome

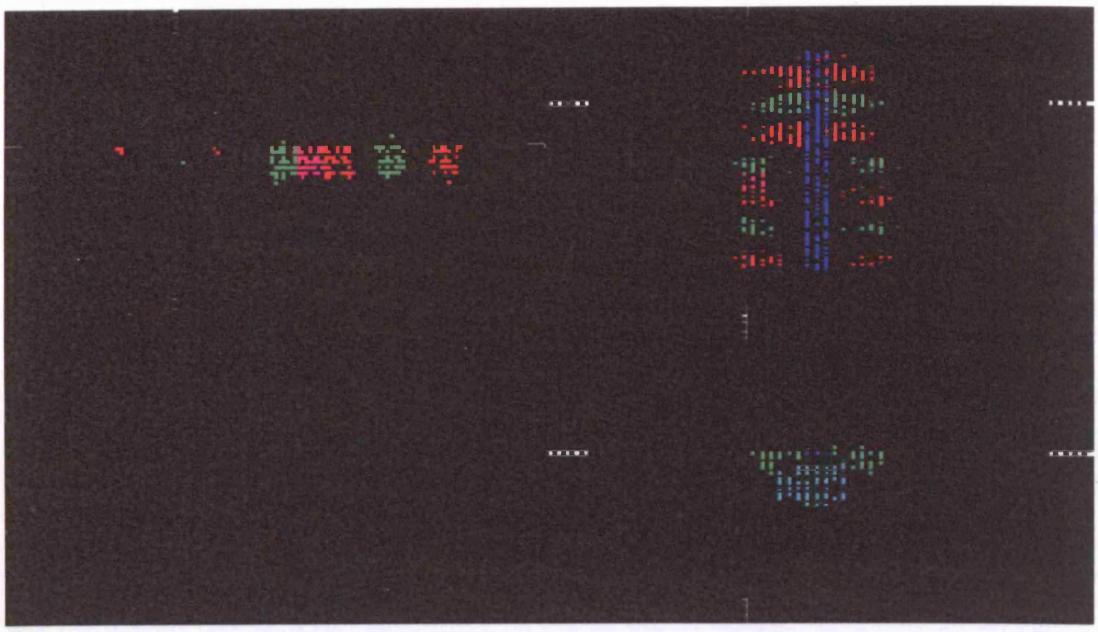

Figure 13-5: frame 0299 x 22 y 33 z 44

Figure 13-5 illustrates the initial arrangement of the giant sclerotome immediately before it is commencement of migration towards the midline.

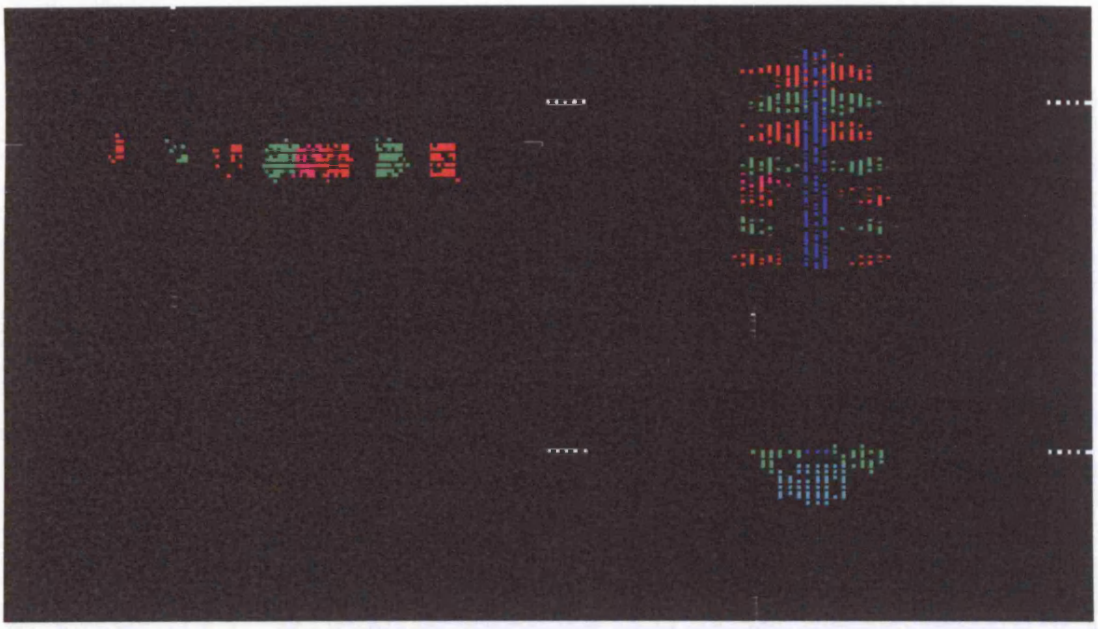

Figure 13-6: frame 0306 x 23 y 33 z 44

Figure 13-6 illustrates the dispersion of the sclerotomal collection, initially as seen in the normal simulation, in this case the green cells of the fourth

left collection and the additional magenta cells. The cells are not seen to spread out in the cranial and caudal directions to the extent that normally occurs.

13.4.1.4 Mixing of the fused sclerotomal cells

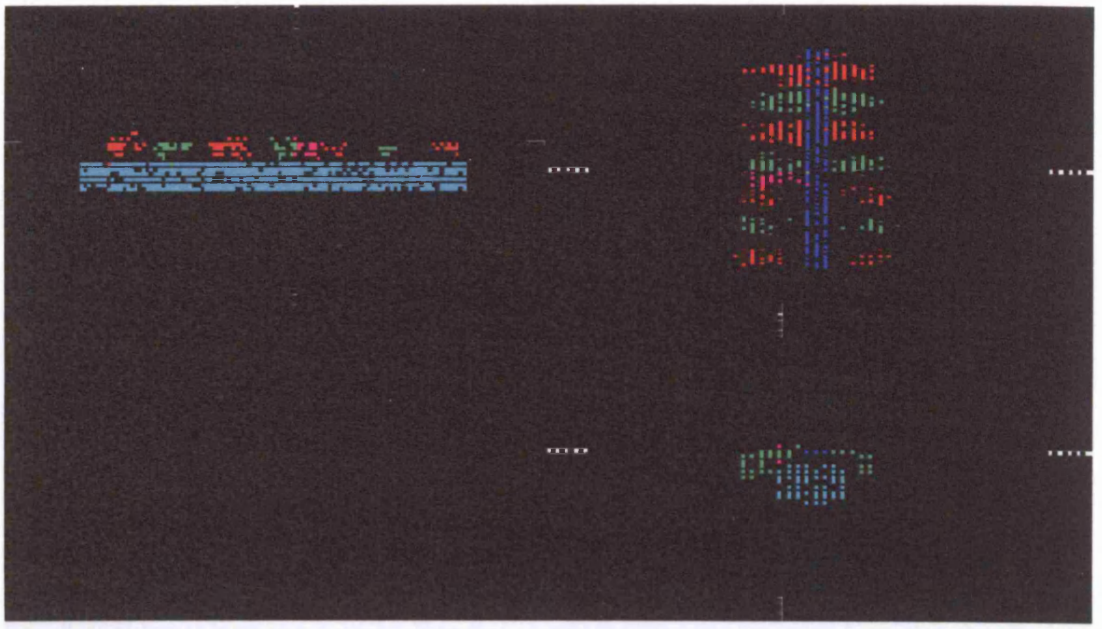

Figure 13-7: frame 0313 x 26 y 33 z 75

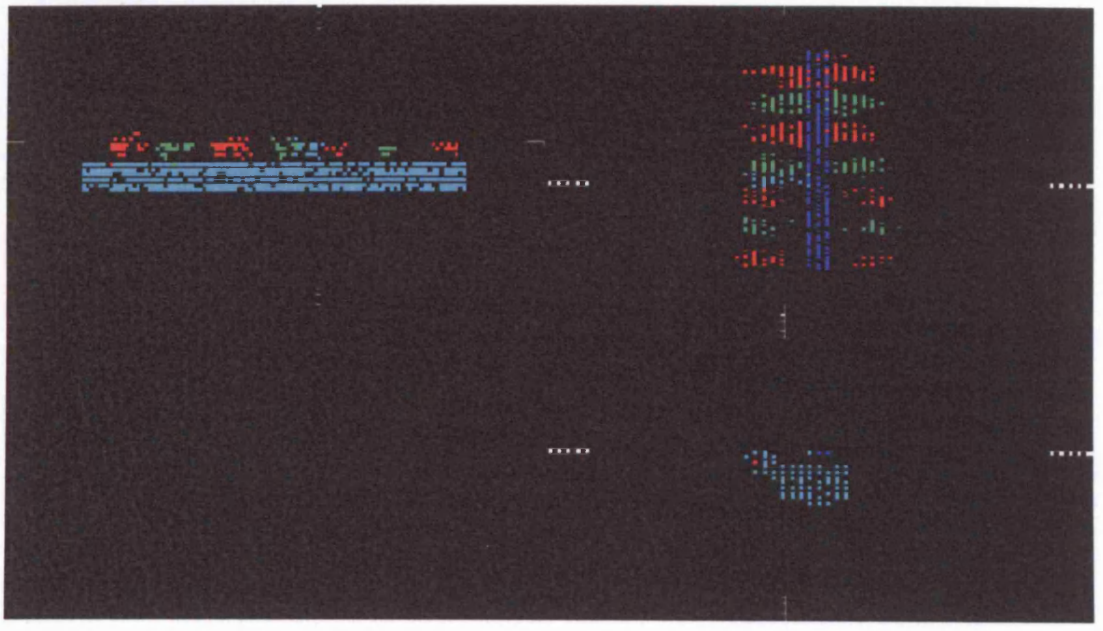

Figure 13-8: frame 0313 x 26 y 33 z 82

Migration towards the notochord continues as demonstrated in Figure 13-7 and Figure 13-8. Amongst the two adjacent migrating cell populations of the additional cells and the left fourth sclerotomal cell collection little mixing occurs. Some caudal movement of the magenta cells occurs against the static red cells of the left fifth sclerotomal cell collection.

13.4.1.5 Migration occurs directly to the notochord

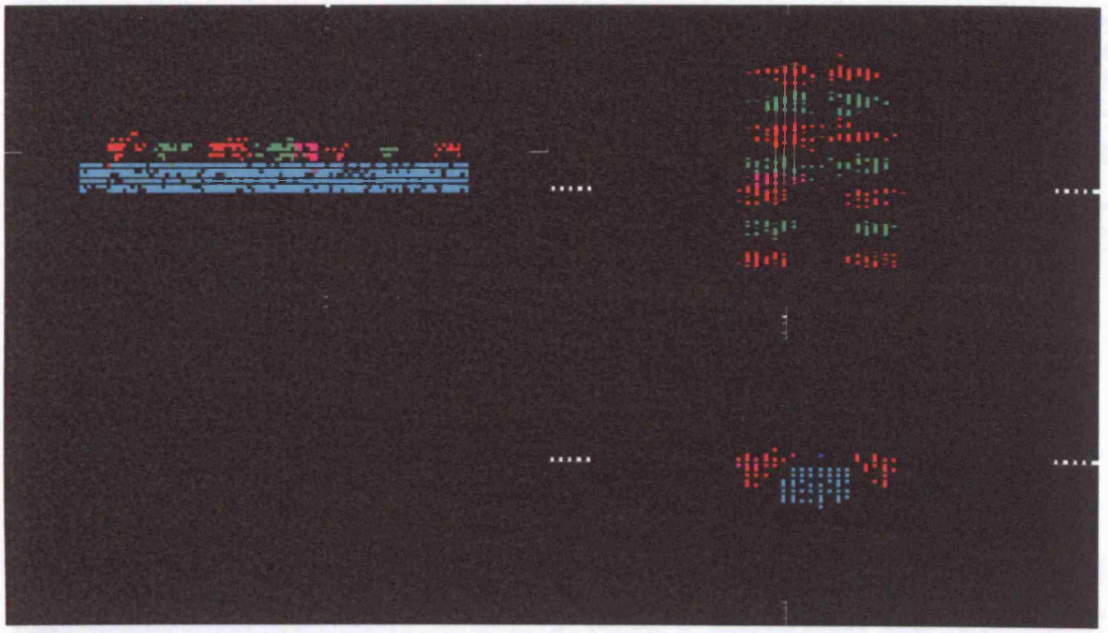

Figure 13-9: frame 0323 x 26 y 32 z 83

The majority of the additional sclerotomal cells migrate directly towards the midline structures as demonstrated in Figure 13-9. Very little encroachment by the additional sclerotomal cells into the area between the left fifth sclerotomal cell collection and the midline structures of the notochord and neural tube occurs.

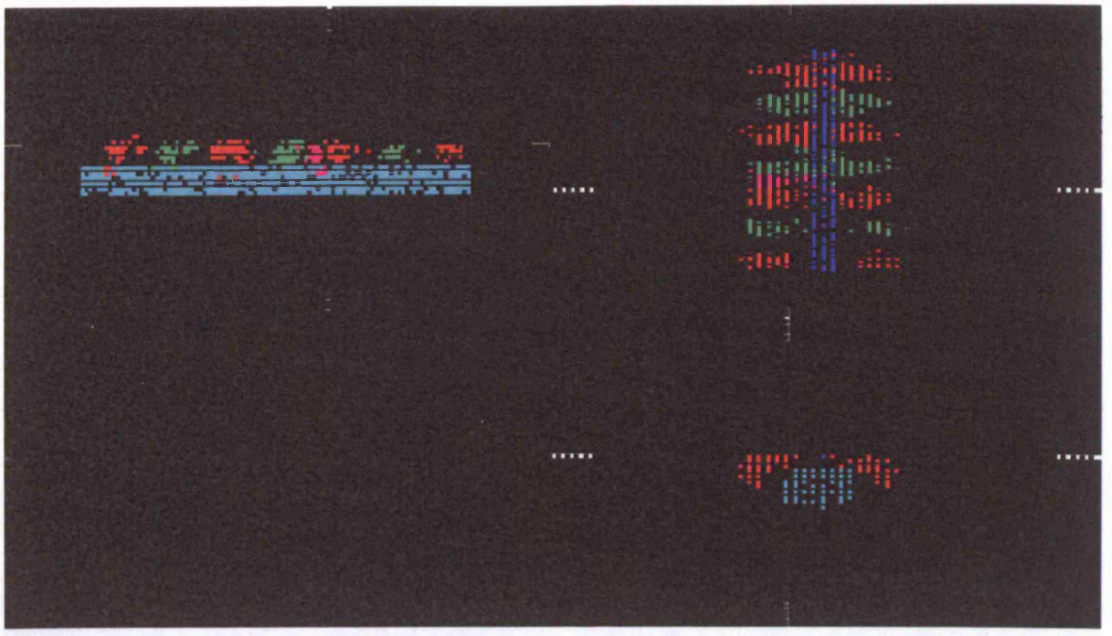

Figure 13-10: frame 0410 x 26 y 33 z 83

Figure 13-10 and Figure 13-11 demonstrate that migration of the fifth sclerotome cell collection occurs in the normal manner.

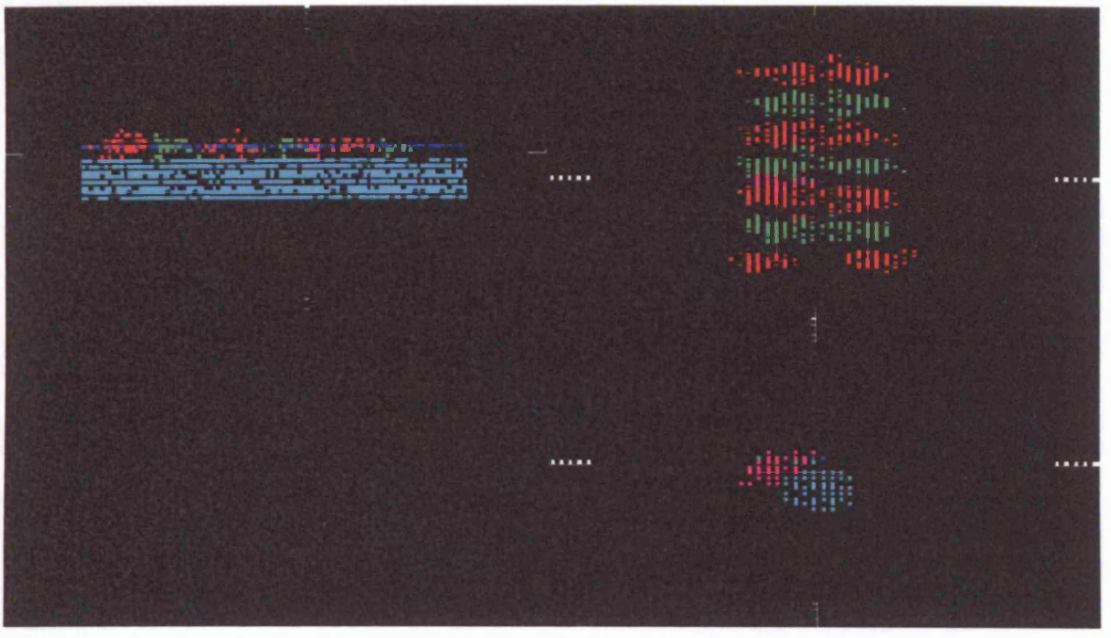

Figure 13-11: frame 0555 x 29 y 32 z 78

Whilst the magenta sclerotomal cells migrate up to the midline structures, none of the cells are seen to cross over the notochord, to the contralateral side.

13.4.1.6 Subsequent development

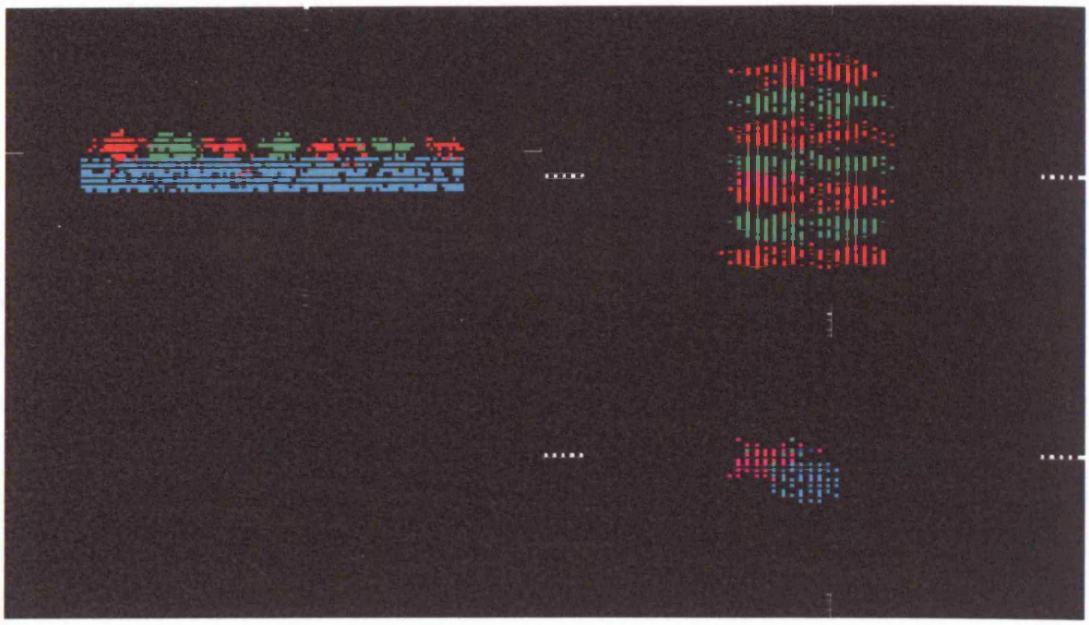

Figure 13-12: frame 0643 x 32 y 32 z 78

The remainder of the developmental process occurs in the normal manner as illustrated in Figure 13-12.

13.5 DISCUSSION

This experiment has demonstrated that malsegmentation resulting in the formation of a giant sclerotomal cell condensation is a potential developmental mechanism through which a hemiblock vertebrae might arise. Although this has not been tested experimentally *in vivo*, it is in accordance with the available biological evidence.

Analysis of the animation (on CDROM) and *Orthoview* frames demonstrates that minimal mixing of the cells from the adjacent sclerotomal collections has occurred, even the collections are physically adjacent. The magenta cells have remained on "their" side of the anatomical midline - which is identical to that seen in the patient with a hemivertebra abnormality. The failure of these cells to cross the midline is most probably related to the concentration profile of the morphogen. In this simulation the "extra" or magenta sclerotomal cells have not fused

with sclerotomal condensations either from the right fourth or fifth sclerotome.

13.6 SUMMARY

This experiment has demonstrated that additional sclerotomal cells between adjacent sclerotome cellular collections will result in the formation of a unilateral fusion between the adjacent cellular condensations. This represents a potential mechanism for formation of a block vertebra.

14 Discussion

This work has focused on firstly, developing a computer program to simulate to manipulate virtual sclerotome cells in order to investigate the mechanisms that underlie the morphogenetic development of the subaxial vertebral column, and secondly, how alteration of these mechanisms might lead to formation of abnormal vertebrae such as those seen in Klippel-Feil syndrome.

The approach adopted was to model the behaviour of the sclerotomal cells during development of the pre-vertebral sclerotomal condensation that is formed around the notochord and anterior neural tube. Observational studies have established that this cellular condensation subsequently undergoes chondrification and then ossification to form the vertebral body[147]. A separate mechanism is responsible for the formation of the neural arch and spinous process[186].

Using a computer simulator to investigate this model has several advantages. It allows the investigator much greater control over the experimental parameters, in particular attributes of cellular behaviour can be controlled and the impact of these attributes on the eventual outcome can be more easily determined than *in vivo* or *in vitro*. The arrangement of the cells can also be controlled, and specific hypotheses can be tested. In this work, the use of the computer simulator has also allowed direct observation and manipulation of the experimental process and cellular behaviour – something which is not possible in most animal experiments.

However, this approach involving a computer model and simulator is not without disadvantages. In particular, the experimental results are only as good as the experimental model and data that are used in the simulation, or to put it another way – rubbish in, rubbish out. Most of the biological processes are probably considerably more complex than the models used to investigate the process, and there is a real danger than over simplification of the model, or mis-understanding of the actual process will lead to the generation of misleading results and subsequent conclusions.

It is worth noting in this context that animal models are also just that - whilst all vertebrate embryos have the same body plan at the phylotypic stage, at which this work has been modelled, there are significant differences between species. For instance, the chick notochord is proportionately much larger than that found in the mouse and human. The total number of somites varies between species; they are of different sizes and possess different numbers of cells[187]. The demands of evolution are such that whilst the biological toolkit, in terms of the structures and many of the genes are similar, each organism has evolved its own unique adaptations to its habitat, and this is reflected in the phenotype.

The adaptation of the vertebral column to the environment is exemplified in vertebrate development. The mammalian vertebral column has evolved from the notochord. The first stage in the evolution of the notochord towards the formation of the mammalian vertebral column was the addition of supplemental cartilages such as a posterior neural arch and an anterior hemal arch. Subsequently in more advanced fish the central notochord was replaced by firm centra which articulate with each other by notochord derived material. As animals moved from the water to land, the stresses and loads on the spine altered. The early amphibians possess an intercentrum which encircles the notochord, paired pleurocentra between the intercentrum and bony neural arch. The subsequent evolutionary stages to the current mammalian arrangement is unknown, however the

centrum of amniotes is considered to be homologous with the pleurocentra.

The form of the centrum varies depending on the organism. The centra of most mammals are acoelous. They have flat ends and are separated by an intervertebral disk. Fish and amphibians possess amphicoelous vertebrae, which have concave ends and surround the notochord, whilst birds possess heterocoelous vertebra. These are hollow and have saddle shaped ends, and allow vertical and lateral flexion, but prevent rotation. The arrangement of the intervertebral disk in the adult chick is different from that of the mammalian disk, with a central suspensory ligament which contains the remnants of the notochord, and synovial saddle joints[4]. These ultimate differences in structure must be borne in mind when these organisms are employed as models to investigate the formation of the human or even the mammalian spine.

14.1 METHOD AND EXPERIMENTAL RESULTS

This work was performed in several stages. The work initially focussed on development of computer algorithms that would reproduce morphogenetic cell behaviour. These algorithms were tested individually and then incorporated into a cell simulator program *vert*. Vert was developed as part of the thesis especially for use in this investigation. It is designed to run simulations "on a biological scale" – that is using realistic biological parameters for the number of cells, the spatial arrangement of the cells, and speed of migration in three dimensions on a biological timescale. To my knowledge, this combination of biological data and model in which cellular behaviour is not pre-ordained, but dependent on external influences on the cell, and its application to a particular clinical problem, in this case the development of bony abnormalities of the subaxial cervical spine has not been previously described.

Initially the performance of *vert* was tested by determining how well the program simulated the normally occurring developmental process. This is described in Chapter 9. In Chapter 10 the experiments which were then

performed to test the variation of the result produced by the simulator, given identical starting conditions. Once it had been established that the simulator was able to reproduce the normal developmental process reliably, it was tested to determine how well it fared on abnormal development. The simulation of the development of a hemivertebra was compared with a series of biological experiments so as to ensure that as far as possible normal and abnormal biology were correctly simulated as described in Chapter 12. Only then was the simulator used to predict the mechanism of block vertebra formation, which is impossible to investigate biologically because of the inability to directly observe the experimental process. This experiment is described in Chapter 13.

14.1.1 Morphogenetic toolkit

The computer algorithms that were developed to simulate cellular behaviour are collectively known as the morphogenetic toolkit. These subroutines, written in C++, successfully implemented algorithms for cellular replication, random movement and migration up a concentration gradient. An account of these algorithms and analysis of the test simulations is described in Chapter 8. These tests have demonstrated that the computer model was able to reproduce biological cell behaviour that has been observed *in vivo* and *in vitro.*

Two variations of the chemotaxis algorithm were implemented using the "zero rule". The zero rule governs whether or not a cell is able to move in the absence of morphogen. Irrespective of whether the zero rule was tested or not, the behaviour of the majority of cells in the simulation was not altered, and the result of the experiment was unchanged. However, on an individual cellular level, using this test resulted in the loss of a single cell of the ten in the simulation. A by product of this experiment is to demonstrate the difference between the behaviour of an individual cell and a mass of cells. This leads to the following conclusions (i) when the behaviour of a large number of cells is being investigated, the general behaviour of the algorithm is more important in the outcome than the finer details of the implementation and (ii) it is important to analyse the

behaviour of the mass of cells rather than individual cells, because on an individual level cellular behaviour may be entirely different from that of the mass of cells.

14.1.2 Simulator program – vert

The actual computer program used to perform the biological simulations in the work described in this thesis is known as "vert". This program was written using the Microsoft Visual C++ development environment, initially running on a Windows NT and later on a Windows 2000 platform. Three dimensional graphics display was performed using the industry standard OpenGL platform using the Microsoft implementation of the OpenGL 1.2 specification. In order to manipulate the virtual sclerotomal cells, vert incorporated the algorithms developed as part of the morphogenetic toolkit.

14.1.3 Normal development

The normal developmental process was examined in experiments 1,2 and 3. These experiments were performed following development of the morphogenetic toolkit, and having demonstrated that the toolkit simulated the behaviour of "real" cells, these experiments sought to demonstrate whether the simulator program could be used within the context of the theoretical model described in Chapter 6, to investigate mammalian development of the cellular condensation that ultimately forms the vertebral body. To this end, this group of experiments specifically tested the ability of vert to (i) simulate "normal" biology, (ii) the experimental reliability of the system and (iii) the relative importance of the different morphogenetic mechanisms in normal development.

14.1.3.1 Experiment 1: normal biology

Experiment 1 was designed to test the formation of a normal vertebral body. The results of this experiment demonstrate that the developmental process forming the anterior cellular condensation requires only a morphogenetic gradient, a chemotactic response in cells to the morphogen, replication and random movement of the cells responding to

the morphogen and that the cells be located in an orderly segmented manner either side of the notochord / neural tube in order to form a normal phenotype.

14.1.3.2 Experiment 2: experimental reliability

Experiment 2 verifies the reproducibility of the simulation process. The analysis performed of identical experiments has shown that the gross morphology of the structures generated is consistent, despite variability on an individual cellular level.

14.1.3.3 Experiment 3: morphogenetic mechanisms in normal development

Experiment 3 dissects the mechanisms used to form the pre-vertebral cellular condensation. This experiment has demonstrated that both cellular migration and cellular replication are essential to the formation of the normal pre-vertebral cellular condensation seen in experiments 1 and 2. Without cellular migration, the collections of sclerotomal cells simply enlarge, but do not meet or fuse across the midline structures Figure 14-1.

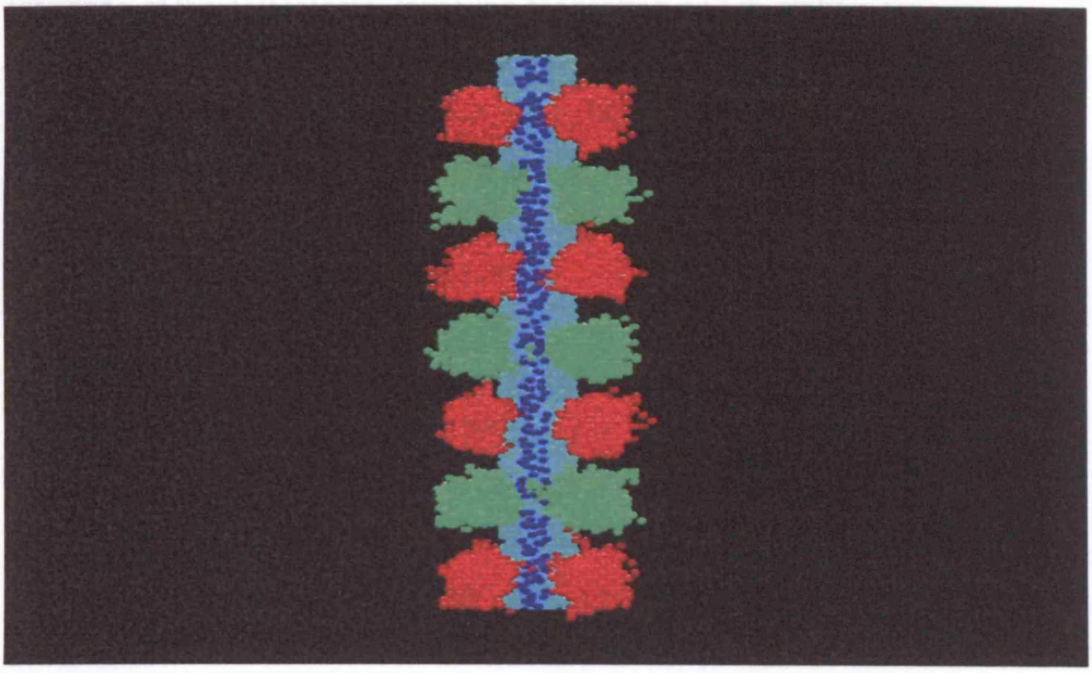

Figure 14-1: Final frame from simulation without cellular migration.

Cellular migration without replication builds cellular condensations that are more elongated than usual and only have tenuous fusions across the midline Figure 14-2.

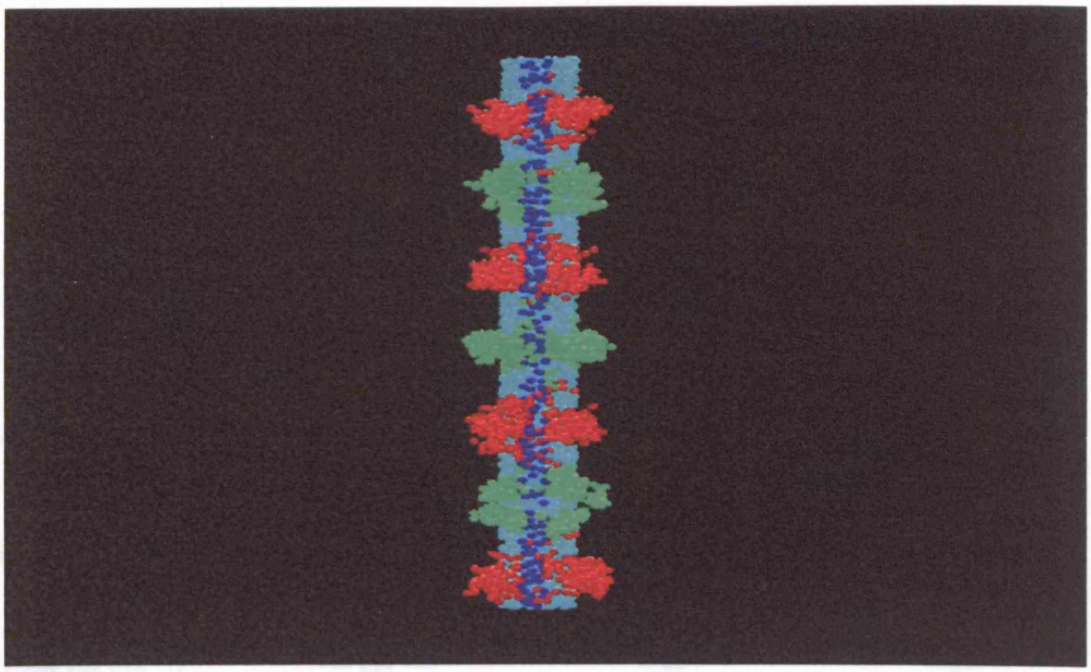

Figure 14-2: Final frame from simulation without cellular replication.

The results of this group of experiments demonstrates the validity of the theoretical model described in Chapter 6 and suggest that a co-ordinated response of the sclerotome, involving replication and migration are required to generate the pre-vertebral cellular condensation. Without migration, the sclerotomal cells will not meet and fuse across the midline structures, however, without replication, whilst the sclerotome cells will migrate to approach the midline, fusion with the contralateral sclerotomal condensation will at best be tenuous.

Although in this work, the processes of cellular replication and migration occur simultaneously, it may well be that this is not the case in the mammalian embryo. The internal state of a cell about to replicate is different from that undergoing cellular migration. Biological experiment evidence suggests that the *shh* and *Mfh* genes promote cellular replication in the *Pax-1* cells in the sclerotome. In the light of these results, I postulate that the following sequence of events then occurs following during the formation of the vertebral centra:

- Stage 1: segmentation of the paraxial mesoderm to form somites, which subsequently partition into sclerotome and dermatomyotome.

- Stage 2: migration of the sclerotomal cells towards to anterior midline structures of the neural tube and notochord.
- Stage 3: replication of the sclerotomal cells creates the prevertebral cellular condensation around the anterior midline structures.
- Stage 4: chondrification and ossification of the prevertebral cellular condensation to form the vertebral body.

This process is summarised in Figure 14-3.

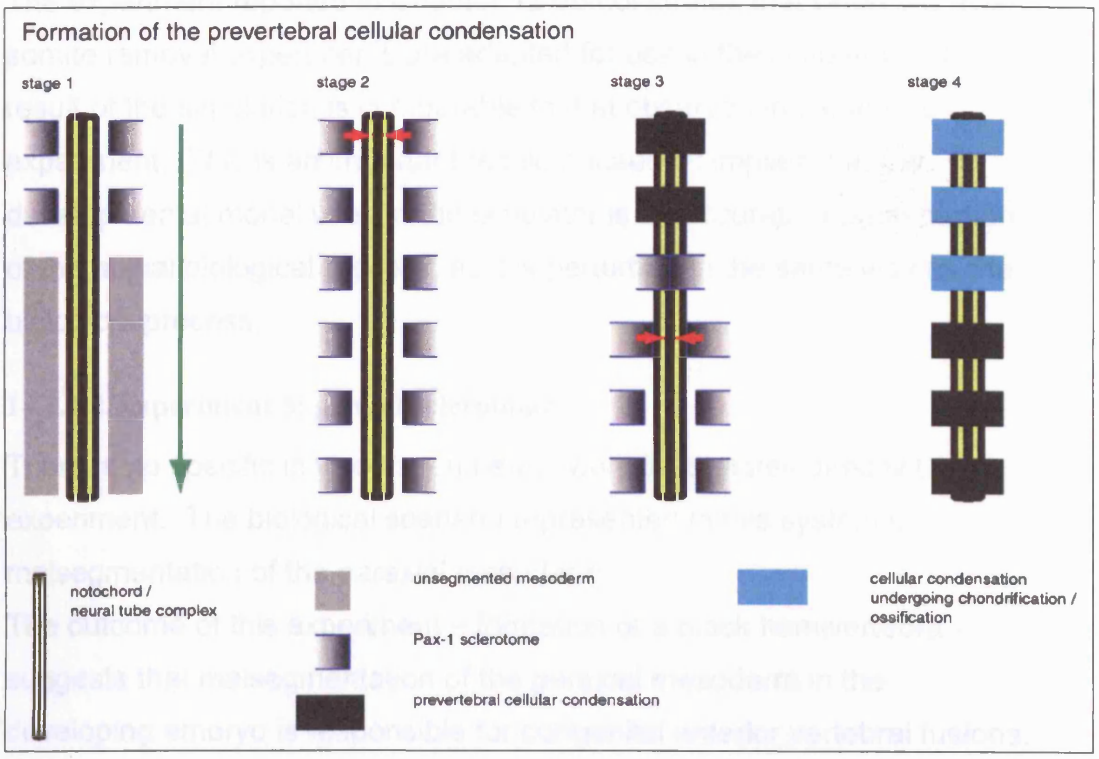

Figure 14-3 Schematic representation of normal development. Sclerotomal cells migrate medially as shown by the red arrows in a craniocaudal sequence (green arrow).

This process is in keeping with the postulated role for the Pax genes, acting as selector and replication control genes[188] and the other available *in vitro* and *in vivo* experimental evidence.

14.1.4 Abnormal development

Following the successful outcome of the experiments to simulate normal development, a second group of experiments was performed. The developmental scenario was perturbed along the lines of known biological experiments, the idea being to test whether the outcome of the simulator was perturbed in a similar manner to that occurring in the biological

system. Much work has been performed on the contribution of a specific somite to the vertebral column, largely to determine whether resegmentation occurs in the avian and mammalian embryos[121,189-191]. However, this work has also demonstrated the consequence of loss of a somite on the eventual morphology of the vertebral column[181-183].

14.1.4.1 Experiment 4: loss of sclerotome

The experiment reported in Chapter 12 demonstrates that when the avian somite removal experiments are adapted for use in the simulator, the result of the simulation is comparable to that observed in the *in vivo* experiment. This is an important result, because it implies that the developmental model used in the simulator is an accurate representation of the actual biological process, as it is perturbed in the same way as the biological process.

14.1.4.2 Experiment 5: gain of sclerotome

There is no specific in vivo experimental work that relates directly to this experiment. The biological scenario represented in this system is malsegmentation of the paraxial mesoderm.
The outcome of this experiment – formation of a block hemivertebra – suggests that malsegmentation of the paraxial mesoderm in the developing embryo is responsible for congenital anterior vertebral fusions. This result, can be, perhaps predicted by the largely linear migration of the cells noted in the previous experiments, and suggests that the morphology of the anterior vertebral column mirrors that of the paraxial mesoderm several developmental stages previously.

14.1.5 Generic outcome measures

Much of the analysis of outcome so far reported is based on the form of the structure generated by the migrating sclerotomal cells. The generic outcome measures offer an alternative method of analysis of the outcome based upon experimentally derived data from biological experiments about cell behaviour / sclerotome morphogenesis.

14.1.5.1 Cell mixing from adjacent sclerotomes

In biological models, mixing of cells from adjacent sclerotomes has not been observed to any substantial degree. In all of the experiments reported in this thesis, mixing of cells from adjacent sclerotomes was not noted. Even in experiment 3, where the additional cells were placed immediately adjacent to sclerotomal cells, between the left fourth and fifth sclerotomes, very little interface mixing was observed.

14.1.5.2 Preservation of disk space between prevertebral cellular condensations

Cell free space between adjacent sclerotomes, that will in time be occupied by the intervertebral disk, was preserved between the adjacent sclerotome cells in all experiments, except when additional cells were added in experiment 3 and in experiment 5. Very little cranial or caudal "drift" of the sclerotomal cells into this space was noted during cellular migration, although adjacent to the notochord, a perinotochordal tube of cells was noted in the final structure, as described by Verbout[192]. These results suggest that cell migration is largely linear in nature.

14.1.5.3 Presence of sclerotomal cell fusion across midline / around notochord

This was observed to occur in those experiments in which cells present on each side of the midline and able to migrate and replicate as demonstrated in experiment 1 and 5. Tenuous midline fusion was observed in experiment 3 when cells were only allowed to migrate and replication did not occur. From the experimental results the requirements for midline fusion are:

- cells migrate from both sides of the midline to surround the midline structures
- replication of the cells occurs.

Unpaired sclerotomal cells, such as those seen in experiment 4, migrate only to the midline, but not beyond, as discussed below. Irregular segmentation in the cranio-caudal dimension does not affect midline fusion, so long as there are cells either side of the midline.

14.1.6 Behaviour of unpaired sclerotomal cells

The similarity of the behaviour of the additional magenta coloured cells in the experimental simulation of a fused vertebra and the unpaired right fourth sclerotomal cell collection in experimental simulation of a hemivertebra is worthy of note. In both situations the cells behave identically, in that they migrate to the source of the morphogen, but do not cross the midline. Neither do the cells intermingle with cells from the adjacent somites. The experimental evidence from the computer simulator demonstrates that most cells migrate towards the midline in a fairly direct manner. These cells are most likely to be prevented from crossing the midline because this is were the highest concentration of morphogen is found. The chemotaxis algorithm does not allow for migration down a concentration gradient.

14.2 MORPHOGENETIC MECHANISMS

These experiments, taken together, suggest that abnormalities of the spinal vertebrae can be caused by abnormalities of the spatial arrangement of the sclerotomal cells prior to migration. The experiments demonstrate that the necessary morphogenetic mechanisms formation of the pre-vertebral cellular condensation are

- concentration gradient of morphogen
- sclerotomal cells that migrate up a concentration gradient (of morphogen)
- cellular replication
- random movement

14.2.1 The morphogen concentration profile

The morphogen concentration profile has not been investigated in this work - primarily because an easily understood representation in three dimensions would require volume rendering with transparency and a special colour scale. Unfortunately, the resources to perform this sort of image display are not available on a desktop personal computer.

This is unfortunate, because correlation of the morphogen concentration profile with cellular migration might provide further insights into the developmental mechanisms, at least as employed in this simulation. The morphogen profile can be estimated, however, given the boundary conditions of a diffusion sink, and continued secretion of morphogen by the notochord cells. The profile generated is probably linear, in line with the notochord, with a sharp fall off in concentration, until the boundaries of the simulation are reached.

Fan demonstrated the diffusibility of *sonic hedgehog*[88], and ability to induce Pax-1 expression in the sclerotome. The notochord has been demonstrated to secrete *shh*[87,102,103,193,194]. It is therefore reasonable to assume that a concentration of *shh* exists from the notochord to the region of the sclerotomes. However, two important questions in this respect still require answers: (i) whether this is the actual morphogenetic agent that the sclerotomal cells respond to, or whether there is another morphogen not yet elucidated, and (ii) what is the profile of the morphogen in the biological system. Both of these questions will require in vivo experimental work in order to resolve these issues.

14.2.2 The balance of replication *versus* migration in the formation of the vertebral column

The algorithms, as implemented in this work, do not separate replication and migration into mutually exclusive events; ie within one frame a cell is able to replicate and migrate. This is unlikely to occur in the real biological situation. Perhaps a better implementation would have been to dis-allow replication if a cell had migrated within a frame.

The replication constant at 6%, when compared with experimental data of cellular somite cell replication, is probably a slight over estimate. The experiments have demonstrated that the role of replication appears to be most important in generating a cellular condensation around the notochord and anterior neural tube. The actual mechanism of replication in this function is to join or fuse the two cell masses across the midline.

Replication is not responsible for the movement of cells from the position of the laterally placed sclerotome to the midline structures.

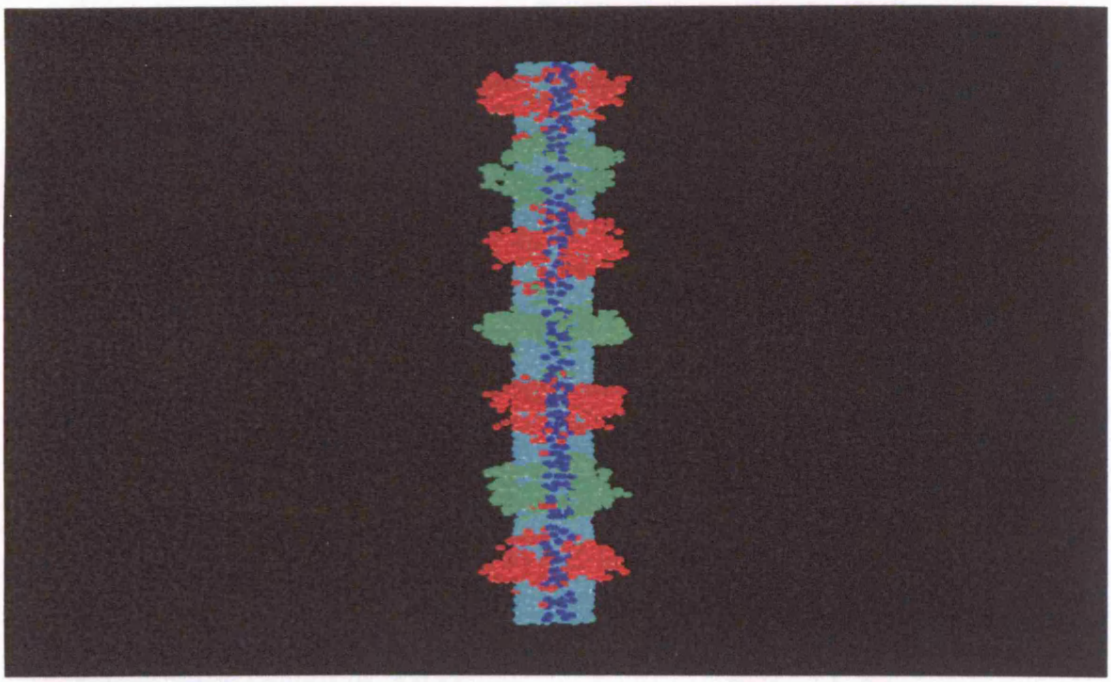

Figure 14-4 Simulation performed with adnoto dataset and 2% replication.

The simulation final frame pictured in Figure 14-4 was obtained when the replication constant had been reduced to 2%. The frame demonstrates that the size of the cellular condensation that is formed is less than in the earlier experiments, however, it can be clearly seen that cells have migrated from their initial lateral position to surround the anterior midline structures. The fact that the cells have migrated towards the midline, but that cells from either side of the midline structures have not fused implies that fusion occurs as a result of replication, rather than migration.

14.2.3 What is the relationship of somite malsegmentation to the observed congenital vertebral abnormalities

The results discussed above have demonstrated that, in this work at least, sclerotomal cell migration is predominantly linear, and that the pre-vertebral cellular condensation is formed by fusion across the midline of sclerotomal cells from both sides of the midline.

Malsegmentation – alternatively known as irregular segmentation – can be induced by teratogen or heat shock [97], or genetically inherited as in the *Pudgy* murine mutant[32] and leads to the formation of irregular somites from the paraxial mesoderm. In this situation, the spread of *Pax-1* positivity increases in the cranio-caudal dimension, as is seen in the figure below from Barnes etal[97].

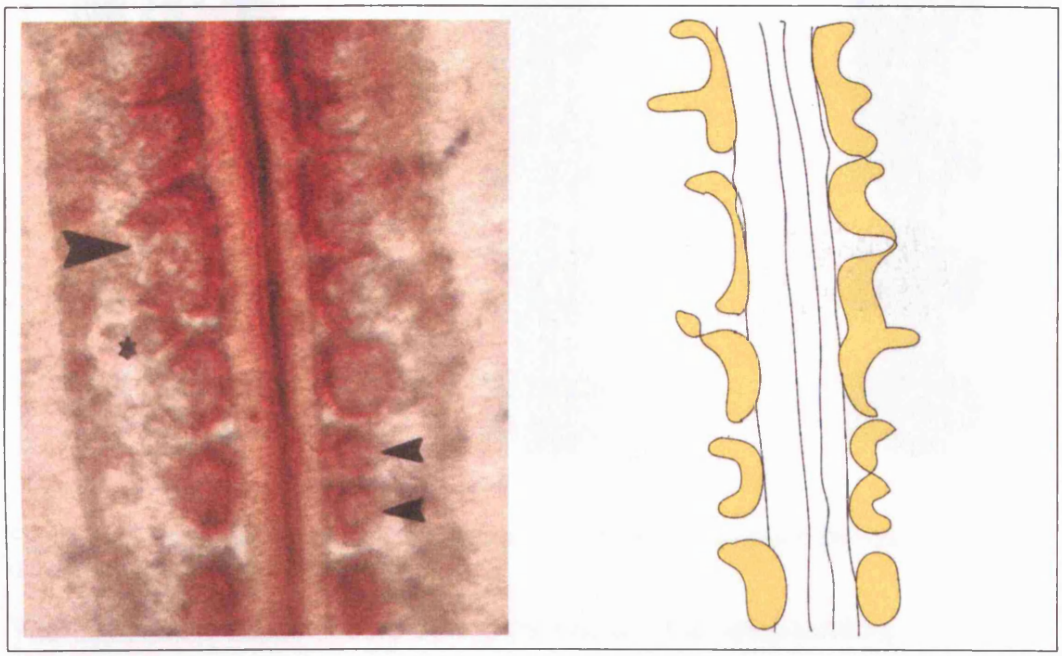

Figure 14-5 Malsegmentation of paraxial mesoderm following heatshock. Original illustration from Tuan etal on left, tracing of Pax-1 expression on right.

The length in the craniocaudal dimension of the "front" across which cells will migrate from their original lateral position to the perinotochordal position will therefore be increased, so increasing the craniocaudal length of the cellular condensation fated to form the vertebral body. This is illustrated in Figure 14-6.

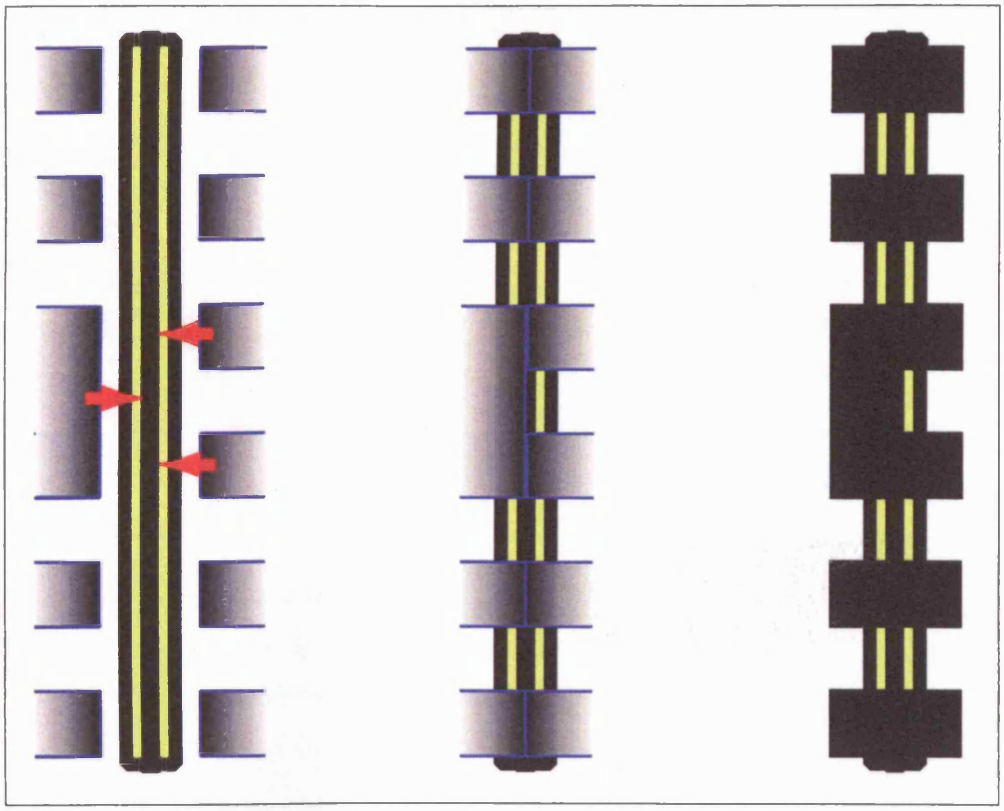

Figure 14-6 Schematic illustration to demonstrate how an increased in the craniocaudal dimension leads to a block vertebra.

The opposite process occurs during formation of a hemivertebra. Sclerotomal cells are lost from the contralateral side. Ipsilateral cells migrate towards the midline but because of the lost cells fusion across the midline does not occur. The unpaired sclerotomal cells continue to development normally, hence undergo chondrification and ossification, leading to the formation of a ipsilateral hemivertebra. This is illustrated in Figure 14-7.

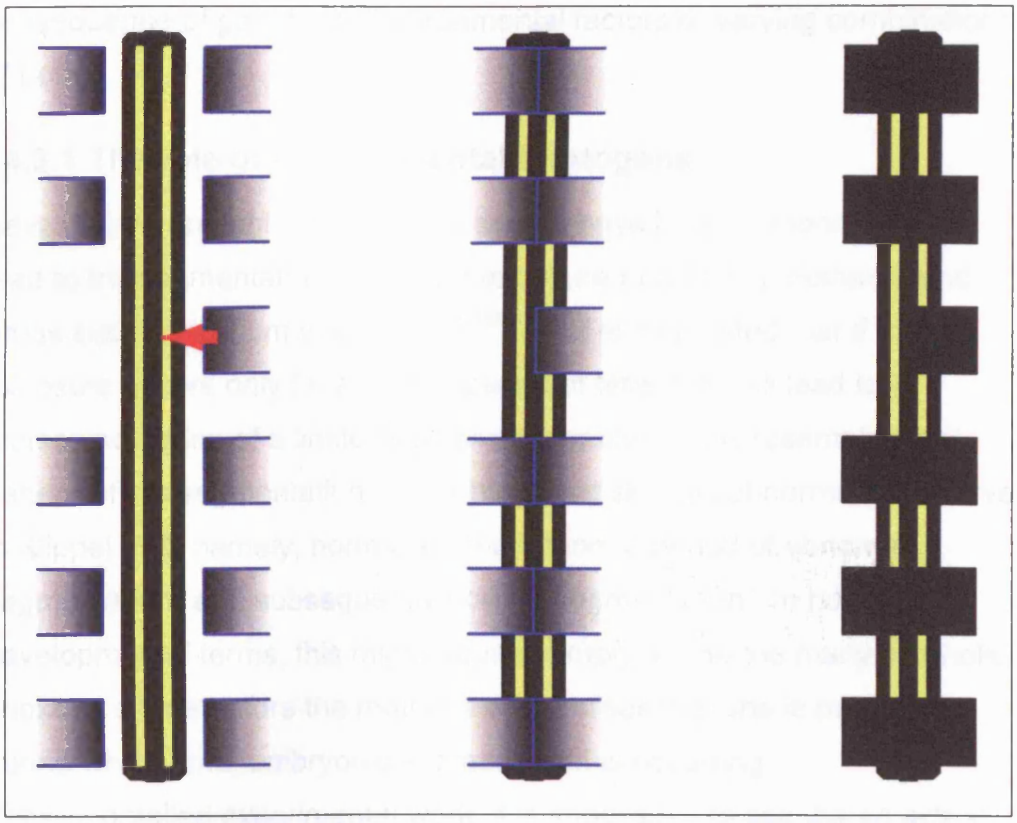

Figure 14-7 Schematic illustration demonstrating the formation of a hemivertebra.

It is important to consider whether the elongated vertebral body formed is from just one segment, or whether it is two or more segments fused together because of the extreme reduction in the space between the lateral sclerotome cells. The work performed in this thesis has not attempted to resolve this point. However, as very little cranial or caudal drift was noted, it is more likely to be the former rather than latter. In the clinical situation, this maybe resolved by examination of the posterior elements, if normal, or the number of spinal nerves seen per motion segment.

14.3 THE MECHANISM OF MALSEGMENTATION IN THE DEVELOPING EMBRYO ?

In order for this work to be a convincing explanation of the clinical / embryological abnormalities observed in man and animals, there has to be a valid explanation for the alterations to the arrangement of the sclerotomal cells. Disturbance of the segmentation phenotype maybe a

consequence of genetic or environmental factors or varying combinations of both.

14.3.1 The role of environmental teratogens

Several environmental teratogenic agents have been demonstrated to lead to malsegmentation, including exposure to ethanol, methanol and drugs such as sodium valproate[184,195,196]. It is suggested that if the exposure occurs only for a limited period of time, this will lead to malsegmentation of a limited number of somites. This resembles that pattern of malsegmentation and subsequent skeletal abnormality observed in Klippel-Feil, namely, normal segmentation, a period of abnormal segmentation, and subsequently normal segmentation. In human developmental terms, this might equate simply to one too many alcoholic drinks at a time before the mother even realises that she is pregnant, during which time, embryonic segmentation is occurring.
Without detailed experimental work, it is impossible to ascribe an actual mechanism of action to the teratogenic influence on segmentation. Indeed, different agents probably work through different mechanisms.

14.3.2 Candidate genes

The process of segmentation is incompletely understood, although there is broad agreement of the basic principles of epithelialization, A/P polarity and segmentation. The genes involved in regulation of each process are listed in Table 14-1(from figure 5, Genetic Regulation of Somite Formation, Rawls etal)[125].

Somite formation Epithelialization	A/P polarity	Segmentation
Paraxis	MesP2	Presenilin1
	Presenillin1	Notch-Delta
	Notch-Delta (Dll1)	RBP-Jκ

Table 14-1: signalling factors controlling somite formation

A simplistic view of the responsible genes is that disturbance of anyone of the genes involved in the segmentation process might be responsible for

the abnormal cervical vertebrae discussed in this work. However, this view is not supported by experimental data.

The experiments performed for this work have demonstrated that the cause of the abnormal vertebral body forms is either a consequence of misplaced sclerotomal cells, not enough, or complete absence of these cells. Malsegmentation of the paraxial mesoderm is the most likely cause of the former, and may also cause the latter.

14.3.2.1 Phenotype of genetic mutations

Mutation of the *Notch1* gene will result in asymmetrical and delayed segmentation of the paraxial mesoderm[197]. In mice without *Dll1* expression, a segmented pattern forms, but anterior-posterior polarity does not develop and the pattern of spinal nerves and ganglia is not preserved[198]. *Dll3* mutation in humans leads to a Spondylocostal dysplasia phenotype[199]. Mice lacking *Presenilin1* have irregular rostal somites and absence of caudal somites[200]. Absence of paraxis leads to a shortened vertebral column, with the caudal vertebral replaced by an unsegmented cartilaginous mass[135].

14.3.2.2 Inherited mutation or teratogenic insult

The mechanism of malsegmentation is likely to be due to either mutations within the genes encoding for the proteins or abnormal protein forms. Genetic mutations might be either inherited, eg *undulated, tail kinks, pudgy* or de novo mutations related to teratogenesis. Abnormal protein forms might be a consequence of genetic mutations or direct teratogenic assault on the protein molecule. Mutations that are inherited will affect the whole of the vertebral column, whilst those that are transient, such as the action of a teratogen over a period of time will alter the phenotype of the vertebral bodies undergoing morphogenesis during teratogenic exposure.

14.3.3 Basic abnormal vertebral body types

The experiments performed in this thesis have suggested how the normal vertebral developmental mechanism is perturbed and the following types of vertebral malformation arise:

- block vertebra
- hemivertebra
- butterfly vertebra

14.3.3.1 Block vertebra

Formation of a block vertebra was examined in Chapter 13. Loss of segmentation results in the formation of a giant somite, which expresses *Pax-1* throughout its cranio-caudal extent in the ventro-medial region. In patients in whom there is no family or previous history of vertebral abnormalities, this is most likely to reflect a teratogenic insult occurring at the time of segmentation, and causing malsegmentation.

14.3.3.2 Hemivertebra

Generation of this abnormal form was examined in Chapter 12. Loss of the contralateral sclerotome results in the formation of an ipsilateral cellular condensation, which reaches but does not cross the midline. This is likely to arise from malsegmentation in a similar manner to that of a block vertebra.

14.3.3.3 Butterfly vertebra

A potential explanation for the formation of this abnormal form was investigated in Chapter 11. Lack of cellular migration results in the formation of two laterally placed cellular condensations, which if they subsequently undergo chondrification / ossification will morphologically resemble a butterfly vertebra.

14.3.3.4 Waisted vertebra

This refers to the vertebra that is often described occurring in Klippel-Feil. The body of the vertebra is said to be waisted or constricted in the medio-lateral dimension. Lack of cellular replication of the sclerotome cells, as

investigated in Chapter 11 is a potential mechanism for the formation of this type.

14.3.4 Complex abnormal vertebral body malformations

These forms, such as the massive fusion, multiple level fusion and the chaotic form are likely to arise from abnormal segmentation occurring at multiple cranio-caudal levels. Consecutive bilateral block vertebrae will form a massive fusion, whilst random segmentation, unpaired across the midline will lead to the generation of a chaotic form. These mechanisms are illustrated in Figure 14-8.

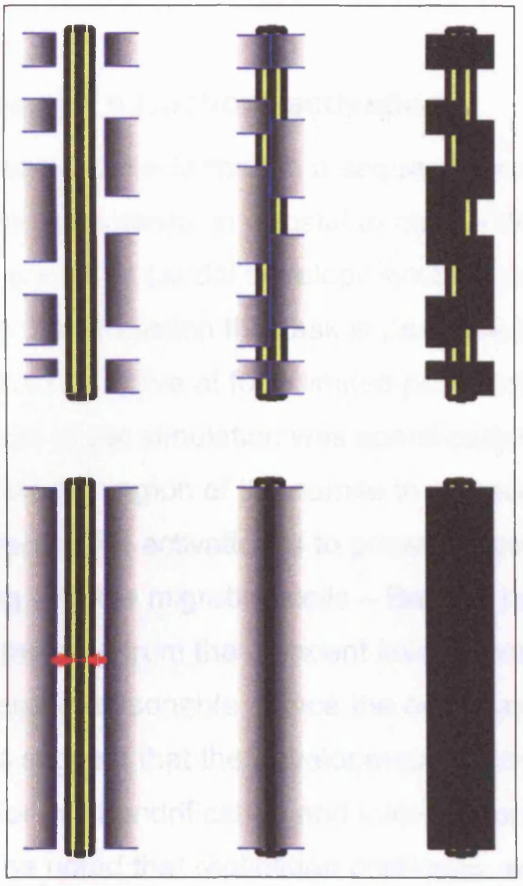

Figure 14-8 Formation of complex vertebral body malformations - chaotic form (above) and massive fusion (below)

14.4 HOW GOOD IS THE THEORETICAL MODEL ?

It is important to critically consider how well the theoretical model utilised in this work represents the actual processes occurring in the human embryo, as differences between the two are likely to lead to different outcomes and hence incorrect conclusions being drawn.

14.4.1 Anatomical considerations

The theoretical model described earlier in this work is based upon classical embryological observations and more recent laboratory investigations into gene expression. The model accurately simulates anatomical properties, such as dimensions and number of cells that are involved in vertebral column formation, albeit in the mouse, as these can be seen and have been extensively investigated over many years [33,147,168,192,201,202].

14.4.2 Sclerotome and notochord activation

In the embryo, the somites are formed in a sequential manner from the insegmented paraxial mesoderm, in a rostal to caudal direction. In an attempt to emulate cranial to caudal developmental process that is seen in somite formation, in the simulation this task is performed by only allowing the sclerotome cells to be active at for a limited period of time, as outlined in Table 9-1. The aim of the simulation was specifically to model the migration of cells from the region of the somite to surrounding the notochord. The effect of the activation is to prevent more cranial or caudal cells from interfering with the migrating cells – Bagnall has demonstrated that little mixing of the cells from the adjacent levels occurs – and I believe the activation process is reasonable. Once the cells have migrated, animal experiments suggest that the developmental process continues, including the initiation of chondrification and intervertebral disk formation. It should however, be noted that replication continues, which may well be the case during chondrification. I feel that the process of staged activation is a reasonable representation of this stage of development.

The notochord, however, remains active - and hence able to release morphogen - for the duration of the simulation. Expression of notochord genes has been less clearly elucidated during sclerotome migration and formation of the vertebral body anlagen.

In the developing embryo, expression of notochordal genes at an early stage has been demonstrated (E8)[203]. In particular, expression of *shh* has been demonstrated to occur at the appropriate time for somite, limb and central nervous system patterning functions[102]. Somite dissociation is also seen to occur concurrently with *shh* expression, thereby releasing sclerotomal cells able to migrate to surround the notochord.

14.4.3 Mechanism of sclerotome migration

The mechanism of the migration is unknown. Fan etal have demonstrated *shh* is a diffusible molecule, able to cause the expression of *Pax-1* in sclerotome cells in an *in vivo* model[88]. Gritli-Linde etal investigated the range of action of *shh* and *ihh* in the mouse embryo[204]. They demonstrated that the *shh* ligand is able to move significant distances with direct evidence for the presence of *shh* in several target compartments. Demonstration of the Hedgehog proteins required the preservation of the proteoglycan / glycosaminoglycan matrix, and in the tooth, alterations of this matrix altered *shh* signalling.

Newgreen demonstrated the ability of sclerotomal cells to migrate towards a notochord[148]. In the absence of *Pax-1* expression, as found in the *undulated* mutants there is failure of the sclerotomal condensation to form, and hence malformation of the anterior vertebral structures[115]. It is likely that absence of the *Pax-1* expression results in failure of migration.

I consider it therefore is reasonable to model the cellular migration as described, dependant on *shh* leading to *Pax-1* expression, and subsequent migration towards the notochord. The more precise details of the method are yet to be elucidated.

14.4.4 Anatomical variation between species

It is important to note that significant differences between adult vertebral morphology are found even in closely related species, and that the model is a necessary fusion of the observed embryological processes that occur largely in chicken and mouse vertebral column formation, but incorporating information from sheep development and also data from a number of other animal models, including human development. The consequence of this it that when compared to the developmental process and the phenotype found in any one particular animal, differences between particular animal and the model are likely to be noted. The consequence of this is that the model represents the generality, rather than any one specific animal.

I do not feel that this is a major problem for this work because the described differences between the different animal models usually arise following the sclerotome migration and cellular condensation stage being simulated.

In conclusion, it is felt that the whilst the theoretical model is obviously a simplified version of the real state of affairs, it faithfully represents the major concepts of this stage in the development of the vertebral column.

14.5 CONCURRENT EMBRYONIC EVENTS

There are a number of processes that take place in animal development concurrently with the somite formation / sclerotome migration that have not been incorporated into this model. In particular the effect of the three dimensional folding that takes place in a number of embryos at about the time of segmentation, and is involved in neural tube closure has not been replicated. Additionally, the developmental processes occurring in the intermediate and lateral mesoderm have not been considered. Clearly the co-ordinated interaction of all of these processes is required in order to form the complete embryo, and disruption of one can lead to abnormalities in another. It can only be speculated as to the effect of not including these processes. I suspect that the effect is not great at the stage in

development under investigation, when a relatively small process of vertebral column formation has been investigated as in this case. A more complete model, perhaps from mesoderm formation to vertebral body chondrification is likely to be more affected, but in the case described in this work, the changes - morphological and genetic - outside of vertebral column formation are likely to be limited and therefore have only a constant influence if at all on the vertebral column formation process being investigated.

14.6 HOW DO THE EXPERIMENTAL RESULTS RELATE TO FORMATION OF THE INTERVERTEBRAL DISK ?

Formation of the intervertebral disk is said to arise from notochord proliferation, but has not been extensively investigated as that of vertebral body formation. The studies reported in the literature suggest that the nucleus pulposus component of the intervertebral disk is of notochordal derivation[205,206]. Studies have suggested that the notochord simply proliferates in the space between the adjacent developing vertebral bodies. The annulus appears to be of fibrous origin, and may develop at a later stage when the joint capsules and ligamentous components of the vertebral column form.

This model would fit well with the results found in this work. At the completion of the simulation, gaps between adjacent midline cellular condensations are noted - referred to in the text as the putative disk space - and it is likely that notochordal proliferation at these locations leads to the development of at least a rudimentary intervertebral disk. As discussed later, this scenario could be tested without major modifications to the simulation.

A small, partly formed disk - termed a rudimentary disk - is also sometimes observed in congenital fusions. If the disordered arrangement of the sclerotomal cells leads to reduced space around the notochord into which

cells might proliferate, it can be seen how a smaller more rudimentary disk might result.

14.7 FROM EMBRYO TO CLINIC

The object of this work was to use the computer simulator to understand how congenital vertebral abnormalities arise. In order to do this the phenotypes created by the computer simulator have been compared with those seen in patients. A wide range of vertebral abnormalities have been described, ranging from simple block vertebra to a complex fusion of the cervical vertebra as described by Klippel and Feil in their index case[7,40,105].

14.7.1 Abnormal vertebral segmentation

A review of the major series of cases of abnormal vertebral segmentation reported in the literature demonstrates several major patterns of subaxial vertebral malformations[40,105,207]. These patterns are listed in Table 14-2. Figure 14-9 illustrates type I and type IV.

Type	Name	Description
I	massive fusion	complete fusion from high in subaxial spine eg C3 to cervico-thoracic junction eg T1
II	single level	block vertebra formation eg C3-4, occasionally repeated lower in cervical spine
III	multiple levels	two or three consecutive fusions eg from C3 to C6
IV	chaotic	multiple block vertebra and hemivertebra

Table 14-2: different forms of vertebral fusion

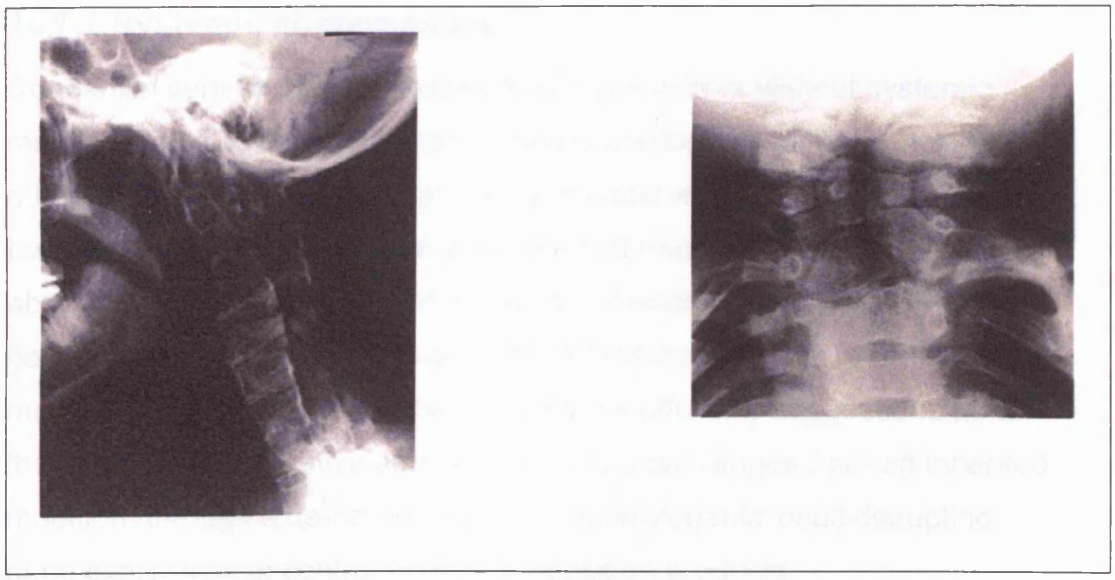

Figure 14-9 Abnormal forms of vertebral segmentation: LEFT - Type I, RIGHT Type IV

The experimental results discussed above have provided developmental mechanisms for simple isolated abnormalities such as block vertebra and / or hemivertebra. The more complex malformations can be classified according to whether there is a combination of axial and subaxial abnormalities, or whether the abnormality is limited to one or other of these regions. From the literature the most common pattern of abnormality is that of atlas assimilation to the occiput and C2-3 fusion[40,41]. The present work has not investigated the formation of the atlanto-axial complex, which results from a complex re-arrangement of the otherwise evolutionally lost components of the vertebra. This pattern has been attributed to an altered Hox expression pattern leading to anterior homeotic transformation[105].

The work offers an explanation for the massive fusions of the cervical spine – the one bone spine – such as those described by David etal[42], and Nguysen and Tyrrel[207]. In the most extreme example of these cases, fusion is found from the occupit to the cervico-thoracic region. Extrapolation of the results of experiment 5 (giant somite) across multiple vertebral levels would lead to the formation of a massive fusion in the cervical spine, similar to those described by David and Nguysen.

14.7.2 Systemic abnormalities

Congenital vertebral abnormalities may occur with or without systemic manifestations. Vertebral abnormalities occurring in combination with other systemic abnormalities are likely to occur as a consequence of the Lubinsky-Optiz hypothesis which states that multiple congenital abnormalities arise because of disruption of discrete developmental fields[208]. Whilst this hypothesis states the mechanism that gives rise to multiple congenital abnormalities, it does not offer any suggestions as to the origin of the causative agent. This, as before ranges from an inherited mutation, through a de-novo mutation to a teratogenic insult disrupting gene expression or control of gene expression products.

It is also interesting to speculate on the presence or absence of associated systemic malformations occurring with the vertebral fusions. Vertebral fusions occurring with cardiovascular defects are more likely with fetal alcohol syndrome, whilst those seen in Klippel-Feil syndrome are more likely to be associated with genito-urinary malformations. As discussed in the paragraph above, it is likely that these associations represent either a different time of teratogenic insult, or a different mechanism of action of the teratogen.

14.7.3 Cervical spinal cord abnormalities

Several papers have reported on the rare occurrence of cervical spinal cord malformations associated with bony vertebral malformations, and several explanations have been advanced for this association[43,209-211]. David etal[43], have divided the split cord malformation into those with a partial dorsal split and those with a complete split – diastematomyelia. They suggest that the underlying cause in the formation of a diastematomyelia is adhesion between the endoderm and the ectoderm, whereas a partial dorsal split is caused by incomplete closure of the cervical neural tube. The theory suggested by David etal is a refinement of that initially proposed by Bremer[212] and Pang[209]. David etal were not able to link the vertebral malformations observed in the genetic mechanism proposed for the split cord malformation, however, it is likely

that both malformations arise as a consequence of a teratogenic insult, which disturbs more than one developmental process in the locality.

Whilst, except for the single level ipsilateral fusion and single hemivertebra, the malformations discussed above and listed in Table 14-2 have not been explicitly modelled in this work, it is likely that they arise from a combination of one or more of the basic abnormal vertebral body types.

14.7.4 Klippel-Feil Syndrome

This was defined by Klippel and Feil in 1912[7]. It consists of a short neck, low hairline and restricted cervical movements. These clinical characteristics were due to a cervico-dorsal fusion (illustrated in Figure 2-3 earlier in thesis). In more recent years, the term Klippel-Feil has become synomous with any form of vertebral malsegmentation, thereby encompassing a wide variety of vertebral malformations. It is partly this which makes an accurate definition of the aetiology of the condition difficult, and partly, that most cases of vertebral malsegmentation are sporadic rather than inherited. Additionally, it is likely that many cases are never identified, and in those that are identified, this usually occurs long after birth, when any recollection of an abnormality or ingestion of teratogen by the subjects mother at the very beginning of pregnancy is limited.

14.7.4.1 Congenital or acquired ?

Several human pedigrees have been reported in the literature of congenital vertebral segmentation abnormalities[19]. However, only Clark has isolated a causative gene. Inherited congenital vertebral segmentation abnormalities are common in horses[31] and laboratory mice[32,131]. In mice, the gene responsible for the deformity has been identified, and several different mutations have been correlated with different phenotypical forms. The human gene *HuP48* gene is analogous to the murine *Pax-1* gene[213]. Analysis of the *HuP48* gene in a series of individual with vertebral segmentation abnormalities did not demonstrate genetic mutations[213]. However, the location of the malformed vertebra in

these individuals is somewhat different to that of the *undulated* phenotype. Affected humans demonstrated cervical malformations, whilst the malformations seen in the *undulated* phenotype are most common in the lumbar region.

The most closely related murine mutant to Klippel-Feil is *Tail-Kinks*. This is a recessive mutant, and both sexes are fertile and viable[210]. Figure 14-10, taken from Gruneberg[32], page 177, illustrates the loss of height in the cervical region of the spine and the chaotic nature of the cervical vertebrae. The nature of the abnormality in *Tail-Kinks* has not been extensively investigated, although Gruneberg classified this mutation as a sclerotomal disorder[32]. In the classification of vertebral abnormalities presented above, this phenotype is closest to that of type IV (Table 14-2).

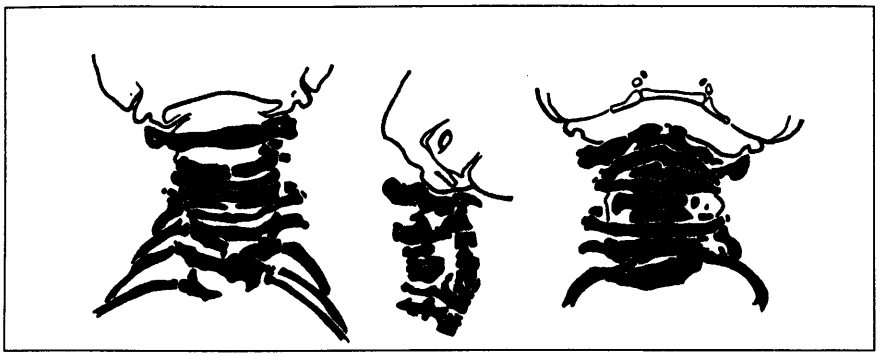

Figure 14-10 Cervical region of the tail kinks mouse. From Gruneberg, 1963

It is likely that the spectrum of vertebral segmentation abnormalities contains both inherited and acquired forms.

14.7.4.2 Developmental mechanism

Within the literature there is little recent discussion of the developmental mechanism of the Klippel-Feil phenotype. Bavinck and Weaver proposed that an abnormality of the blood supply to the developing vertebra might be responsible for the defects[47]. Generally, it appears to be accepted that the deformity arises through an abnormality of segmentation, although the precise mechanism is uncertain.

The work performed in this thesis has demonstrated that the most likely developmental mechanism for Klippel-Feil is abnormal segmentation,

whether of inherited or acquired (teratogenic) aetiology. Abnormal linear arrangement of the sclerotomal cells as demonstrated in Figure 14-5 leads to abnormal midline cellular condensations at a single level. Malsegmentation at several cranio-caudal levels can result in the formation of a more complex abnormality.

14.7.4.3 Do mutations occur predominantly in the cervical spine ?

This work has studied the cervical spine, this region of the spine being the site of the malformations described in the Klippel-Feil syndrome. It however clear that these malformations are not limited to this region. Abnormalities such as spondylocostal dysplasia affect all regions of the spine.

The literature does not report any studies which have systematically investigated the incidence of vertebral abnormalities by region, and therefore it is not known whether one region is more affected or susceptible to malformations that other regions.

Tams investigations in mice demonstrated the number of cells in the cervical somites is less than the number in thoracic and lumbar regions[168]. It can be speculated that when larger numbers of cells are involved, it might become more difficult to disrupt certain morphogenetic processes such as chondrification. This is because, in processes that are dependant on a critical number of cells in order to commence, such as chondrification, a relatively greater proportion of cells must be non-functional, for example, as a response to teratogenic insult, in order to prevent the process from occurring.

14.8 NEW EMBRYOLOGICAL PERSPECTIVES

14.8.1 Subaxial vertebral development

The work described in this thesis has demonstrated that the morphological mechanisms of sclerotomal migration, cellular replication, establishment of a morphogenetic concentration gradient and regular segmental

arrangement of the sclerotomal cells are essential for the normal formation of the anterior vertebral body, and that perturbation of one or more of the developmental mechanisms or the regular sclerotomal arrangement will result in abnormal forms.

14.8.2 Resegmentation

The concept of resegmentation of the somites, first introduced by Remak in 1850[214] remains one of the most controversial topics of vertebral column development. Somites give rise to the segmental myotome and the segmental vertebrae. In order that the musculature act across the vertebrae, the vertebrae are displaced by half a segment. Remak considered this displacement arose by combination of the caudal half of the anterior vertebra with the cranial half of the next anterior vertebra. Verbouts view of resegmentation – that it does not occur – appeared to be firmly quashed by a series of avian and murine experiments over the last 15 years[189,190,215-217]. However, recent experiments performed by Fleming etal[218] have suggested that in zebrafish resegmentation does not occur. Instead, they have found that ossified vertebral bodies appear to arise by the secretion of bone matrix from the notochord without an intermediate cartilage stage. Fleming etal have also demonstrated that notochords cultured in isolation are able to secrete bone matrix in vivo[218].

These findings imply that the model of resegmentation may not apply in all vertebrates. An explanation for the variability of resegmentation might be the different evolutionary adaptation of the components of the vertebral body.

14.9 FURTHER WORK

This work has focussed on a particular and discrete developmental stage in the formation of the vertebral column. In order to carry out this work, a simulation program has been developed. The suggestions outlined below can be divided into two groups - (i) those that might be investigated using the current simulator, or following minor modifications, and (ii) those that

would require substantial further work, either in designing a theoretical model and framework and / or refining the computer simulator.

14.9.1 Simulations using the current theoretical model and simulation program

There are a number of ways in which the theoretical model described above might be altered to investigate the effect on the cellular condensation. These include

- different patterns of notochord activation, as discussed above. In particular (i) whole notochord activated together at start time, and deactivated at the end of the simulation, and (ii) once a segment of the notochord has been activated, it remains in an active state until the simulation is complete
- alter the spacing between the starting clusters of sclerotomal cells, and the number of cells in each cluster. This would be interesting to determine whether the model requires a critical number of sclerotomal cells in order to produce robust results, particularly, as discussed above, regarding the region of the vertebral column prone to vertebral malformations and the increasing size of caudal sclerotome noted by Tam in the mouse.
- alter the diffusion, replication and secretion constants in the theoretical model, in particular to allow the notochord to replicate, and investigate formation of the intervertebral disk, as discussed above.

14.9.2 Simulations requiring further development of the theoretical model and simulation program

- The most obvious step would be to develop a model to describe the formation of the cranio-vertebral junction. Subaxial congenital abnormalities of the cervical spine often co-exist with those of the cranio-vertebral junction, however, the embryology of this region of the spine is considerably more complex than that of the subaxial region.

- Another area which might be investigated is that of spinal cord development, perhaps in combination with the vertebral column. Clearly, the two develop in synergy, and combined abnormalities are well described, although less common than those seen purely in the vertebral component of the spinal column.
- It would also be interesting to model the combined development of the spinous process and vertebral body. Bony malformations of anterior and posterior elements are often noted together.

14.10 SUMMARY

This chapter has discussed and placed in biological context the experimental findings in the work performed for this thesis. Using a realistic biological model it has been possible to demonstrate cells move towards the midline structures. This is achieved using only replication and migration up a concentration gradient. Furthermore this work has demonstrated that hemivertebrae arise from loss of the contralateral sclerotomal cells, butterfly vertebra when cellular replication has been inhibited, and disruption of the segmentation boundaries leads to fusion across the motion segments. Additionally this work has shown how the simple malformations can be combined to produce more complex malformations.

15 Conclusions

1. It is possible to model the stage in vertebral body development from sclerotome formation to cellular condensation using a cellular automata model.
2. During the normal formation of the vertebral body sclerotomal cells migrate medially in a direct manner to form a condensation around the notochord and anterior neural tube.
3. Abnormalities of segmentation causes malposition of the sclerotomal cells. Because the sclerotomal cells migrate medially in a direct manner, irregular segmentation will be reproduced in the midline cellular condensation. Lack of cells laterally causes a contralateral hemi-vertebra, whereas lack of segmentation between adjacent forming somites leads to the formation of a giant somite causing a vertebral fusion.
4. Cellular reproduction is required in order for the sclerotomal cells to fuse around the midline structures.
5. The likely cause for malsegmentation in the human embryo is exposure to an environmental teratogen such as ethanol or sodium valproate at a time before the embryos mother knows of her pregnancy.

16 References

1. Sinnatamby CS: Head, neck and spine, Last's Anatomy: regional and applied,10th Edition. Edinburgh: Churchill Livingstone, 1999, pp 414-424

2. Sinnatamby CS: Head, neck and spine, Last's Anatomy,10th Edition. Edinburgh: Churchill Livingstone, 1999, pp 425-432

3. Haldeman SD, Kirkaldy-Willis WH, Bernard TN: Introduction, An Atlas of Back Pain,1st Edition. London: Parthenon Publishing, 2002, pp 7-14

4. Hildebrand M: Analysis of vertebrate structure,4th edition. New York: John Wiley and Sons, 1995,

5. Drews U: Human Development, Color Atlas of Embryology,1st Edition. Stuttgart: Theime, 1995, pp 40-131

6. The Adult and Pediatric Spine,3rd edition. Philadelphia: Lippincott Williams and Wilkins, 2004,

7. Klippel M, Feil A: Un cas d'absence des vertebres cervicales. Nouv Iconog Salpetriere 25:223-250, 1912

8. Thorogood PV: The Relationship between Genotype and Phenotype: some basic concepts, in Thorogood PV (ed): Embryos, Genes and Birth Defects,1st Edition. Chichester: John Wiley and Sons, 1997, pp 1-16

9. Apley AG, Solomon L: The Hip, Apleys system of orthopaedics and fractures,7th Edition Edition. Oxford: Butterworth-Heinemann, 1993, pp 383-431

10. Crockard HA, Stevens JM: Craniovertebral junction anomalies in inherited disorders: part of the syndrome or caused by the disorder ? European Journal of Pediatrics 154:504-512, 1995

11. Brown N: Chemical teratogens: Hazards, tools and clues, in Thorogood PV (ed): Embryos, genes and birth defects,1st Edition. Chichester: John Wiley and Sons, 1997, pp 69-88

12. Drews U: Causes of malformation, Color atlas of embryology,1st Edition. Stuttgart: Theime, 1995, pp 358-365

13. Duncan PA, Shapiro LR, Stangel JJ, et al: The MURCS association: Mullerian duct aplasia, renal aplasia and cervicothoracic somite dysplasia. Journal of Pediatrics 95:399-402, 1979

14. Gilbert S: Environmental regulation of animal development, Developmental Biology,6th Edition. Sunderland, Massachusetts: Sinauer Associates, 2000, pp 649-678

15. Conlon RA: Retinoic acid and pattern formation in vertebrates. Trends in Genetics 11:314-319, 1995

16. Connor JM, Ferguson-Smith MA: Congenital Malformations, Essential Medical Genetics,2nd Edition. Oxford: Blackwell Scientific Publications, 1987, pp 163-180

17. Scarborough J, Aiton JF, Machlan JC, et al: The study of early human embryos using interactive three dimensional computer reconstructions. Journal of Anatomy 191:117-122, 1997

18. Brown MW, Templeton AW, Hodges FJ: The incidence of acquired and congenital fusions in the cervical spine. American Journal of Roentgenology 92:1255-1259, 1964

19. Clarke RA, Singh S, McKenzie H, et al: Familial Klippel-Feil syndrome and paracentric inversion inv(8)(q22.2q23.3). American Journal of Human Genetics 57:1364-1370, 1995

20. Ohashi HK, Wakui H, Nishimoto M, et al: Klippel-Feil syndrome and de novo balanced autosomal translocation [46,XX,t(5;17)(q11.2;q23)]. American Journal of Human Genetics 51:A294, 1992

21. Steinbok P: Dysraphic lesions of the cervical spinal cord. Neurosurgery Clinics of North America 6:367-376, 1995

22. Ackerman LL, Menezes A, Follett KA: Cervical and thoracic dermal sinus tracts. A case series and review of the literature. Pediatric Neurosurgery 37:137-147, 2003

23. Urasaki E, Yasukouchi H, Yokota A: Atlas hypoplasia manifesting as myelopathy in a child - case report. Neurologia Medico-Chirurgica 41:160-162, 2001

24. May D, Jenny B, Faundez A: Cervical cord compression due to a hypoplastic atlas. Case report. Journal of Neurosurgery: Spine 94:133-136, 2001

25. de Graaff R: Congenital block vertebrae C2-C3 in patients with cervical myleopathy. Acta Neurochirurgica 61:111-126, 1982

26. Jaskwhich D, Ali RM, Patel TC, et al: Congenial Scoliosis. Current Opinion in Pediatrics 12:61-66, 2000

27. Smith MD: Congenital scoliosis of the cervical or cervicothoracic spine. Orthopedic Clinics of North America 25:301-310, 1994

28. Pizzutillo PD, Woods M, Nicholson L, et al: Risk factors in Klippel-Feil syndrome. Spine 19:2110-2116, 1994

29. Lincolin JD: Cervical vertebral malformations / malarticulations syndrome in large dogs. Veterinary Clinics of North America - Small Animal Practice 22:923-935, 1992

30. Wagner PC, Grant BD, Reed SM: Cervical vertebral malformations. Veterinary Clinics of North America- Equine Practice 3:385-396, 1987

31. Watson AG, Mayhew IG: Familial congenital occipitoatlantoaxial malformation (OAAM) in the arabian horse. Spine 11:334-339, 1986

32. Gruneberg H: The Pathology of Development: a study of inherited skeletal disorders in animals,1st edition edition. Oxford: Blackwell Scientific Publications, 1963,

33. Collins P: Embryology and Development, in Williams PL, Bannister LH, Berry MM, et al (eds): Grays Anatomy,38th Edition. New York: Churchill Livingstone, 1995, pp 91-342

34. Wilting J, Ebensperger C, Muller TS, et al: Pax-1 in the development of the cervico-occipital transitional zone. Anatomy and Embryology 192:221-227, 1995

35. Lufkin T, Mark M, Hart CP, et al: Homeotic transformation of the occipital bones of the skull by ectopic expression of a homeobox gene. Nature 359:835-841, 1992

36. Guille JT, Sherk HH: Congenital osseous anomalies of the upper and lower cervical spine in children. Journal of Bone and Joint Surgery 84-A:277-288, 2002

37. Watanabe Y, Le Douarin N: A role for BMP-4 in the development of subcutaneous cartilage. Mechanisms of Development 57:69-78, 1996

38. Monsoro-Burq A-H, Duprez D, Watanabe Y, et al: The role of bone morphogenetic proteins in vertebral development. Development 122:3607-3616, 1996

39. Gunderson CH, Greenspan RH, Glaser GH, et al: The Klippel-Feil syndrome: genetic and clinical re-evaluation of cervical fusion. Medicine 46:491-512, 1967

40. Gray SW, Romaine CB, Skandalakis JE: Congenital fusion of the cervical vertebrae. Surgery, Obstetrics and Gynaecology373-385, 1964

41. David, K. M, Thorogood, P. V, Stevens, J. M, and Crockard, H. A. The dysmorphic cervical spine in Klippel-Feil syndrome: interpretations from developmental biology. Neurosurgical Focus . 1999.

42. David KM, Thorogood PV, Stevens JM, et al: The one bone spine: a failure of notochord / sclerotome signalling ? Clinical Dysmorphology 6:303-314, 1997

43. David KM, Copp AJ, Stevens JM, et al: Split cervical spinal cord with Klippel-Feil syndrome: seven cases. Brain 119:1859-1872, 1996

44. Kessel M, Gruss P: Homeotic transformations of murine verterbae and concomitant alteration of Hox codes induced by retinoic acid. Cell 67:89-104, 1991

45. Kessel M, Balling R, Gruss P: Variations of cervical vertebrae after expression of a Hox-1.1 transgene in mice. Cell 61:301-308, 1990

46. Kieny M, Mauger A, Sengel P: Early regionalization of the somitic mesoderm as studied by the development of the axial skeleton of the chick embryo. Developmental Biology 28:142-161, 1972

47. Bavrinck ON, Weaver DD: Subclavian artery supply distribution sequence: Hypothesis of a vascular etiology for Poland, Klippel-Feil syndrome and Mobius anomalies. American Journal of Medical Genetics 23:903-918, 1986

48. Sheffield, L. J. A dominantly inherited syndrome of palate and vertebral abnormalities. Sixth Annual General Meeting Human

Genetics Society of Australia, Adelaide, Australia, August 23-25 . 1982.

49. Morgan MK, Onofrio BM, Bender CE: Famalial os odointoideum. Case report. Journal of Neurosurgery 70:636-639, 1989

50. Clarke RA, Kearsley JH, Walsh DA: Patterned expression in familial Klippel-Feil syndrome. Teratology 53:152-157, 1996

51. Mortier GR, Lachman RS, Bocian M, et al: Multiple vertebral segmentation defects: analysis of 26 new patients and review of the literature. American Journal of Medical Genetics 61:310-319, 1996

52. Treadwell SJ, Smith DF: Cervical spine abnormalities in fetal alcohol syndrome. Spine 7:331-334, 1982

53. Sherk HH, Black JD: Bony anomalies of the mid and lower cervical spine, in Pang D (ed): Disorders of the Pediatric Spine,1st edition Edition. New York: Raven Press, 1995, pp 125-136

54. Thompson DNP, Slaney SF, Hall CM, et al: Congenital cervical spinal fusion: a study in Apert syndrome. Pediatric Neurosurgery 25:20-27, 1996

55. Anderson PJ, Hall CM, Evans RD, et al: The cervical spine in Crouzon syndrome. Spine 22:402-405, 1997

56. Burke D, Wilkes D, Blundell TL, et al: Fibroblast growth factor receptors: lessons from the genes. Trends in Biochemical Science 23:59-62, 1998

57. Wilkie AOM, Slaney SF, Oldridge M, et al: Apert syndrome results from localized mutations of FGFR2 and is allelic with Crouzon syndrome. Nature Genetics 9:165-172, 1995

58. Bard JB: The molecular basis of morphogenesis, Morphogenesis: the cellular and molecular processes of developmental anatomy,1st Edition. Cambridge: Cambridge University Press, 1992, pp 65-119

59. Elsdale TR, Bard JB: Cellular interactions in mass cultures of human diploid fibroblasts. Nature 236:152-155, 1972

60. Elsdale TR, Bard JB: Collagen substrata for studies on cell behaviour. Journal of Cell Biology 54:626-637, 1972

61. Bard JB, Hay ED: The behaviour of fibroblasts from the developing avian cornea: their morphology and movement in situ and in vivo. Journal of Cell Biology 67:400-418, 1975

62. Bard JB, Higginson K: Fibroblast-collagen interactions in the formation of the secondary stroma of the chick cornea. Journal of Cell Biology-816, 1977

63. Erickson CA: Morphogenesis of the neural crest, in Browder L (ed): Developmental Biology - a comprehensive synthesis,1st edition Edition. New York: Plenum Press, 1986, pp 481-543

64. Gail MH, Boone CW: The locomotion of mouse fibroblasts in tissue culture. Biophysical Journal 10:980-993, 1970

65. Gail MH, Boone CW: Effect of colcemid on fibroblast activity. Experimental Cell Research 65:221-227, 1971

66. Ambrose EJ: Experimental Cell Research **8**:54, 1961

67. Bray D: Cell movements: from molecules to motility,2nd edition. Garland Science, 2000,

68. Random Walk. Wkikpedia - the free encyclopedia . 26-4-2006. 30-4-2006.

69. Bonner JT: Evidence for the formation of cell aggregates by chemotaxis in the development of the slime mould *Dictyostelium Discoideum*. Journal of Experimental Zoology 106:1-26, 1947

70. Konijn TM, van der Meene JGC, Bonner JT, et al: The acrasin activity of adenosine - 3' 5' - cyclic phosphate. Proceedings of the National Academy of Science, USA 58:1152-1154, 1967

71. Bonner JT, Berkley DS, Hall EM, et al: Acresin, acrasinase and sensitivity to acrasin in *Dictyostellium Discoideum*. Developmental Biology 20:72-87, 1969

72. MacKay SA: Computer simulation of aggregation in *Dictyostelium discoideum*. Journal of Cell Science 33:1-16, 1978

73. Dallon JC, Othmer HG: A discrete cell model with adaptive signalling for aggregation of *Dictyostelium discoideum*. Philosophical Transactions of the Royal Society 352 B:391-417, 1997

74. Gurdon JB, Standley H, Dyson S, et al: Single cells can sense their position in a morphogen gradient. Development 126:5309-5317, 1999

75. Gilbert S: Cell-cell communication in development, Developmental Biology,6th Edition. Sunderland, Massachusetts: Sinauer Associates, 2000, pp 143-184

76. Gustafson T, Wolpert L: Cellular movement and contact in sea urchin morphogenesis. Biological Review 42:442-498, 1967

77. Malinda KM, Fisher GW, Ettensohn CA: Four dimensional microscopic analysis of the filopodial behavior of primary mesenchyme cells during gastrulation in the sea urchin embryo. Developmental Biology 172:552-566, 1995

78. Muller TS, Ebensperger C, Neubuser A, et al: Expression of Pax-1 and Pax-9 is instrinsically regulated in the pharyngeal endoderm, but depends on environmental influences in the paraxial mesoderm. Developmental Biology 178:403-417, 1996

79. Bard JB: The morphogenetic properties of the mesenchyme, Morphogenesis: the cellular and molecular processes of developmental biology,1st Edition. Cambridge: Cambridge University Press, 1992, pp 120-180

80. Wood A, Thorogood PV: An ultrastructural and morphometric analysis of an in vivo contact guidance system. Development 101:363-381, 1987

81. Linask KL, Lash JW: A role for fibronectin in the migration of avian precardiac cells. I. Dose dependant effects of fibronectin antibody. Developmental Biology 129:315-323, 1988

82. Linask KL, Lash JW: A role for fibronectin in the migration of avian precardiac cells. II. Rotation of the heart forming region during different stages and its effects. Developmental Biology 129:324-329, 1988

83. Abercombie M: Contact inhibition: the phenomenon and its biological implications. In Vitro 26:249-261, 1967

84. Gilbert S: Principles of experimental embryology, Developmental Biology,6th edition Edition. Sunderland, Massachusetts: Sinauer Associates, 2000, pp 49-78

85. Waddington CH: Organisers and Genes edition. Cambridge: Cambridge University Press, 1940,

86. Spemann H: Embryonic Development and Induction edition. New Haven: Yale University Press, 1938,

87. Fan C-M, Tessier-Lavigne M: Patterning of mammalian somites by surface ectoderm and notochord: evidence for sclerotome induction by a hedgehog homolog. Cell 79:1175-1186, 1994

88. Fan C-M, Porter JA, Chiang C, et al: Long range sclerotome induction by sonic hedgehog: direct role of the amino-terminal cleavage product and modulation by the cyclic AMP signalling pathway. Cell 81:457-465, 1995

89. Drews U: General Embryology, Color Atlas of Embryology,1st Edition. Stuttgart: Thieme, 1995, pp 132-205

90. Takeichi M: The cadherins: cell-cell adhesion molecules controlling animal morphogenesis. Development 102:639-655, 1988

91. Chuong CM, Widelitz RB, Jiang TX, et al: Roles of adhesion molecules NCAM and tenascin in limb skeletogenesis: analysis with antibody pertubation, exogenous gene expression, talpid mutants ad activin stimulation. Prog Clin Bio Res 383 Part B:465-474, 1993

92. Hay ED: Collagen and other matrix glycoproteins in embryogenesis, in Hay ED (ed): Cell Biology of extracellular matrix,2st edition Edition. New York: Plenum Press, 1991, pp 419-462

93. Wolpert L: Morphogenesis: change in form in the early embryo, Principles of Development,1st Edition. London: Current Biology, 1998, pp 231-268

94. Kerr JF, Wyllie AH, Currie AR: Apoptosis: a basic biological phenomenon with wide ranging implications in tissue kinetics. British Journal of Cancer 26:239-257, 1972

95. Ebensperger C, Wilting J, Brand-Saberi B, et al: Pax 1, a regulator of sclerotome development is induced by notochord and floor plate signals in avian embryos. Anatomy and Embryology 191:297-310, 1995

96. Peters H, Wilm B, Sakai N, et al: Pax-1 and Pax-9 synergistically regulate vertebral column development. Development 126:5399-5408, 1999

97. Barnes GL, Hsu CW, Mariani BD, et al: Chicken Pax-1 gene: structure and expression during embryonic somite development. Differentiation 61:13-23, 1996

98. Deutsch U, Dressler GR, Gruss P: Pax 1, a member of the paired box homologous murine gene family is expressed in segmented structures during development. Cell 53:617-625, 1988

99. Neubuser A, Koseki H, Balling R: Characterization and developmental expression of Pax9, a paired box containing gene related to Pax1. Developmental Biology 170:701-716, 1995

100. Gruss P, Walther C: Pax in development. Cell 69:719-722, 1992

101. Chiang C, Litingtung Y, Lee E, et al: Cyclopia and defective axial patterning in mice lacking sonic hedgehog gene function. Nature 383:407-413, 1996

102. Marti E, Takada R, Bumcrot DA, et al: Distribution of sonic hedgehog peptides in the developing chick and mouse embryo. Development 121:2537-2547, 1995

103. Roelink H: Tripartite signalling of pattern: interactions between hedgehogs, BMPs, and Wnts in the control of vertebrate development. Current Opinion in Neurobiology 6:33-40, 1996

104. Brand-Saberi B, Ebensperger C, Wilting J, et al: The ventralizing effect of the notochord on somite differentiation in chick embryos. Anatomy and Embryology 188:239-245, 1993

105. David KM, McLachlan JC, Aiton JF, et al: Cartilaginous development of the human craniovertebral junction as visualised by a new three-dimensional computer reconstruction technique. Journal of Anatomy 192:269-277, 1998

106. Turing AM: The chemical basis of morphogenesis. Philosophical Transactions of the Royal Society 237 B:37-72, 1952

107. Bard JB, Lauder I: How well does Turings theory of morphogenesis work ? Journal of Theoretical Biology 45:501-531, 1974

108. Meinhardt H: Models of Biological Pattern Formation,1st edition edition. London: Academic Press, 1982,

109. Slack JMW: Theoretical embryology, in Slack JMW (ed): From egg to embryo,2nd Edition. Cambridge: Cambridge University Press, 1991, pp 34-66

110. Meinhardt H, Gierer A: Pattern formation by local self activation and lateral inhibition. BioEssays 22:753-760, 2000

111. Ermentrout GB, Edelstein-Keshet L: Cellular automata approaches to biological modelling. Journal of Theoretical Biology 160:97-133, 1993

112. Young DA: ??? Mathematical Bioscience 72:51-58, 1984

113. Murray JD: Mathematical Biology,2nd, corrected edition. Berlin: Speinger, 1993,

114. Nijhout HF, Wray GA, Kremen C, et al: Ontogeny, phylogeny and evolution of form: an algorithmic approach. Systematic Zoology 35:445-457, 1986

115. Dietrich S, Kessel M: The Vertebral Column, in Thorogood PV (ed): Embryos, Genes and Birth Defects,1st edition Edition. Chichester: John Wiley and Sons, 1997, pp 281-302

116. Watanabe Y, Duprez D, Monsoro-Burq A-H, et al: Two domains in vertebral development: antagonistic regulation by SHH and BMP4 proteins. Development 125:2631-2639, 1998

117. Pourquie O, Fan C-M, Coltey M, et al: Lateral and axial signals involved in avian somite patterning: a role for BMP4. Cell 84:461-471, 1996

118. Hamburger V, Hamilton HL: A series of normal stages in the development of the chick embryo. Journal of Morphology 88:49-92, 1951

119. Theiler K: The House Mouse edition. New York: Springer-Verlag, 1972,

120. O'Rahilly, R. and Muller, F. Developmental stages in human embryos. (637). 1987. Washington, DC, USA, Carnegie Institution.

121. Christ B, Schmidt C, Huang R, et al: Segmentation of the vertebrate body. Anatomy and Embryology 197:1-8, 1998

122. Stern C, Fraser S, Keynes R, et al: A cell lineage analysis of segmentation in the chick embryo. Development Supplement 104:231-244, 1988

123. Bronner-Fraser M: Rostrocaudal differences within Somites that confer segmental pattern to trunk neural crest migration, in Ordahl C (ed): Somitogenesis Part 1,1st edition Edition. San Diego: Academic Press, 2000, pp 279-296

124. Stern CD, Keynes R: Interactions between somite cells: the formation and maintance of segment boundaries in the chick embryo. Development 99:261-272, 1987

125. Rawls A, Wilson-Rawls J, Olson EN: Genetic regulation of somite formation, in Ordahl C (ed): Somitogenesis Part 1,1st edition Edition. San Diego: Academic Press, 2000, pp 132-154

126. Stockdale FE, Nikovits W, Christ B: Molecular and cellular biology of avian somite development. Developmental Dynamics 219:304-321, 2000

127. Palmeirim I, Henrique D, Ish-Horowicz D, et al: Avian hairy gene expression identifies a molecular clock linked to vertebrate segmentation and somitogenesis. Cell 91:639-648, 1997

128. Pourquie O: The segmentation clock: converting embryonic time into spatial pattern. Science 301:328-330, 2003

129. Rida PCG, Le Minh N, Jiang Y-J: A notch feeling of somite segmentation and beyond. Developmental Biology 265:2-22, 2004

130. Kusumi K, Sun ES, Kerrebrock AW, et al: The mouse *pudgy* mutation disrupts Delta homologue Dll3 and initiation of early somite boundaries. Nature Genetics 19:274-278, 1998

131. Johnson DR: The Genetics of the Skeleton: Animal Models of Skeletal Development,1st edition edition. Oxford: Oxford University Press, 1986,

132. Stern CD, Vasiliauskas D: Segmentation: a view from the border, in Ordahl C (ed): Somitogenesis Part 1,1st edition Edition. San Diego: Academic Press, 2000, pp 107-131

133. Brand-Saberi B, Christ B: Evolution and development of distinct cell lineages dervived from somites, in Ordahl C (ed): Somitogenesis Part 2,1st Edition. San Diego: Academic Press, 2000, pp 2-42

134. Johnson J, Rhee J, Parsons SM, et al: The anterior/posterior polarity of somites is disrupted in paraxis deficit mice. Developmental Biology 229:176-187, 2001

135. Burgess R, Rawls A, Brown D, et al: Requirement of the paraxis gene for somite formation and musculoskeletal patterning. Nature 384:570-573, 1996

136. Radice GL, Rayburn H, Matsunami H, et al: Developmental defects in mouse embryos lacking N-cadherin. Developmental Biology 181:64-78, 1997

137. Goulding MD, Chalepakis D, Deutsch U, et al: Pax-3, a novel murine DNA binding protein expressed during early neurogenesis. EMBOJ 10:1135-1147, 1991

138. Williams BA, Ordahl C: Pax-3 expression in segmental mesoderm marks early stages in myogenic cell specification. Development 120:785-796, 1994

139. Hoadley L: The differentiation of isolated chick primodia in chorio-allantoic grafts. II. The effect of the presence of the spinal cord, ie innervation on the differentiation of the somitic region. Journal of Experimental Zoology 42:143-162, 1925

140. Dockter JL: Sclerotome induction and differentiation, in Ordahl C (ed): Somitogenesis part 2,1st Edition. San Diego: Academic Press, 2000, pp 77-128

141. Wallin J, Wilting J, Koseki H, et al: The role of Pax-1 in axial skeleton development. Development 120:1109-1121, 1994

142. Peters H, Doll U, Niessing J: Differential expression of the chicken Pax-1 and Pax-9 gene: in situ hybridization and immunohistochemical analysis. Developmental Dynamics 203:1-16, 1995

143. Dietrich S, Schubert FR, Gruss P: Altered Pax gene expression in murine notochord mutants: the notochord is required to initiate and maintain ventral identity in the somite. Mechanisms of Development 44:189-207, 1993

144. Dietrich S, Gruss P: undulated phenotypes suggest a role of Pax-1 for the development of vertebral and extraverterbal structures. Developmental Biology 167:529-548, 1995

145. McMahon JA, Takada S, Zimmerman LB, et al: Noggin-mediatated antagonism of BMP signalling is required for growth and patterning of the neural tube and somite. Genes and Development 12:1438-1452, 1998

146. Williams L: The somites of the chick. American Journal of Anatomy 11:55-100, 1910

147. Christ B, Huang H, Wilting J: The development of the avian vertebral column. Anatomy and Embryology 202:179-194, 2000

148. Newgreen DF, Scheel M, Kastner V: Morphogenesis of the sclerotome and neural crest in avian embryos: in vivo and in vitro studies on the role of notochordal extracellular material. Cell and Tissue Research 244:299-313, 1986

149. Newgreen DF: Spreading explants of embryonic chick mesenchymes and epithelia on fibronectin and laminin. Cell and Tissue Research 236:265-277, 1984

150. Sanders EJ, Prasad S: The culture of chick embryo mesoderm cells in hydrated collagen gells. Journal of Experimental Zoology 226:81-92, 1983

151. Leeson CR, Threadgold LT, Sinclair NRSC: Histochemical observations upon the development of the notochord in the chick. Acta Anatomy 46:91-97, 1961

152. Gotz W, Osmers R, Herken R: Localisation of extracellular matrix components in the embryonic human notochord and axial mesenchyme. Journal of Anatomy 186:111-121, 1995

153. Hayes AJ, Benjamin M, Ralphs JR: Extracellular matrix in the development of the intervertebral disk. Matrix Biology 20:107-121, 2001

154. Smits P, Lefebvre V: Sox5 and Sox6 are required for notochord extracellular matrix sheath formation, notochordal cell survival and development of the nucleus pulposus of intervertebral discs. Development 130:1135-1148, 2003

155. Lettice LA, Purdie LA, Carlson GJ, et al: The mouse bagpipe gene controls development of axial skeleton, skull, and spleen. Proceedings of the National Academy of Sciences of the United States of America 96:9695-9700, 1999

156. Tribioli C, Lufkin T: The murine Bapx1 homeobox gene plays a critical role in embryonic development of the axial skeleton and spleen. Development 126:5699-5711, 1999

157. Rodrigo I, Hill RE, Balling R, et al: Pax-1 and Pax-9 activate Bapx-1 to induce chondrogenic differentiation in the sclerotome. Development 130:473-482, 2003

158. Tribioli C, Lufkin T: Molecular cloning, chromosomal mapping and developmental expression of BAPX1, a novel human homeobox-containing gene homologous to Drosphila bagpipe. Gene 203:225-233, 1997

159. Tribioli C, Frasch M, Lufkin T: Bapx1: an evolutionary conserved homologue of the Drosophila bagpipe homeobox gene is expressed in splanchnic mesoderm and the embryonic skeleton. Mechanisms of Development 65:145-162, 1997

160. Zeng L, Kempf H, Murtaugh LC, et al: Shh establishes an Nkx3.2 / Sox9 autoregulatory loop that is maintained by BMP signals to induce somitic chondrogenesis. Genes and Development 16:1990-2005, 2002

161. Stroustrup B: The C++ Programming Language,3rd edition. Addison Wesley, 1997,

162. Lorensen WE, Cline HE: Marching cubes: a high resolution 3D surface construction algorithm. Computer Graphics 21:163-169, 1987

163. Introduction to Implicit Surfaces,1st edition. Morgan Kaufmann, 1997,

164. Crank J: The mathematics of diffusion,2nd edition. Oxford: Oxford University Press, 1975,

165. Kaufman MH: The atlas of mouse development,2nd edition edition. London: Academic Press, 1995,

166. Balling R, Deutsch U, Gruss P: *undulated*, a mutation affecting the development of the mouse skeleton has a point mutation in the paired box of Pax 1. Cell 55:531-535, 1988

167. Wilm B, Dahl E, Peters H, et al: Targeted disruption of Pax1 defines it null phenotype and proves haploinsufficiency. Proceedings of the National Academy of Science, USA 95:8692-8697, 1998

168. Tam PPL: The control of somitogenesis in mouse embryos. Journal of Embryology and Experimental Morphology 65:103-128, 1981

169. Oster G: Biophysics of the leading lamella. Cell Motility and the Cytoskeleton 10:164-171, 1988

170. Noble PB: Extracellular matrix and cell migration: locomotory characteristics of MOS-11 cells within a three dimensional hydrated collagen lattice. Journal of Cell Science 87:241-248, 1987

171. Dow JAT, Lackie JM, Crocket KV: A simple microcomputer based system for real time analysis of cell behaviour. Journal of Cell Science 87:171-182, 1987

172. Felder S, Kam Z: Human neutrophil motility: time dependent three dimensional shape and granule diffusion. Cell Motility and the Cytoskeleton 28:285-302, 1994

173. Wood A, Thorogood PV: Patterns of cell behavior underlying somitogenesis and notochord formation in intact vertebrate embryos. Developmental Dynamics 201:151-167, 1994

174. Thorogood PV, Wood A: Analysis of in vivo cell movement using transparent tissue systems. Journal of Cell Science 8:395-413, 1987

175. Gulyas BJ: A re-examination of the cleavage patterns in eutherian mammalian eggs: rotation of the blastomere pairs during the second cleavage in the rabbit. Journal of Experimental Zoology 193:235-248, 1975

176. Press WH, Flannery BP, Teukolsky SA, et al: Random Numbers, Numerical Recipes in C: The art of scientific computing,1st Edition. Cambridge: Cambridge University Press, 1988, pp 204-241

177. Snow MHL, Tam PPL: Is compensatory growth a complicating factor in mouse teratology. Nature 279:555-557, 1979

178. Dalgleish AE: A study of the development of thoracic vertebrae in the mouse assisted by autoradiography. Acta Anatomy 122:91-98, 1985

179. Chernoff EAG, Lash JW: Cell movement in somite formation and development of the chick: inhibition of segmentation. Developmental Biology 87:212-219, 1981

180. Sonel B, Yalcin P, Ozturk EA, et al: Butterfly vertebra: a case report. Journal of Clinical Imaging 25:206-208, 2001

181. Bagnall KM, Sanders EJ, Higgins SJ, et al: The effects of somite removal of vertebral formation in the chick. Anatomy and Embryology 178:183-190, 1983

182. Bagnall KM, Sanders EJ, Higgins SJ, et al: The effects on vertebral development of removing a single somite from a 2 day old chick embryo, in Bellairs R, Ede DA, Lash JW (eds): Somites in Developing Embryos,1st edition Edition. New York: Plenum Press, 1984, pp 69-78

183. Jungel-Wass K, Christ B, Brand-Saberi B: Defect repair after somite removal in avian embryos is not true regeneration. Anatomy and Embryology 198:225-265, 1998

184. Barnes GL, Mariani BD, Tuan RS: Valproic acid-induced somite teratogenesis in the chick embryo: relationship with Pax-1 gene expression. Teratology 54:93-102, 1996

185. Smith CA, Tuan RS: Functional involvement of Pax-1 in somite development: somite dysmorphogenesis in chick embryos treated with Pax-1 paired box antisense oligodeoxynucleotide. Teratology 52:333-345, 1995

186. Monsoro-Burq A-H, Le Douarin N: Duality of Molecular Signals Involved in Vertebral Chondrogenesis, in Ordahl C (ed): Current Topics in Developmental Biology Volume 48 Edition. San Diego: Academic Press, 2000, pp 43-75

187. Theiler K: Vertebral malformations. Advances in Anatomy, Embryology and Cell Biology 112:1-99, 1988

188. Dahl E, Koseki H, Balling R: Pax genes and organogenesis. BioEssays 19:755-765, 1997

189. Bagnall KM, Higgins SJ, Sanders EJ: The contribution made by cells from a single somite to tissues within a body segment and assessment of their integration with similar celss from adjacent segments. Development 107:931-943, 1989

190. Bagnall KM, Higgins SJ, Sanders EJ: The contribution made by a single somite to the vertebral column: experimental evidence in support of resegmentation using the chick-quail chimaera model. Development 103:69-85, 1988

191. Pourquie O, Coltey M, Teillet M-A, et al: Control of dorsoventral patterning of somitic derivatives by notochord and floor plate. Proceedings of the National Academy of Science, USA 90:5242-5246, 1993

192. Verbout AJ: The development of the vertebral column,1st edition. Berlin: Springer Verlag, 1985, pp 1-122

193. Epstein D, McMahon AP, Joyner AL: Regionalization of sonic hedgehog transcription along the anterioposterior axis of the mouse central nervous system is regulated by Hnf3-dependent and independent mechanisms. Development 126:281-292, 1999

194. Johnson RL, Laufer E, Riddle RD, et al: Ectopic expression of sonic hedgehog alters dorsal-ventral patterning of somites. Cell 79:1165-1173, 1994

195. Sanders EJ, Cheung E: Ethanol treatment induces a delayed segmentation anomaly in the chick embryo. Teratology 41:289-297, 1990

196. Connelly LE, Rogers JM: Methanol causes posteriorization of cervical vertebrae in mice. Teratology 55:138-144, 1997

197. Conlon RA, Reaume AG, Rossant J: Notch 1 is required for the co-ordinate expression of somites. Development 121:1533-1545, 1995

198. De Angelis MH, McIntyre J, Gossler A: Maintance of somite borders in mice requires the Delta homologue Dll1. Nature 386:717-721, 1997

199. Bulman MP, Kusumi K, Frayling TM, et al: Mutations in the human delta homologue DLL3 cause axial skeletal defects in spondylocostal dysostosis. Nature Genetics 24:438-441, 2000

200. Wong PC, Zheng H, Chen H, et al: Presenilin 1 is required for Notch1 and Dll1 expression in the paraxial mesoderm. Nature 387 May 15:288-292, 1997

201. Tam PPL, Trainor PA: Specification and segmentation of the paraxial mesoderm. Anatomy and Embryology 189:275-305, 1994

202. Christ B, Wilting J: From somites to vertebral column. Annals of Anatomy 174:23-32, 1992

203. Sasaki H, Hogan BL: Differential expression of multiple fork head related genes during gastrulation and axial pattern formation in the mouse embryo. Development 118:49-59, 1993

204. Gritli-Linde A, Lewis P, McMahon AP, et al: The whereabouts of a morphogen: direct evidence for short and graded long-range activity of hedgehog signaling peptides. Developmental Biology 236:364-386, 2001

205. Walmsley R: The development and growth of the intervertebral disk. Edinburgh Medical Journal 60:343-363, 1953

206. Hunter CJ, Matyas JR, Duncan NA: Functional significance of cell clusters in the notochordal nucleus pulposus. Spine 29:1099-1104, 2004

207. Nguyen VD, Tyrrel R: Klippel-Feil syndrome: patterns of bony fusion and wasp-waist sign. Skeletal Radiology 22:519-523, 1993

208. Martinez-Frias ML, Bermejo E, Martinez S, et al: Jarcho-Levin and Casamassima syndromes: differential diagnosis and frequency in Spain. An Esp Pediatr 48:510-514, 1998

209. Pang D: Split cord malformation: Part II: Clinical syndrome. Neurosurgery 31:481-500, 1992

210. Pang D, Dias MS, Ahab-Barmada M: Split cord malformation: Part I: a unified theory of embryogenesisfor double spinal cord malformations. Neurosurgery 31:451-480, 1992

211. Ulmer JL, Elster AD, Ginsberg LE, et al: Klippel-Feil syndrome: CT and MR of acquired and congenital abnormalities of the cervical spine and cord. Journal of Computer Assisted Tomography 17:215-224, 1993

212. Bremer JL: Dorsal intestinal fistula: accessory neurenteric canal: diastematomyelia. Archives of Pathology 54:132-138, 1952

213. Smith CA, Tuan RS: Human PAX gene expression and development of the vertebral column. Clinical Orthopaedics and Related Research 302:241-250, 1994

214. Remak R: Untersuchungen uber die Entwicklung der Wirbeltiere edition. Berlin: Reimer, 1855,

215. Bagnall KM: The migration and distribution of somite cells after labelling with the carbocyanine dye, DiI: the relationship of this distribution to segmentation in the vertebrate body. Anatomy and Embryology 185:317-324, 1992

216. Huang R, Zhi Q, Brand-Saberi B, et al: New experimental evidence for somite resegmentation. Anatomy and Embryology 202:195-200, 2000

217. Aoyama H, Asamoto K: The developmental fate of the rostal/caudal half of a somite for vertebra and rib formation: experimental confirmation of resegmentation theory using chick-quail chimeras. Mechanisms of Development 99:71-82, 2000

218. Fleming A, Keynes R, Tannahill D: A central role for the notochord in vertebral patterning. Development 131:873-880, 2004

17 Appendix A

17.1 THEILER STAGES OF MOUSE DEVELOPMENT

([C57BL x CBA] F1 generation hybrid mice)

Stage	embryonic age	size	somites	description
1	0-1			fertilised cell in oviduct
2	1-2			two cells in oviduct
3	2-2.5			cleavage, 4 to 8 cells, then morula formation
4	2.5-3.5			blastocyst – zona intact
5	3.5-4			blastocyst – zona absent
6	4-4.5			attaching blastocyst
7	4.5-5.5			embryo impanted, egg cylinder
8	5.5-6			differentiation of egg cylinder
9	6-6.5			primitive streak formation, gastrulation, first evidence of mesoderm
10	6.5-7.5			primitive streak and groove, Hensens node
11	7-7.5			neural plate, head process developing, neural folds closing in cervical / occipital region. Heart differentiation
12	7.5-8.5	1-4 5-7		first branchial arch, formation of heart, 1 to 3 somites, later 4 to 7.
13	8.5-9	8-12		Between 8 and 12 somites. Embryo turning, first and second branchials seen
14	8.5-9	13-20		Between 13 and 20 somites. Cephalic neural folds, formation, closure of rostal neuropore. Third arch, optic vesicle formation, forelimb ridge
15	9-9.75	21-29	1.8-3.3	Caudal neuropore decreasing, three branchial arches, optic cup, forelimb bud, tracheal diverticulum
16	9.75-10.25	30-34	3-4	Caudal neuropore closure, fourth branchial arch appearance, otocyst, hindlimb bud
17	10-10.5	35-39	3.5-5	differentiation of cephalic neural tube, tail elongation and thinning, umbilical hernia
18	10.5-11	40-44	5-6	Formation / closure of lense vesicle, deep nasal pit, cervical somites indistinct
19	11-11.5	45-47	6-7	distal forelimb bud paddle shaped, auditory hillocks first evident
20	11.5-12	48-51	7-8	earliest signs of fingers, splayed out digits, foot plate seen, brain vesicles recognised
21	12.5-13	52-55	8-9	anterior part of foot indented, elbow and wrist regions seen, 5 row of whiskers
22	13.5-14	56- >60	9-10	fingers well defined, long bones of limbs seen, hair follicles
23	14.5-15		10-11.5	toes separated, eyelids open
24	15.5-16		11.5-14	repositioning of umbilical hernia, eyelids closing
25	16.5-17		13.6-16	skin wrinkled, eyelids closed, no evidence of umbilical hernia
26	17.5-18		17-19	elongated whiskers, eyes barely visible through closed eyelids, external ear covers auditory meatus

From Kaufman, MH, Bard, JBL The Anatomical Basis of Mouse Development

17.2 CARNEIGE STAGES OF HUMAN DEVELOPMENT

Stage	Days post conception	Length (mm)	Description
First week: migration through the fallopian tube			
1			fertilised oocyte
2	2-3		cleavage, differentiation into inner and outer cells
3	4-5		free blastocyst with trophoblast and inner cell mass
Second week: implantation			
4	5-6		blastocyst attaching to uterine wall
5	7-12	.1-.2	implantation, bilaminar embryonic disk
6	13-15	.2	primitive streak and embryonic mesoderm
7	15-17	.4	formation of notochord
8	17-19	1-1.5	primitive pit, notochordal canal, neurenteric canal
9	19-21	1.5-2.5	1 to 3 somites, neural and head folds, cardiac primordium
Fourth week: folding			
10	22-23	2-3.5	4-12 somites, neural folds fuse, two pharyngeal arches, optic sulcus
11	23-26	2.5-4.5	13-20 somites, rostal neuropore closes, optic vesicle
12	26-30	3-5	21-29 somites, caudal neuropore closes, three pharyngeal arches, arm buds appear
13	28-32	4-6	30 somites, leg buds, lense placode, otic vesicle
Organogenesis: weeks 5 to 8			
14	31-35	5-7	lens pit and optic cup, endolymphatic duct
15	35-38	7-9	cerebral vesicle, lense vesicle, nasal pit, facial swellings, hand plate
16	37-42	8-11	pigmented eye, auricular hillocks visible
17	42-44	11-14	relative enlargment of head and trunk elongation. Nasolacrimal groove, distinct auricular hillocks. Finger rays
18	44-48	13-17	elbows and toe rays. Appearance of nipples, distinct nose apex and eyelids, onset of ossification
19	48-51	16-18	elongation and straightening of trunk
20	51-53	18-22	upper limbs longer and bend at elbow
21	53-54	22-24	hands and feet turned inwards
22	54-56	23-28	eyelids and external ears develop
23	56-60	27-31	rounded head, body and limbs developed

from Drews, L Atlas of Embryology, Theime